Neural Plasticity

Post-Stroke Neural Plasticity: Functional and Structural Reorganization during Stroke Recovery 2022

Lead Guest Editor: Xiaozheng Liu
Guest Editors: Yating Lv, Yu Zheng, Xize Jia, Xiaofu He, and Zhiyong Zhao

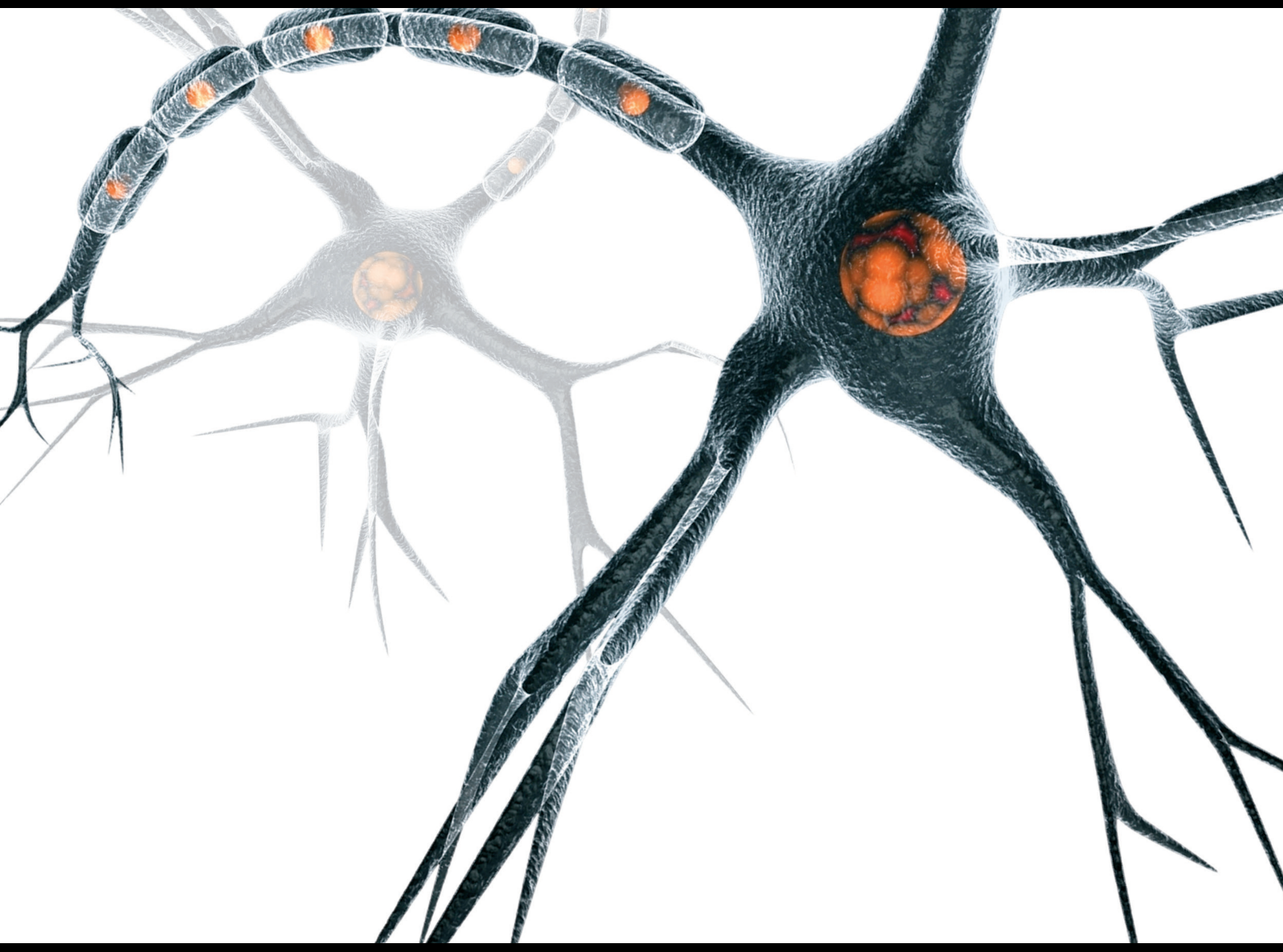

Post-Stroke Neural Plasticity: Functional and Structural Reorganization during Stroke Recovery 2022

Neural Plasticity

Post-Stroke Neural Plasticity: Functional and Structural Reorganization during Stroke Recovery 2022

Lead Guest Editor: Xiaozheng Liu
Guest Editors: Yating Lv, Yu Zheng, Xize Jia, Xiaofu He, and Zhiyong Zhao

Contents

Hindawi
Neural Plasticity
Volume 2023, Article ID 2403175, 10 pages
https://doi.org/10.1155/2023/2403175

Research Article

Premotor and Posterior Parietal Cortex Activity is Increased for Slow, as well as Fast Walking Poststroke: An fNIRS Study

Shannon B. Lim[1,2] **Sue Peters**[3] **Chieh-ling Yang**[4] **Lara A. Boyd**[1,5] **Teresa Liu-Ambrose**[1,5,6] **and Janice J. Eng**[1,2,6]

[1]*Department of Physical Therapy, University of British Columbia, Vancouver, BC, Canada*
[2]*Rehabilitation Research Program, GF Strong Rehabilitation Centre, Vancouver, BC, Canada*
[3]*School of Physical Therapy, Western University, London, ON, Canada*
[4]*Department of Occupational Therapy and Graduate Institute of Behavioral Sciences, College of Medicine, Chang Gung University, Taoyuan City, Taiwan*
[5]*The David Mowafaghian Centre for Brain Health, University of British Columbia, Vancouver, BC, Canada*
[6]*Centre for Aging SMART at Vancouver Coastal Health, Vancouver, BC, Canada*

Correspondence should be addressed to Janice J. Eng; janice.eng@ubc.ca

Received 15 August 2022; Revised 14 June 2023; Accepted 14 September 2023; Published 13 October 2023

Academic Editor: Xi-Ze Jia

Background and Purpose. The ability to change gait speeds is important for interacting with the surrounding environment. Gait speed modulation poststroke is often impaired and is related to decreased walking independence after stroke. Assessment of brain activation during walking at different speeds can provide insight into important regions for facilitating gait recovery. The purpose is to determine: (1) the symmetry of brain activation as individuals increase or decrease their gait speed, (2) the activation levels in frontal to parietal brain regions during walking at different speeds, and (3) the relationship between an individual's stroke impairment or their ability to modulate their gait speed and change in their brain activation. *Methods*. Twenty individuals in the chronic stage of stroke walked: (1) at their normal pace, (2) slower than normal, and (3) as fast as possible. Functional near-infrared spectroscopy was used to assess bilateral prefrontal, premotor, sensorimotor, and posterior parietal cortices during walking. *Results*. No significant differences in laterality were observed between walking speeds. The ipsilesional prefrontal cortex was overall more active than the contralesional prefrontal cortex. Premotor and posterior parietal cortex activity were larger during slow and fast walking compared to normal-paced walking with no differences between slow and fast walking. Greater increases in brain activation in the ipsilesional prefrontal cortex during fast compared to normal-paced walking related to greater gait speed modulation. *Conclusions*. Brain activation is not linearly related to gait speed. Ipsilesional prefrontal cortex, bilateral premotor, and bilateral posterior parietal cortices are important areas for gait speed modulation and could be an area of interest for neurostimulation.

1. Introduction

While adequate gait speed is an important factor for successful ambulation within the community, the ability to change gait speed is also important for safe interaction with the environment. For example, the ability to appropriately increase gait speed is important for crossing the street before a light turns red and the ability to slow down gait is important before stepping up onto a curb. This ability to change walking speed has been related to balance performance [1] and falls risk [2]. In fact, older adults who demonstrate a decreased ability to adapt their walking speed are almost five times more likely to be at high risk of falls [3]. After a stroke, the ability to change gait speed is often impaired [4] and individuals who are not able to increase gait speed exhibit lower functional ambulation [5].

Investigation of brain activation while walking at different speeds may provide some insight into gait speed impairments. In healthy adults, slow walking (0.4–0.6 m/s) primarily results in activation of the premotor and supplementary motor area of both cortices [6]. As walking speed increases to 0.7 and 0.8 m/s, bilateral prefrontal and sensorimotor cortices also become active [6]. When healthy older adults were asked to

walk at different speeds, the greatest activation was found at the fastest walking speed [7]. Harada et al. [7] also found that the prefrontal cortex activity increase was greater for individuals that have a slower fast gait speed (<1.67 m/s) compared to those who had a faster gait. In addition, when gait speed continuously changes on one leg using a split-belt treadmill, healthy adults show increased activation within the supplementary motor area and posterior parietal cortex compared to walking at a stable speed [8]. It is possible that impaired gait speed modulation poststroke may be explained by abnormal activation in these prefrontal, premotor, supplementary motor, sensorimotor, or posterior parietal cortical areas.

To date, the impact of stroke on functional activation changes with speed modulation is unknown. Previous studies have shown indications of asymmetric brain activations with greater ipsilesional prefrontal [9], contralesional sensorimotor [9, 10], and contralesional posterior parietal [9] cortices relating to faster walking speeds poststroke. The changes in the amplitude of activation during walking at different speeds poststroke are also unclear. Bansal et al. [11] recently demonstrated that their lower-functioning stroke group had a limited capacity to increase their gait speed compared to their higher-functioning stroke group. Although not measured in their study, it is possible that this impairment is related to their participant's capacity to activate certain brain regions.

To help understand the impact stroke has on gait speed modulation, the purposes of this study are to explore: (1) the symmetry of brain activation as individuals increase or decrease their gait speed, (2) the activation levels in frontal to parietal brain regions during walking at different speeds, and (3) the relationship between an individual's stroke impairment or their ability to modulate their gait speed and change in their brain activation. Specifically, we hypothesized that: (1) fast walking would show asymmetrical activity with greater ipsilesional prefrontal, contralesional sensorimotor, and contralesional posterior parietal activation; (2) a graded activation would be observed with a lower magnitude of activation observed in slow walking and the highest activation with fast walking; and (3) the magnitude of brain activation changes from fast and slow compared to normal-paced walking would relate to impairment and gait speed modulation ability.

2. Methods

2.1. Participant Recruitment. Participants were recruited through convenience sampling via posters at private clinics, local rehabilitation centers, and online platforms. Information regarding the study was also distributed through phone or mail to previous participants who have agreed to be contacted for future studies. Study details were approved by the University of British Columbia Research Ethics Board (H18-01003) and written and informed consent was provided by all participants.

2.2. Participant Screening. Individuals were screened for eligibility by telephone. Inclusion criteria were as follows: age greater or equal to 18 years; telephone minimental state exam greater than 21/26 [12, 13] indicating no moderate or severe cognitive impairment; stroke incident greater than 6 months previous (chronic stroke); single known stroke; one-sided hemiparesis; able to walk independently (gait aids allowed) for 1-min bouts; and able to understand and follow directions in English. Exclusion criteria were musculoskeletal injury impairing walking and neurological injury other than stroke.

2.3. Demographic Data. Age, sex, global cognition (using the Montreal Cognitive Assessment), and gait aid used were collected. Stroke details were obtained from medical charts when available. When medical charts were not available, details on time poststroke and stroke type (ischemic/hemorrhagic) were collected through verbal reports by the participants. Lesion location was determined from structural MRI obtained through medical records or collected for this study when eligible.

2.4. Task Procedure. The walking tasks were completed in a 50-m hallway. Participants completed one to two familiarization trials of each walking condition. Participants stood at either end of the hallway to begin each trial. The starting end was randomly determined by the researcher. After a minimum 30 s of quiet stance, a verbal "go" from the researcher specified the start of the walking trial; a verbal "stop" indicated the end of the trial. All participants were told to keep their head position consistent and to avoid unnecessary talking throughout the walking trials. Walking trials were 30 s long and were performed four to five times. A wheelchair and spotter were positioned behind the participant for safety during all trials. At the end of each walking trial, participants stood for 5 s before sitting in the wheelchair. The spotter then pushed the participant to the end of the hallway to start the next trial. All trials had at least 30 s of standing immediately before the start of the trial—this allowed for the brain signals to return to baseline.

Participants performed three walking conditions: normal-paced walking speed (*NORM*), slow speed (*SLOW*), and fast speed (*FAST*). Overground walking was chosen to resemble daily walking conditions and to investigate limitations to changing one's gait speed. All participants first completed the *NORM* condition and then either the *SLOW* or *FAST* condition (randomized). For the *SLOW* condition, participants were told to walk slower than their normal pace and for the *FAST* condition, participants were told to walk as fast as they could without running. The PychoPy3.0 program was used for randomizing the conditions and triggering/timing the trials [14].

2.5. Functional Brain Activation. Functional brain activity was measured by functional near-infrared spectroscopy (fNIRS). All data collection and analysis regarding fNIRS were completed in accordance with best practice guidelines [15, 16]. fNIRS was chosen, opposed to other imaging devices, due to its ability to be wireless, portable, and robust to motion artifacts. Further information on the advantages and details of fNIRS have been discussed in previous reviews [17–19]. The NIRSport2 (NIRx Medical Technology, Germany) was used, which had 16 LED emitters that released near-infrared light at 760 and 850 nm for measurement of both deoxygenated

(HbR) and oxygenated (HbO) hemoglobin, respectively, and 23 silicon photodetectors. Optodes were connected to the fNIRS collection device, which was worn as a backpack by the participants. fNIRS data were continuous sampled at 4.36 Hz through Aurora 1.4 (NIRx Medical Technologies, Berlin, Germany). The probe configuration for this experiment was similar to our previous studies [9, 20, 21] with 48 long separation channels (~30–35 mm apart) and 8 short separation channels (8 mm apart). Two different distances were chosen to control for extracerebral systemic changes such as breathing, heartbeat, and mayer waves [22]. As previous studies have primarily shown significant findings with HbO and little change in HbR, results will focus on HbO findings. HbO is also more reproducible and stable over time [23], has the highest correlation to fMRI BOLD measures [24]. For transparency, detailed HbR findings are reported in Tables S4 and S5.

2.6. Probabilistic Localization. Several approaches were taken to improve the accuracy of localizing functional brain activation. First, spatial locations of the optodes on each participant's scalp were digitally collected using a 3D digitizer (Polhemus Patriot, USA) and the software PHOEBE [25]. To control for the location of digitization within the optode holder (7 mm diameter), a custom interface between the optode holder and the digitizing stylus was 3D printed to consistently place the stylus at the center of the optode holder. The 3D digitations were then imported to AtlasViewer [26], which was used to project the channels to the Colin27 atlas brain. Montreal Neurological Institute coordinates and Automated Anatomical Labeling projections were provided by AtlasViewer and were then translated into Brodmann labels using the Allen Human Brain Atlas [27] and the Yale BioImage Suite Package web application [28]. This labeling system was then used to categorize channels into regions of interest: PFC, PMC (which was also combined with SMA), SMC, and PPC on the ipsilesional and contralesional hemispheres. Individual MRIs were then used to determine the location of the stroke lesion. If stroke lesions were present along the cortex, channels that were projected to lesion sites were removed (i.e., not analyzed).

2.7. Stroke Lower Extremity Impairment. The lower extremity portion of the Fugl-Meyer assessment [29] was used to determine motor impairment after stroke. This assessment was completed by a trained physiotherapist, has excellent inter- [30] and intra-rater [31] reliability, and is a recommended outcome measure for individuals living after stroke [32].

2.8. Gait Speed Modulation. Gait speeds were first calculated for every trial by determining the distance walked during the 30-s trials. Average gait speed was calculated for each condition and the differences in gait speed were calculated between *NORM* to *FAST* and between *NORM* to *SLOW*. These differences were used to determine gait speed modulation ability.

2.9. Analysis. To determine if the tasks were performed as intended, task performance differences in gait speed were determined by paired *t*-tests between NORM and FAST and between NORM and SLOW. A Bonferroni corrected alpha of 0.025 was used to reduce Type 1 error. HomER2 [33] was used to preprocess the fNIRS data. HomER2 functions and corresponding parameters are indicated within square brackets. First, noisy channels were removed (enPruneChannels: SNRtresh = 6.67, dRange = 5e-4 to 1e+00, SDrange:0 −45) before converting the signal into optical density (hmrIntensity2OD). 0.5 s time windows were used to identify motion artifacts in data for signals exceeded either 20 standard deviations above the mean signal for each channel or a change greater than five times in amplitude (hmrMotionArtifactByChannel: tMotion = 0.5, tMask = 1.0, STDEVthresh = 20.0, AMPthresh = 5.00). Once identified, motion correction was applied using a wavelet transformation with a 1.5 interquartile range (hmrMotionCorrectWavelet: iqr = 1.5) [34–36]. The remaining motion artifacts were assessed again using the same parameters as above (hmrMotionArtifactByChannel: tMotion = 0.5, tMask = 1.0, STDEVthresh = 20.0, AMPthresh = 5.00). The number of channels removed from further analysis for each participant can be found in Tables S2 and S3. A lowpass filter of 0.15 Hz was then applied to the data (hmrBandpassFilt: lpf = 0.15) and converted to hemoglobin concentration using the modified Beer–Lambert equation (hmrOD2Conc: ppf = 6.0, 6.0) [37, 38]. A general linear model with an ordinary least squares approach [39, 40] and a 0.5 s width and 0.5 s step consecutive Gaussian basis function [41] was used to estimate the hemodynamic response. Superficial contributions to the signal were also removed by regressing out the data from the short separation channel that has the highest correlation to each channel [40–44]. Any drift within the signal was corrected using a third-order polynomial correction [40] (hmrDeconvHRF_DriftSS:trange = −20.0 35.0, glmSolveMethod = 1, idxBasis = 1, paramsBasis = 0.5 0.5, rhoSD_ssThresh = 15.0, flagSSmethod = 1, driftOrder = 3, flagMotionCorrect = 0). Once preprocessed, data were exported to a custom Matlab script for baseline corrections (−15 to 0 s before walking onset) and region of interest averaging. Brain activations during the task were calculated by averaging hemoglobin amplitudes during the first 20 s of walking. The first 20 s of the task were chosen for analysis, opposed to the entire 30-s walking task because some participants walked fast enough to reach the end of the straight walking track before the 30 s was up. Thus, 20 s was chosen as all participants were walking along the straight path during this period.

Aim 1: To assess activation symmetry, a laterality index was calculated for each region of interest [45]. The laterality index was calculated as follows:

$$\text{Laterality index} = \frac{\text{Ipsilesional activation} - \text{Contralesional activation}}{|\text{Ipsilesional activation}| + |\text{Contralesional activation}|}. \quad (1)$$

Using this equation, a positive value indicates more activation in the ipsilesional hemisphere whereas a negative value indicates more activation in the contralesional

hemisphere. The laterality index was then compared between conditions using linear mixed-effects models in the statistical package "lme4" within the R Studio software. Participants were set as random effects and condition (*NORM*, *FAST*, *SLOW*) were included as fixed effects.

Aim 2: To look at the effects of condition (*NORM*, *SLOW*, *FAST*) on brain activation, linear mixed-effects models (one for each region of interest: PFC, PMC, SMC, PPC) were used. Within this model, participants were included as random effects, condition was included as fixed effect, and if it significantly improved the model, hemisphere was also added as a fixed effect.

Aim 3: Relationships between changes in brain activation and stroke lower extremity impairment and gait speed modulation were determined using Pearson's correlations. Change in brain activation was calculated for each region of interest (PFC, PMC, SMC, PPC). These changes in brain activation were determined by calculating the difference between average brain activation during *NORM* and average brain activation during *FAST* or *SLOW*. Correlations were assessed for each region separately: ipsilesional PFC, PMC, SMC, PPC and contralesional PFC, PMC, SMC, PPC.

All relevant assumptions and diagnostics were checked for each statistical test. Appropriate modifications were made and reported when necessary. Due to the relatively small sample size, results are reported using a standard alpha of 0.05 in order not to miss potential effects. Data are also shown with a Bonferroni correction for reducing Type 1 error by running multiple models ($p \leq 0.0125 = 0.05/4$ models and regions) and a Benjamini–Hochberg false discovery rate of 5% to correct for multiple Pearson's correlations.

3. Results

Twenty-two individuals were eligible and consented to the study and 20 participants completed the study. Two eligible participants were not able to attend data collection sessions due to restrictions as a result of the COVID-19 pandemic. Average demographic data and gait performance are displayed in Table 1. Overall, participants completed the tasks as intended. Compared to the *NORM* condition, an average increase in gait speed of 30% was calculated for the *FAST* condition and an average decrease of 21% was calculated for the *SLOW* condition. One participant ended up increasing their gait speed during *SLOW* compared to *NORM* by 0.03 m/s, another participant was not able to increase their gait speed during the *FAST* condition compared to *NORM*. Further details on individual stroke demographics and performance can be found in Table S1.

The overall hemodynamic waveform showed a typical shape with increases in HbO and smaller amplitude decreases in HbR starting within the first 5 s of walking for all conditions (Figure 1).

Aim 1: No significant differences in laterality were observed between the three walking speeds (Figure 2 and Table 2, Aim 1).

Aim 2: Linear mixed models showed an effect of speed for the PMC and PPC regions. Compared to the *NORM* condition, *FAST* and *SLOW* conditions showed increased activation for both PMC and PPC. No significant differences were found between the *FAST* and *SLOW* conditions. Ipsilesional PFC showed significantly greater activation compared to the contralesional side (Table 2, Aim 2).

Aim 3: The magnitude of gait speed increase from *NORM* to *FAST* showed a moderate positive correlation to the amount of brain activation increase in ipsilesional PFC. Less impairment (i.e., higher FMLE scores) related to greater ipsilesional PFC activation changes from *NORM* to *FAST*, with a moderate but not significant correlation after correction for multiple comparisons. No significant relationships were found with the contralesional hemisphere (Table 3).

4. Discussion

This is the first study to investigate brain activation during modulation of gait speed poststroke. Results for Aim 1 were supportive of the null hypothesis while results for Aim 2 and 3 partially supported the alternate hypotheses.

4.1. Laterality. Although previous works have suggested some hemispheric differences with different walking speeds, the current study showed no changes in laterality with the three walking speeds. Despite not observing an overall change in hemispheric activation, participants exhibited a greater level of ipsilesional prefrontal cortex activation throughout. This is similar to our previous study where ipsilesional PFC was also elevated compared to the contralesional side and had a significant relationship with performance [8].

4.2. Premotor and Posterior Parietal Regions Involved in Speed Modulation. The current study showed that PMC and PPC play a role in modulating gait speeds, with the increase in PPC activity during *FAST* compared to *NORM* walking showing the largest difference. This increase in brain activity during *FAST* and *SLOW* walking occurred despite having participants of varying impairment levels (Fugl-Meyer lower extremity score range: 18–34) and gait speed abilities (normal-paced gait speed range: 0.14–1.39 m/s). Notably, no significant correlations were observed between PMC or PPC changes and impairment. This may indicate that these regions are involved in the task of changing gait speeds itself, and not as a regulator of the amount of gait speed change. Interestingly, our previous work in individuals poststroke showed that PMC activation does not change during normal-paced walking compared to standing [9]. PMC is known to be involved in motor planning and preparation [46, 47] and the supplementary motor area, which we included in our PMC region, is involved in online motor adjustments [8]. This finding suggests that continuous planning or movement preparation is not required for walking at a comfortable speed, which may arguably be quite automatic for the independent walkers in our studies, whereas a change from normal-paced walking requires more planning and

Table 1: Summary of participant details.

	$N = 20$
Age [mean (SD)]	64 (7.6) years
Sex (female/male)	7/13
Chronicity [mean (SD)]	82 (67.4) months
Lesion depth (cortical/subcortical/mixed)	0/17/3
Lesion side (left/right)	7/13
FM-LE (34 max)	27 (4.9)
MoCA (30 max)	26 (2.6)
Gait aids (none/walking stick(s)/4-point cane/4 wheeled walker)	12/6/1/1
Normal gait speed [mean (SD)]	0.83 (0.346) m/s Range: 0.14–1.39 m/s
Slow gait speed [mean (SD)]	0.64 (0.34) m/s* Range: 0.10–1.32 m/s $t(19) = 3.05$, $p = 0.007$, CI = 0.06–0.31
Fast gait speed [mean (SD)]	1.08 (0.45) m/s* Range: 0.14–1.88 m/s $t(19) = -7.65$, $p < 0.001$, CI = −0.30 to −0.17

Note: *Significantly different than the *NORM* condition. FM-LE = Fugl-Meyer lower extremity; MoCA = Montreal Cognitive Assessment; CI = 95% confidence interval.

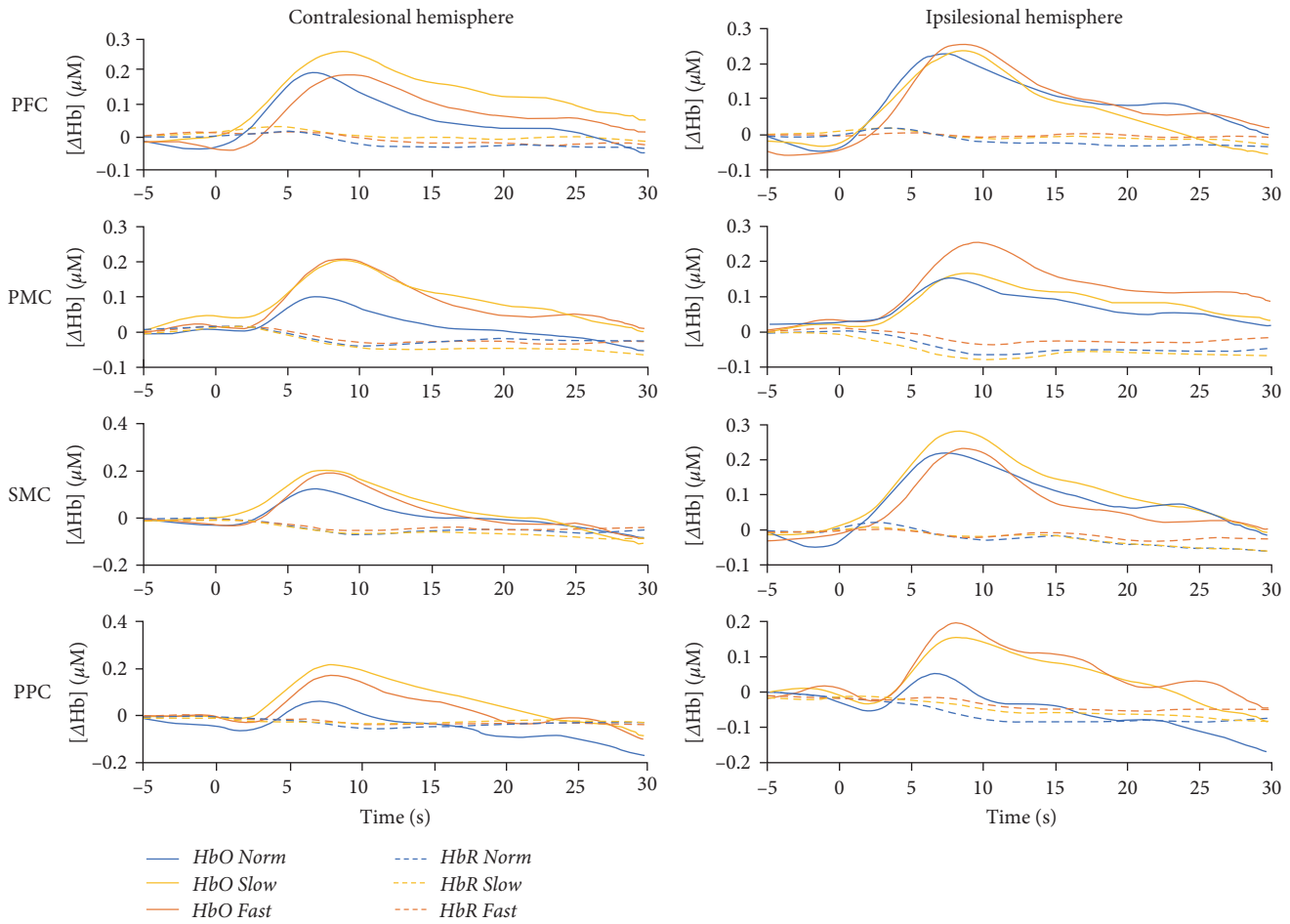

Figure 1: Average ($N = 20$) activation for oxyhemoglobin (HbO) and deoxyhemoglobin (HbR) during each walking condition. PFC = prefrontal cortex; PMC = premotor cortex; SMC = sensorimotor cortex; PPC = posterior parietal cortex.

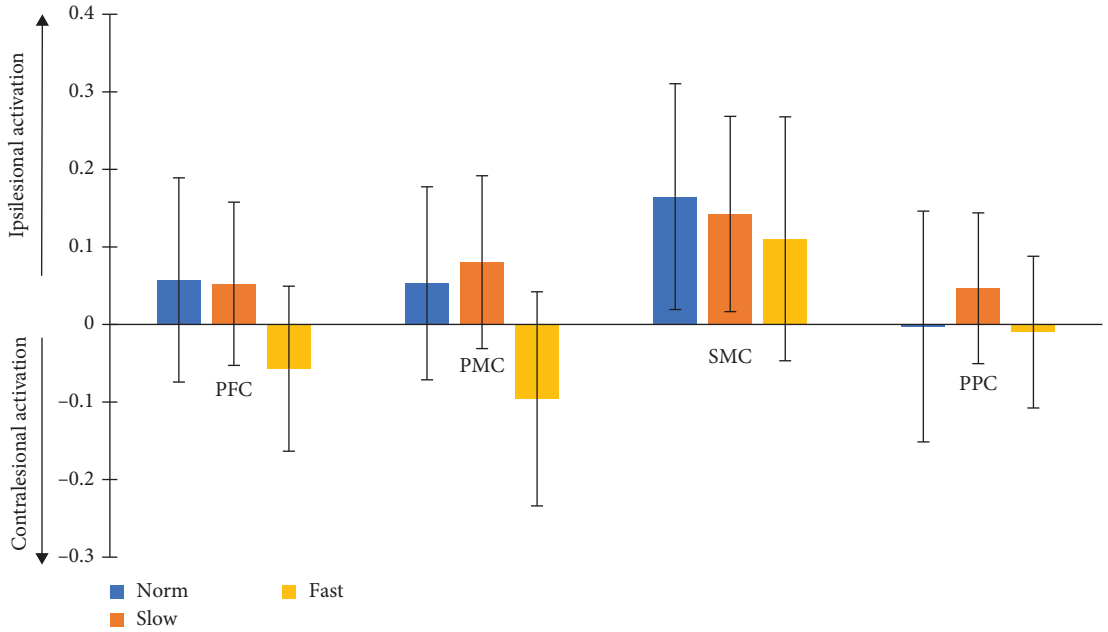

Figure 2: Average and standard error ($N = 20$) change in laterality index for HbO during each walking condition. Positive values indicate more activation along the ipsilesional hemisphere and negative values indicate more activation along the contralesional hemisphere. PFC = prefrontal cortex; PMC = premotor cortex; SMC = sensorimotor cortex; PPC = posterior parietal cortex.

Table 2: Linear mixed-effects models results.

ROI	Predictors	Estimates	Confidence interval	p	ICC	N_{subj}	Observations	Marginal R^2/conditional R^2
(a). Aim 1: laterality index ~ condition + (1|participant)								
PFC	(Intercept)	0.057449	−0.167247–0.282145	0.610	0.74	20	60	0.011/0.739
	Condition (*FAST*)	−0.114453	−0.277834–0.0489273	0.166				
	Condition (*SLOW*)	−0.004908	−0.168288–0.158473	0.952				
PMC	(Intercept)	0.053142	−0.191337–0.297621	0.665	0.73	20	60	0.020/0.737
	Condition (*FAST*)	−0.149032	−0.328234–0.030171	0.101				
	Condition (*SLOW*)	0.027203	−0.152000–0.206405	0.762				
SMC	(Intercept)	0.164832	−0.115489–0.445153	0.243	0.72	18	54	0.001/0.720
	Condition (*FAST*)	−0.054382	−0.264360–0.155596	0.605				
	Condition (*SLOW*)	−0.022304	−0.232282–0.187674	0.832				
PPC	(Intercept)	−0.002626	−0.231353–0.226100	0.982	0.51	19	57	0.003/0.516
	Condition (*FAST*)	−0.007294	−0.232649–0.218060	0.948				
	Condition (*SLOW*)	0.049297	−0.176058–0.274652	0.663				
(b). Aim 2: HbO ~ condition + Hemisphere + (1|participant) and HbO ~ condition + (1|participant)								
PFC	(Intercept)	0.091497	−0.006430–0.189424	0.067	0.34	20	801	0.011/0.345
	Condition (*FAST*)	0.033987	−0.014290–0.082264	0.167				
	Condition (*SLOW*)	0.000406	−0.047871–0.048683	0.987				
	Hemisphere (ipsi)	0.067867	0.027958–0.107776	*0.001**				
PMC	(Intercept)	0.048776	−0.059401–0.156953	0.376	0.38	20	636	0.007/0.383
	Condition (*FAST*)	0.069844	0.013942–0.125746	*0.014*				
	Condition (*SLOW*)	0.060211	0.004309–0.116113	*0.035*				
SMC	Intercept)	0.089338	−0.018620–0.197295	0.105	0.37	20	441	0.003/0.375
	Condition (*FAST*)	0.044168	−0.021419–0.109755	0.186				
	Condition (*SLOW*)	0.004477	−0.061110–0.070063	0.893				
PPC	(Intercept)	0.001145	−0.111003–0.113293	0.984	0.32	19	471	0.016/0.332
	Condition (*FAST*)	0.119288	0.048082–0.190495	*0.001**				
	Condition (*SLOW*)	0.077668	0.006462–0.148875	*0.033*				

Note: Predictors indicate the fixed effects levels within the variables in the model. Reference level was the *NORM* condition and the contralesional hemisphere, when applicable. Estimates indicate the difference between the reference level and the predictor level. Italic p-values indicate a significant difference at alpha of 0.05. *Indicates significant differences with $p \leq 0.0125$ (0.05/4: Bonferroni correction for four models). PFC = prefrontal cortex; PMC = premotor cortex; SMC = sensorimotor cortex; PPC = posterior parietal cortex; ipsi = ipsilesional hemisphere.

Table 3: Pearson's correlation results for Aim 3 with comparisons to between brain activation changes, gait speed modulation, and impairment.

Region of interest		Gait speed modulation				Impairment (Fugl-Meyer lower extremity)			
		NORM minus *SLOW*		*FAST* minus *NORM*		*NORM* minus *SLOW*		*FAST* minus *NORM*	
		r	*p*	*r*	*p*	*r*	*p*	*r*	*p*
Contralesional hemisphere	PFC	−0.222	0.360	0.402	0.079	0.009	0.969	0.323	0.165
	PMC	−0.326	0.173	−0.183	0.439	−0.006	0.981	−0.155	0.513
	SMC	−0.234	0.350	0.237	0.330	0.388	0.101	0.375	0.114
	PPC	−0.295	0.234	0.353	0.138	0.208	0.394	0.235	0.332
Ipsilesional hemisphere	PFC	−0.282	0.241	0.598	*0.005**	0.172	0.469	0.503	*0.024*
	PMC	−0.310	0.197	0.204	0.387	−0.118	0.620	0.250	0.287
	SMC	−0.104	0.682	0.201	0.410	−0.025	0.919	0.249	0.303
	PPC	−0.382	0.117	0.137	0.576	0.186	0.446	0.242	0.318

Note: Change in brain activation and gait speed modulations were calculated as a change from the *SLOW* to *NORM* condition and change from the *NORM* to *FAST* condition. Italic *p*-values indicate significant relationships with an alpha of 0.05. *Indicates significant relationships after Benjamini–Hochberg correction for multiple comparisons (using a false discovery rate of 5%). PFC = prefrontal cortex; PMC = premotor cortex; SMC = sensorimotor cortex; PPC = posterior parietal cortex.

online adjustments. The impact of a stroke on motor control and balance [48] may require these individuals to similarly activate PMC and PPC during both slow and fast walking—speeds they do not regularly walk at and, therefore, are more novel. Previous work has also suggested that PPC is important for gait adaptation [49, 50]. Both studies used a split-belt treadmill with healthy adults and showed involvement of the PPC by recording activation with electroencephalography [50] or suppressing the region with transcranial direct stimulation [49].

4.3. Ipsilesional PFC Activation Relates to Gait Speed Modulation and Impairment. The only significant correlation observed was with brain activation changes from *NORM* to *FAST* walking in ipsilesional PFC. Ipsilesional PFC activity was also overall higher compared to the contralesional side. PFC activity is often elevated when learning or performing a new task [51] or a complex task [52]. The complexity of walking at a different speed may require an increase in PFC whereby individuals who are able to perform the task better (i.e., greater gait speed modulation) and are less impaired (i.e., higher Fugl-Meyer scores) are able to increase PFC activation to a greater extent. PFC also plays an important role in regulating information relayed to various areas of the cortex, such as sensory information to the PPC [53]. Interestingly, we also showed the greatest PPC activation for *FAST* walking. Sauvage et al. [54], found increased PPC activation with their slow compared to fast leg movements and suggested that this was a result of a greater need for fine voluntary control requiring greater attention for selecting relevant sensory feedback. After stroke, sensory integration is often impaired and varies depending on the type of sensory information [53]. Impaired sensory integration may be observable through heightened PPC, indicating decreased overall efficiency, and an increased need for PFC to regulate the incoming sensory information for successful task performance.

Clinically, the results from our study indicate that PMC, PPC, and ipsilesional PFC may be important targets for noninvasive stimulation techniques such as repetitive transcranial magnetic stimulation or transcranial direct stimulation. Using these stimulation techniques to upregulate activity may help an individual gain the ability to modulate their gait speeds.

Data Availability

The imaging data in Excel format used to support the findings of this study have been deposited into Janice Eng's Dataverse on the Borealis Canadian Dataverse Repository.

Additional Points

Limitations. Our previous systematic review consolidating investigations of brain activation during walking in the stroke population [55] found 22 studies with an average of 13 participants in the studies. Although our sample size exceeded this average, we acknowledge that we were not powered to detect some smaller effects and our results are limited to our small sample size. In addition, a lack of a healthy older-adult group limits some of our interpretations of whether the results observed are attributed to the effect of stroke or aging. However, our hemisphere-dependent findings suggest that our results are not exclusively a product of aging and some stroke-specific compensations are needed when walking at different speeds.

We acknowledge that walking at different speeds, particularly for the *FAST* condition, may have introduced more motion artifacts compared to the slower speeds [56]. Unfortunately, we are not able to calculate the number of motion artifacts within each condition, however, upon visual inspection of the raw data motion artifacts were not more abundant during the *FAST* condition for the majority of participants. The exact speed of walking and the change in walking speed was not uniform across all participants. This was done intentionally to determine if the participants' ability to modulate their walking speed was related to their brain activity. As a result of the different walking speeds, we introduced more

variability and may have reduced the ability to detect brain activations. Future studies should investigate if brain activity changes are related to specific increases or decreases in gait speed.

Conflicts of Interest

The authors declare that they have no conflicts of interest.

Acknowledgments

University of British Columbia Four-Year Fellowship (SBL), Canadian Institute of Health Research (Fellowship for SBL and SP; Foundation Grant FND143340 to JJE), the Michael Smith Foundation for Health Research (SP), the Canada Research Chairs Program (JJE, TLA, LAB). and the Heart and Stroke Foundation Partnership for Stroke Recovery (Post-doc award to CLY).

Supplementary Materials

Table S1: individual participant demographics and performance details. Table S2: channel numbers associated with regions of interest and excluded channel due to lesion or preprocessing. Table S3: number of channels excluded by region. Table S4: results from Aim 1 and 2 for deoxyhemoglobin (HbR) results. Table S5: Pearson's correlation results for Aim 3 with comparisons to between brain activation changes, gait speed modulation, and impairment. (*Supplementary Materials*)

References

[1] M. Hösl, M. Egger, J. Bergmann, T. Amberger, F. Mueller, and K. Jahn, "Tempo-spatial gait adaptations in stroke patients when approaching and crossing an elevated surface," *Gait & Posture*, vol. 73, pp. 279–285, 2019.

[2] D. J. Geerse, M. Roerdink, J. Marinus, and J. J. van Hilten, "Walking adaptability for targeted fall-risk assessments," *Gait & Posture*, vol. 70, pp. 203–210, 2019.

[3] M. J. D. Caetano, S. R. Lord, M. A. Brodie et al., "Executive functioning, concern about falling and quadriceps strength mediate the relationship between impaired gait adaptability and fall risk in older people," *Gait & Posture*, vol. 59, pp. 188–192, 2018.

[4] I. Jonkers, S. Delp, and C. Patten, "Capacity to increase walking speed is limited by impaired hip and ankle power generation in lower functioning persons post-stroke," *Gait & Posture*, vol. 29, no. 1, pp. 129–137, 2009.

[5] K. B. Lee, S. H. Lim, E. H. Ko, Y. S. Kim, K. S. Lee, and B. Y. Hwang, "Factors related to community ambulation in patients with chronic stroke," *Topics in Stroke Rehabilitation*, vol. 22, no. 1, pp. 63–71, 2015.

[6] H. Y. Kim, E. J. Kim, and J. S. H. You, "Adaptive locomotor network activation during randomized walking speeds using functional near-infrared spectroscopy," *Technology and Health Care*, vol. 25, no. S1, pp. 93–98, 2017.

[7] T. Harada, I. Miyai, M. Suzuki, and K. Kubota, "Gait capacity affects cortical activation patterns related to speed control in the elderly," *Experimental Brain Research*, vol. 193, no. 3, pp. 445–454, 2009.

[8] D. C. Hinton, A. Thiel, J.-P. Soucy, L. Bouyer, and C. Paquette, "Adjusting gait step-by-step: brain activation during split-belt treadmill walking," *NeuroImage*, vol. 202, Article ID 116095, 2019.

[9] S. B. Lim, C.-L. Yang, S. Peters, T. Liu-Ambrose, L. A. Boyd, and J. J. Eng, "Phase-dependent brain activation of the frontal and parietal regions during walking after stroke—an fNIRS study," *Frontiers in Neurology*, vol. 13, Article ID 904722, 2022.

[10] A. R. Luft, L. Forrester, R. F. Macko et al., "Brain activation of lower extremity movement in chronically impaired stroke survivors," *NeuroImage*, vol. 26, no. 1, pp. 184–194, 2005.

[11] K. Bansal, D. J. Clark, E. J. Fox, C. Conroy, P. Freeborn, and D. K. Rose, "Spatiotemporal strategies adopted to walk at fast speed in high- and low-functioning individuals post-stroke: a cross-sectional study," *Topics in Stroke Rehabilitation*, vol. 30, no. 1, pp. 1–10, 2023.

[12] M. F. Folstein, S. E. Folstein, and P. R. McHugh, "Mini-mental state". A practical method for grading the cognitive state of patients for the clinician," *Journal of Psychiatric Research*, vol. 12, no. 3, pp. 189–198, 1975.

[13] L. A. Newkirk, J. M. Kim, J. M. Thompson, J. R. Tinklenberg, J. A. Yesavage, and J. L. Taylor, "Validation of a 26-point telephone version of the mini-mental state examination," *Journal of Geriatric Psychiatry and Neurology*, vol. 17, no. 2, pp. 81–87, 2004.

[14] J. Peirce, J. R. Gray, S. Simpson et al., "PsychoPy2: experiments in behavior made easy," *Behavior Research Methods*, vol. 51, no. 1, pp. 195–203, 2019.

[15] J. C. Menant, I. Maidan, L. Alcock et al., "A consensus guide to using functional near-infrared spectroscopy in posture and gait research," *Gait & Posture*, vol. 82, pp. 254–265, 2020.

[16] M. A. Yücel, A. Lühmann, F. Scholkmann et al., "Best practices for fNIRS publications," *Neurophotonics*, vol. 8, no. 1, Article ID 012101, 2021.

[17] M. Ferrari and V. Quaresima, "A brief review on the history of human functional near-infrared spectroscopy (fNIRS) development and fields of application," *NeuroImage*, vol. 63, no. 2, pp. 921–935, 2012.

[18] V. Quaresima and M. Ferrari, "A mini-review on functional near-infrared spectroscopy (fNIRS): where do we stand, and where should we go?" *Photonics*, vol. 6, no. 3, Article ID 87, 2019.

[19] C. Huo, G. Xu, W. Li et al., "A review on functional near-infrared spectroscopy and application in stroke rehabilitation," *Medicine in Novel Technology and Devices*, vol. 11, Article ID 100064, 2021.

[20] S. Brigadoi and R. J. Cooper, "How short is short? Optimum source–detector distance for short-separation channels in functional near-infrared spectroscopy," *Neurophotonics*, vol. 2, no. 2, Article ID 025005, 2015.

[21] S. B. Lim, S. Peters, C.-L. Yang, L. A. Boyd, T. Liu-Ambrose, and J. J. Eng, "Frontal, sensorimotor, and posterior parietal regions are involved in dual-task walking after stroke," *Frontiers in Neurology*, vol. 13, Article ID 904145, 2022.

[22] M. M. Plichta, M. J. Herrmann, C. G. Baehne et al., "Event-related functional near-infrared spectroscopy (fNIRS): are the measurements reliable?" *NeuroImage*, vol. 31, no. 1, pp. 116–124, 2006.

[23] G. Strangman, J. P. Culver, J. H. Thompson, and D. A. Boas, "A quantitative comparison of simultaneous BOLD fMRI and

NIRS recordings during functional brain activation," *NeuroImage*, vol. 17, no. 2, pp. 719–731, 2002.

[24] L. Pollonini, H. Bortfeld, and J. S. Oghalai, "PHOEBE: a method for real time mapping of optodes-scalp coupling in functional near-infrared spectroscopy," *Biomedical Optics Express*, vol. 7, no. 12, pp. 5104–5119, 2016.

[25] C. M. Aasted, M. A. Yücel, R. J. Cooper et al., "Anatomical guidance for functional near-infrared spectroscopy: AtlasViewer tutorial," *Neurophotonics*, vol. 2, no. 2, Article ID 020801, 2015.

[26] M. J. Hawrylycz, E. S. Lein, A. L. Guillozet-Bongaarts et al., "An anatomically comprehensive atlas of the adult human brain transcriptome," *Nature*, vol. 489, no. 7416, pp. 391–399, 2012.

[27] C. M. Lacadie, R. K. Fulbright, J. Arora, and R. T. Constable, "Papademetris Brodmann areas defined in MNI space using a new tracing tool in BioImage suite," in *Proceedings of the 14th Annual Meeting of the Organization for Human Brain Mapping*, Melbourne, Australia, 2008.

[28] A. R. Fugl-Meyer, L. Jääskö, I. Leyman, S. Olsson, and S. Steglind, "The post-stroke hemiplegic patient. 1. a method for evaluation of physical performance," *Journal of Rehabilitation Medicine*, vol. 7, no. 1, pp. 13–31, 1975.

[29] P. W. Duncan, M. Propst, and S. G. Nelson, "Reliability of the Fugl-Meyer assessment of sensorimotor recovery following cerebrovascular accident," *Physical Therapy*, vol. 63, no. 10, pp. 1606–1610, 1983.

[30] K. J. Sullivan, J. K. Tilson, S. Y. Cen et al., "Fugl-Meyer assessment of sensorimotor function standardized training procedure for clinical practice and clinical trials," *Stroke*, vol. 42, no. 2, pp. 427–432, 2011.

[31] G. Kwakkel, N. A. Lannin, K. Borschmann et al., "Standardized measurement of sensorimotor recovery in stroke trials: consensus-based core recommendations from the stroke recovery and rehabilitation roundtable," *International Journal of Stroke*, vol. 12, no. 5, pp. 451–461, 2017.

[32] T. J. Huppert, S. G. Diamond, M. A. Franceschini, and D. A. Boas, "HomER: a review of time-series analysis methods for near-infrared spectroscopy of the brain," *Applied Optics*, vol. 48, no. 10, pp. D280–D298, 2009.

[33] B. Molavi and G. A. Dumont, "Wavelet-based motion artifact removal for functional near-infrared spectroscopy," *Physiological Measurement*, vol. 33, no. 2, pp. 259–270, 2012.

[34] L. M. Hocke, I. K. Oni, C. C. Duszynski, A. V. Corrigan, B. D. Frederick, and J. F. Dunn, "Automated processing of fNIRS data—a visual guide to the pitfalls and consequences," *Algorithms*, vol. 11, no. 5, Article ID 67, 2018.

[35] Y.-C. Liu, Y.-R. Yang, Y.-A. Tsai, C.-F. Lu, and R.-Y. Wang, "Brain activation and gait alteration during cognitive and motor dual task walking in stroke—a functional near-infrared spectroscopy study," *IEEE Transactions on Neural Systems and Rehabilitation Engineering*, vol. 26, no. 12, pp. 2416–2423, 2018.

[36] S. Peters, S. B. Lim, D. R. Louie, C.-L. Yang, and J. J. Eng, "Passive, yet not inactive: robotic exoskeleton walking increases cortical activation dependent on task," *Journal of NeuroEngineering and Rehabilitation*, vol. 17, no. 1, Article ID 107, 2020.

[37] L. Kocsis, P. Herman, and A. Eke, "The modified Beer–Lambert law revisited," *Physics in Medicine and Biology*, vol. 51, no. 5, pp. N91–N98, 2006.

[38] A. Sassaroli and S. Fantini, "Comment on the modified Beer–Lambert law for scattering media," *Physics in Medicine and Biology*, vol. 49, no. 14, pp. N255–N257, 2004.

[39] J. C. Ye, S. Tak, K. E. Jang, J. Jung, and J. Jang, "NIRS-SPM: statistical parametric mapping for near-infrared spectroscopy," *NeuroImage*, vol. 44, no. 2, pp. 428–447, 2009.

[40] C. M. Aasted, M. A. Yücel, S. C. Steele et al., "Frontal lobe hemodynamic responses to painful stimulation: a potential brain marker of nociception," *PLoS One*, vol. 11, no. 11, Article ID e0165226, 2016.

[41] M. A. Yücel, J. Selb, C. M. Aasted et al., "Mayer waves reduce the accuracy of estimated hemodynamic response functions in functional near-infrared spectroscopy," *Biomedical Optics Express*, vol. 7, no. 8, pp. 3078–3088, 2016.

[42] L. Gagnon, R. J. Cooper, M. A. Yücel, K. L. Perdue, D. N. Greve, and D. A. Boas, "Short separation channel location impacts the performance of short channel regression in NIRS," *NeuroImage*, vol. 59, no. 3, pp. 2518–2528, 2012.

[43] M. A. Yücel, C. M. Aasted, M. P. Petkov, D. Borsook, D. A. Boas, and L. Becerra, "Specificity of hemodynamic brain responses to painful stimuli: a functional near-infrared spectroscopy study," *Scientific Reports*, vol. 5, no. 1, Article ID 9469, 2015.

[44] M. A. Yücel, J. Selb, C. M. Aasted et al., "Short separation regression improves statistical significance and better localizes the hemodynamic response obtained by near-infrared spectroscopy for tasks with differing autonomic responses," *Neurophotonics*, vol. 2, no. 3, Article ID 035005, 2015.

[45] M. L. Seghier, "Laterality index in functional MRI: methodological issues," *Magnetic Resonance Imaging*, vol. 26, no. 5, pp. 594–601, 2008.

[46] S. Yazawa Ikeda, T. Kunieda, S. Ohara et al., "Cognitive motor control in human pre-supplementary motor area studied by subdural recording of discrimination/selection-related potentials," *Brain*, vol. 122, no. 5, pp. 915–931, 1999.

[47] M. Weinrich and S. P. Wise, "The premotor cortex of the monkey," *Journal of Neuroscience*, vol. 2, no. 9, pp. 1329–1345, 1982.

[48] M. Roerdink, A. C. H. Geurts, M. de Haart, and P. J. Beek, "On the relative contribution of the paretic leg to the control of posture after stroke," *Neurorehabilitation and Neural Repair*, vol. 23, no. 3, pp. 267–274, 2009.

[49] D. R. Young, P. J. Parikh, and C. S. Layne, "The posterior parietal cortex is involved in gait adaptation: a bilateral transcranial direct current stimulation study," *Frontiers in Human Neuroscience*, vol. 14, Article ID 581026, 2020.

[50] T. C. Bulea, J. Kim, D. L. Damiano, C. J. Stanley, and H.-S. Park, "Park prefrontal, posterior parietal and sensorimotor network activity underlying speed control during walking," *Frontiers in Human Neuroscience*, vol. 9, Article ID 247, 2015.

[51] P. A. Reuter-Lorenz and D. C. Park, "Human neuroscience and the aging mind: a new look at old problems," *The Journals of Gerontology Series B: Psychological Sciences and Social Sciences*, vol. 65, no. 4, pp. 405–415, 2010.

[52] A. M. C. Kelly and H. Garavan, "Human functional neuroimaging of brain changes associated with practice," *Cerebral Cortex*, vol. 15, no. 8, pp. 1089–1102, 2005.

[53] K. E. Brown, J. L. Neva, S. J. Feldman, W. R. Staines, and L. A. Boyd, "Sensorimotor integration in chronic stroke: baseline differences and response to sensory training," *Restorative Neurology and Neuroscience*, vol. 36, no. 2, pp. 245–259, 2018.

[54] C. Sauvage, P. Jissendi, S. Seignan, M. Manto, and C. Habas, "Brain areas involved in the control of speed during a motor sequence of the foot: real movement versus mental imagery," *Journal of Neuroradiology*, vol. 40, no. 4, pp. 267–280, 2013.

[55] S. B. Lim, D. R. Louie, S. Peters, T. Liu-Ambrose, L. A. Boyd, and J. J. Eng, "Brain activity during real-time walking and with walking interventions after stroke: a systematic review," *Journal of NeuroEngineering and Rehabilitation*, vol. 18, no. 1, Article ID 8, 2021.

[56] R. Vitorio, S. Stuart, L. Rochester, L. Alcock, and A. Pantall, "fNIRS response during walking—artefact or cortical activity? A systematic review," *Neuroscience & Biobehavioral Reviews*, vol. 83, pp. 160–172, 2017.

Hindawi
Neural Plasticity
Volume 2023, Article ID 8510213, 14 pages
https://doi.org/10.1155/2023/8510213

Research Article

Acupuncture Alters Brain's Dynamic Functional Network Connectivity in Stroke Patients with Motor Dysfunction: A Randomised Controlled Neuroimaging Trial

Yahui Wang,[1,2] **Mengxin Lu**,[1] **Ruoyi Liu**,[1] **Liping Wang**,[1] **Yue Wang**,[3] **Lingling Xu**,[1] **Kang Wu**,[1] **Chen Chen**,[1] **Tianzhu Chen**,[1] **Xinyue Shi**,[1] **Kuangshi Li**,[1] **and Yihuai Zou**[1]

[1]*Department of Neurology, Dongzhimen Hospital, Beijing University of Chinese Medicine, Beijing, China*
[2]*Department of Rehabilitation Medicine, Beijing Tsinghua Changgung Hospital, School of Clinical Medicine, Tsinghua University, Beijing, China*
[3]*China-Japan Friendship Hospital, Beijing, China*

Correspondence should be addressed to Yihuai Zou; zouyihuai2004@163.com

Received 19 October 2022; Revised 19 March 2023; Accepted 25 May 2023; Published 20 June 2023

Academic Editor: Xi-Ze Jia

Objectives. Neuroimaging studies have confirmed that acupuncture can promote static functional reorganization in poststroke patients with motor dysfunction. But its effect on dynamic brain networks remains unclear. This study is aimed at investigating how acupuncture affected the brain's dynamic functional network connectivity (dFNC) after ischemic stroke. *Methods*. We conducted a single-center, randomised controlled neuroimaging study in ischemic stroke patients. A total of 53 patients were randomly divided into the true acupoint treatment group (TATG) and the sham acupoint treatment group (SATG) at a ratio of 2 : 1. Clinical assessments and magnetic resonance imaging (MRI) scans were performed on subjects before and after treatment. We used dFNC analysis to estimate distinct dynamic connectivity states. Then, the temporal properties and strength of functional connectivity (FC) matrix were compared within and between the two groups. The correlation analysis between dynamic characteristics and clinical scales was also calculated. *Results*. All functional network connectivity (FNC) matrices were clustered into 3 connectivity states. After treatment, the TATG group showed a reduced mean dwell time and found attenuated FC between the sensorimotor network (SMN) and the frontoparietal network (FPN) in state 3, which was a sparsely connected state. The FC between the dorsal attention network (DAN) and the default mode network (DMN) was higher after treatment in the TATG group in state 1, which was a relative segregated state. The SATG group preferred to increase the mean dwell time and FC within FPN in state 2, which displayed a local tightly connected state. In addition, we found that the FC value increased between DAN and right frontoparietal network (RFPN) in state 1 in the TATG group after treatment compared to the SATG group. Correlation analyses before treatment showed that the Fugl-Meyer Assessment (FMA) lower score was negatively correlated with the mean dwell time in state 3. FMA score showed positive correlation with FC in RFPN-SMN in state 3. FMA-lower score was positively correlated with FC in DAN-DMN and DAN-RFPN in state 1. *Conclusions*. Acupuncture has the potential to modulate abnormal temporal properties and promote the balance of separation and integration of brain function. True acupoint stimulation may have a more positive effect on regulating the brain's dynamic function. *Clinical Trial Registration*. This trial is registered with Chinese Clinical Trials Registry (ChiCTR1800016263).

1. Introduction

Stroke remains the second leading cause of death and the third leading cause of disability worldwide, according to the latest Global Burden of Disease study [1]. In China, ischemic stroke is the leading cause of mortality and disability, resulting in an increasing annual disease burden [2]. Motor dysfunction is the most common symptom of ischemic stroke, with more than 70% of stroke survivors suffering from a varying degree of motor dysfunction [3]. Rehabilitation services, which promote spontaneous neurological recovery and experience-dependent plasticity, are the primary approaches

for promoting functional recovery and independence of patients with stroke [4–6].

Acupuncture, as a vital part of Traditional Chinese Medicine, has gained increasing acceptance worldwide and has been applied in different forms to treat diseases in more than 180 countries around the world [7–10]. In China, acupuncture is widely used in the treatment of stroke patients with motor dysfunction [11]. American Heart Association/American Stroke Association Guideline also indicated that facilitating acupuncture may be effective as an adjunctive treatment for motor recovery and walking mobility [6]. Of note, *Shou Zu Shi Er Zhen* is the representative needling prescription in China for the treatment of poststroke patients with motor dysfunction, and its effectiveness has been identified by several randomised clinical trials [12–15]. However, its underlying mechanism remains unclear.

As a noninvasive neuroimaging technology, functional magnetic resonance imaging (fMRI) lays the foundation for real-time measurement of whole-brain activity and helps advance the understanding of neuroplasticity modulated by acupuncture [16, 17]. Neuroimaging evidence has demonstrated the facilitating effect of acupuncture in the regulation of brain functional reorganization, comprising activation of motor-related cortical areas [18–20], increasing motor-cognition connectivity and decreasing compensation of contralesional motor cortex, and modulating effective connectivity of resting-state networks in patients with post-stroke hemiplegia [21, 22]. However, these studies mainly focus on instant acupuncture effects. Our previous work provided evidence for long-term acupuncture intervention effects using the voxel-mirrored homotopic connectivity method. We confirmed that *Shou Zu Shi Er Zhen* acupuncture prescription can integrate information among motor, vision, hearing processing, and cognitive brain regions, thereby promoting motor function recovery [23].

Despite such progress, the assessment of brain function is still limited by an assumption that the brain activity is constant throughout recording periods in resting state [24]. Recent studies have confirmed the time-varying properties of functional brain networks [25, 26]. Dynamic functional network connectivity (dFNC), which combines independent component analysis and sliding window approach, reflects temporal variations in functional network connectivity at much faster timescales (seconds-minutes) [24, 25]. Several studies have confirmed that acupuncture can affect the brain's dynamic functional connectivity (FC), such as decreasing temporal variability in chronic tinnitus and regulating dynamic alterations of brain activity in migraine patients [27, 28]. So far, no study has shown the acupuncture effect on dFNC in stroke patients. However, there is evidence suggesting that the brain's preference for distinct dynamic connection patterns was altered after ischemic stroke, and the specific patterns may be critical for neurological function recovery [29].

Therefore, the goal of the present study was to investigate how acupuncture affected the brain's dynamic connections following ischemic stroke based on dFNC analysis. We hypothesized that acupuncture might modulate dynamic properties of brain functional networks in poststroke patients, while true acupoint stimulation has a more positive effect.

2. Materials and Methods

2.1. Study Design. This was a single-center, randomised controlled neuroimaging study, with patients and assessors blinded for group allocation. According to the order of admission, the stroke patients were randomly divided into the true acupoint treatment group (TATG) and the sham acupoint treatment group (SATG) at a ratio of 2 : 1 using a random number table. Based on conventional treatment, the TATG group received *Shou Zu Shi Er Zhen* acupuncture treatment, while the SATG group received sham acupuncture treatment. All patients were evaluated using clinical scales and underwent MRI scan before and after acupuncture treatment. The trial was registered in the Chinese Clinical Trial Registry (Registration number: ChiCTR 1800016263). The study protocol had been published previously [30].

2.2. Participants. A total of 53 patients who matched the selection criteria were recruited from Dongzhimen Hospital affiliated to Beijing University of Chinese Medicine (Beijing, China) from March 2018 to December 2021. The inclusion criteria were as follows: (1) patients with ischemic stroke; (2) within 6 weeks from onset; (3) single lesion of ischemic infarct restricted to the unilateral hemisphere involving the internal capsule, basal ganglia, corona radiata, and its neighboring regions; (4) right-handed before stroke; (5) 35-80 years of age; (6) consciousness and stable condition; (7) not taken any psychiatric medications in 1 month. The exclusion criteria were as follows: (1) severe primary diseases of heart, liver, kidneys, hematologic system, immune system disease, tumors, and psychiatric disorders; (2) pregnant or lactating women; (3) any MRI contraindications; (4) any brain abnormalities except infarction identified by MRI. Seven patients did not complete the second MRI scan for personal reasons, and six patients were excluded due to severe head motion during scanning. Therefore, a total of 40 patients were included in the final analysis. Figure 1 shows the flow chart of this study.

2.3. Interventions. Ande brand disposable acupuncture needles (size 0.25×40 mm) were used. Patients in the TATG group received *Shou Zu Shi Er Zhen* acupuncture treatment, which consist of bilateral Hegu (LI4), Quchi (LI11), Neiguan (PC6), Zusanli (ST36), Yanglingquan (GB34), and Sanyinjiao (SP6). After skin disinfection, acupuncture needles were inserted vertically into the skin to a depth of 20-30 mm. Following needle insertion, acupuncture manipulations of twirling and lifting were conducted on all needles to allow patients to obtain *De qi*, a combination of sensations including soreness, dullness, numbness, heaviness, and other feelings [31]. It was believed to play an important role in acupuncture efficacy. Needles were kept in situ for 30 minutes. The patients received five treatment sessions per week for 2 weeks (10 sessions in total). Patients in the SATG group received sham acupuncture treatment. The location of sham acupoints was referred to the method published in JAMA by Liu et al., with 20 mm beside the true acupoints [32]. The location of all acupoints is shown in Supplementary Material 1. We would avoid *De qi* sensations in the manipulation in the SATG group. Besides that, other treatment procedures were

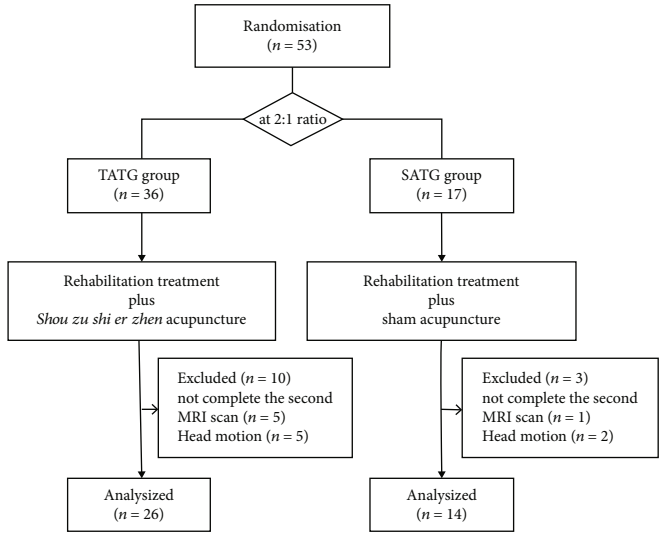

Figure 1: The study flow chart.

the same as the TATG group. And all the patients received routine medication and rehabilitation treatment.

2.4. Clinical Assessments. We used the National Institutes of Health Stroke Scale (NIHSS) to assess the severity of neurological deficit and the Fugl-Meyer Assessment (FMA) to evaluate the motor function at baseline and after the acupuncture treatment. SPSS 20 was applied for statistical analysis. Paired samples t-test was used for within-group comparisons. Independent sample t-test was used to compare the difference between the two groups. Statistical significance was set at $P < 0.05$.

2.5. MRI Data Acquisition. All MRI data were acquired from a 3.0 Tesla scanner (Siemens, Sonata, Germany) at Dongzhimen Hospital, Beijing, China. The parameters of gradient echoplanar imaging (EPI) were as follows: echo time (TE) = 30 ms, repetition time (TR) = 2000 ms, matrix = 64 × 64, field of vision (FOV) = 225 mm × 225 mm, slice thickness = 3.5 mm, and flip angle (FA) = 90°. The functional scan lasted for 6 minutes, and 179 image volumes were obtained. And the T1-weighted imaging (T1WI) scan lasted for 4 minutes and 10 seconds, with the following parameters: TE = 2.53 ms, TR = 1900 ms, matrix = 256 × 256, FOV = 250 mm × 250 mm, slice thickness = 1.0 mm, and FA = 9°.

2.6. Preprocessing of fMRI Data. The resting-state fMRI data were preprocessed using DPABI software [33] in MATLAB (version R2018a, MathWorks, Inc., Natick, MA, USA). For the left hemispheric lesions ($n = 18$), the functional images were flipped along the midsagittal plane in order to reduce the spatial heterogeneity of lesions. Thus, all lesions were located on the right hemisphere. The probability map and detailed information of the lesion location in each patient are shown in Supplementary Material 1. The first 10 time points were removed to stabilize MRI signal and remained 169 volumes. Then, the remaining volumes were slice-timing corrected to correct time differences between slices. Head motion correction was performed, and the patients were excluded when the maximum translation exceeded 3 mm and rotational parameters exceeded 3 degrees in any direction. Next functional images were normalized to the standard Montreal Neurological Institute space by using T1 image unified segmentation, resliced into $3 \times 3 \times 3\ mm^3$. Afterward, images were smoothed using a Gaussian kernel with a 4 mm full width at half maximum, regressed with 24-parameter regression, white matter, and cerebrospinal fluid signal. Finally, the data were bandpass filtered with 0.01-0.1 Hz. Global signal regression was not performed.

2.7. Intrinsic Connectivity Networks. For all preprocessing data, spatial independent component analysis (ICA) was carried out to identify intrinsic connectivity network independent components (ICs) using the Group ICA Toolbox (GIFT version 4.0b, http://icatb.sourceforge.net). Firstly, the number of ICs was automatically estimated from the imaging data of all the patient, and 56 ICs were obtained. Following that, the principal component analysis was performed to reduce dimensionality. Secondly, Group ICA was conducted using the infomax algorithm to extract independent spatial maps and time courses of each component [34]. Lastly, the back-reconstruction [35] and Fisher's z-transformation were performed for each independent component of the subjects so that the transformed data approximately obeyed a normal distribution with standard deviation of the mean. Multiple regression analysis was applied to analyze the spatial correlation between the extracted components and the resting brain network templates [36]. The IC selection referred to previous criteria [37]: (1) peak coordinates of ICs located primarily in the gray matter; (2) almost no spatial overlap with blood vessels, ventricles, and suspicious artifacts; (3) dominated by low-frequency signals (<0.1 Hz). Following these steps, 11 ICs were kept for further analysis and arranged into different functional networks, including the default mode network (DMN), sensorimotor network (SMN), dorsal attention network (DAN), left frontoparietal network (LFPN), and right frontoparietal network (RFPN). And then, we performed

the following postprocessing steps on the time courses of 11 ICs: (1) detrending linear, quadratic, and cubic trends; (2) removing spikes; (3) low-pass filtering with a cut-off frequency of 0.15 Hz. To estimate functional network connectivity, Pearson's correlations were performed using postprocessed time courses between ICs throughout the whole scanning and then converted to z values using Fisher's z-transformation to improve the normality [25, 38].

2.8. Dynamic Functional Network Connectivity

2.8.1. Sliding Window Analysis. Sliding window analysis, the most common method in dFNC analysis, was used to construct brain functional network in GIFT toolbox. Previous studies had confirmed that the window length of 20-30 TR can better reflect the dynamic characteristics of the brain [39, 40]. Thus, we selected a window length of 20TR, in step of 1TR, computing 149 individual windows. These time windows were convolved with a Gaussian value of $\sigma = 3$ TRs and computed via the L1-regularized precision matrix. To obtain z values and stabilize variance for further analyses, Fisher's z-transformation was applied to the functional connectivity matrices.

2.8.2. Clustering Analysis. Based on the windowed functional connectivity matrices of all participants, a k-means clustering algorithm was applied to detect reoccurring FC patterns. We used the city-block distance with 500 iterations and 150 replicates to assess the similarity between all time windows. The optimal number of clustering states was estimated by the elbow criterion. The number was determined to be 3, which meant 3 FC states, exhibiting different FC patterns.

2.8.3. Temporal Properties and Connectivity Strength of Dynamics States. Three parameters were measured to assess the temporal properties of FNC: (1) fraction time (the frequency of each state); (2) mean dwell time (the average time a subject spent in any state without converting to another state); (3) number of transitions (switching times between different states). Besides, the connectivity strength of 3 states within the TATG group and the SATG group was also calculated. Analysis of covariance (ANCOVA) was used to compare the mean changes from before treatment to after treatment between groups. Disease duration and lesion volume were taken as covariates. And paired samples t-test was adopted to compare the changes before and after treatment in each group. The P value for the above analysis was set to 0.05 and corrected for false discovery rate (FDR) correction.

2.9. Correlation Analysis. Pearson's correlation was carried out to assess the relationship between clinical characteristics and dFNC parameters at baseline in all subjects, as well as FC values showing significant changes in any state before and after treatment (level of significance: $P < 0.05$).

2.10. Validation Analysis. We used different sliding window lengths and number of clusters to verify the stability of our results. The numbers of clusters were set at 4 and 5, and the sliding window lengths were set at 22TRs and 30TRs (detailed information in Supplementary Material 2).

3. Results

3.1. Demographic Characteristics. A total of 40 patients completed the whole study, including 26 patients in the TATG group and 14 patients in the SATG group. There was no significant difference in age, gender, and duration of disease between the TATG group and the SATG group ($P > 0.05$). The detailed data is presented in Table 1.

3.2. Clinical Information. For the clinical data, no statistical differences were observed in NIHSS and FMA scores pretreatment and posttreatment between the two groups (all $P > 0.05$). Intragroup comparisons showed that FMA-lower score, FMA total score, and NIHSS score improved after treatment compared with those before treatment in both the TATG group and the SATG group (all $P < 0.05$). In addition, the FMA-upper score increased after treatment in the TATG group ($P < 0.05$), while this result was not found in the SATG group ($P > 0.05$). The clinical information was provided in Table 2.

3.3. Intrinsic Connectivity Networks and Dynamic Functional Connectivity States. We identified five resting-state networks from the 11 ICs, including the default mode network (DMN: ICs 51, 56), the sensorimotor network (SMN: ICs 41, 48), the dorsal attention network (DAN: ICs 16, 27), the left frontoparietal network (LFPN: ICs 1, 53), and the right frontoparietal network (RFPN: ICs 12, 45, 50). Spatial maps of 11 ICs are shown in Figure 2. All FNC matrices were clustered into 3 connectivity states. State 1 presented a relatively complicated connectivity pattern, which was characterized by partly strong positive connections within networks (such as DMN and DAN) and predominantly negative and neutral internetwork connections (between DAN and LFPN, between SMN and other networks, etc.), along with less positive connections (between FPN and DMN). Therefore, we referred to this state as the relative segregated state. The overall frequency of state 1 accounted for 23.22% of all time windows. State 2 seemed to display a more densely intranetwork connection, especially in FPN. We called it the local tightly connected state. The frequency of state 2 was lower than state 1 at 19.60%. State 3 had the longest time window percentage of 57.18%. This state exhibited sparse intra-/internetwork connectivity, which meant no high positive or negative connections within or between networks. And we called this the sparsely connected state. All states are shown in Figure 3.

3.4. Temporal Properties. There were no statistical differences observed between the two groups in mean change of fraction time, mean dwell time, and number of transitions. The detailed results are listed in Table 3. The TATG group showed a significantly shorter mean dwell time in state 3 after treatment than that before treatment ($P < 0.05$, FDR correction), while the SATG group revealed a longer mean dwell time in state 2 after treatment ($P < 0.05$, FDR correction). Detailed information are shown in Table 4 and Figure 4.

Table 1: Demographic features of stroke patients.

	The TATG group ($n = 26$)	The SATG group ($n = 14$)	P value
Sex (male/female)	18/8	10/4	0.885
Age (years)	59.38 ± 11.61	59.14 ± 8.77	0.946
Disease duration (days)	15.89 ± 20.70	20.07 ± 15.34	0.831
Lesion side (left/right)	12/14	6/8	0.842
Lesion volume (ml)	2.96 ± 2.85	4.75 ± 3.97	0.127

Values were expressed as mean ± standard deviation. TATG: true acupuncture treatment group; SATG: sham acupuncture treatment group. The chi-square test was used to compare the distribution of sex and lesion side between the two groups.

Table 2: Clinical assessment before and after treatment in the two groups.

Clinical scales	The TATG group			The SATG group		
	Before treatment	After treatment	P value	Before treatment	After treatment	P value
FMA-UE	41.23 ± 23.87	46.42 ± 22.57	<0.0001*	45.50 ± 24.49	49.42 ± 23.39	0.058
FMA-LE	27.50 ± 7.58	30.19 ± 5.06	<0.0001*	27.64 ± 7.08	30.64 ± 4.49	0.013*
FMA	68.73 ± 37.38	76.61 ± 25.65	<0.0001*	73.14 ± 30.71	80.07 ± 27.56	0.016*
NIHSS	3.46 ± 2.42	2.46 ± 2.24	<0.0001*	3.64 ± 3.24	2.50 ± 3.05	0.002*

Values were expressed as mean ± standard deviation. TATG: true acupuncture treatment group; SATG: sham acupuncture treatment group. FMA: Fugl-Meyer. FMA-UE: FMA for the upper extremity. FMA-LE: FMA for the lower extremity. NIHSS: National Institute of Health Stroke Scale. The P value represents the difference before and after treatment in the TATG group or the SATG group. * represents $P < 0.05$.

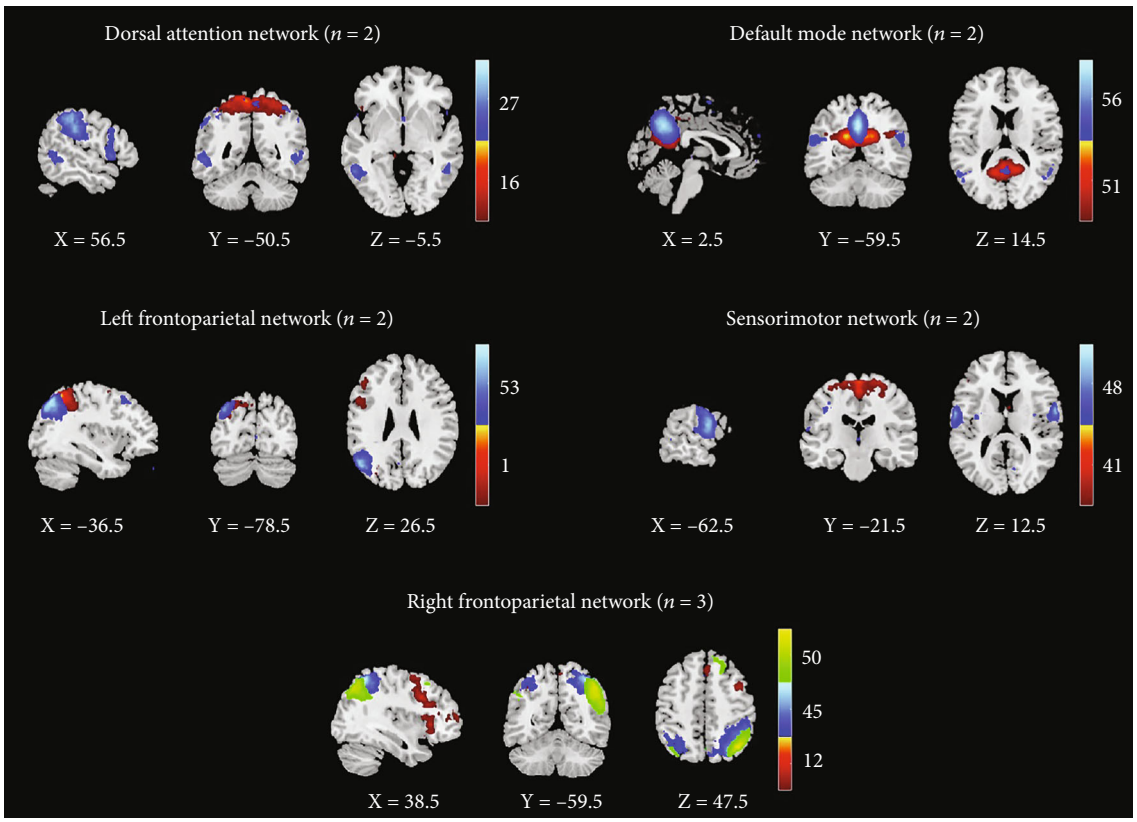

Figure 2: Spatial maps of all 11 independent components. They were assigned to 5 networks: the default mode network, the sensorimotor network, the dorsal attention network, the left frontoparietal network, and the right frontoparietal network. Different color represents the location of independent component of the peak point in each network.

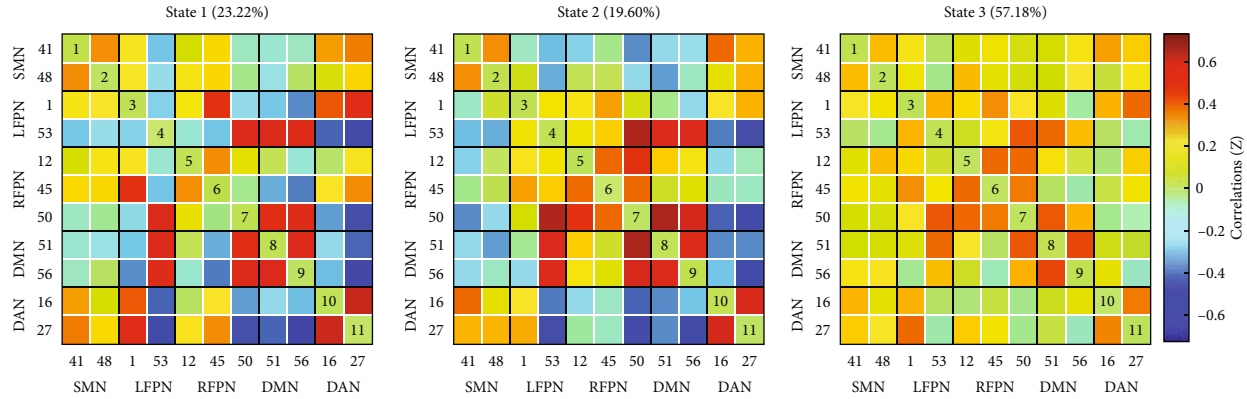

Figure 3: Three different dynamic functional connectivity states. Each matrix represents a stable connectivity state within the data. The percentage of occurrences in each state is also listed. The warm color indicates stronger positive connectivity, and the cold color implies stronger negative connectivity.

3.5. Strength of Dynamics States. We analyzed the alterations of FC within and between groups for each state. The TATG group showed increased FC between DAN and DMN in state 1 and reduced FC between RFPN and SMN in state 2 and FPN and SMN in state 3 after treatment (all $P < 0.05$). The SATG group had elevated FC in FPN (between LFPN and RFPN, within RFPN) in state 2 after treatment ($P < 0.05$).

Group difference showed positive effect between DAN and RFPN in state 1 ($P < 0.05$), which means increased FC between DAN and RFPN in state 1 in the TATG group compared to the SATG group. Altered connectivity pairs are shown in Figure 5.

3.6. Correlation between Clinical Measures and dFNC Parameters. Correlation analyses were carried out to detect whether dFNC parameters were related to clinical characteristics. The mean dwell time was negatively correlated with FMA-lower score in state 3 ($r = -0.266$, $P = 0.049$). We speculate that better motor recovery may be associated with short time spent in state 3 to some extent. We also found a negative correlation trend between mean dwell time and NIHSS score in state 1 ($r = -0.236$, $P = 0.071$). In addition, FMA score showed positive correlation with FC in RFPN-SMN in state 3 ($r = 0.331$, $P = 0.037$). FMA-lower score was positively correlated with FC in DAN-DMN and DAN-RFPN in state 1 ($r = 0.405$, $P = 0.016$ and $r = 0.394$, $P = 0.012$) (see in Figure 6).

3.7. Validation Analysis. Due to the different settings of dynamic analysis parameters, the results are different to some extent. But most of our main results were well replicated when using different parameters. These observations indicated that acupuncture can indeed improve the abnormal temporal properties and functional network connectivity in stroke patients. One interesting finding was that the number of transitions significantly increased after treatment in the TATG group when the number of clusters $k = 3$ and the length of sliding time windows $W = 22$TRs. Previous studies reported that such variability may lead to greater cognitive and behavioral flexibility [41, 42]. Thus, we speculated that true acupuncture has the potential to improve the brain's flexibility.

4. Discussion

4.1. Acupuncture Improves Motor Function in Stroke Patients with Hemiplegia. From Traditional Chinese Medicine, *Shou Zu Shi Er Zhen* has the effect of harmonizing qi and blood, balancing yin and yang, harmonizing the spleen and stomach, and regulating body constituent and spirit [30, 43]. Current evidence suggested that conventional treatment combined with *Shou Zu Shi Er Zhen* therapy is more effective in improving FMA score and lowering NIHSS score compared to conventional treatment in patients with post-stroke hemiplegia, exerting the effectiveness of acupuncture [13–15]. In this study, we found significant improvements in the FMA score (FMA-upper, FMA-lower, and FMA total) and NIHSS score in the TATG group after treatment, which is in accordance with previous studies.

4.2. Acupuncture Alters Brain's Dynamic Functional Network Connectivity. After treatment, the TATG group showed a reduced mean dwell time in state 3, as manifested sparse connections within and between brain functional networks. Previous studies demonstrated that such weakly connected state resembled stationary functional connectivity, representing the average of a great number of additional states that were infrequent to be separated or insufficiently distinct [25]. Furthermore, recent studies suggested that a significantly longer mean dwell time of this weakly connected state was observed in stroke patients compared to healthy individuals and may prevent the recovery of neurological function [29, 44–46]. With disease remission, the mean dwell time in weakly state decreases and tends to normal time [44]. Our correlation analysis revealed that the motor dysfunction improved with a reduction of mean dwell time in state 3. The stroke patients who received *Shou Zu Shi Er Zhen* treatment displayed a significant decrease in mean dwell time in state 3, indicating the positive effects of acupuncture in ameliorating the abnormal temporal properties. One study considered that a weakly connected pattern was more likely

Table 3: Comparison in temporal properties between the two groups.

	Fraction time (%)			Mean dwell time (TR)			Number of transitions
	State 1	State 2	State 3	State 1	State 2	State 3	
Mean difference (TATG-SATG)	4.900	-4.200	-0.600	1.919	-2.966	-6.886	1.503
95% confidence interval (lower bound, upper bound)	-10.50020.200	-17.500 9.000	-15.300, 14.000	-6.391, 10.230	-10.107, 4.175	-31.153, 17.380	-1.335, 4340
F	0.417	0.428	0.008	0.221	0.716	0.334	1.164
P	0.523	0.518	0.931	0.641	0.404	0.567	0.289

TATG: true acupuncture treatment group; SATG: sham acupuncture treatment group.

Table 4: Comparison in temporal properties within the two groups.

		Fraction time (%)			Mean dwell time (TR)			Number of transitions
		State 1	State 2	State 3	State 1	State 2	State 3	
The TATG group	Before treatment	24.08 ± 19.70	21.73 ± 21.51	54.18 ± 29.54	12.38 ± 8.54	11.06 ± 9.55	35.08 ± 38.59	6.92 ± 3.42
	After treatment	28.55 ± 15.55	24.96 ± 15.71	46.49 ± 15.94	14.61 ± 6.88	14.25 ± 9.03	21.35 ± 10.97	8.11 ± 2.59
	t	-1.133	-0.805	1.716	-1.068	-1.456	2.096	-1.563
	P	0.268	0.428	0.098	0.296	0.158	0.046*	0.131
The SATG group	Before treatment	21.62 ± 21.92	15.63 ± 18.23	62.75 ± 28.28	11.39 ± 10.63	8.74 ± 10.70	44.37 ± 46.14	6.5 ± 3.83
	After treatment	22.82 ± 19.67	23.30 ± 23.09	53.88 ± 23.96	12.42 ± 8.53	15.14 ± 15.60	33.50 ± 36.39	6.5 ± 3.27
	t	-0.189	-1.588	1.622	-0.296	-2.313	1.113	0
	P	0.853	0.136	0.129	0.772	0.038*	0.286	1

Values were expressed as mean ± standard deviation. TATG: true acupuncture treatment group; SATG: sham acupuncture treatment group. The P value represents the difference before and after treatment in the TATG group or the SATG group. * represents $P < 0.05$.

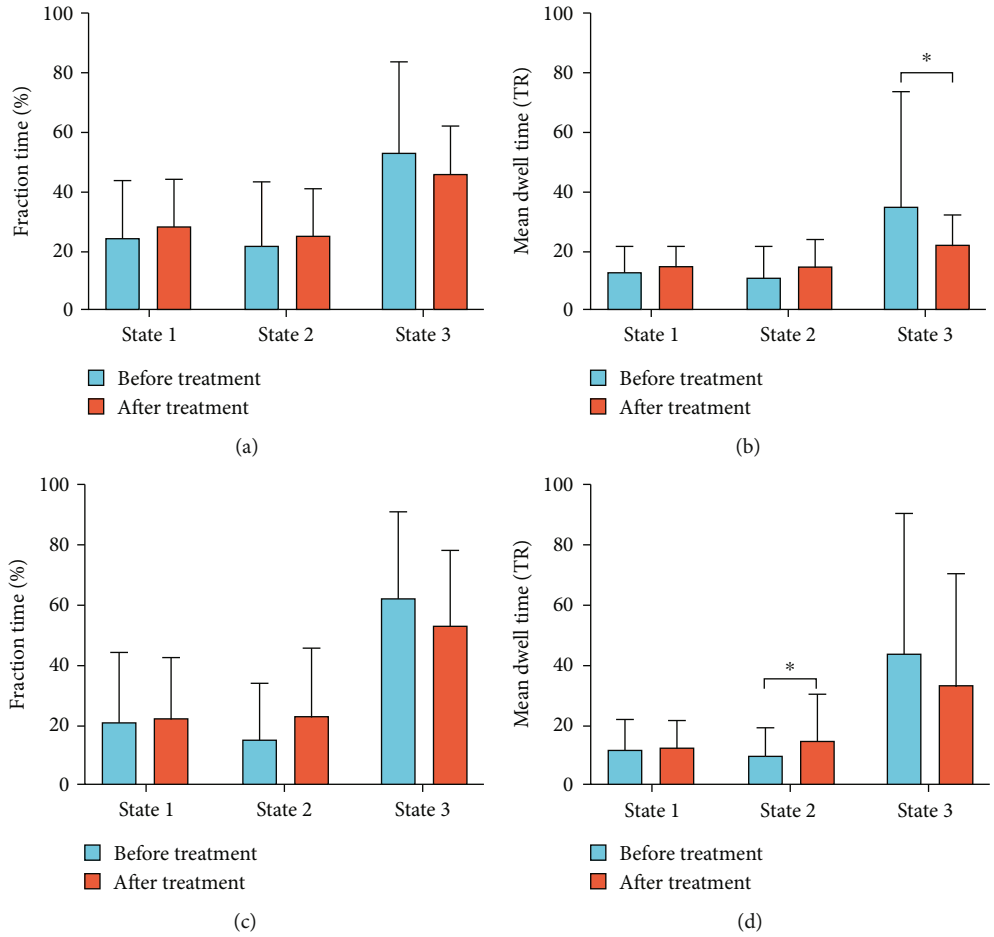

Figure 4: Changes in dynamic properties before and after treatment in the TATG group and the SATG group. (a) Change in fraction time before and after treatment in the TATG group. (b) Change in mean dwell time before and after treatment in the TATG group. (c) Change in fraction time before and after treatment in the SATG group. (d) Change in mean dwell time before and after treatment in the SATG group. TATG: true acupuncture treatment group. SATG: sham acupuncture treatment group. * represents $P < 0.05$.

to be altered and converted to another connection pattern or to construct a new function matrix [29]. Hence, we speculate that acupuncture has the potential to enhance such alteration and promote abnormal whole-brain functional connectivity toward normal patterns.

In addition, we found attenuated connectivity between SMN and FPN in state 3 in the TATG group after treatment. SMN is involved in perceptual and motor function, and FPN participates in many cognitive tasks consisting of attention, working memory, and motor control [22, 47]. Several studies report that increased FC between SMN and FPN at earlier time after stroke contributed to complete motor planning and execution by integrating information related to the motor-related goal and spatial information, reflecting a compensation strategy for the damaged motor system [22, 47, 48]. As stroke patients recover, the higher FC between brain networks will be decreased. However, prolonged compensatory brain activity is believed to a maladaptive plasticity, which leads to poorer motor performance [49, 50]. Therefore, acupuncture may facilitate aberrant functional network normalization during stroke rehabilitation.

Besides, we found both fraction time and mean dwell time in state 1 that had an increasing tendency after *Shou Zu Shi Er Zhen* acupuncture treatment. State 1 was characterized by partially high intranetwork connectivity, as well as low internetwork connectivity with few positive connections. We referred to this state as the relative segregated state, which can be explained by the concept of functional segregation [51, 52]. Functional segregation reflects better cognitive abilities and information processing for specific tasks [53]. Recent evidence shows that the mean dwell time of such state significantly decreased in stroke patients, suggesting reduced functional segregation to be a sign of impaired function [45, 54]. In our study, there was a negative trend between NIHSS score and the mean dwell time in state 1, meaning reduced mean dwell time in segregated state in parallel to worse neurological deficits. Nevertheless, this interpretation should be viewed with caution due to limited statistical power. Notably, the connectivity between DAN and DMN in state 1 was positively correlated with FMA score and was higher in the TATG group after treatment than before. DAN is related to motor attention task, especially in spatial attention and pointing movements

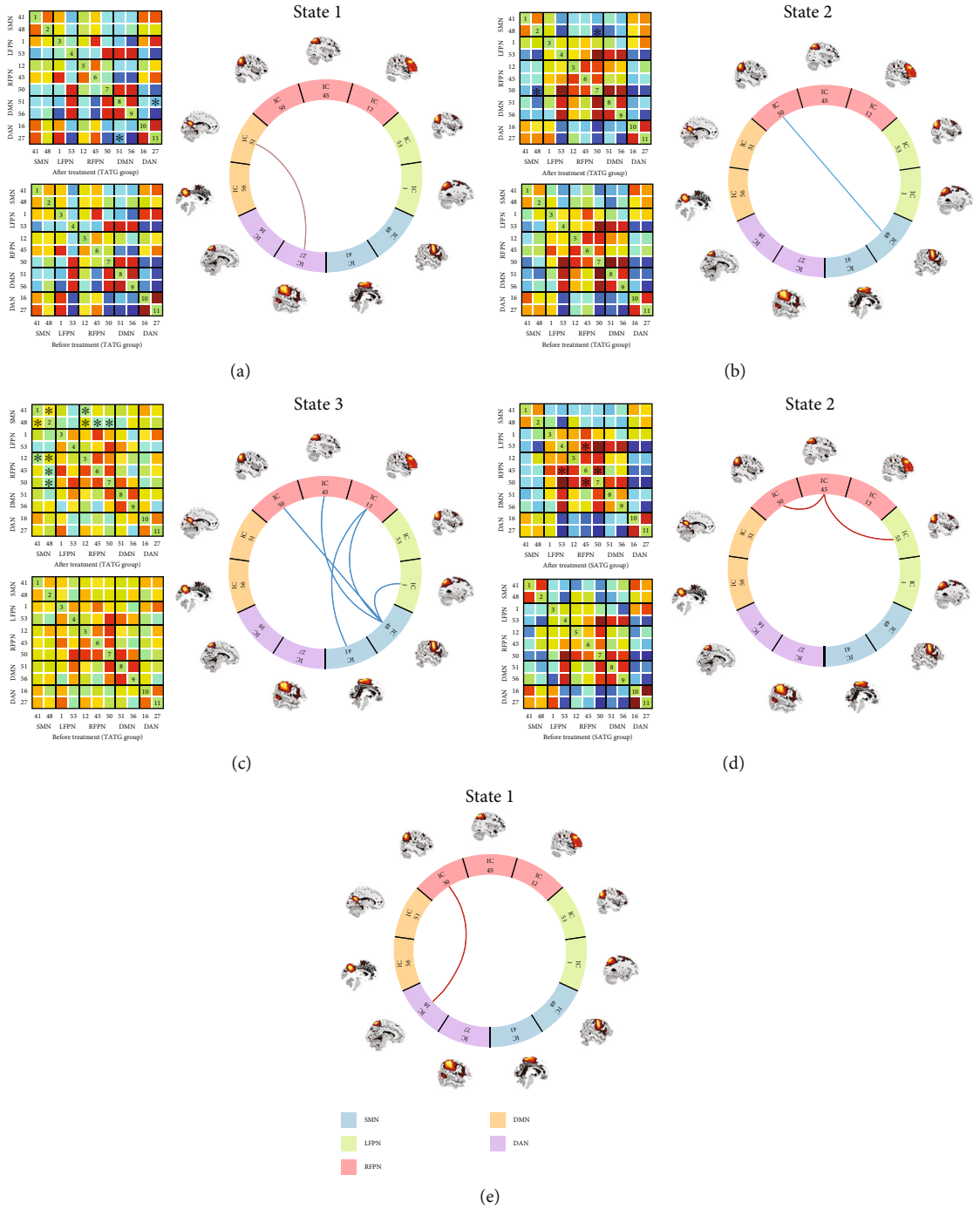

Figure 5: Differences in functional connectivity among distinct states. Specific connectivity matrix (left) and circle plots of significant difference in connectivity states (right) (a–d). The significant difference in specific state is marked by asterisk (* represents $P < 0.05$). In circle plots, red lines indicate increased functional connectivity (FC) between or within networks. Blue lines indicate decreased FC between or within networks. (a–d) The significant connectivity differences after treatment compared to before treatment in the TATG group or the SATG group. (a) Increased FC between DAN and DMN in state 1 in the TATG group. (b) Reduced FC between RFPN and SMN in state 2 in the TATG group. (c) Reduced FC between FPN and SMN in state 3 in the TATG group. (d) Increased FC in FPN in state 2 in the SATG group. (e) Positive effect between DAN and RFPN in state 1 between the two groups, which means increased FC between DAN and RFPN in state 1 in the TATG group compared to the SATG group. SMN: sensorimotor network. LFPN: left frontoparietal network. RFPN: the right frontoparietal network. DMN: default mode network. DAN: dorsal attention network.

[55]. DMN is associated with self-referential and spontaneous cognition, and this network is anticorrelated with DAN in the resting state [56]. Neuroimaging evidence revealed that the enhanced negative connectivity may compensate for decreased cognitive function in Parkinson's disease [57]. Prior studies suggested that acupuncture therapy

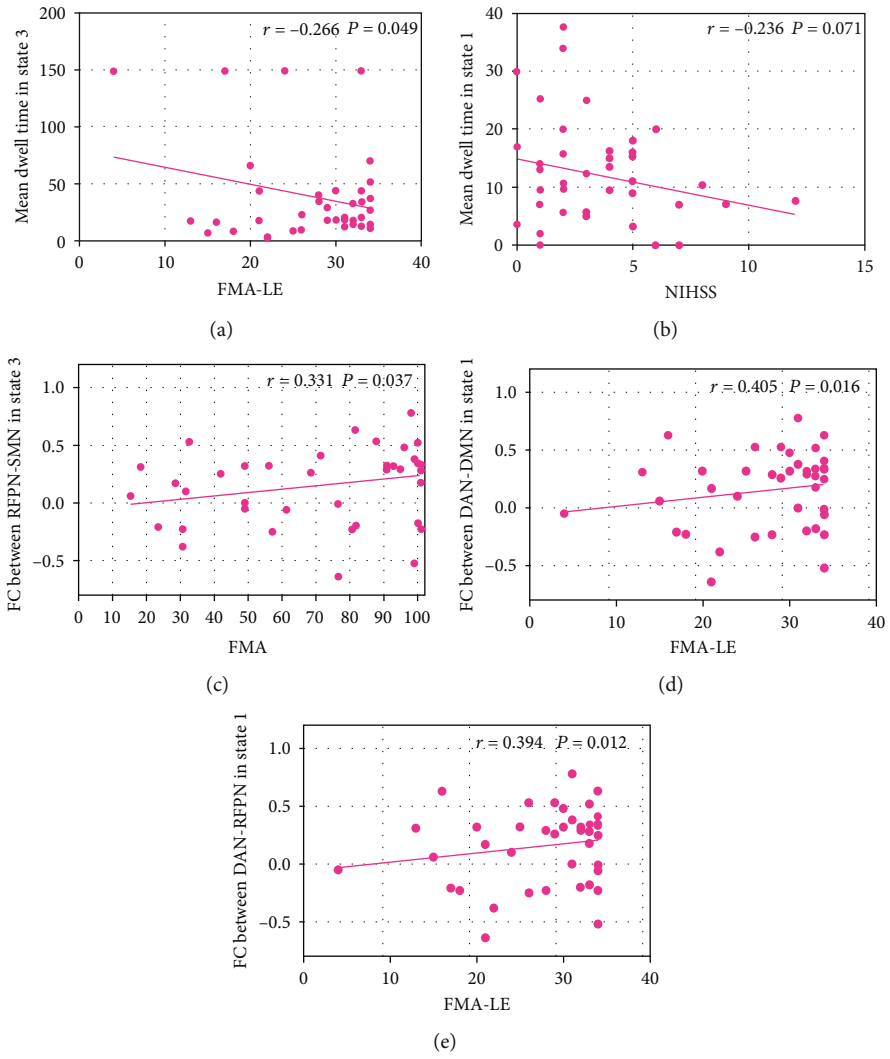

Figure 6: Correlation between clinical measures and dFNC parameter. (a) Negative correlation between mean dwell time and FMA-LE score in state 3. (b) Negative correlation trend between mean dwell time and NIHSS score in state 1. (c) Positive correlation between FMA score and FC in RFPN-SMN in state 3. (d) Positive correlation between FMA-LE score and FC in DAN-DMN in state 1. (e) Positive correlation between FMA-LE score and FC in DAN-RFPN in state 1. FMA: Fugl-Meyer. FMA-LE: FMA for the lower extremity. NIHSS: National Institute of Health Stroke Scale.

could help patients improve their cognitive function [58, 59]. Our result showed an increased FC between DAN and DMN after true acupuncture treatment; that is, the negative FC between the two networks decreased. Thus, we presume that acupuncture promotes higher-order cognitive information integration without the need for functional compensation induced by increased negative FC between DAN and DMN. And the result also revealed that decreased FC between DAN and DMN was positively related to good motor recovery, supporting our speculation to some extent.

In terms of sham acupuncture treatment, we found increased mean dwell time, as well as elevated FC within FPN in state 2 after treatment. FPN is mainly involved in the cognitive control process such as attention and memory [60]. Fu et al. approved that FPN was the causal hub and inputted most information from other brain networks in the resting state for stroke patients [22]. Interestingly, after needling stimulation, they found that LFPN converted into the network outputting most information to other brain networks, reflecting that acupuncture may help transmit information by thinking and decision-making. Considering our results, we speculated that sham acupuncture also had a certain effect on brain functional activity, which may help to strengthen communication within FPN to support cognitive process and motor preparation.

4.3. Differences in Functional Connectivity between True and Sham Acupuncture. Acupuncture points are distributed on the meridians, with specific names, definite locations and clear therapeutic ranges. Acupoint specificity is considered the core scientific issue in the practice of acupuncture at the Society for Acupuncture Research International Symposium held in 2007 [31]. Several studies have demonstrated that acupoint stimulation in stroke patients induces significant activation of more brain areas and stronger effective connections between functional networks in comparison to

sham acupuncture [61]. We found that the FC value increased between DAN and RFPN in state 1 in the TATG group compared to the SATG group. And further analysis showed that stronger FC between DAN and RFPN was associated with better motor performance. Accordingly, we supposed that true acupuncture may enhance the integration of movement-related and cognitive formation. In terms of temporal properties, there was a trend toward a greater decline in mean dwell time in the weakly connected state (state 3), as well as a larger increase in mean dwell time in the relative segregated state (state 1) in patients treated with true acupuncture compared to sham acupuncture, and these alterations were closely related with motor recovery. Interestingly, the mean dwell time in state 2 increased significantly after sham acupuncture, with elevated FC within FPN in state 2. However, no clinical relevance was observed for these indicators in state 2. Such changes suggest that sham acupoint stimulation also has some impact on brain function but may not be sufficient to achieve therapeutic effects.

4.4. Limitations. This work has several limitations. In this study, we failed to confirm the advantages of true acupuncture from the clinical perspective. Some evidence suggests that sham acupuncture also creates some effects, which may underestimate the true acupuncture treatment effect [11]. And although the sample size met the requirement of a minimum sample size for statistical power in neuroimaging research [62, 63], it was still relatively small for a clinical study. Our neuroimaging results also need to be validated via independent datasets with larger sample sizes. Besides, due to the limitation of the objective conditions, we only performed two weeks of acupuncture intervention for stroke patients, which is not the optimal duration of treatment for rehabilitation. Further studies should provide long-course acupuncture treatment to explore the mechanism underlying how acupuncture promotes brain neuroplasticity. In addition, there is evidence suggesting that stroke severity is related to temporal properties and dynamic connectivity of the brain. In the present study, most patients were mild to moderate, and our conclusions may not be adapted to patients with severe motor dysfunction.

5. Conclusion

This is the first study to investigate the alteration of dynamic brain function induced by acupuncture treatment in stroke patients with motor dysfunction based on dFNC analysis. We identified the relationship between dynamic properties and motor function in poststroke patients. Our findings demonstrated that acupuncture has the potential to modulate abnormal temporal properties and promote the balance of separation and integration of brain function. True acupoint stimulation may have a more positive effect on regulating the brain's dynamic function. Our findings provide additional evidence for exploring the association between acupuncture therapy and neuroplasticity.

Data Availability

The data used to support the findings of this study will be available upon reasonable request, which can be directed to the corresponding author.

Ethical Approval

This study has been approved by the ethics committee of Dongzhimen Hospital affiliated to Beijing University of Chinese Medicine (DZMEC-KY-2018-04), Beijing, China. All participants signed informed consent before the beginning of this study.

Conflicts of Interest

The authors declare that they have no conflicts of interest.

Authors' Contributions

YHW wrote the manuscript. YHZ conceptualized and designed the study. MXL, RYL, LPW, and YW collected the clinical and fMRI data. YHW and KSL analyzed the fMRI data. MXL, KW, and CC completed the evaluation of the clinical scale. TZC, LLX, and XYS performed the acupuncture manipulation. Yahui Wang, Mengxin Lu, and Ruoyi Liu contributed equally to this work and share the first authorship.

Acknowledgments

We are indebted to our patients for generously supporting our study. We would like to thank Dr. Mingsheng Lyu for providing picture processing help and thank Lekai Luo for his guidance in data processing. This work was supported by the Natural Science Foundation of China (Grant No. 81873257) and the Natural Science Foundation of Beijing (Grant No. 7182104).

Supplementary Materials

The supplementary materials provide more detailed information. The probability map and detailed information of the lesion location in each patient are shown in Supplementary Material 1. The location of all acupoints is also shown in Supplementary Material 1. The results of validation analysis are shown in Supplementary Material 2. *(Supplementary Materials)*

References

[1] GBD, "Global, regional, and national burden of stroke and its risk factors, 1990-2019: a systematic analysis for the Global Burden of Disease Study 2019," *The Lancet Neurology*, vol. 20, no. 10, pp. 795–820, 2021.

[2] L. Wang, B. Peng, H. Zhang, and Y. Wang, "Brief report on stroke prevention and treatment in China, 2020," *Chinese Journal of Cerebrovascular Diseases*, vol. 19, pp. 136–144, 2022.

[3] N. E. Mayo, S. Wood-Dauphinee, S. Ahmed et al., "Disablement following stroke," *Disability and Rehabilitation*, vol. 21, no. 5-6, pp. 258–268, 1999.

[4] W. S. Kim, S. Cho, J. Ku et al., "Clinical application of virtual reality for upper limb motor rehabilitation in stroke: review

of technologies and clinical evidence," *Journal of Clinical Medicine*, vol. 9, no. 10, p. 9, 2020.

[5] D. J. Reinkensmeyer and M. L. Boninger, "Technologies and combination therapies for enhancing movement training for people with a disability," *Journal of Neuroengineering and Rehabilitation*, vol. 9, no. 1, p. 17, 2012.

[6] M. Gittler and A. M. Davis, "Guidelines for adult stroke rehabilitation and recovery," *Journal of the American Medical Association*, vol. 319, no. 8, pp. 820-821, 2018.

[7] J. X. Pan and P. L. J. al ZNZe, "Strategic thinking of evidence-based medicine in promoting the internationalization of acupuncture and moxibustion from the perspective of belt and road initiative," *Chinese Journal of traditional Chinese Medicine*, vol. 35, pp. 3287–3289, 2020.

[8] A. Yang, H. M. Wu, J. L. Tang et al., "Acupuncture for stroke rehabilitation," *Cochrane Database of Systematic Reviews*, vol. 2016, no. 8, p. CD004131, 2016.

[9] J. Wen, X. Chen, Y. Yang et al., "Acupuncture medical therapy and its underlying mechanisms: a systematic review," *The American Journal of Chinese Medicine*, vol. 49, no. 1, pp. 1–23, 2021.

[10] NIH Consensus Conference, "Acupuncture," *JAMA*, vol. 280, no. 17, pp. 1518–1524, 1998.

[11] Y. T. Fei, H. J. Cao, R. Y. Xia et al., "Methodological challenges in design and conduct of randomised controlled trials in acupuncture," *BMJ*, vol. 376, article e064345, 2022.

[12] Medicine BhoTC, *'Gold Needle' WangLeting*, Beijing Publishing House, Beijing, 1984.

[13] Z. Sun, "Clinical observation of cerebral infarction treated with shou zu shi er zhen in 150 cases," *China Modern Medicine*, vol. 16, pp. 82-83, 2009.

[14] H. Li, L. Tian, and X. Du, "Wang's 12 needle acupuncture combined with Western medicine for 30 cases of hemiplegia after ischemic stroke," *Traditional Chinese Medicinal Research*, vol. 29, pp. 56–58, 2016.

[15] X. Wang, H. Zhang, X. Ding, and Yangyang, "The effect of "hands and feet twelve acupuncture" on the quality of life of patients," *World Journal of Integrated Traditional and Western Medicine*, vol. 15, pp. 1684–1687, 2020.

[16] J. Zhang, Z. Li, Z. Li et al., "Progress of acupuncture therapy in diseases based on magnetic resonance image studies: a literature review," *Frontiers in Human Neuroscience*, vol. 15, article 694919, 2021.

[17] Z. Zhou, S. Chen, Y. Li et al., "Comparison of sensory observation and somatosensory stimulation in mirror neurons and the sensorimotor network: a task-based fMRI study," *Frontiers in Neurology*, vol. 13, article 916990, 2022.

[18] Y. Huang, J. Q. Chen, X. S. Lai et al., "Lateralisation of cerebral response to active acupuncture in patients with unilateral ischaemic stroke: an fMRI study," *Acupuncture in Medicine*, vol. 31, no. 3, pp. 290–296, 2013.

[19] M. K. Li, Y. J. Li, G. F. Zhang et al., "Acupuncture for ischemic stroke: cerebellar activation may be a central mechanism following Deqi," *Neural Regeneration Research*, vol. 10, no. 12, pp. 1997–2003, 2015.

[20] J. D. Schaechter, B. D. Connell, W. B. Stason et al., "Correlated change in upper limb function and motor cortex activation after verum and sham acupuncture in patients with chronic stroke," *Journal of Alternative and Complementary Medicine*, vol. 13, no. 5, pp. 527–532, 2007.

[21] X. Chen, H. Zhang, and Y. Zou, "A functional magnetic resonance imaging study on the effect of acupuncture at GB34 (Yanglingquan) on motor-related network in hemiplegic patients," *Brain Research*, vol. 1601, pp. 64–72, 2015.

[22] C. H. Fu, K. S. Li, Y. Z. Ning et al., "Altered effective connectivity of resting state networks by acupuncture stimulation in stroke patients with left hemiplegia: a multivariate granger analysis," *Medicine (Baltimore)*, vol. 96, no. 47, article e8897, 2017.

[23] L. Jiang, *Mechanism based on bilateral cerebral connections of acupuncture effect on hemiplegia after cerebral infarction*, Beijing University of Chinese Medcine, 2020.

[24] R. M. Hutchison, T. Womelsdorf, E. A. Allen et al., "Dynamic functional connectivity: promise, issues, and interpretations," *NeuroImage*, vol. 80, pp. 360–378, 2013.

[25] E. A. Allen, E. Damaraju, S. M. Plis, E. B. Erhardt, T. Eichele, and V. D. Calhoun, "Tracking whole-brain connectivity dynamics in the resting state," *Cerebral Cortex*, vol. 24, no. 3, pp. 663–676, 2014.

[26] C. Chang and G. H. Glover, "Time-frequency dynamics of resting-state brain connectivity measured with fMRI," *NeuroImage*, vol. 50, no. 1, pp. 81–98, 2010.

[27] Y. Wei, W. Zhang, Y. Li et al., "Acupuncture treatment decreased temporal variability of dynamic functional connectivity in chronic tinnitus," *Frontiers in Neuroscience*, vol. 15, article 737993, 2022.

[28] Y. Chen, Y. Kang, S. Luo et al., "The cumulative therapeutic effect of acupuncture in patients with migraine without aura: evidence from dynamic alterations of intrinsic brain activity and effective connectivity," *Frontiers in Neuroscience*, vol. 16, article 925698, 2022.

[29] A. K. Bonkhoff, F. A. Espinoza, H. Gazula et al., "Acute ischaemic stroke alters the brain's preference for distinct dynamic connectivity states," *Brain*, vol. 143, no. 5, pp. 1525–1540, 2020.

[30] L. Jiang, H. Geng, M. Lu et al., "Acupuncture for poststroke hemiplegia focusing on cerebral bilateral connections: study protocol for a randomised controlled neuroimaging trial," *BMJ Open*, vol. 10, no. 4, article e034548, 2020.

[31] J. J. Xing, B. Y. Zeng, J. Li, Y. Zhuang, and F. R. Liang, "Acupuncture point specificity," *International Review of Neurobiology*, vol. 111, pp. 49–65, 2013.

[32] Z. Liu, Y. Liu, H. Xu et al., "Effect of electroacupuncture on urinary leakage among women with stress urinary incontinence: a randomized clinical trial," *Journal of the American Medical Association*, vol. 317, no. 24, pp. 2493–2501, 2017.

[33] C. G. Yan, X. D. Wang, X. N. Zuo, and Y. F. Zang, "DPABI: data processing & analysis for (resting-state) brain imaging," *Neuroinformatics*, vol. 14, no. 3, pp. 339–351, 2016.

[34] A. J. Bell and T. J. Sejnowski, "An information-maximization approach to blind separation and blind deconvolution," *Neural Computation*, vol. 7, no. 6, pp. 1129–1159, 1995.

[35] E. B. Erhardt, S. Rachakonda, E. J. Bedrick, E. A. Allen, T. Adali, and V. D. Calhoun, "Comparison of multi-subject ICA methods for analysis of fMRI data," *Human Brain Mapping*, vol. 32, no. 12, pp. 2075–2095, 2011.

[36] B. T. Yeo, F. M. Krienen, J. Sepulcre et al., "The organization of the human cerebral cortex estimated by intrinsic functional connectivity," *Journal of Neurophysiology*, vol. 106, no. 3, pp. 1125–1165, 2011.

[37] D. Cordes, V. M. Haughton, K. Arfanakis et al., "Mapping functionally related regions of brain with functional connectivity MR imaging," *American Journal of Neuroradiology*, vol. 21, no. 9, pp. 1636–1644, 2000.

[38] Y. Li, K. Wu, X. Hu et al., "Altered effective connectivity of resting-state networks by tai chi chuan in chronic fatigue syndrome patients: a multivariate granger causality study," *Frontiers in Neurology*, vol. 13, article 858833, 2022.

[39] N. Leonardi and D. Van De Ville, "On spurious and real fluctuations of dynamic functional connectivity during rest," *NeuroImage*, vol. 104, pp. 430–436, 2015.

[40] S. Wang, H. Cai, Z. Cao et al., "More than just static: dynamic functional connectivity changes of the thalamic nuclei to cortex in Parkinson's disease with freezing of gait," *Frontiers in Neurology*, vol. 12, article 735999, 2021.

[41] H. A. Marusak, V. D. Calhoun, S. Brown et al., "Dynamic functional connectivity of neurocognitive networks in children," *Human Brain Mapping*, vol. 38, no. 1, pp. 97–108, 2017.

[42] R. M. Hutchison and J. B. Morton, "Tracking the brain's functional coupling dynamics over development," *The Journal of Neuroscience*, vol. 35, no. 17, pp. 6849–6859, 2015.

[43] Y. Wang, L. Wang, M. Lu, Y. Wang, and Y. Zou, "Exploring the clinical value and effect mechanism of hand-foot twelve needles in the treatment of stroke based on the theory of "harmonization of form and spirit"," *Journal of Traditional Chinese Medicine*, vol. 63, pp. 327–331, 2022.

[44] R. Xiao, L. Zuo, Y. Zhou, and Y. Chen, "Functional magnetic resonance imaging study on the changes of dynamic brain functional," *Chinese Journal of Stroke*, vol. 16, pp. 996–1005, 2021.

[45] Y. Wang, C. Wang, P. Miao et al., "An imbalance between functional segregation and integration in patients with pontine stroke: a dynamic functional network connectivity study," *NeuroImage: Clinical*, vol. 28, article 102507, 2020.

[46] A. K. Bonkhoff, M. D. Schirmer, M. Bretzner et al., "Abnormal dynamic functional connectivity is linked to recovery after acute ischemic stroke," *Human Brain Mapping*, vol. 42, no. 7, pp. 2278–2291, 2021.

[47] T. K. Lam, D. R. Dawson, K. Honjo et al., "Neural coupling between contralesional motor and frontoparietal networks correlates with motor ability in individuals with chronic stroke," *Journal of the Neurological Sciences*, vol. 384, pp. 21–29, 2018.

[48] C. S. Inman, G. A. James, S. Hamann, J. K. Rajendra, G. Pagnoni, and A. J. Butler, "Altered resting-state effective connectivity of fronto-parietal motor control systems on the primary motor network following stroke," *NeuroImage*, vol. 59, no. 1, pp. 227–237, 2012.

[49] C. Mei, J. Ni, and C. Shan, "Progress in the study of mechanisms of brain area recovery and functional connectivity after motor impairment in stroke," *Chinese Journal of Rehabilitation Medicine*, vol. 33, pp. 239–243, 2018.

[50] A. W. Dromerick, C. E. Lang, R. Birkenmeier, M. G. Hahn, S. A. Sahrmann, and D. F. Edwards, "Relationships between upper-limb functional limitation and self-reported disability 3 months after stroke," *Journal of Rehabilitation Research and Development*, vol. 43, no. 3, pp. 401–408, 2006.

[51] K. J. Friston, "Functional and effective connectivity: a review," *Brain Connectivity*, vol. 1, no. 1, pp. 13–36, 2011.

[52] R. Wang, M. Liu, X. Cheng, Y. Wu, A. Hildebrandt, and C. Zhou, "Segregation, integration, and balance of large-scale resting brain networks configure different cognitive abilities," *Proceedings of the National Academy of Sciences of the United States of America*, vol. 118, no. 23, 2021.

[53] G. S. Wig, "Segregated Systems of human brain networks," *Trends in Cognitive Sciences*, vol. 21, no. 12, pp. 981–996, 2017.

[54] J. S. Siegel, B. A. Seitzman, L. E. Ramsey et al., "Re-emergence of modular brain networks in stroke recovery," *Cortex*, vol. 101, pp. 44–59, 2018.

[55] P. Mengotti, A. S. Käsbauer, G. R. Fink, and S. Vossel, "Lateralization, functional specialization, and dysfunction of attentional networks," *Cortex*, vol. 132, pp. 206–222, 2020.

[56] M. E. Raichle, "The brain's default mode network," *Annual Review of Neuroscience*, vol. 38, no. 1, pp. 433–447, 2015.

[57] Q. Yu, Q. Li, W. Fang et al., "Disorganized resting-state functional connectivity between the dorsal attention network and intrinsic networks in Parkinson's disease with freezing of gait," *The European Journal of Neuroscience*, vol. 54, no. 7, pp. 6633–6645, 2021.

[58] W. He, M. Li, X. Han, and W. Zhang, "Acupuncture for mild cognitive impairment and dementia: an overview of systematic reviews," *Frontiers in Aging Neuroscience*, vol. 13, article 647629, 2021.

[59] L. Zhou, Y. Wang, J. Qiao, Q. M. Wang, and X. Luo, "Acupuncture for improving cognitive impairment after stroke: a meta-analysis of randomized controlled trials," *Frontiers in Psychology*, vol. 11, article 549265, 2020.

[60] S. T. Witt, H. van Ettinger-Veenstra, T. Salo, M. C. Riedel, and A. R. Laird, "What executive function network is that? An image-based meta-analysis of network labels," *Brain Topography*, vol. 34, no. 5, pp. 598–607, 2021.

[61] L. Liu, X. Li, F. Wang, Y. Ji, B. Qu, and D. Cao, "Activating the brain fMRI cerebral functional imaging by needling gall bladder channel of foot- Shaoyang meridian point and he sea point," *Acta Chinese Medicine and Pharmacology*, vol. 42, pp. 74–77, 2014.

[62] D. Szucs and J. P. Ioannidis, "Sample size evolution in neuroimaging research: an evaluation of highly-cited studies (1990-2012) and of latest practices (2017-2018) in high-impact journals," *Neuroimage*, vol. 221, article 117164, 2020.

[63] J. E. Desmond and G. H. Glover, "Estimating sample size in functional MRI (fMRI) neuroimaging studies: statistical power analyses," *Journal of Neuroscience Methods*, vol. 118, no. 2, pp. 115–128, 2002.

Hindawi
Neural Plasticity
Volume 2023, Article ID 6297653, 13 pages
https://doi.org/10.1155/2023/6297653

Research Article

Imbalance of Microbacterial Diversity Is Associated with Functional Prognosis of Stroke

Xintong Zhang,[1] **Xiangyu Wang**,[2] **Hong Zhao**,[1] **Risheng Cao**,[3] **Yini Dang**,[4] **and Binbin Yu**[1]

[1]*Department of Rehabilitation Medicine, The First Affiliated Hospital of Nanjing Medical University, Jiangsu, China*
[2]*Department of Rehabilitation Medicine, The Affiliated Lianyungang Oriental Hospital of Kangda College of Nanjing Medical University, Jiangsu, China*
[3]*Department of Science and Technology, The First Affiliated Hospital of Nanjing Medical University, Jiangsu, China*
[4]*Department of Gastroenterology, The First Affiliated Hospital of Nanjing Medical University, Jiangsu, China*

Correspondence should be addressed to Risheng Cao; rishengcao@njmu.edu.cn, Yini Dang; yeani_hi@126.com, and Binbin Yu; coldrain24@163.com

Received 30 October 2022; Revised 25 November 2022; Accepted 11 April 2023; Published 8 May 2023

Academic Editor: Xi-Ze Jia

Objectives. There is mounting evidence to suggest that the pathophysiology of stroke is greatly influenced by the microbiota of the gut and its metabolites, in particular short-chain fatty acids (SCFAs). The primary purpose of the study was to evaluate whether the levels of SCFAs and the gut microbiota are altered in poststroke patients and to examine the relationship between these alterations and the physical condition, intestinal health, pain, or nutritional status of patients. *Methods*. Twenty stroke patients and twenty healthy controls were enrolled in the current study, and their demographics were matched. Gas chromatography was used to determine the fecal SCFAs, and 16S rRNA gene sequencing was used to evaluate their fecal microbiota. Microbial diversity and richness were examined using the diversity indices alpha and beta, and taxonomic analysis was utilized to determine group differences. The relationships between the gut microbiome and fecal SCFAs, discriminant bacteria, and poststroke clinical outcomes were analyzed. *Results*. Less community richness (ACE and Chao) was observed in the poststroke patients ($P < 0.05$), but the differences between the poststroke group and the healthy control group in terms of species diversity (Shannon and Simpson) were not statistically significant. The makeup of the poststroke gut microbiota was distinct from that of the control group, as evidenced by beta diversity. Then, the relative abundances of the taxa in the poststroke and control groups were compared in order to identify the specific microbiota changes. At the level of phylum, the poststroke subjects showed a significant increase in the relative abundances of *Akkermansiaceae*, *Fusobacteriota*, *Desulfobacterota*, *Ruminococcaceae*, and *Oscillospirales* and a particularly noticeable decrease in the relative abundance of *Acidobacteriota* compared to the control subjects ($P < 0.05$). In regard to SCFA concentrations, lower levels of fecal acetic acid ($P = 0.001$) and propionic acid ($P = 0.049$) were found in poststroke subjects. *Agathobacter* was highly correlated with acetic acid level ($r = 0.473$, $P = 0.002$), whereas *Fusobacteria* ($r = -0.371$, $P = 0.018$), *Flavonifractor* ($r = -0.334$, $P = 0.034$), *Desulfovibrio* ($r = -0.362$, $P = 0.018$), and *Akkermansia* ($r = -0.321$, $P = 0.043$) were negatively related to acetic acid levels. Additionally, the findings of the correlation analysis revealed that *Akkermansia* ($r = -0.356$, $P = 0.024$), *Desulfovibrio* ($r = -0.316$, P = 0.047), and *Alloprevotella* ($r = -0.366$, $P = 0.020$) were significantly negatively correlated with high-density lipoprotein cholesterol. In addition, the Neurogenic Bowel Dysfunction score ($r = 0.495$, $P = 0.026$), Barthel index ($r = -0.531$, $P = 0.015$), Fugl-Meyer Assessment score ($r = -0.565$, $P = 0.009$), Visual Analogue Scale score ($r = 0.605$, P = 0.005), and Brief Pain Inventory score ($r = 0.507$, $P = 0.023$) were significantly associated with alterations of distinctive gut microbiota. *Conclusions*. Stroke generates extensive and substantial alterations in the gut microbiota and SCFAs, according to our findings. The differences of intestinal flora and lower fecal SCFA levels are closely related to the physical function, intestinal function, pain, or nutritional status of poststroke patients. Treatment strategies aimed at modulating the gut microbiota and SCFAs may have the potential to enhance the clinical results of patients.

1. Introduction

Stroke is the main cause of disability and death, respectively, and imposes huge individual and societal burdens [1, 2]. Although advanced stroke emergency treatments, such as endovascular thrombectomy and intravenous thrombolysis, can improve the physical and mental status of some patients, the prognosis of most stroke patients is still poor [3].

Recent studies have focused on the finding of the microbiome-gut-brain axis, which describes the relationship between the gut and the brain via gut bacteria [4]. The microbiome-gut-brain axis consists primarily of gut microbiota and its metabolites, neurological (enteric, central, and autonomic nervous systems), immunological, and hormonal pathways, of which gut microbiota is an important component [5, 6]. Stroke is commonly associated with hypertension, diabetes, hyperlipidemia, and low physical activity, all of which have major influences on the gut microbiota [7]. In addition, stressful stimuli at the onset of stroke, limb paralysis, neurogenic intestinal dysfunction, neuropathic pain, malnutrition, and other problems caused by stroke will lead to microbiome disturbances [3, 8, 9]. On the other hand, the gut microbiota and its metabolites, such as the highly concerned short-chain fatty acids (SCFAs), may affect poststroke outcomes through multiple pathways, including intestinal leakage, local and systemic inflammation, and endotoxemia [10]. The gut microbiota and its metabolites have great potential to become therapeutic targets for stroke.

Some studies have demonstrated the existence of significant intestinal flora disturbance in poststroke patients [11, 12]. Our previous study also found that stroke may lead to changes in gut microbiota structure, especially a significant decrease in the abundance of SCFA-producing microbiota, but the level of SCFAs was not explored in that study [13]. A recent study reported that reduced SCFAs, especially acetate, were associated with poor motor functional outcomes after stroke [14]. However, that study did not explore the relationship between SCFAs and other complications, such as gastrointestinal dysfunction, pain, and malnutrition. These complications may have potential interactions with intestinal flora and SCFAs, which are also important factors affecting the long-term prognosis of stroke patients [9, 15–17].

We carried out this research to evaluate the following two hypotheses by comparing the gut microbiota composition and SCFA levels of poststroke patients with those of healthy individuals: (1) the makeup of the gut microbiota and levels of SCFAs in poststroke patients differ significantly from those of healthy controls, and (2) the alteration of gut microbiota composition and SCFA level in poststroke patients may be potentially related to physical function, intestinal function, pain, and nutritional status.

2. Methods and Materials

2.1. Study Design and Patient Enrollment. An individual-center prospective observational case-control research was conducted. Patients were recruited from the regular medical wards or the stroke unit at the Affiliated Lianyungang Oriental Hospital of Kangda College of Nanjing Medical University from 19 January 2022 to 29 July 2022. The inclusion criteria were as follows: (1) age of between 18 years and 80 years, (2) ischemic/hemorrhagic stroke as confirmed by computerised tomography (CT) or magnetic resonance imaging (MRI), and (3) were able to provide a vocal response to the directions they were given and provided informed consent [18]. Patients were excluded from the study if (1) diagnosed with silent cerebral infarction or transient ischemic attack (TIA), (2) with serious cognitive impairments or mental dysfunctions, and (3) current participation in another clinical trial or participation in another clinical trial in the 6 months prior to enrolment [19]. Age-, gender-, and risk factor-matching healthy subjects served as the controls. Prior to conducting the study, ethics approval using an approval code was acquired (Institutional Review Board, 2022-041-01). The clinical trial was formally registered in advance with the Clinical Trials Registry (registration number: NCT03938311). Prior to enrolment, consent was acquired with knowledge.

2.2. Clinical Assessment and Sample Collection. The following demographic data was collected: age, gender, and subtype of stroke. Clinical assessments were conducted by a trained researcher. The degree of physical symptoms, such as pain, was assessed using tools such as the Visual Analogue Scale (VAS) as well as the Brief Pain Inventory (BPI). A VAS value of 0 showed that there was no pain, while a VAS score of 10 indicated severe pain [20, 21]. The BPI was used to characterize pain severity and functional interference in daily life. On a scale from 0 (never interferes) to 10 (totally interferes), participants evaluate each item [22, 23]. Bowel function was assessed by using the Neurogenic Bowel Dysfunction (NBD) score, for which a higher score indicates worse bowel function [24, 25]. Scores on the Barthel index (BI) range from 0 to 100, with higher scores showing better performance in activities of daily living (ADL) [26, 27]. The Fugl-Meyer Assessment, often known as the FMA score, was used to evaluate either the upper or lower extremity motor function, and higher score represents better function [28, 29]. Patients' fresh stool samples were taken and stored at a temperature of -80 degrees Celsius for use in DNA extraction at a later time.

2.3. DNA Extraction, 16S rRNA Gene Amplification, and Sequencing. Using the Qiagen QIAamp DNA Stool Mini Kit (Qiagen, catalogue number 51504, Hilden, Germany) and following the manufacturer's instructions, bacterial genomic DNA was extracted from the prepared frozen cecal samples. The DNA concentration and purity were evaluated both with a NanoDrop-2000 spectrophotometer (NanoDrop Technologies, Wilmington, DE, USA). For the microbial community diversity analysis, the V3-V4 region of the bacterial 16S rRNA gene was targeted with the barcoded primer pair 341F/806R (341F: CCTAYGGGRBGCASCAG, 806R: GGACTCNNGGGTATCTAAT). The Illumina 16S Metagenomic Sequencing Library preparation protocol was followed to perform the 16S rRNA gene amplification and index PCR for sequencing (Illumina, San Diego, CA, USA).

2.4. Quantification of SCFAs in Stool Samples. According to other reports, gas chromatography-mass spectrometry (GC-MS) was used to quantify numerous SCFAs (acetic acids, butyric acids, propionic acids, caproic acids, isobutyric acids, isovaleric acids, and valeric acids) in fecal samples [30].

2.5. Bioinformatic Gut Microbiota Analyses. Using QIIME v.1.9.1 (QIIME permits analysis of high-throughput community sequencing data) and USEARCH v.10.0, the 16S rRNA gene sequences were processed in this investigation (Magnit search and clustering orders). The raw FASTQ files had their quality filtered by Trimmomatic, and then, USEARCH merged them based on the following criteria: the removal of barcodes and primers, the removal of low-quality reads, and the detection of nonredundancy readings. Sequences assigned by the UPARSE software to the same operational taxonomic units (OTUs) had a 97% similarity rate (version 7.0.1001). With the QIIME software displayed, alpha diversity indices such as ACE, Chao, Shannon, and Simpson were computed, and beta diversity was evaluated using principal coordinate analysis (PCA) and nonmetric multidimensional scaling (NMDS). Linear discriminant analysis (LDA) and linear discriminant effect size (LEfSe) techniques were used to assess metagenomic biomarkers among groups utilizing the Galaxy Online Analysis Platform.

2.6. Statistical Analysis. The means and standard deviations of continuous variables are shown. The categorical variables are represented by numbers (percentages). Microbiota data and SCFA levels were tested by one-way analysis of variance (ANOVA) and the Wilcoxon rank-sum test. Alpha diversity and beta diversity among groups were tested by the Wilcoxon rank-sum test. Using the Bonferroni correction, the P values were adjusted for multiple testing. Pearson correlation was used to estimate the correlations between bacterial or SCFA levels and clinical evaluations. P values under 0.05 were used to determine whether a difference between groups was significant. With SPSS 24.0, all statistical evaluations were completed (SIBM SPSS, Armonk, NY, USA). Software called GraphPad Prism 5.0 was used to plot the data (La Jolla, CA, USA).

3. Results

3.1. Participant Demographics. Twenty patients with a clinical diagnosis of stroke were evaluated (average age 64 ± 13 years; gender, male : female 11 : 9) and were recruited. In the meantime, 20 healthy persons of the same age and gender were examined (average age 60 ± 8 years; gender, male : female 6 : 14) who attended annual physical examinations and were also recruited. The clinical features and demographics of stroke patients and controls are shown in Table 1.

3.2. Poststroke Subjects Harbor an Altered Gut Microbiota Composition. As shown in Figure 1(a), 900 and 93 OTUs were individually identified from the control group and the poststroke group, and there were 634 OTUs that overlapped between the two groups. Between the poststroke and control groups, there were significant differences ($P < 0.05$) in terms of community richness (ACE and Chao) when comparing bacterial alpha diversity (Figures 1(b) and 1(c)).The differences between each group were not statistically significant when assessing the species diversity of the microbiota (Shannon and Simpson) (Figures 1(d) and 1(e)). PCA and NMDS were used to determine differences in bacterial community composition between the two groups. Poststroke samples were predominantly dissimilar from those of healthy controls, indicating variations in the community structure of the microbiota between the two groups (Figures 1(f) and 1(g)).

We evaluated the average relative abundances of the taxa in the poststroke and control groups to identify the precise changes in the microbiota. At the phylum level, poststroke patients have significantly less *Acidobacteriota* than controls (0.0005% vs. 0.2710%), whereas the abundance of *Fusobacteriota* was considerably increased in poststroke patients (0.9640%) compared to controls (0.0961%). Furthermore, we also observed that *Desulfobacterota* was enriched in poststroke samples compared to control samples (Figure 2(a)). LEfSe was utilized to discover substantial changes in the bacterial composition of the poststroke and control groups. Significantly higher levels of *Akkermansiaceae*, *Fusobacteriota*, *Desulfobacterota*, *Ruminococcaceae*, and *Oscillospirales* were found in the poststroke individuals (Figures 2(b) and 2(c)).

3.3. The Levels of SCFAs in the Poststroke Group Differ Significantly from Those of the Control Group. In Figure 3, the amounts of acetic acid, butyric acid, propionic acid, caproic acid, isobutyric acid, isovaleric acid, and valeric acid in feces are displayed. The concentration of acetic acid was dramatically reduced in patients with stroke (67.60 ± 36.98) compared with controls (212.28 ± 95.25, $P = 0.001$). Between the two groups, there were no discernible variations in butyric acid levels ($P = 0.070$). Compared with healthy control group (160.41 ± 27.36), the propionate concentration was significantly decreased in the poststroke group (114.54 ± 65.72, $P = 0.049$). However, there were no appreciable variations in the concentrations of caproic acid, isobutyric acid, isovaleric acid, or valeric acid between the groups.

3.4. Correlation between the Intestinal Microbiota and Fecal SCFA Levels. At the genus level, a Pearson correlation was employed to establish a relationship between the differentially abundant taxa and the levels of SCFAs in the feces (shown in Figure 4). The relative abundance of *Agathobacter* was highly correlated with acetic acid level ($r = 0.473$, $P = 0.002$), whereas the relative abundances of *Fusobacteria* (increased considerably in the poststroke group, $r = -0.371$, $P = 0.018$), *Flavonifractor* ($r = -0.334$, $P = 0.034$), *Desulfovibrio* (increased considerably in the poststroke group, $r = -0.362$, $P = 0.018$), and *Akkermansia* (increased considerably in the poststroke group, $r = -0.321$, $P = 0.043$) were negatively correlated with acetic acid level. Furthermore, we discovered a negative association between *Fusobacteria* and butyrate ($r = -0.362$, $P = 0.022$). Additionally, there was a positive correlation between the amounts of isovaleric acid and isobutyric acid and the presence of *Desulfovibrio*, *Akkermansia*, *Parabacteroides*, *Alistipes*, and *Odoribacter*.

Table 1: Characteristics of study participants.

	Poststroke group ($n = 20$)	Control group ($n = 20$)	P value
Age in year, mean (SD)	63.55 (12.63)	59.95 (8.02)	0.290
Gender, n (%)			0.201
Male	11 (55.00)	6 (30.00)	
Female	9 (45.00)	14 (70.00)	
Height in centimeter, mean (SD)	167.55 (6.19)	163.50 (6.49)	0.069
Weight in kilogram, mean (SD)	66.80 (8.03)	62.90 (5.53)	0.238
BMI in kg/m^2, mean (SD)	23.79 (2.57)	23.47 (2.01)	0.265
SBP in mmHg, mean (SD)	127.10 (20.45)	118.10 (16.82)	0.390
DBP in mmHg, mean (SD)	78.35 (10.33)	76.00 (8.37)	0.434
Smoking status, n (%)			0.723
Nonsmoker	7 (35.00)	9 (45.00)	
Current smoker	7 (35.00)	7 (35.00)	
Previous smoker	6 (30.00)	4 (20.00)	
Alcohol intake, n (%)			0.326
No drinking	7 (35.00)	12 (60.00)	
Light drinking	8 (40.00)	6 (30.00)	
Heavy drinking	5 (25.00)	2 (10.00)	
Medical history, n (%)			
Hypertension	15 (75.00)	9 (45.00)	0.053
Diabetes mellitus	9 (45.00)	2 (10.00)	0.013
Dyslipidemia	7 (35.00)	2 (10.00)	0.058
Laboratory findings			
Total protein (g/L)	62.00 (5.00)	64.81 (6.04)	0.118
Albumin (g/L)	39.48 (3.28)	39.99 (3.07)	0.615
Total bilirubin (μmol/L)	12.15 (3.01)	14.63 (6.59)	0.134
Direct bilirubin (μmol/L)	2.00 (0.76)	2.04 (0.96)	0.500
ALT (U/L)	24.55 (17.18)	22.05 (14.09)	0.425
AST (U/L)	24.30 (9.38)	24.45 (9.09)	0.919
Urea (mmol/L)	6.17 (1.86)	5.86 (2.88)	0.689
Creatinine (μmol/L)	68.17 (22.38)	76.66 (38.83)	0.403
Uric acid (μmol/L)	290.44 (116.44)	278.10 (103.76)	0.726
Glucose (mmol/L)	6.63 (1.69)	5.62 (1.19)	0.035
Cholesterol (mmol/L)	4.67 (1.14)	5.05 (1.08)	0.280
Triglyceride (mmol/L)	1.58 (0.76)	1.50 (0.62)	0.654
HDL-C (mmol/L)	0.99 (0.29)	1.06 (0.15)	0.329
LDL-C (mmol/L)	2.07 (0.83)	2.27 (0.45)	0.359
Stroke characteristics			
Type of stroke, n (%)			
Hemorrhage stroke	7 (35.00)		
Ischemic stroke	7 (65.00)		
Duration of stroke, n (%)			
No more than 3 months	11 (55.00)		
More than 3 months	9 (45.00)		
Side of hemiparesis, n (%)			
Left	8 (40.00)		
Right	12 (60.00)		
FMA-UE score, mean (SD)	15.8 (10.94)		
FMA-LE score, mean (SD)	16.30 (6.07)		

Table 1: Continued.

	Poststroke group ($n = 20$)	Control group ($n = 20$)	P value
Barthel index score, mean (SD)	43.00 (17.73)		
VAS score, mean (SD)	4.55 (1.36)		
NBD score, mean (SD)	14.55 (5.38)		
BPI score, mean (SD)			
Activity of daily living	4.75 (1.52)		
Emotion	4.80 (1.40)		
Sleep	3.85 (1.35)		
Work	4.55 (1.43)		
Walk	4.90 (1.65)		
Relationship	4.95 (0.89)		
Interests	5.85 (1.09)		

SD: standard deviation; BMI: body mass index; SBP: systolic blood pressure; DBP: diastolic blood pressure; ALT: alanine aminotransferase; AST: aspartate aminotransferase; HDL-C: high-density lipoprotein cholesterol; LDL-C: low-density lipoprotein cholesterol; FMA-UE: Fugl-Meyer Assessment Upper Extremity Scale; FMA-LE: Fugl-Meyer Assessment Lower Extremity Scale; VAS: Visual Analogue Scale; NBD: Neurogenic Bowel Dysfunction; BPI: Brief Pain Inventory.

3.5. Correlations among Fecal SCFA Concentrations, Distinct Bacterial Species, and Clinical Variables. In order to determine whether there are any significant relationships between various clinical indexes, including blood parameters, functional parameters, SCFA levels, and clinical parameters and distinct bacterial species, Pearson correlation analysis was used. Isovaleric acid ($r = -0.344$, $P = 0.030$) and isobutyric acid ($r = -0.335$, $P = 0.034$) were negatively correlated with serum total protein (TP). Valeric acid ($r = -0.338$, $P = 0.032$) and caproic acid ($r = -0.390$, $P = 0.012$) were negatively correlated with cholesterol (Figure 5(a)). Furthermore, isovaleric acid ($r = 0.636$, $P = 0.003$), isobutyric acid ($r = 0.606$, $P = 0.005$), and valeric acid ($r = 0.456$, $P = 0.043$) were positively correlated with NBD (Figure 5(b)).

The correlation analysis results demonstrated that *Akkermansia* ($r = -0.356$, $P = 0.024$), *Desulfovibrio* ($r = -0.316$, $P = 0.047$), and *Alloprevotella* ($r = -0.366$, $P = 0.020$) were significantly negatively correlated with HDL-C. *Akkermansia* was also negatively correlated with LDL-C ($r = -0.390$, $P = 0.012$) and TP ($r = -0.370$, $P = 0.019$). In addition, *Desulfovibrio* was significantly positively correlated with glucose (GLU) ($r = 0.352$, $P = 0.025$) (Figure 5(c)). *Akkermansia* ($r = 0.495$, $P = 0.026$), *Odoribacter* ($r = 0.467$, $P = 0.038$), *Alistipes* ($r = 0.579$, $P = 0.007$), *Parabacteroides* ($r = 0.522, P = 0.018$), and *Parasutterella* ($r = 0.465, P = 0.039$) were positively correlated with NBD. *Akkermansia*, *Odoribacter*, and *Desulfovibrio* were also negatively correlated with BI, FMA-UE, and FMA-LE ($P < 0.05$). Both *Paraprevotella* and *Sutterella* were positively correlated with portions of the BPI (ADL and walking) ($P < 0.05$), and both *Akkermansia* ($r = 0.605$, $P = 0.005$) and *Odoribacter* ($r = 0.471$, $P = 0.036$) were positively correlated with VAS (Figure 5(d)).

4. Discussion

Several investigations have documented differences in the gut microbiome composition between poststroke patients and healthy subjects. In this study, we discovered that stroke patients had lower species diversity and evenness. The findings are consistent with the studies using rodent experimental stroke models [31]. Multiple studies have showed a considerable rise in the prevalence of Prevotella and a decrease in the prevalence of *Bacteroides* in stroke patients. We also observed a considerable reduction of *Bacteroides* in stroke patients, consistent with the study of Yin et al. [19]. *Bacteroides* play a leading role in the intestinal microbiota and were found to be associated with obesity [32, 33]. Furthermore, it has been found that a decrease in *Bacteroides* in cases of obesity and overweight is also recognized as one of the important risk factors for the ischemic stroke [34]. In addition, *Bacteroides* taxa have been shown to ferment polysaccharides to both acetate and propionate [35]. Previous studies have demonstrated a decreased relative abundance of *Akkermansia* in poststroke patients [36, 37]. In contrast, *Akkermansia* increased significantly after stroke in the current study. There has been a study indicating that an increase in the number of *Akkermansia* bacteria in the poststroke may facilitate the *Akkermansia*-assisted healing of wound damage and reinforce the epithelial integrity of the intestinal mucosa [38]. Meanwhile, some studies have shown greater abundance of *Akkermansia* in hypertensive subjects and it related to an overall proinflammatory environment, which is considered to be one of the mechanisms of stroke occurrence [39, 40]. Therefore, it is tempting to hypothesize that this microbiota member may have a role in stroke, and future research may uncover more unique activities of *Akkermansia*.

Our findings also revealed a decline in the amounts of fecal acetic acid and propionic acid in stroke patients. The most prevalent SCFAs are acetic, butyric, and propionic acids [41], and it appears that maintaining the function of the gut barrier involves a significant amount of SCFA generation [42]. Multiple mechanisms have been identified by which SCFAs affect the host, involving the control of acetylation and methylation of histones, the regulation of G-protein coupled receptors, the facilitation of the secretion

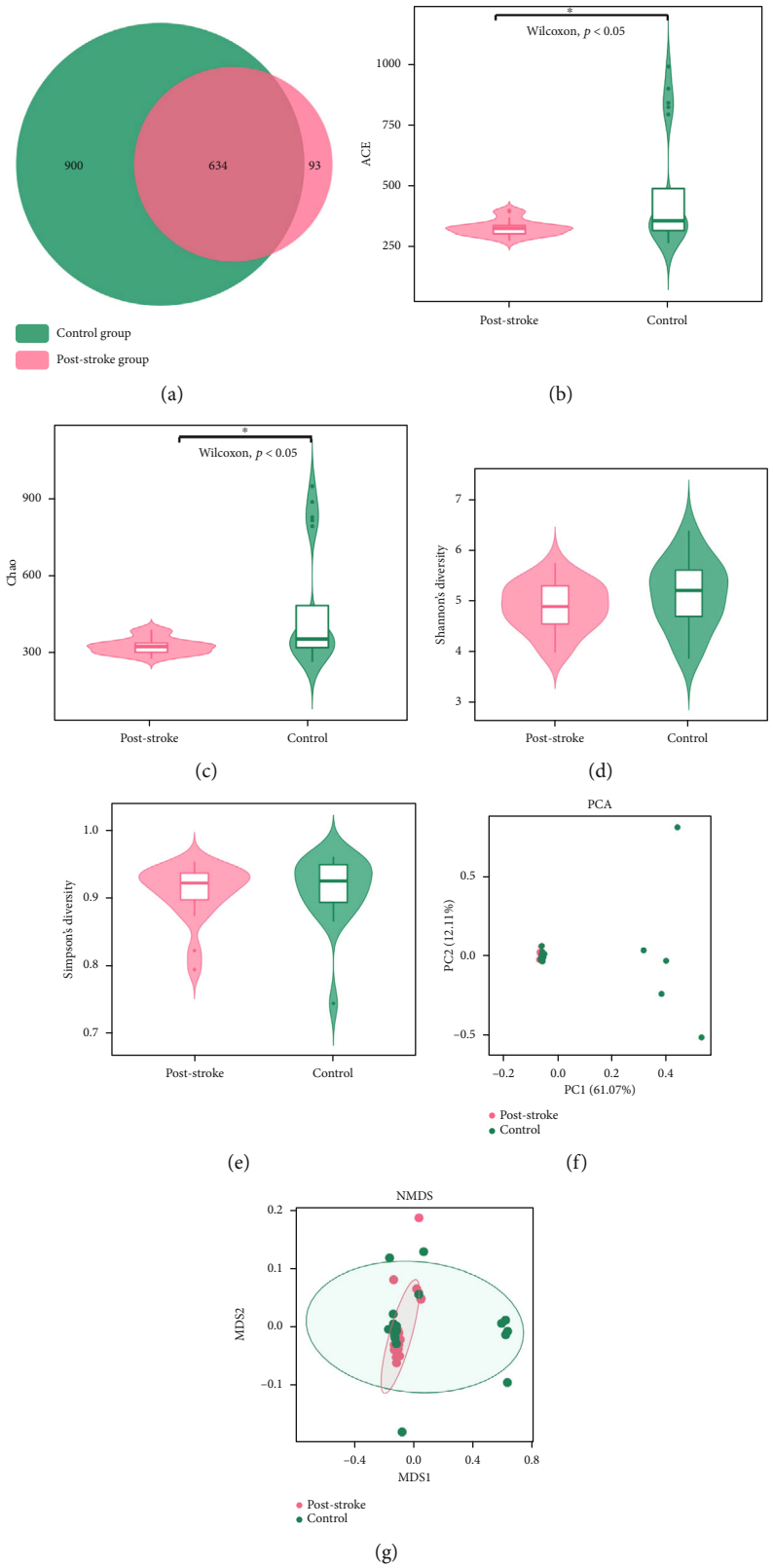

Figure 1: Gut microbiota diversity in poststroke and control subjects. (a) Venn diagram of common OTUs. (b–e) Alpha diversity at the OTU level as measured by the ACE (b), Chao (c), Shannon (d), and Simpson (e) index. (f, g) Beta diversity shown by PCA (f) and NMDS (g) based on weighted UniFrac distance. OTU: operational taxonomic unit; PCA: principal component analysis; NMDS: nonmetric multidimensional scaling.

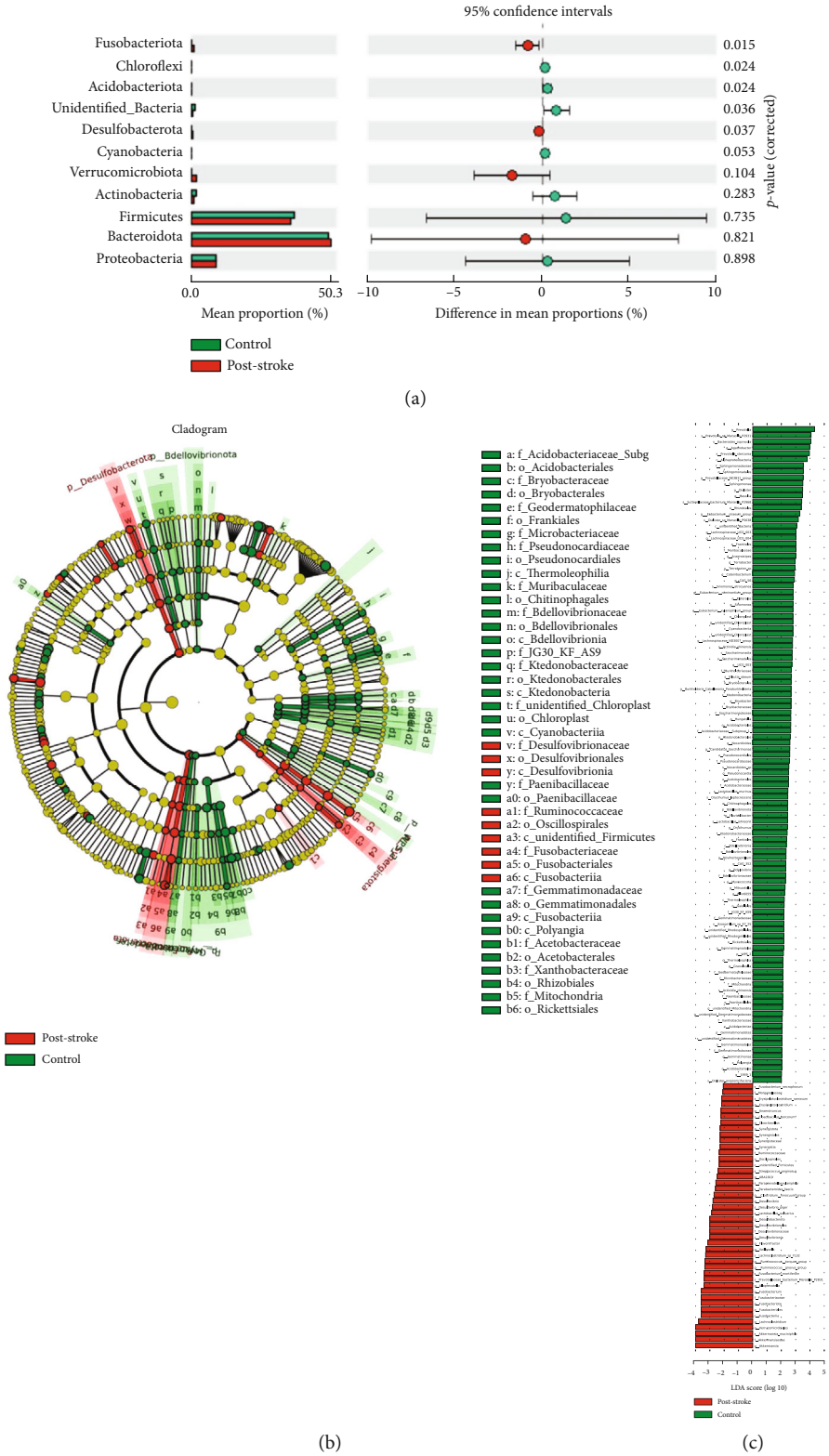

Figure 2: Compositional changes in the gut microbiota of poststroke and healthy controls. (a) The mean relative abundances of taxa at the phylum level in poststroke and control subjects. The red and green bars represent the relative abundances of taxa in poststroke patients and healthy controls, respectively. (b) LEfSe-generated cladograms. (c) LDA scores for the differentially abundant bacterial taxa (LDA score > 2.0). Taxa enriched in the control group are shown by green bars, whereas taxa enriched in the poststroke group are represented by red bars. LEfSe: linear discriminant effect size; LDA: linear discriminant analysis.

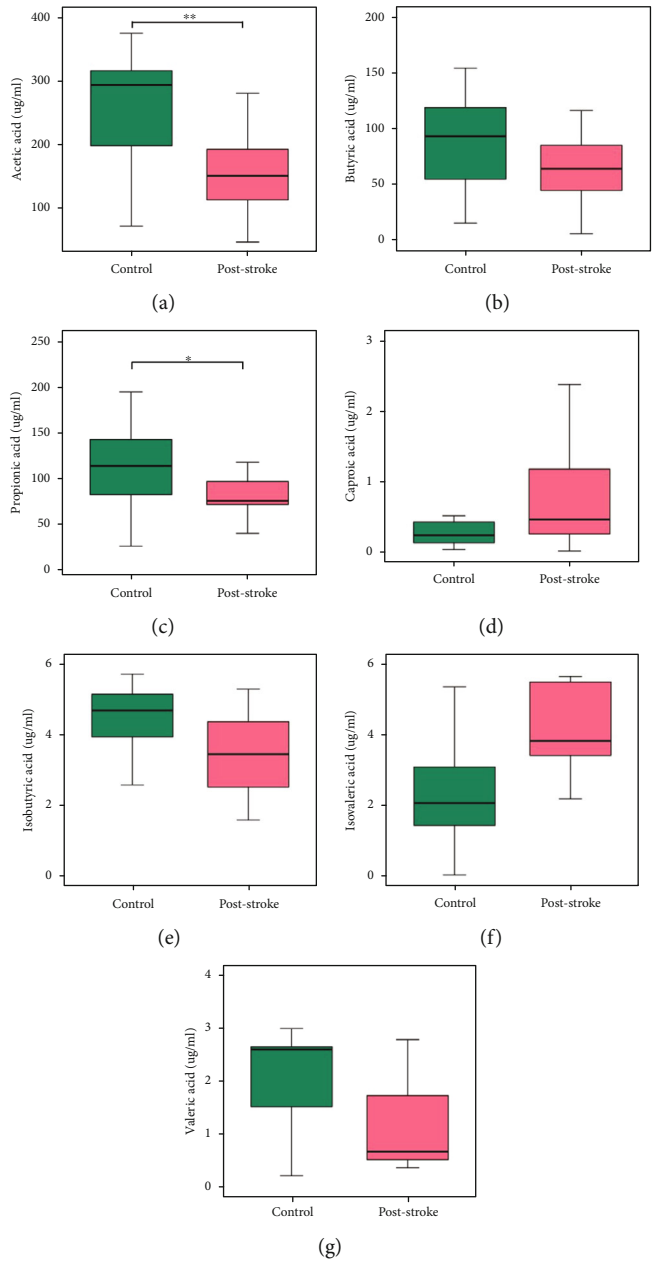

Figure 3: Fecal levels of SCFAs of poststroke and control patients. Boxplots showing the absolute concentration distribution of SCFAs measured in microgram per milliliter in the control group and poststroke group. (a) Acetic acid, (b) butyric acid, (c) propionic acid, (d) caproic acid, (e) isobutyric acid, (f) isovaleric acid, and (g) valeric acid. $^{*}P$ value ≤ 0.05; $^{**}P$ value ≤ 0.01; Wilcoxon rank-sum test. SCFAs: short-chain fatty acids.

of various hormones and neurochemicals, and the stimulation of signals through the vagus nerve [3]. SCFAs also serve as a source of energy in the mitochondria, which results in an exceptionally rapid absorption of these molecules in humans [43]. Acetic acid and propionic acid are the two primary metabolites that are produced by the microbiome of the gut, and they are responsible for regulating the actions of the microbiome-gut-brain axis. It has been demonstrated that certain concentrations of acetate and propionate exert a direct effect on the brain. The most frequent SCFA, acetate, is digested by the liver and subsequently transported to peripheral tissues, where it participates in cholesterol metabolism and lipogenesis and may have a role in the regulation of central appetite [44]. Acetate also acts as a fuel for the brain, and it easily penetrates through the blood–brain barrier from the periphery and is metabolized in the brain [45]. Previous research demonstrated that rats receiving fecal microbiota transplants from depressed patients showed increased fecal acetate and total SCFA concentrations as well as depression-like behavior [46]. According to Maltz et al., mice suffering from psychosocial stress exhibit a decrease in fecal acetate, which is accompanied by an increase in inflammation in the gut [47]. Additionally, the current study confirmed a negative association between fecal acetic acid

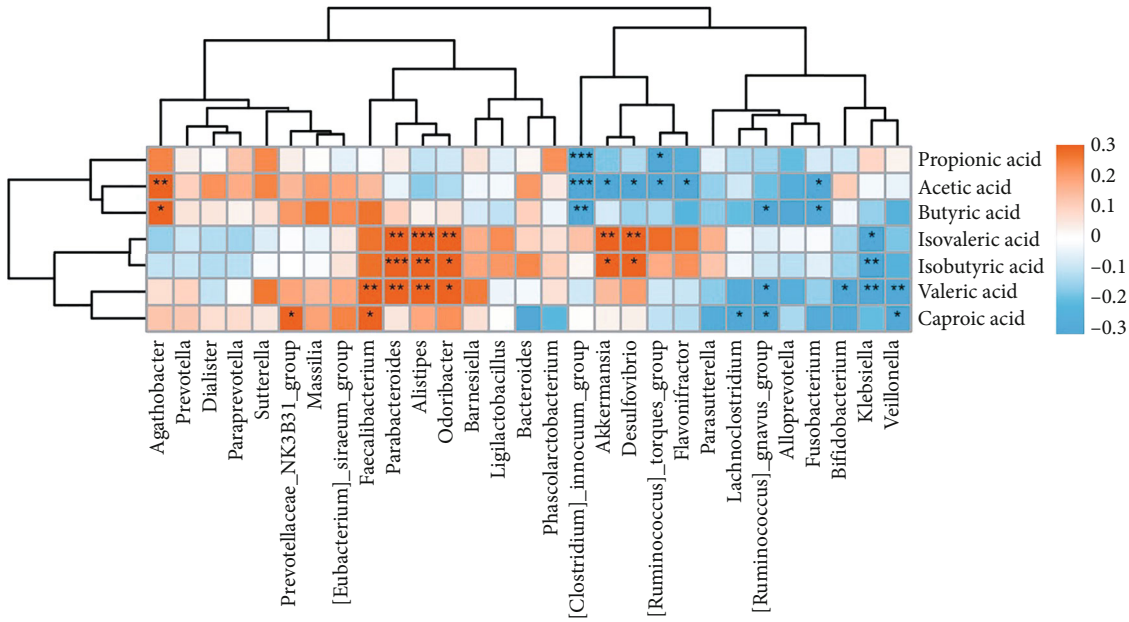

Figure 4: Correlation of the gut microbiota with fecal SCFA levels. SCFA: short-chain fatty acid.

and *Fusobacteria*, *Desulfovibrio*, and *Akkermansia*, which were significantly increased in poststroke patients. Propionate is the only SCFA that, after being digested, has the potential to be a significant source of glucose; it can be utilized for the production of energy and may have a role in decreasing cholesterol levels [48]. Some investigations have shown that propionate and butyrate can directly alter brain physiology and behavior by working on microglial cells and astrocytes to enhance anti-inflammatory activity and control general brain maintenance by scavenging damaged or unneeded neurons, synapses, and infectious agents [49, 50]. Collectively, our results and the aforementioned evidence indicate that acetate and propionate may govern the gut-brain axis in poststroke patients by modulating the immune system and energy metabolism.

Despite the fact that there was not a discernible change in the concentrations of caproic, valeric, isobutyric, isovaleric, or butyric acid between the two groups of our study, we found a negative correlation between *Fusobacteria* and butyrate, and *Fusobacteria* abundance was significantly higher in poststroke patients. There is evidence that butyrate stimulates vascular endothelial growth factor, which may play central roles in neurogenesis, angiogenesis, and functional recovery in the aftermath of stroke [51]. Furthermore, lower fecal butyrate concentrations were also associated with a high risk of stroke [52]. This might indicate that butyrate is involved in the progression of ischemic stroke. Isovaleric acid and isobutyric acid were negatively correlated with serum total protein, and valeric acid and caproic acid were negatively correlated with cholesterol. Isobutyrate, isovalerate, valerate, and caproate are generally considered the typical products of fat and protein fermentation, and they may have the ability to influence lipid metabolism, which affects the lipid profile of the host circulation in the disease state of stroke [35, 53]. These are the research directions warranting further investigation of these metabolites that have relatively low content.

According to the findings of our study, alterations in certain bacteria of the gut appear to be connected with improvements in pain, bowel function, ADL, and motor function of poststroke patients, prompting further investigation into the clinical impact of gut microbiota in this patient population. Some typical SCFA-producing bacteria, *Akkermansia* and *Odoribacter*, were found to be positively associated with VAS and NBD but negatively correlated with BI, FMA-UE, and FMA-LE. SCFAs are essential for intestinal barrier maintenance and microbial regulation [54]. Butyrate has a powerful anti-inflammatory effect on macrophages in the central nervous system, which can inhibit the inflammatory response, thus realizing the important role of nerve protection [55, 56]. Moreover, our current study is particularly concerned about chronic pain associated with stroke. Although SCFAs are crucial for regulating immune responses, their significance in neurological illnesses, particularly chronic pain, has just recently been recognized [57, 58]. SCFAs modulate the production of inflammatory mediators by macrophages, which is mainly associated with the attenuation of histone deacetylase (HDAC) activity and is able to attenuate pain behaviors [59, 60]. In a rat permanent middle cerebral artery occlusion model, valproic acid and butyrate, as HDAC inhibitors, presented antineuroinflammatory and neuroprotective effects after stroke [61]. This suggested that SCFAs may play a significant role as key mediators in the modulation of pain in poststroke patients. However, the mechanism underlying this phenomenon is not singular; there may be multiple mechanisms that influence each other and promote each other to ultimately achieve functional recovery.

Despite its innovative findings and clinical relevance, the present study included a number of limitations. Larger samples and multicenter studies would be required for further validation of the findings because the study was restricted to just one center, with a somewhat small patient enrollment. Then, the study investigated the changes in microbiota and

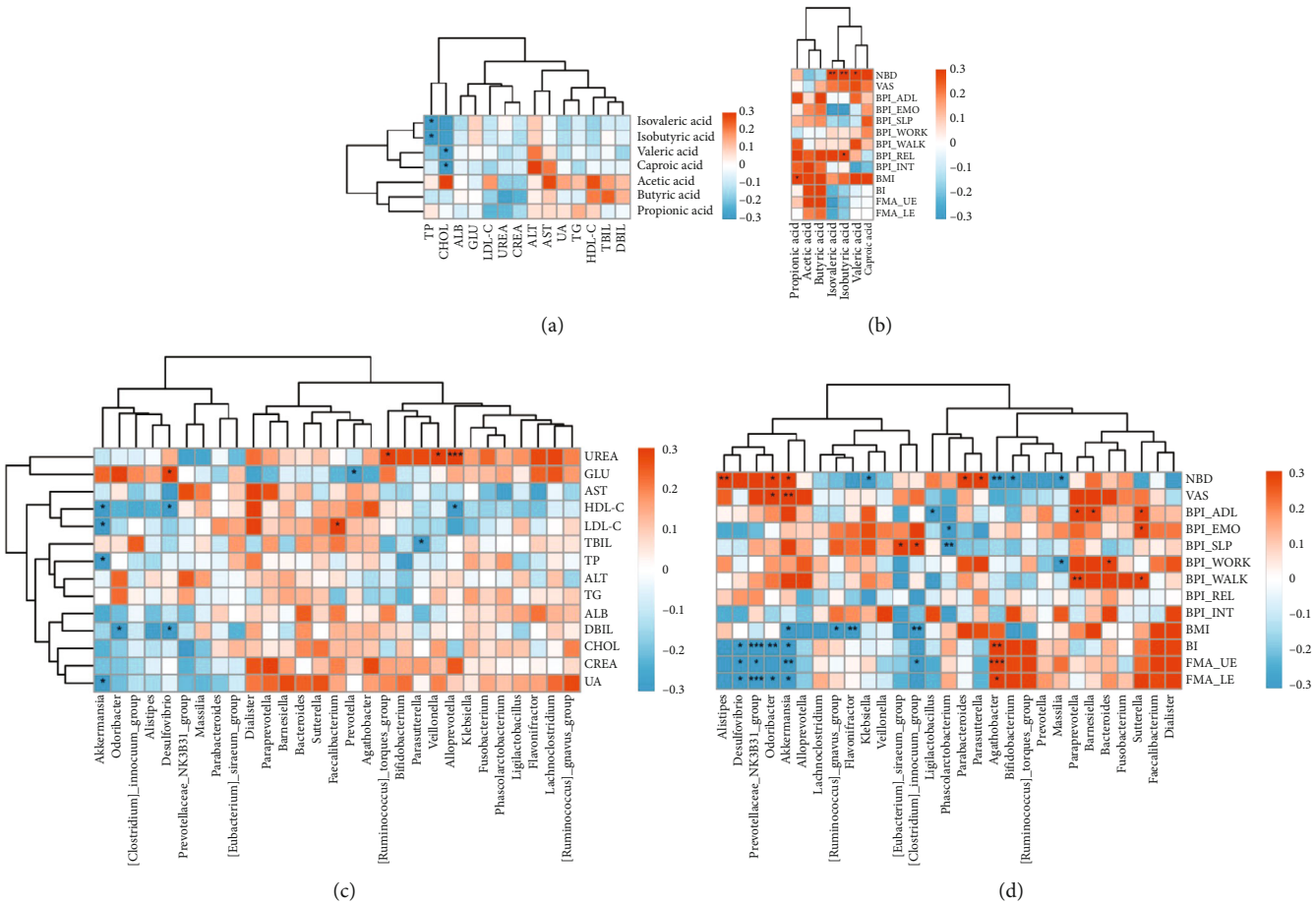

Figure 5: Correlations of fecal SCFA levels with serum index and poststroke clinical variation. (a) Correlation between fecal SCFA levels with serum index; (b) correlation between fecal SCFA levels with poststroke clinical variation; (c) correlation between differentiated bacterial genus with serum index; (d) correlation between differentiated bacterial genus with poststroke clinical variation. SCFA: short-chain fatty acid; DBil: direct bilirubin; TBil: total bilirubin; HDL-C: high-density lipoprotein cholesterol; TG: triglyceride; UA: uric acid; ALT: alanine aminotransferase; AST: aspartate aminotransferase; CREA: creatinine; UREA: urea; LDL-C: low-density lipoprotein cholesterol; GLU: glucose; ALB: albumin; CHOL: cholesterol; TP: total protein; NBD: Neurogenic Bowel Dysfunction; VAS: Visual Analogue Scale; BPI: Brief Pain Inventory; BMI: body mass index; BI: Barthel index; FMA-UE: Fugl-Meyer Assessment Upper Extremity Scale; FMA-LE: Fugl-Meyer Assessment Lower Extremity Scale.

SCFA levels following stroke and showed that there may be links between changes in the gut microbiota and clinical functional parameters. However, the scope of our clinical indicators is limited and needs to be further expanded and more needs to be done to adjust for the effects from the risk factors of stroke including dysglycemia and dyslipidemia. Further studies focusing on possible biological mechanisms are needed. Finally, grading for the severity of stroke in terms of mild, moderate, and severe was not performed, so the correlation between the severity of disease and gut microbiota could not be analyzed. This will be addressed specifically in future experiments.

5. Conclusion

In conclusion, a shift in the gut microbiota and its connection with fecal SCFAs was identified in poststroke patients in comparison to healthy controls. Significant associations were detected between alterations in SCFA levels, as well as distinctive gut microbiota and poststroke clinical outcomes or functional prognosis. Treatment strategies aimed at modulating the gut microbiota and SCFAs may have the potential to relieve pain and improve the functional prognosis after stroke.

Data Availability

The data used to support the findings of this study are available from the corresponding authors upon request.

Conflicts of Interest

The authors declare that there is no conflict of interest regarding the publication of this article.

Authors' Contributions

Xintong Zhang and Xiangyu Wang contributed equally to this work.

Acknowledgments

This work was supported the National Key Research & Development Program of the Ministry of Science and Technology of the People's Republic of China (Grant numbers 2018YFC2002300 and 2018YFC2002301) and the Nanjing Municipal Science and Technology Bureau (Grant number 2019060002).

References

[1] E. Parr, P. Ferdinand, and C. Roffe, "Management of acute stroke in the older person," *Geriatrics (Basel, Switzerland)*, vol. 2, no. 3, p. 27, 2017.

[2] C. O. Johnson, M. Nguyen, G. A. Roth et al., "Global, regional, and national burden of stroke, 1990-2016: a systematic analysis for the Global Burden of Disease Study 2016," *The Lancet Neurology*, vol. 18, no. 5, pp. 439–458, 2019.

[3] S. B. Chidambaram, A. G. Rathipriya, A. M. Mahalakshmi et al., "The influence of gut dysbiosis in the pathogenesis and management of ischemic stroke," *Cell*, vol. 11, no. 7, 2022.

[4] L. H. Morais, H. L. Schreiber IV, and S. K. Mazmanian, "The gut microbiota-brain axis in behaviour and brain disorders," *Nature Reviews Microbiology*, vol. 19, no. 4, pp. 241–255, 2021.

[5] C. Benakis, C. Poon, D. Lane et al., "Distinct commensal bacterial signature in the gut is associated with acute and long-term protection from ischemic stroke," *Stroke*, vol. 51, no. 6, pp. 1844–1854, 2020.

[6] J. Khlevner, Y. Park, and K. G. Margolis, "Brain-gut axis: clinical implications," *Gastroenterology Clinics of North America*, vol. 47, no. 4, pp. 727–739, 2018.

[7] T. G. Dinan and J. F. Cryan, "The microbiome-gut-brain axis in health and disease," *Gastroenterology Clinics of North America*, vol. 46, no. 1, pp. 77–89, 2017.

[8] J. A. Clark and C. M. Coopersmith, "Intestinal crosstalk: a new paradigm for understanding the gut as the "motor" of critical illness," *Shock (Augusta, Ga)*, vol. 28, no. 4, pp. 384–393, 2007.

[9] B. Lin, Y. Wang, P. Zhang, Y. Yuan, Y. Zhang, and G. Chen, "Gut microbiota regulates neuropathic pain: potential mechanisms and therapeutic strategy," *The Journal of Headache and Pain*, vol. 21, no. 1, p. 103, 2020.

[10] C. Benakis, C. Martin-Gallausiaux, J. P. Trezzi, P. Melton, A. Liesz, and P. Wilmes, "The microbiome-gut-brain axis in acute and chronic brain diseases," *Current Opinion in Neurobiology*, vol. 61, pp. 1–9, 2020.

[11] N. Li, X. Wang, C. Sun et al., "Change of intestinal microbiota in cerebral ischemic stroke patients," *BMC Microbiology*, vol. 19, no. 1, p. 191, 2019.

[12] D. J. Xu, K. C. Wang, L. B. Yuan et al., "Compositional and functional alterations of gut microbiota in patients with stroke," *Nutrition, Metabolism, and Cardiovascular Diseases : NMCD*, vol. 31, no. 12, pp. 3434–3448, 2021.

[13] Y. Dang, X. Zhang, Y. Zheng et al., "Distinctive gut microbiota alteration is associated with poststroke functional recovery: results from a prospective cohort study," *Neural Plasticity*, vol. 2021, Article ID 1469339, 16 pages, 2021.

[14] C. Tan, Q. Wu, H. Wang et al., "Dysbiosis of gut microbiota and short-chain fatty acids in acute ischemic stroke and the subsequent risk for poor functional outcomes," *JPEN Journal of Parenteral and Enteral Nutrition*, vol. 45, no. 3, pp. 518–529, 2021.

[15] C. R. Camara-Lemarroy, B. E. Ibarra-Yruegas, and F. Gongora-Rivera, "Gastrointestinal complications after ischemic stroke," *Journal of the Neurological Sciences*, vol. 346, no. 1-2, pp. 20–25, 2014.

[16] A. M. Valdes, J. Walter, E. Segal, and T. D. Spector, "Role of the gut microbiota in nutrition and health," *BMJ (Clinical research ed)*, vol. 361, article k2179, 2018.

[17] C. J. Schwarzbach and A. J. Grau, "Complications after stroke : clinical challenges in stroke aftercare," *Der Nervenarzt*, vol. 91, no. 10, pp. 920–925, 2020.

[18] B. W. Haak, W. F. Westendorp, T. S. R. van Engelen et al., "Disruptions of anaerobic gut bacteria are associated with stroke and post-stroke infection: a prospective case-control study," *Translational Stroke Research*, vol. 12, no. 4, pp. 581–592, 2021.

[19] J. Yin, S. X. Liao, Y. He et al., "Dysbiosis of gut microbiota with reduced trimethylamine-N-oxide level in patients with large-artery atherosclerotic stroke or transient ischemic attack," *Journal of the American Heart Association*, vol. 4, no. 11, 2015.

[20] M. F. Kilkenny, N. A. Lannin, C. S. Anderson et al., "Quality of life is poorer for patients with stroke who require an interpreter: an observational Australian registry study," *Stroke*, vol. 49, no. 3, pp. 761–764, 2018.

[21] L. Turner-Stokes and S. Rusconi, "Screening for ability to complete a questionnaire: a preliminary evaluation of the AbilityQ and ShoulderQ for assessing shoulder pain in stroke patients," *Clinical Rehabilitation*, vol. 17, no. 2, pp. 150–157, 2003.

[22] A. Turan, H. Essber, W. Saasouh et al., "Effect of intravenous acetaminophen on postoperative hypoxemia after abdominal surgery: the FACTOR randomized clinical trial," *JAMA*, vol. 324, no. 4, pp. 350–358, 2020.

[23] H. Harno, E. Haapaniemi, J. Putaala et al., "Central poststroke pain in young ischemic stroke survivors in the Helsinki Young Stroke Registry," *Neurology*, vol. 83, no. 13, pp. 1147–1154, 2014.

[24] M. González Viejo, M. Avellanet, L. Montesinos Magraner, K. Rojas Cuotto, P. Launois Obregón, and J. C. Perrot Gonzalez, "Spanish validation of the Neurogenic Bowel Dysfunction score - _NBD score_ \- in patients with central neurological injury," *Medicina Clinica*, vol. 157, no. 8, pp. 361–367, 2021.

[25] D. Darrow, D. Balser, T. I. Netoff et al., "Epidural spinal cord stimulation facilitates immediate restoration of dormant motor and autonomic supraspinal pathways after chronic neurologically complete spinal cord injury," *Journal of Neurotrauma*, vol. 36, no. 15, pp. 2325–2336, 2019.

[26] N. J. Klinedinst, S. B. Dunbar, and P. C. Clark, "Stroke survivor and informal caregiver perceptions of poststroke depressive symptoms," *Journal of Neuroscience Nursing*, vol. 44, no. 2, pp. 72–81, 2012.

[27] Z. Liu, Y. Liu, X. Tu et al., "High serum levels of malondialdehyde and 8-OHdG are both associated with early cognitive impairment in patients with acute ischaemic stroke," *Scientific Reports*, vol. 7, no. 1, p. 9493, 2017.

[28] Z. Wang, J. Pan, L. Wang, and P. Chen, "Clinical efficacy of comprehensive nursing in patients with cerebral hemorrhagic hemiplegia," *American Journal of Translational Research*, vol. 13, no. 5, pp. 5526–5532, 2021.

[29] N. Lodha, P. Patel, J. M. Shad, A. Casamento-Moran, and E. A. Christou, "Cognitive and motor deficits contribute to longer

braking time in stroke," *Journal of Neuroengineering and Rehabilitation*, vol. 18, no. 1, p. 7, 2021.

[30] X. Jin, Y. Ru, X. Zhang et al., "The influence of in vitro gastrointestinal digestion and fecal fermentation on the flowers of Juglans regia: changes in the active compounds and bioactivities," *Frontiers in Nutrition*, vol. 9, article 1014085, 2022.

[31] A. Houlden, M. Goldrick, D. Brough et al., "Brain injury induces specific changes in the caecal microbiota of mice via altered autonomic activity and mucoprotein production," *Brain, Behavior, and Immunity*, vol. 57, pp. 10–20, 2016.

[32] P. J. Turnbaugh, R. E. Ley, M. A. Mahowald, V. Magrini, E. R. Mardis, and J. I. Gordon, "An obesity-associated gut microbiome with increased capacity for energy harvest," *Nature*, vol. 444, no. 7122, pp. 1027–1031, 2006.

[33] J. Y. Yang, Y. S. Lee, Y. Kim, et al., "Gut commensal *Bacteroides acidifaciens* prevents obesity and improves insulin sensitivity in mice," *Mucosal Immunology*, vol. 10, no. 1, pp. 104–116, 2017.

[34] A. Cardoneanu, S. Cozma, C. Rezus, F. Petrariu, A. M. Burlui, and E. Rezus, "Characteristics of the intestinal microbiome in ankylosing spondylitis," *Experimental and Therapeutic Medicine*, vol. 22, no. 1, p. 676, 2021.

[35] L. P. Johnson, G. E. Walton, A. Psichas, G. S. Frost, G. R. Gibson, and T. G. Barraclough, "Prebiotics modulate the effects of antibiotics on gut microbial diversity and functioning in vitro," *Nutrients*, vol. 7, no. 6, pp. 4480–4497, 2015.

[36] W. Ji, Y. Zhu, P. Kan et al., "Analysis of intestinal microbial communities of cerebral infarction and ischemia patients based on high throughput sequencing technology and glucose and lipid metabolism," *Molecular Medicine Reports*, vol. 16, no. 4, pp. 5413–5417, 2017.

[37] Y. Chang, H. G. Woo, J. H. Jeong, G. H. Kim, K. D. Park, and T. J. Song, "Microbiota dysbiosis and functional outcome in acute ischemic stroke patients," *Scientific Reports*, vol. 11, no. 1, p. 10977, 2021.

[38] D. Stanley, R. J. Moore, and C. H. Y. Wong, "An insight into intestinal mucosal microbiota disruption after stroke," *Scientific Reports*, vol. 8, no. 1, p. 568, 2018.

[39] X. Dan, Z. Mushi, W. Baili et al., "Differential analysis of hypertension-associated intestinal microbiota," *International Journal of Medical Sciences*, vol. 16, no. 6, pp. 872–881, 2019.

[40] G. Silveira-Nunes, D. F. Durso, L. R. A. de Oliveira Jr. et al., "Hypertension is associated with intestinal microbiota dysbiosis and inflammation in a Brazilian population," *Frontiers in Pharmacology*, vol. 11, p. 258, 2020.

[41] J. Kim, H. Lee, J. An et al., "Alterations in gut microbiota by statin therapy and possible intermediate effects on hyperglycemia and hyperlipidemia," *Frontiers in Microbiology*, vol. 10, p. 1947, 2019.

[42] Y. Y. Sun, M. Li, Y. Y. Li et al., "The effect of _Clostridium butyricum_ on symptoms and fecal microbiota in diarrhea-dominant irritable bowel syndrome: a randomized, double-blind, placebo-controlled trial," *Scientific Reports*, vol. 8, no. 1, p. 2964, 2018.

[43] J. M. Medina, R. Fernández-López, J. Crespo, and F. Cruz, "Propionate fermentative genes of the gut microbiome decrease in inflammatory bowel disease," *Journal of Clinical Medicine*, vol. 10, no. 10, p. 2176, 2021.

[44] M. Ziętek, Z. Celewicz, J. Kikut, and M. Szczuko, "Implications of SCFAs on the parameters of the lipid and hepatic profile in pregnant women," *Nutrients*, vol. 13, no. 6, p. 1749, 2021.

[45] W. K. Wu, E. A. Ivanova, and A. N. Orekhov, "Gut microbiome: a possible common therapeutic target for treatment of atherosclerosis and cancer," *Seminars in Cancer Biology*, vol. 70, pp. 85–97, 2021.

[46] J. R. Kelly, Y. Borre, C. O' Brien et al., "Transferring the blues: depression-associated gut microbiota induces neurobehavioural changes in the rat," *Journal of Psychiatric Research*, vol. 82, pp. 109–118, 2016.

[47] R. M. Maltz, J. Keirsey, S. C. Kim et al., "Social stress affects colonic inflammation, the gut microbiome, and short-chain fatty acid levels and receptors," *Journal of Pediatric Gastroenterology and Nutrition*, vol. 68, no. 4, pp. 533–540, 2019.

[48] S. Aoe, K. Mio, C. Yamanaka, and T. Kuge, "Low molecular weight barley β-glucan affects glucose and lipid metabolism by prebiotic effects," *Nutrients*, vol. 13, no. 1, 2021.

[49] H. N. Sanchez, J. B. Moroney, H. Gan et al., "B cell-intrinsic epigenetic modulation of antibody responses by dietary fiber-derived short-chain fatty acids," *Nature Communications*, vol. 11, no. 1, p. 60, 2020.

[50] P. Mehrpouya-Bahrami, K. N. Chitrala, M. S. Ganewatta et al., "Blockade of CB1 cannabinoid receptor alters gut microbiota and attenuates inflammation and diet-induced obesity," *Scientific Reports*, vol. 7, no. 1, p. 15645, 2017.

[51] S. de Maistre, N. Vallée, S. Gaillard, C. Duchamp, and J. E. Blatteau, "Stimulating fermentation by the prolonged acceleration of gut transit protects against decompression sickness," *Scientific Reports*, vol. 8, no. 1, p. 10128, 2018.

[52] X. Zeng, X. Gao, Y. Peng et al., "Higher risk of stroke is correlated with increased opportunistic pathogen load and reduced levels of butyrate-producing bacteria in the gut," *Frontiers in Cellular and Infection Microbiology*, vol. 9, p. 4, 2019.

[53] J. Lee, V. R. Venna, D. J. Durgan et al., "Young versus aged microbiota transplants to germ-free mice: increased short-chain fatty acids and improved cognitive performance," *Gut Microbes*, vol. 12, no. 1, pp. 1–14, 2020.

[54] X. Li, C. He, N. Li et al., "The interplay between the gut microbiota and NLRP3 activation affects the severity of acute pancreatitis in mice," *Gut Microbes*, vol. 11, no. 6, pp. 1774–1789, 2020.

[55] M. W. Bourassa, I. Alim, S. J. Bultman, and R. R. Ratan, "Butyrate, neuroepigenetics and the gut microbiome: can a high fiber diet improve brain health?," *Neuroscience Letters*, vol. 625, pp. 56–63, 2016.

[56] R. Chen, Y. Xu, P. Wu et al., "Transplantation of fecal microbiota rich in short chain fatty acids and butyric acid treat cerebral ischemic stroke by regulating gut microbiota," *Pharmacological Research*, vol. 148, article 104403, 2019.

[57] Z. Li, T. Sun, Z. He et al., "SCFAs ameliorate chronic postsurgical pain-related cognition dysfunction via the ACSS2-HDAC2 Axis in rats," *Molecular Neurobiology*, vol. 59, no. 10, pp. 6211–6227, 2022.

[58] F. Zhou, X. Wang, B. Han et al., "Short-chain fatty acids contribute to neuropathic pain via regulating microglia activation and polarization," *Molecular Pain*, vol. 17, article 1744806921996520, 2021.

[59] R. Guo, L. H. Chen, C. Xing, and T. Liu, "Pain regulation by gut microbiota: molecular mechanisms and therapeutic potential," *British Journal of Anaesthesia*, vol. 123, no. 5, pp. 637–654, 2019.

[60] P. M. Cholan, A. Han, B. R. Woodie et al., "Conserved anti-inflammatory effects and sensing of butyrate in zebrafish," *Gut Microbes*, vol. 12, no. 1, pp. 1–11, 2020.

[61] H. J. Kim, M. Rowe, M. Ren, J. S. Hong, P. S. Chen, and D. M. Chuang, "Histone deacetylase inhibitors exhibit anti-inflammatory and neuroprotective effects in a rat permanent ischemic model of stroke: multiple mechanisms of action," *The Journal of Pharmacology and Experimental Therapeutics*, vol. 321, no. 3, pp. 892–901, 2007.

Hindawi
Neural Plasticity
Volume 2023, Article ID 2382980, 10 pages
https://doi.org/10.1155/2023/2382980

Research Article

The Effect of Swallowing Action Observation Therapy on Resting fMRI in Stroke Patients with Dysphagia

Ming Zeng,[1] **Zhongli Wang**,[1] **Xuting Chen**,[1] **Meifang Shi**,[1] **Meihong Zhu**,[1] **Jingmei Ma**,[1] **Yunhai Yao**,[1] **Yao Cui**,[2] **Hua Wu**,[1] **Jie Shen**,[1] **Lingfu Xie**,[3] **Jianming Fu**,[1] **and Xudong Gu**[1]

[1]*Department of Rehabilitation Medicine, The Second Affiliated Hospital of Jiaxing University, The Second Hospital of Jiaxing City, Jiaxing, Zhejiang Province 314000, China*
[2]*Department of Physical Therapy, Beijing Bo'ai Hospital, China Rehabilitation Research Center, Capital Medical University School of Rehabilitation Medicine, Beijing 100068, China*
[3]*First Clinical Medical College, Nanchang University, Nanchang, Jiangxi Province 330031, China*

Correspondence should be addressed to Jianming Fu; fjm_7758@163.com and Xudong Gu; jxgxd@hotmail.com

Received 18 November 2022; Revised 7 February 2023; Accepted 6 April 2023; Published 21 April 2023

Academic Editor: Yating Lv

Objective. Many stroke victims have severe swallowing problems. Previous neuroimaging studies have found that several brain regions scattered in the frontal, temporal, and parietal lobes, such as Brodmann's areas (BA) 6, 21, and 40, are associated with swallowing function. This study sought to investigate changes in swallowing function and resting-state functional magnetic resonance imaging (rs-fMRI) in stroke patients with dysphagia following action observation treatment. It also sought to detect changes in brain regions associated with swallowing in stroke patients. *Methods*. In this study, 12 healthy controls (HCs) and 12 stroke patients were recruited. Stroke patients were given 4 weeks of action observation therapy. In order to assess the differences in mfALFF values between patients before treatment and HCs, the fractional amplitude of low-frequency fluctuations (fALFF) in three frequency bands (conventional frequency band, slow-4, and slow-5) were calculated for fMRI data. The significant brain regions were selected as regions of interest (ROIs) for subsequent analysis. The mfALFF values were extracted from ROIs of the three groups (patients before and after treatment and HCs) and compared to assess the therapeutic efficacy. *Results*. In the conventional band, stroke patients before treatment had higher mfALFF in the inferior temporal gyrus and lower mfALFF in the calcarine fissure and surrounding cortex and thalamus compared to HCs. In the slow-4 band, there was no significant difference in related brain regions between stroke patients before treatment and HCs. In the slow-5 band, stroke patients before treatment had higher mfALFF in inferior cerebellum, inferior temporal gyrus, middle frontal gyrus, and lower mfALFF in calcarine fissure and surrounding cortex compared to HCs. We also assessed changes in aberrant brain activity that occurred both before and after action observation therapy. The mfALFF between stroke patients after therapy was closed to HCs in comparison to the patients before treatment. *Conclusion*. Action observation therapy can affect the excitability of certain brain regions. The changes in brain function brought about by this treatment may help to further understand the potential mechanism of network remodeling of swallowing function.

1. Introduction

One of the most typical causes of neurological disability in adults is stroke, and in some countries, it is also the leading cause of mortality. In the last ten years, the incidence and prevalence of stroke have increased. Every year, more than 2 million new stroke patients are diagnosed in China. Because of the aging population, the high prevalence of risk factors such as high blood pressure, and poor management, this burden is likely to grow even more [1]. Dysphagia is a

serious after-stroke complication that increases the risk of dehydration, malnutrition, aspiration pneumonia, and death [2]. According to an epidemiological survey, dysphagia affected 51.14 percent of the 2872 hospitalized stroke patients [3].

However, treatments for dysphagia caused by stroke are still limited. Traditional treatments include alternative feeding methods, dietary adjustment, behavioral and postural techniques, peripheral sensory and motor stimulation techniques, or active exercise designed to enhance the function of selected muscle groups and shorten exercise time at the beginning of swallowing [4, 5]. These techniques are designed to ensure the safety and proper food intake of stroke patients with dysphagia. Although these techniques have achieved some success, the effective recovery of dysphagia after stroke remains a challenge [2].

Swallowing is a complex sensory movement that involves the interaction between the cerebral cortex and subcortical nerves. The rehabilitation of swallowing function in stroke patients is impacted by a variety of factors, including the location of brain injury and the activation of brain swallowing-related cortical neuronal networks during swallowing [6]. Because the actual situation of stroke patients varies greatly, it is very important to set specific treatment plans for different patients; this makes treating dysphagia challenging for all stroke rehabilitation teams.

In recent years, due to the discovery of mirror neuron (MN) and ongoing research, a new rehabilitation method for stroke dysphagia has been developed. MN is a special type of neuron that triggers when one person performs an action or notices another person performing an action with a similar purpose [7]. The action observation therapy used in this study is based on this theory, but there is no completely unified discussion on the specific distribution of MN in the brain. The action observation therapy is a new method of rehabilitation which has become increasingly popular in recent years. Patients can improve their function by carefully observing the relevant motion videos and trying to imitate them. It is widely used in the study of recovery of poststroke dysfunction, such as swallowing and limb function [8].

Resting functional magnetic resonance imaging (fMRI) measures blood oxygen level-dependent (BOLD) signals, which are used to measure the spontaneous fluctuations of the brain. It has been widely used in Parkinson's disease [9, 10], Alzheimer's disease [11, 12], stroke [13, 14], and other diseases. Park et al. [15] found that in contrast to healthy people, stroke patients had decreased connection in the contralateral M1 and occipital cortex and increased functional connectivity in the bilateral thalamus, cerebellum, and ipsilateral frontal and parietal cortex. Additionally, it was discovered that motor recovery half a year after stroke was favorably connected with the functional relationship between the ipsilateral M1 area and contralateral thalamus, auxiliary motor area, and middle frontal gyrus. The synchronization of brain activity between regions is reflected in functional connections. Local indicators have also been used in stroke research recently. ALFF [16] was proposed by Zang et al. in 2007, which measures the oscillation's amplitude at low frequencies. Based on this, fALFF has been enhanced. The calculation of fALFF [17] value was first proposed by Zou et al. Generally, by computing the proportion of a certain frequency band's power spectrum to its whole spectrum, one can determine the fALFF. This approach can enhance the sensitivity and specificity of detecting spontaneous brain activity in fMRI by suppressing the nonspecific signal components. In the study of Zhan et al. [18], the value of fALFF was calculated, and it was found that the values of fALFF in the cerebellum, anterior lobe, precentral gyrus, superior frontal gyrus, and parietal lobe increased after scalp acupuncture intervention. A potential clinical measure for predicting motor impairment is thought to be the fALFF value of the ipsilateral precentral and postcentral gyrus. Researchers discovered that low-frequency oscillations (LFOs) with a frequency range of 0.073-0.025 Hz (slow-3: 0.073-0.198 Hz, slow-2: 0.198-0.25 Hz) are frequently found within the white matter and LFOs with a frequency range of 0.01-0.073 Hz (slow-4: 0.027-0.073 Hz, slow-5: 0.01-0.027 Hz) embody the spontaneous activities of neurons in the gray matter [19]. Prior research [20] largely concentrated on the variation of fALFF in conventional frequency band. However, no research has focused on whether there is band specificity in the brain regions that differ between stroke patients and healthy people in multifrequency bands. Therefore, this study intends to use rs-fMRI to conduct a multiband analysis of regional brain movement in healthy people and stroke patients, to find out the possible relationship between MN and action observation therapy from the mechanism level, and to evaluate the therapeutic effect of action observation therapy more comprehensively and deeply.

2. Materials and Methods

2.1. Participants. From June 2019 to January 2022, a case-control observational study was carried out in the Second Hospital of Jiaxing (Zhejiang, China). In this study, 12 stroke patients and 12 healthy controls (HCs) who were matched for age and gender were recruited. The inclusion criteria were in line with the latest stroke diagnostic criteria [21], and the patients with dysphagia were confirmed by swallowing angiography after the first stroke. The following were some of the patient exclusion criteria: (1) MRI contraindications, (2) mental and psychological diseases, (3) muscle disease, (4) oropharyngeal organic disease, (5) esophageal disease, and (6) unilateral spatial neglect. Each subject was assessed by general condition assessment and swallowing function assessment; the former includes Barthel index [22], Nutritional Risk Screening 2002 (NRS2002) [23], and John Hopkins Fall Risk Assessment Tool (JHFRAT) [24], while the latter was assessed by Eating Assessment Tool-10 (EAT-10) [25]. The Ethics Committee of the Second Affiliated Hospital of Jiaxing University approved this study (no. jxey-2018SKZ03), and it was conducted in accordance with the ethical guidelines outlined in the Declaration of Helsinki. A formal informed consent form was signed by each participant. The China Clinical Trial Registry has this trial listed (ChiCTR1900021849). Figure 1 depicts the detailed enrolling process; Figure 2 depicts the lesion area in 12 stroke patients; Tables 1 and 2 depict the detailed participant characteristics.

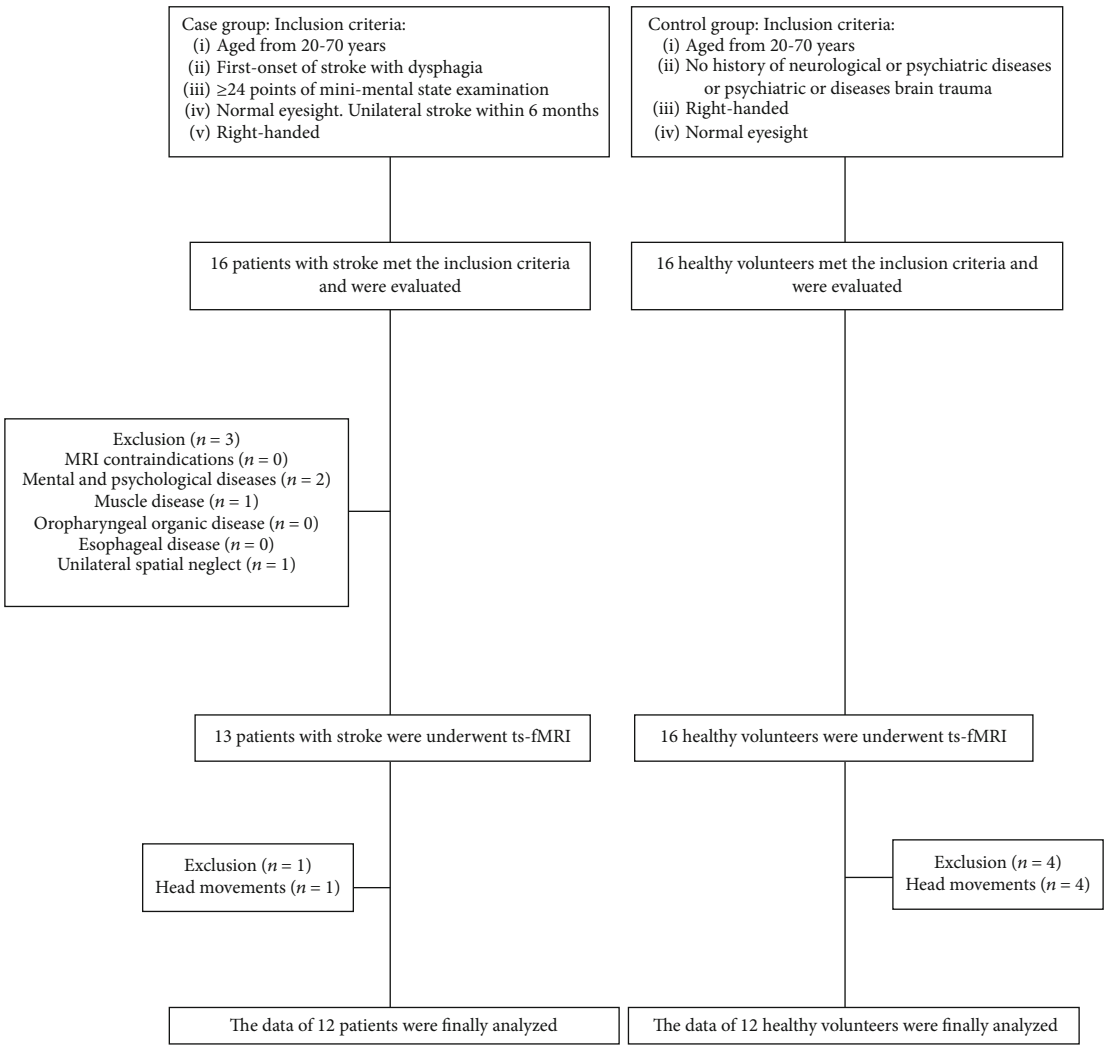

Figure 1: A schematic illustration of the participant selection process used in the present study.

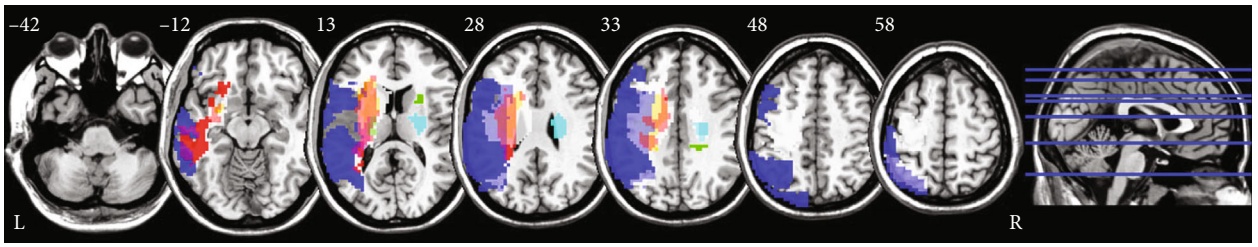

Figure 2: Focal area overlap map in stroke patients.

Table 1: Demographic and clinical characteristics of stroke patients and HCs.

Group	Course of disease (day)	Stroke classification		Lesion site		
		Cerebral infarction	Cerebral hemorrhage	Lateral ventricle	Frontal/temporal/parietal lobe	Basal ganglia
Healthy controls						
Stroke patients	34.25 ± 16.43*	9*	3*	2*	4*	6*

The stroke classification and lesion site between the two groups were compared using the chi-square test, and the course of disease was compared using the independent two-sample T-test. *$P < 0.001$, there was a statistical difference between the two groups.

Table 2: Demographic and clinical characteristics of stroke patients and HCs.

	Healthy controls ($n = 12$)	Stroke patients ($n = 12$)	Test statistic	P value
Age (year)	51.17 ± 13.02	66.08 ± 10.01	-3.147	0.005
Gender (male/female)	6/6	8/4	0.685	0.4076
Edu years (year)	12.08 ± 4.19	6.00 ± 1.81	4.619	<0.001
General function				
Barthel index	100	31.67 ± 18.13	13.055	<0.001
Nutritional Risk Screening 2002 (NRS2002)	0	1.83 ± 1.59	-4.004	<0.001
John Hopkins Fall Risk Assessment Tool (JHFRAT)	0	10.50 ± 4.03	-9.017	<0.001
Swallowing function				
Eating Assessment Tool-10 (EAT-10)	0	Pretreatment 32.00 ± 4.45	-24.901	<0.001
		Posttreatment 20.58 ± 4.46	8.486	<0.001

The gender distribution between the two groups was compared using the chi-square test, and the age, education year, Barthel index, NRS2002, JHFRAT, and EAT-10 scores were compared using the independent two-sample T-test. A paired T-test was used to compare the EAT-10 scores for the stroke group before and after treatment.

Table 3: Difference in brain regions of mfALFF between stroke patients before treatment and healthy controls.

Brain area	Voxel size	MNI coordinates	Peak T-value
Conventional band (0.01-0.08 Hz)			
Temporal_Inf_R	72	60 -21 -30	7.3028
Calcarine_L	145	-9 -87 6	-5.7019
Thalamus_L	49	-6 -15 12	-4.9552
Slow-4 band: 0.027-0.073			
NA			
Slow-5 band: 0.01-0.027			
Cerebellum_7b_L	54	-24 -75 -54	5.1098
Temporal_Inf_L	50	-33 -9 -45	5.6083
Calcarine_L	672	-12 -87 9	-6.6743
Frontal_Mid_R	89	42 30 45	5.5876

T: statistical value of mfALFF differences between the two groups (negative values: patients before treatment<healthy controls; positive values: patients before treatment>healthy controls); MNI: Montreal Neurological Institute Coordinate System or Template; Temporal_Inf_R: inferior temporal gyrus; Calcarine_L: calcarine fissure and surrounding cortex; Thalamus_L: thalamus; Cerebellum_7b_L: inferior cerebellum; Frontal_Mid_R: middle frontal gyrus.

2.2. Action Observation Therapy. We recorded a video of swallowing action observation of 7 min, which was used to observe the swallowing action of patients. The video includes the following: (a) swallow solid food and observe models chewing and swallowing rice from the front; (b) swallow solid food and observe the model chewing and swallowing an apple directly; (c) swallow solid food and observe the model chewing and swallowing an apple from the side; (d) swallow liquid food and observe the model swallowing yogurt directly; (e) empty swallowing and observe the model's imitation of swallowing three mouthpieces without drinking water (in (a), (b), (c), (d), and (e) swallowing videos, the model will properly raise her head and swallow during the process of chewing and swallowing and zoom in to show the swallowing movements of the model's mouth and throat); (f) facial muscle movement, positive observation of the model to do gill exercise; (g) neck movement, positive observation of the model's neck movement; (h) tongue muscle movement, positive observation of the model before and after the tongue stretching action; (i) tongue muscle resistance movement, observe the model's tongue resistance movement before and after stretching tongue, and use tongue depressor to exert resistance to the model's tongue muscle movement; (j) lip muscle movement, observe the lip movement of the model when making the sound of "e, u, and o"; and (k) lip muscle resistance action, front observation of the model with her lips on the tongue depressor and then against another person to remove the tongue depressor.

The single treatment time of action observation therapy was 10 minutes, once a day, five days a week for four weeks. In addition, each patient in the study received conventional swallowing therapy, including sensory stimulation, lingual resistance training, swallowing position placement, supraglottic swallowing, and Mendelson swallowing, for 30 minutes at a time, once a day, five days a week for four weeks.

2.3. MRI Data Acquisition. All stroke patients completed two MRI examinations (before and after treatment), while healthy controls completed only one MRI examination. The MRI was performed using a 3.0 T superconducting MRI equipment with a typical 32-channel head coil (Philips,

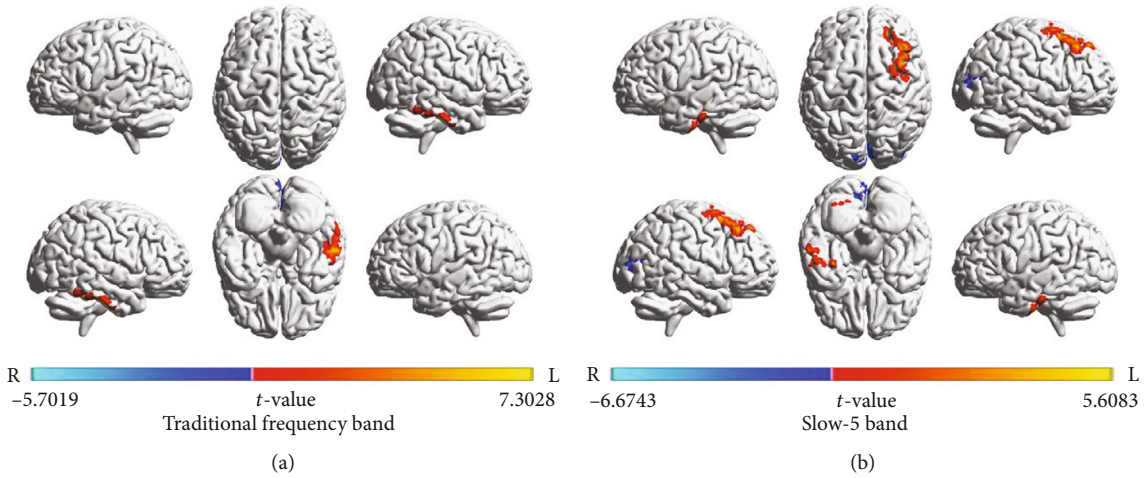

Figure 3: Difference of brain regions in three frequency bands between patients before treatment and HCs.

Table 4: The mfALFF values of these clusters were extracted for every participant and compared between each pair of the three groups in traditional band.

MNI coordinates	Brain region	Contrast	*T*-value	*P* value
60 -21 -30	Temporal_Inf_R (aal)	pre vs. con	4.351	0.0003
		pos vs. pre	0.7371	0.478
		pos vs. con	2.961	0.0075
-9 -87 6	Calcarine_L (aal)	pre vs. con	4.64	0.0001
		pos vs. pre	1.103	0.2959
		pos vs. con	4.028	0.0006
-6 -15 12	Thalamus_L (aal)	pre vs. con	3.876	0.0009
		pos vs. pre	0.5864	0.5706
		pos vs. con	3.158	0.0047

Temporal_Inf_R (aal): inferior temporal gyrus; Calcarine_L (aal): calcarine fissure and surrounding cortex; Thalamus_L (aal): thalamus.

Netherlands). The scanning sequences included initial positioning image, high-resolution T1-weighted structural image for segmentation, and registration. Every participant was once again instructed to unwind with their eyes closed, breathe deeply, and minimize head movements and cognitive processes. The use of sponge cushions helped to minimize head motion. Earplugs made of rubber were employed to block out scanner noise.

The following scan parameters were used to acquire anatomical pictures using a high-resolution T1-weighted 3-dimensional fast gradient echo sequence: 170 slices in sagittal position, slice thickness = 1 mm, slice gap = 0 mm, repetition time (TR) = 7.9 ms, echo time (TE) = 3.5 ms, flip angle = 8 ∘ , field of view (FOV) = 256 × 256 mm^2, acquisition matrix = 256 × 256, voxel size = 1 × 1 × 1 mm^3, and total scanning time = 5 min and 2 s.

Fast spin echo sequence uses the following parameters for conventional T2-weighted imaging to validate the lesion's location: 24 slices in axial transverse position, slice thickness = 5 mm, gap = 6 mm, TR = 3000 ms, TE = 80 ms, flip angle = 90 ∘ , FOV = 230 × 190 mm^2, acquisition matrix = 328 × 224, voxel dimensions = 0.4 × 0.4 × 6 mm^3, and total scanning time = 1 min and 30 s.

The following are the resting-state functional magnetic resonance data using echo-planar imaging (EPI) sequence: 46 slices in transverse section, slice thickness = 2.5 mm, slice gap = 0.5 mm, TR = 2000 ms, TE = 20 ms, flip angle = 90 ∘ , FOV = 240 × 240 mm^2, acquisition matrix = 96 × 96, and voxel dimensions = 2.5 × 2.5 × 3 mm^3. A skilled radiologist determined the volume of each patient's lesion. Using MRIcron software (http://www.mricro.com), the contour of the aberrant signal in the T2-weighted image was manually drawn layer by layer, and the T2-weighted image space was standardized to the Montreal Neurological Institute (MNI) space. Each patient's lesion mask was added together to create a lesion overlay, which was then placed on the MRIcron standard template. For all stroke patients, the final lesion overlays were displayed by layer.

2.4. fMRI Data Processing. Statistical Parametric Mapping 12 (SPM12) and RESTPlus version 1.25 were used to process all functional imaging data. To reduce the nonequilibrium effect of magnetization, in order to adapt to the surroundings, the first 10 time points were eliminated. Slice timing was applied to the remaining images for each individual (the number of time layers was 46 and the scanning

Table 5: The mfALFF values of these clusters were extracted for every participant and compared between each pair of the three groups in slow-5 band.

MNI coordinates	Brain region	Contrast	T-value	P value
-24 -75 -54	Cerebellum_7b_L (aal)	pre vs. con	2.887	0.0088
		pos vs. pre	0.3407	0.7404
		pos vs. con	2.896	0.0086
-33 -9 -45	Temporal_Inf_L (aal)	pre vs. con	2.097	0.0483
		pos vs. pre	0.3555	0.7296
		pos vs. con	1.528	0.1415
-12 -87 9	Calcarine_L (aal)	pre vs. con	4.865	<0.0001
		pos vs. pre	2.333	0.0418
		pos vs. con	3.743	0.0012
42 30 45	Frontal_Mid_R (aal)	pre vs. con	2.587	0.0172
		pos vs. pre	1.059	0.3145
		pos vs. con	1.874	0.0749

Cerebellum_7b_L (aal): inferior cerebellum; Temporal_Inf_L (aal): inferior temporal gyrus; Calcarine_L (aal): calcarine fissure and surrounding cortex; Frontal_Mid_R (aal): middle frontal gyrus.

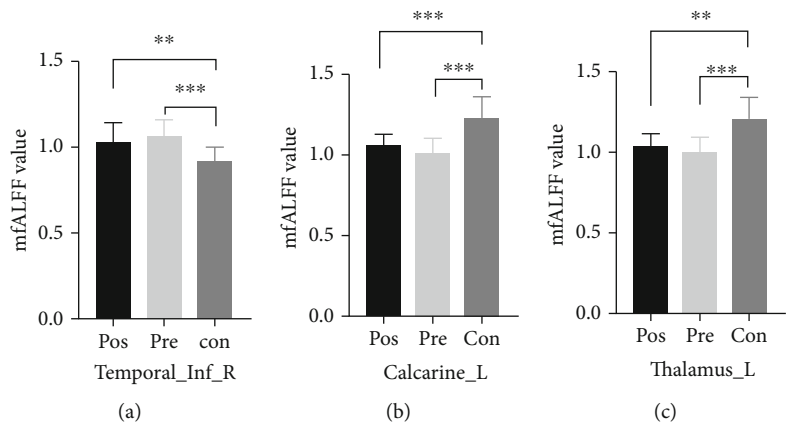

Figure 4: The difference of mfALFF in traditional frequency band between patients before and after treatment and HCs (pos: stroke patients after treatment; pre: stroke patients before treatment; con: healthy controls; ** indicated $P < 0.01$; *** indicated $P < 0.001$).

sequence was interlayer scanning), realignment (participants whose maximum head movement was larger than 3 mm and 3 degrees were excluded), segmentation, and coregistration with the subjects' own structural pictures. The Montreal Neurological Institute (MNI) space was used to normalize all the aligned functional pictures, and the standardized voxel size is $3 \times 3 \times 3\text{mm}^3$ and spatial smoothing of standardized functional images using Gaussian kernel $6 \times 6 \times 6$ mm; after removing the linear trend, the Friston-24 motion parameters, white matter, and cerebrospinal fluid signal were regressed out using detrending.

The fALFF was calculated for the preprocessed data. The frequency bands are, respectively, set to the traditional frequency bands (0.01-0.08 Hz), slow-4 (0.027-0.073 Hz), and slow-5 (0.01-0.027 Hz). Subsequent statistical analysis uses the mfALFF values. We followed the methods of Zhou et al. [26].

2.5. Statistical Analysis. In this study, age and course data were analyzed using the nonparametric test, gender data were analyzed using the Pearson chi-square test, and demographic characteristics were statistically analyzed using SPSS 25.0 software.

By using a two-sample T-test, the values of mfALFF in three frequency bands were compared between HCs and patients before treatment, and age, location of lesion, education level, and so on were taken as covariates. The difference in brain areas between the two groups was determined using the Gaussian random field (GRF) multiple comparison correction method, voxel $P < 0.005$, cluster $P < 0.05$. These several brain areas served as the ROI for the analyses that followed.

For each cluster survived after GRF corrected, the mean mfALFF value was extracted for every participant. Two-sample T-test was used for patients and HCs, and paired T-test was used for patients before and after treatment. Pearson correlation coefficients were calculated to evaluate the correlations between the change rate of regional brain index (mfALFF) and the change rate of swallowing function score in stroke patients before and after treatment. The threshold value was $P < 0.05$.

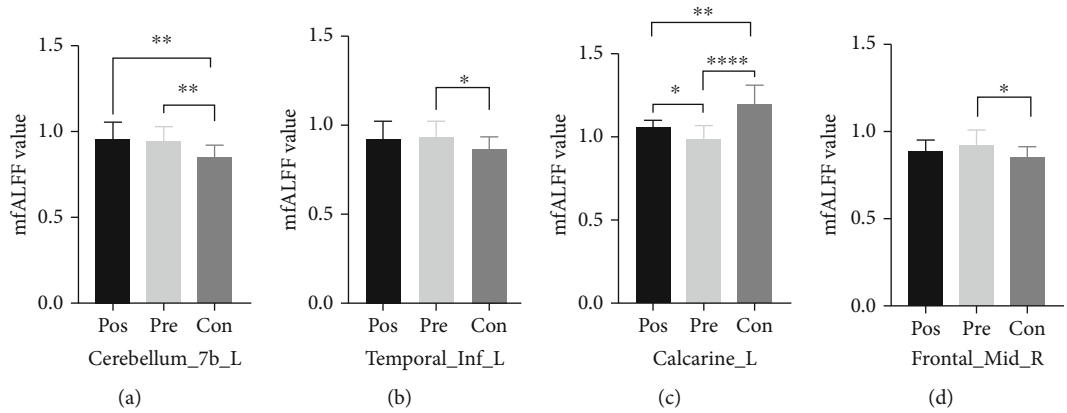

Figure 5: The difference of mfALFF in slow-5 band between patients before and after treatment and HCs (pos: stroke patients after treatment; pre: stroke patients before treatment; con: healthy controls; * indicated $P < 0.05$; ** indicated $P < 0.01$; **** indicated $P < 0.0001$).

Table 6: The correlation between the change rate of regional brain index (mfALFF) and swallowing function score in stroke patients before and after treatment.

Brain area	*r*-value	*P* value	Significant
Temporal_Inf_R (60 -21 -30)	0.683	0.0205	*
Calcarine_L (-9 -87 6)	-0.4467	0.1684	ns
Thalamus_L (-6 -15 12)	0.4112	0.209	ns
Cerebellum_7b_L (-24 -75 -54)	-0.1597	0.6391	ns
Temporal_Inf_L (-33 -9 -45)	0.1228	0.7191	ns
Calcarine_L (-12 -87 9)	-0.299	0.3718	ns
Frontal_Mid_R (42 30 45)	0.1795	0.5974	ns

*There was a correlation between the change rate of mfALFF and the change rate of swallowing function score; ns: there was no significant correlation between the change rate of mfALFF and the change rate of swallowing function score.

3. Results

3.1. Demographic and Clinical Characteristics. Tables 1 and 2 analyze the demographic information and clinical effectiveness of the three groups. There was no discernible gender difference between the patients before treatment and HCs, but there were statistical differences in age, course of disease, stroke classification, lesion site, education years, Barthel index, NRS2002, JHFRAT, and EAT-10. The EAT-10 score of the patients after treatment was lower than that before treatment.

3.2. Results of mfALFF Analysis. In the traditional frequency band, compared with HCs, the mfALFF of inferior temporal gyrus increased, and the calcarine fissure and surrounding cortex and thalamus decreased in stroke patients before treatment. In the slow-4 band, we did not find significant differences in mfALFF values between stroke patients before treatment and HCs. In the slow-5 band, compared with HCs, the mfALFF of inferior cerebellum, inferior temporal gyrus, and middle frontal gyrus increased, while calcarine fissure and surrounding cortex decreased in stroke patients before treatment (Table 3 and Figure 3).

3.3. Effect of Action Observation Therapy. In the ROIs detected in the traditional frequency band, the difference of mfALFF between the patients after treatment and the HCs was less than that before treatment, mainly in the following brain regions: inferior temporal gyrus and thalamus. In slow-4 frequency band, no effective ROIs were found. In the ROIs detected in the slow-5 band, the difference of mfALFF between the patients after treatment and the HCs was less than that before treatment, mainly in the following brain regions: inferior temporal gyrus, calcarine fissure and surrounding cortex, and middle frontal gyrus (Tables 4 and 5 and Figures 4 and 5).

3.4. Correlation Analysis. In this study, correlation analysis was conducted between the change rate of regional brain index (mfALFF) and the change rate of swallowing function score in stroke patients before and after treatment. The results showed that there was a significant correlation between the change rate of mfALFF in inferior temporal gyrus and the change rate of swallowing function score; other ROIs failed to suggest that there was a significant correlation between the change rate of mfALFF and the change rate of swallowing function score (Table 6 and Figure 6).

4. Discussion

In the multiband detection of this study, it was found that action observation therapy could significantly reduce the difference of mfALFF between patients after treatment and HCs compared with that before treatment between patients

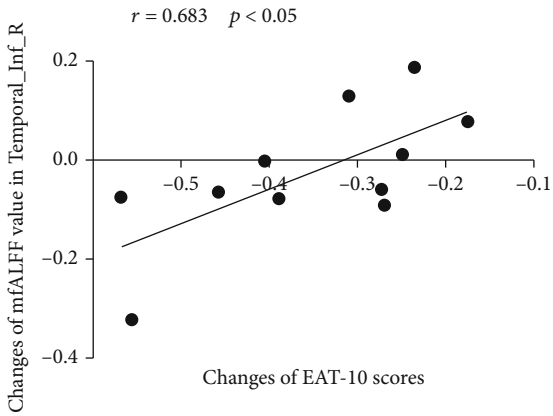

Figure 6: Analysis of the correlation between the change rate of mfALFF and swallowing function score in the inferior temporal gyrus.

and HCs. It is mainly distributed in the following brain regions: inferior temporal gyrus, calcarine fissure and surrounding cortex, thalamus, and middle frontal gyrus, most of which are independent of the lesions. There is also partial overlap between a small part of the brain area and the focus. In addition, we also found that there was a significant correlation between the change rate of mfALFF in the inferior temporal gyrus region and the change rate of swallowing function score before and after action observation therapy. All these results suggest that action observation therapy can indeed improve the swallowing function of stroke patients and change the excitability of brain areas related to swallowing.

Action observation therapy is a new method of rehabilitation, which is mostly used in exercise and speech rehabilitation [27–29]. The theoretical mechanism is believed to be related to MN, which are unique neurons that are activated when one person performs an action and watches another person perform a similar action [7]. Some scholars believe that there is also a MN system related to swallowing in the human brain. Ushioda et al. [30] employed magnetoencephalography to assess the active regions of the cerebral cortex connected to the MN system during swallowing in 10 healthy participants. The experimental group received visual and auditory swallowing stimulation, while the control group received static frame images and artificial sound. It was found that BA6 (premotor cortex and supplementary motor area) and BA40 (superior marginal gyrus) corresponding to the MN system were active between 620 and 720 milliseconds before drinking water was triggered. Jing et al. used task-stated fMRI to identify areas of the brain that were active during observation and swallowing in healthy subjects [31]. They discovered that the MN system, along with the left BA21 (middle temporal gyrus) and left BA6 (supplementary motor area), was engaged in the observation and execution of swallowing movements. However, from the observations obtained in this study alone, we were not able to find strong support for the role of MN in the relevant brain regions, but this does not exclude the possibility that mirror neurons play a role in the swallowing process, and the unsatisfactory results of the study may be influenced by various factors, including the persistent effect of the action observation therapy and individual differences in the site of lesion of the subjects.

There is also some evidence that the temporal lobe is associated with swallowing. Hamdy et al. [32] found that there is a significant asymmetry in the swallowing center between the hemispheres during volitional swallowing, and this recruitment phenomenon can involve the temporal lobe, the primary sensorimotor cortex, and other brain regions. The temporal lobe is believed by PET researchers to be crucial in helping people recognize the quality of their tastes. The prefrontal brain and temporal lobe may be involved in the control of swallowing [33]. The inferior temporal gyrus is connected to taste and appearance of food and may promote swallowing and diet control. Toogood et al. [34] suggested that different stages of swallowing are mediated by different regions. For example, a significant increase in activation in several regions, including bilateral thalamus, can be observed during swallowing preparation, while the increase in excitability during swallowing is mainly in the insular and dorsolateral peripheral cortex. Similarly, Martin et al. [35] found that during active tongue lifting, activation of related brain regions such as the thalamus and precentral/postcentral gyrus increased and that specific areas would mediate the occurrence and execution of a specific swallowing process. In addition, the middle frontal gyrus is also thought to be involved in continuous exercise programs, especially swallowing [36], which is active after swallowing water or saliva [37]. According to the above studies, we speculate that action observation therapy mainly affects the preparation stage of swallowing, including passive observation and unconscious simulation of swallowing movement. Thus, it promotes the activation of a series of brain regions, including the inferior temporal gyrus, middle frontal gyrus, and subcortical nuclei, promotes the swallowing compensatory function in the cortical and subcortical areas, and finally achieves the purpose of improving the swallowing function.

In addition, we also observed signal differences in some cerebellar regions between stroke patients before treatment and HCs, although we did not find the practical significance of cerebellum in the recovery of swallowing function in this study. However, there are still a large number of studies that support the cerebellum to actively participate in the regulation of human swallowing [32]. In early functional neuroimaging studies, chewing, oral and facial movement, lip and tongue movement, and whistling have been shown to activate the cerebellar hemisphere [38]. The cerebellum plays a role in the regulation of supplementary swallowing mechanism. This may explain how dysphagia manifests as delayed swallowing, malfunction of the esophageal sphincter, etc. We think this is also a research direction worth digging.

At the same time, this study also has some shortcomings: first, because the sample size is small and the subjects are not classified, the results of this study are only used as a preliminary exploratory study. Secondly, we only use a single resting-state fMRI to analyze the brain areas of MN, excluding EEG and motor-evoked potentials for further analysis. In order to better understand the impact of exercise observation therapy on the swallowing network, we therefore plan to examine the disease's subtypes on a large sample in the future and select a variety of detection methods to represent changes in brain excitability.

5. Conclusions

Using fALFF, we found that there was band specificity in the different brain regions between patients and healthy people before treatment; that is, the spatial distribution was different in different frequency bands. Observation of action therapy may improve the abnormal brain activity of patients to some extent and assist patients receive better care.

Data Availability

The data used to support the findings of this study are available from the corresponding authors upon reasonable request.

Conflicts of Interest

No conflicts of interest exist, according to the authors, with the publishing of this article.

Authors' Contributions

XDG and JMF guided the experimental design. MZ, ZLW, and XTC conceived, designed, and carried out this experiment. MZ prepared the manuscript after conducting data analysis. ZLW, YC, and LFX reviewed and edited the manuscript. XTC integrated the data and modified the paper. JMM participated in the fMRI. MFS, MHZ, HW, JS, and YHY collected data. The article's submission was approved by all authors who contributed to it. MZ, ZLW, and XTC contributed equally to this work and shared first authorship.

Acknowledgments

This study was supported by the Zhejiang Provincial Natural Science Foundation (no. LQ19H170001), Zhejiang Provincial Medical and Health Science and Technology Project (nos. 2022KY378 and 2022KY383), and Zhejiang Basic Public Welfare Research Project (no. LGF21H170003).

References

[1] S. Wu, B. Wu, M. Liu et al., "Stroke in China: advances and challenges in epidemiology, prevention, and management," *Lancet Neurology*, vol. 18, no. 4, pp. 394–405, 2019.

[2] S. Marchina, J. M. Pisegna, J. M. Massaro et al., "Transcranial direct current stimulation for post-stroke dysphagia: a systematic review and meta-analysis of randomized controlled trials," *Journal of Neurology*, vol. 268, no. 1, pp. 293–304, 2021.

[3] M. Zhang, C. Li, F. Zhang et al., "Prevalence of dysphagia in China: an epidemiological survey of 5943 participants," *Dysphagia*, vol. 36, no. 3, pp. 339–350, 2021.

[4] S. H. Doeltgen and M.-L. Huckabee, "Swallowing neurorehabilitation: from the research laboratory to routine clinical application," *Archives of Physical Medicine and Rehabilitation*, vol. 93, no. 2, pp. 207–213, 2012.

[5] M. Galovic, N. Leisi, M. Müller et al., "Lesion location predicts transient and extended risk of aspiration after supratentorial ischemic stroke," *Stroke*, vol. 44, no. 10, pp. 2760–2767, 2013.

[6] A. Sasegbon, M. Watanabe, A. Simons et al., "Cerebellar repetitive transcranial magnetic stimulation restores pharyngeal brain activity and swallowing behaviour after disruption by a cortical virtual lesion," *The Journal of Physiology*, vol. 597, no. 9, pp. 2533–2546, 2019.

[7] G. Rizzolatti and C. Sinigaglia, "The mirror mechanism: a basic principle of brain function," *Nature Reviews. Neuroscience*, vol. 17, no. 12, pp. 757–765, 2016.

[8] A. Shamili, A. Hassani Mehraban, A. Azad, G. R. Raissi, and M. Shati, "Effects of meaningful action observation therapy on occupational performance, upper limb function, and corticospinal excitability poststroke: a double-blind randomized control trial," *Neural Plasticity*, vol. 2022, Article ID 5284044, 12 pages, 2022.

[9] M. E. Johansson, I. G. M. Cameron, N. M. Van der Kolk et al., "Aerobic exercise alters brain function and structure in Parkinson's disease: a randomized controlled trial," *Annals of Neurology*, vol. 91, no. 2, pp. 203–216, 2022.

[10] S. G. Ryman and K. L. Poston, "MRI biomarkers of motor and non-motor symptoms in Parkinson's disease," *Parkinsonism & Related Disorders*, vol. 73, pp. 85–93, 2020.

[11] R. Ni, "Magnetic resonance imaging in animal models of Alzheimer's disease amyloidosis," *International Journal of Molecular Sciences*, vol. 22, no. 23, p. 12768, 2021.

[12] H. Yang, J. Zhang, and J. Cheng, "Effects of donepezil on the amplitude of low-frequency fluctuations in the brain of patients with Alzheimer's disease: evidence from resting-state functional magnetic resonance imaging," *Neuroreport*, vol. 32, no. 11, pp. 907–912, 2021.

[13] A. E. Ramage, S. Aytur, and K. J. Ballard, "Resting-state functional magnetic resonance imaging connectivity between semantic and phonological regions of interest may inform language targets in aphasia," *Journal of speech, language, and hearing research: JSLHR*, vol. 63, no. 9, pp. 3051–3067, 2020.

[14] A. Crofts, M. E. Kelly, and C. L. Gibson, "Imaging functional recovery following ischemic stroke: clinical and preclinical fMRI studies," *Journal of Neuroimaging: Official Journal of the American Society of Neuroimaging*, vol. 30, no. 1, pp. 5–14, 2020.

[15] C. Park, W. H. Chang, S. H. Ohn et al., "Longitudinal changes of resting-state functional connectivity during motor recovery after stroke," *Stroke*, vol. 42, no. 5, pp. 1357–1362, 2011.

[16] Y.-F. Zang, Y. He, C.-Z. Zhu et al., "Altered baseline brain activity in children with ADHD revealed by resting-state functional MRI," *Brain & Development*, vol. 29, no. 2, pp. 83–91, 2007.

[17] Q.-H. Zou, C.-Z. Zhu, Y. Yang et al., "An improved approach to detection of amplitude of low-frequency fluctuation (ALFF) for resting-state fMRI: fractional ALFF," *Journal of Neuroscience Methods*, vol. 172, no. 1, pp. 137–141, 2008.

[18] Y. Zhan, J. Pei, J. Wang et al., "Motor function and fALFF modulation in convalescent-period ischemic stroke patients after scalp acupuncture therapy: a multi-centre randomized controlled trial," *Acupuncture in Medicine: Journal of the British Medical Acupuncture Society*, 2022.

[19] X.-N. Zuo, A. Di Martino, C. Kelly et al., "The oscillating brain: complex and reliable," *NeuroImage*, vol. 49, no. 2, pp. 1432–1445, 2010.

[20] J.-J. Wang, X. Chen, S. K. Sah et al., "Amplitude of low-frequency fluctuation (ALFF) and fractional ALFF in migraine patients: a resting-state functional MRI study," *Clinical Radiology*, vol. 71, no. 6, pp. 558–564, 2016.

[21] A. Frank, "The latest national clinical guideline for stroke," *Clinical Medicine (London, England)*, vol. 17, no. 5, p. 478, 2017.

[22] S. Gupta, R. Yadav, and A. K. Malhotra, "Assessment of physical disability using Barthel index among elderly of rural areas of district Jhansi (U.P), India," *Journal of Family Medicine and Primary Care*, vol. 5, no. 4, pp. 853–857, 2016.

[23] S. Ahmadi, D. Firoozi, M. Dehghani et al., "Evaluation of nutritional status of intensive care unit COVID-19 patients based on the nutritional risk screening 2002 score," *International Journal of Clinical Practice*, vol. 2022, article 2448161, 6 pages, 2022.

[24] Y. Chen, L. Lv, C. Wu et al., "Assessment of the predictive ability of the Johns Hopkins fall risk assessment tool (Chinese version) in inpatient settings," *Journal of Advanced Nursing*, vol. 78, no. 12, pp. 4054–4061, 2022.

[25] P.-p. Zhang, Y. Yuan, D.-z. Lu et al., "Diagnostic accuracy of the eating assessment tool-10 (EAT-10) in screening dysphagia: a systematic review and meta-analysis," *Dysphagia*, vol. 38, no. 1, pp. 145–158, 2023.

[26] J. Zhou, X. Ma, C. Li et al., "Frequency-specific changes in the fractional amplitude of the low-frequency fluctuations in the default mode network in medication-free patients with bipolar II depression: a longitudinal functional MRI study," *Frontiers in Psychiatry*, vol. 11, article 574819, 2021.

[27] M. Tani, Y. Ono, M. Matsubara et al., "Action observation facilitates motor cortical activity in patients with stroke and hemiplegia," *Neuroscience Research*, vol. 133, pp. 7–14, 2018.

[28] W.-L. Chen, Q. Ye, S.-C. Zhang et al., "Aphasia rehabilitation based on mirror neuron theory: a randomized-block-design study of neuropsychology and functional magnetic resonance imaging," *Neural Regeneration Research*, vol. 14, no. 6, pp. 1004–1012, 2019.

[29] H. Mao, Y. Li, L. Tang et al., "Effects of mirror neuron system-based training on rehabilitation of stroke patients," *Brain and Behavior*, vol. 10, no. 8, article e01729, 2020.

[30] T. Ushioda, Y. Watanabe, Y. Sanjo et al., "Visual and auditory stimuli associated with swallowing activate mirror neurons: a magnetoencephalography study," *Dysphagia*, vol. 27, no. 4, pp. 504–513, 2012.

[31] Y.-H. Jing, T. Lin, W.-Q. Li et al., "Comparison of activation patterns in mirror neurons and the swallowing network during action observation and execution: a task-based fMRI study," *Frontiers in Neuroscience*, vol. 14, p. 867, 2020.

[32] S. Hamdy, J. C. Rothwell, D. J. Brooks, D. Bailey, Q. Aziz, and D. G. Thompson, "Identification of the cerebral loci processing human swallowing with H2 (15) O PET activation," *Journal of Neurophysiology*, vol. 81, no. 4, pp. 1917–1926, 1999.

[33] J. Gao, X. Guan, Z. Cen et al., "Alteration of brain functional connectivity in Parkinson's disease patients with dysphagia," *Dysphagia*, vol. 34, no. 4, pp. 600–607, 2019.

[34] J. A. Toogood, R. C. Smith, T. K. Stevens et al., "Swallowing preparation and execution: insights from a delayed-response functional magnetic resonance imaging (fMRI) study," *Dysphagia*, vol. 32, no. 4, pp. 526–541, 2017.

[35] R. E. Martin, B. J. Mac Intosh, R. C. Smith et al., "Cerebral areas processing swallowing and tongue movement are overlapping but distinct: a functional magnetic resonance imaging study," *Journal of Neurophysiology*, vol. 92, no. 4, pp. 2428–2443, 2004.

[36] J. Tanji, K. Shima, and H. Mushiake, "Multiple cortical motor areas and temporal sequencing of movements," *Brain Research. Cognitive Brain Research*, vol. 5, no. 1-2, pp. 117–122, 1996.

[37] P. Sörös, Y. Inamoto, and R. E. Martin, "Functional brain imaging of swallowing: an activation likelihood estimation meta-analysis," *Human Brain Mapping*, vol. 30, no. 8, pp. 2426–2439, 2009.

[38] X. Ruan, G. Zhang, G. Xu et al., "The after-effects of theta burst stimulation over the cortex of the Su-prahyoid muscle on regional homogeneity in healthy subjects," *Frontiers in Behavioral Neuroscience*, vol. 13, p. 35, 2019.

Hindawi
Neural Plasticity
Volume 2023, Article ID 5044065, 23 pages
https://doi.org/10.1155/2023/5044065

Review Article

From Molecule to Patient Rehabilitation: The Impact of Transcranial Direct Current Stimulation and Magnetic Stimulation on Stroke—A Narrative Review

Anca Badoiu,[1] Smaranda Ioana Mitran,[2] Bogdan Catalin,[2,3] Tudor Adrian Balseanu,[2,3] Aurel Popa-Wagner,[3] Florin Liviu Gherghina,[4] Carmen Valeria Albu,[1] and Raluca Elena Sandu[1]

[1]*Department of Neurology, Clinical Hospital of Neuropsychiatry, 200349 Craiova, Romania*
[2]*Department of Physiology, University of Medicine and Pharmacy of Craiova, 200349 Craiova, Romania*
[3]*Experimental Research Centre for Normal and Pathological Aging, University of Medicine and Pharmacy of Craiova, 200349 Craiova, Romania*
[4]*Department of Physical Medicine and Rehabilitation, University of Medicine and Pharmacy of Craiova, 200349 Craiova, Romania*

Correspondence should be addressed to Florin Liviu Gherghina; florin.gherghina@umfcv.ro
and Carmen Valeria Albu; carmenvaleriaalbu@yahoo.com

Anca Badoiu, Smaranda Ioana Mitran, and Bogdan Catalin contributed equally to this work.

Received 29 July 2022; Revised 10 November 2022; Accepted 28 November 2022; Published 28 February 2023

Academic Editor: Zhiyong Zhao

Stroke is a major health problem worldwide, with numerous health, social, and economic implications for survivors and their families. One simple answer to this problem would be to ensure the best rehabilitation with full social reintegration. As such, a plethora of rehabilitation programs was developed and used by healthcare professionals. Among them, modern techniques such as transcranial magnetic stimulation and transcranial direct current stimulation are being used and seem to bring improvements to poststroke rehabilitation. This success is attributed to their capacity to enhance cellular neuromodulation. This modulation includes the reduction of the inflammatory response, autophagy suppression, antiapoptotic effects, angiogenesis enhancement, alterations in the blood-brain barrier permeability, attenuation of oxidative stress, influence on neurotransmitter metabolism, neurogenesis, and enhanced structural neuroplasticity. The favorable effects have been demonstrated at the cellular level in animal models and are supported by clinical studies. Thus, these methods proved to reduce infarct volumes and to improve motor performance, deglutition, functional independence, and high-order cerebral functions (i.e., aphasia and hemineglegence). However, as with every therapeutic method, these techniques can also have limitations. Their regimen of administration, the phase of the stroke at which they are applied, and the patients' characteristics (i.e., genotype and corticospinal integrity) seem to influence the outcome. Thus, no response or even worsening effects were obtained under certain circumstances both in animal stroke model studies and in clinical trials. Overall, weighing up risks and benefits, the new transcranial electrical and magnetic stimulation techniques can represent effective tools with which to improve the patients' recovery after stroke, with minimal to no adverse effects. Here, we discuss their effects and the molecular and cellular events underlying their effects as well as their clinical implications.

1. Introduction

Stroke represents one of the main causes of death and a major cause of disability worldwide, with most survivors reporting a decrease in life quality [1, 2]. With an annual increase in its incidence, stroke involves significant economic costs both direct and indirect [3, 4]. As most patients present far beyond the therapeutic window for thrombectomy/thrombolysis,

rehabilitation is their only option to improve physical, cognitive, communicative, emotional, and social status [2, 5]. A plethora of rehabilitation programs aimed to improve motor function, balance, walking, and daily living activities have been developed and are being used by healthcare professionals. For example, thousands of repetitions of reach-to-grasp movements are necessary to have an impact on the functional recovery of the upper limb after stroke [6]. Specific recovery strategies seem to work better than others depending mainly on the extent of the infarct area. As such, patients who do not suffer a visual impairment can be subjected to movement performance therapies using mirrors, video, or graphical representations of three-dimensional motion capture as feedback [7, 8]. The major aim of any physical therapy is to promote neuroplasticity and motor recovery after a stroke [9]. The amount and intensity of exercise, personal implication and/or determination, and task-oriented training play a crucial role in the outcome [10]. However, physical recovery is highly dependent on the severity of the stroke. A severe stroke (significant brain tissue damage) induces multiple neurological impairments leading to a considerable loss of function [11]. For those patients, rehabilitation is particularly focused on both function restoration (not always possible or often incomplete) and reduction of immobility-related complications, a burden for caregivers of severe stroke survivors.

With classical rehabilitation having certain limitations in severe cases of stroke, modern techniques such as transcranial magnetic stimulation (TMS) and transcranial direct current stimulation (tDCS) started to make their way as an alternative or complementary method in impacting the consequences of stroke. Being relatively inexpensive and easy to administer [12], in recent years, these noninvasive brain stimulation (NIBS) techniques were applied for the treatment of a variety of conditions in different specialties such as psychiatry, neurology, and rehabilitation. In poststroke rehabilitation, they seem to bring improvements mainly through a cellular process of neuromodulation [13–15], as they counteract the molecular and cellular mechanisms involved in the pathophysiology of cerebral ischemia [16–20]. These NIBS techniques exert their neuroprotective [19–22] or neuroregenerative [23–26] characteristics principally by modifying brain excitability [18, 27–29]. However, their effects were not always favorable, and they seem to be influenced by the type of protocol used [21, 28] or by the heterogenous capacity of individuals to induce M1 plasticity, both in healthy and poststroke-treated patients [30–32]. Regarding protocols, a meta-analysis on 445 stroke patients evidenced that bilateral transcranial electric stimulation and cathodal tDCS over the contralesional hemisphere were superior to other stimulation montages/patterns/protocols [33]. Promising results were also obtained with different protocols of NIBS applied to poststroke survivors. A meta-analysis of more than 600 subacute and chronic poststroke patients revealed the beneficial effects of combined TMS and mirror therapy and tDCS and mirror therapy on upper extremity dysfunction [34].

The moment at which NIBS is applied after stroke affects patients' recovery. For example, encouraging results were observed after repetitive tDCS, with amelioration of the motor and somatosensory functions in patients during the first-month poststroke [35]. Interestingly, a similar positive outcome was also reported for chronic patients [34, 36, 37] or even severely ill patients [38]. Clear benefits were observed on motor function with TMS being applied during the acute phase of stroke [39–41], while more diverging results were obtained in the subacute or chronic phases by using only NIBS [42–44]. Another beneficial result of NIBS on poststroke patients is the reduction in depression scale scores [45–47] and improvement of aphasia [48], episodic memory, working memory [49], or attention [50, 51].

In this review, we will focus on reported experimental and clinical findings underlying the molecular, cellular, and clinical reasoning behind modern poststroke rehabilitation strategies. The present work reflects both our own experience and literature search online using resources from PubMed, Clarivate, and other scientific databases.

2. Transcranial Electric Stimulation Overview

Transcranial electric stimulation (TES) is a noninvasive method used to modulate brain functions (i.e., motor, sensory, and cognitive) with applicability to many neurological conditions such as stroke [52], multiple sclerosis [53, 54], epilepsy [55], Alzheimer's disease [56, 57], and Parkinson's disease [58, 59]. It uses scalp electrodes to deliver positive (cathodal) or negative (anodal) currents to specific cortical regions. The low intensity of the current (1-2 mA) does not trigger an action potential but rather alters neuronal excitability by modifying the membrane polarization [18]. Anodal stimulation generates depolarization, while cathodal stimulation results in hyperpolarization [27, 60]. The main effect of TES can be the modulation of ongoing neural oscillations [61, 62] or neuroplasticity induction [63, 64]. Thus, the neurophysiological effects of TES can be classified as immediate [65] and long-lasting [66]. While immediate effects are due to changes in synaptic activity level and neuronal membrane properties [62, 65], long-lasting effects outlast the period of stimulation and are generated through modifications of intracellular calcium dynamics and mechanisms of synaptic plasticity supporting long-term potentiation (LTP) or long-term depression (LTD) [63, 64].

In practice, three different approaches to TES are known: transcranial direct stimulation (tDCS) [18, 67], transcranial alternating current stimulation (tACS) [68, 69], and transcranial random noise stimulation (tRNS) [70]. The main difference between these three approaches lies in the way the current is delivered. In tDCS, the electrical current flows unidirectionally from the anode to the cathode. In tACS, the current flows sinusoidally with a particular frequency and stimulation amplitude from the anode to the cathode in one half-cycle and in the reverse direction in the second half-cycle. In tRNS, alternating current oscillates at random frequencies [71, 72]. Generally, two protocols of tDCS are used for the treatment of stroke. Unilateral tDCS involves the placement of an active electrode, either anodal or cathodal, over the brain area (i.e., primary motor cortex-M1) with a contralateral cathodal or anodal supraorbital reference electrode. Dual tDCS is a technique used by placing

both electrodes simultaneously over the hemispheres: the cathode is placed over the M1 of the nonlesioned hemisphere, and the anode is placed over the M1 of the lesioned hemisphere [73].

2.1. Experimental Data Supporting the Therapeutic Use of TES. Studies done on animal stroke models showed that TES provides *neuroprotection* [17, 21, 22, 74–76] by attenuating some of the ischemia-induced cerebral injury mechanisms such as glutamate excitotoxicity [77–80], neuroinflammation [81–83], oxidative stress [84–86], blood-brain barrier dysfunction [87, 88], apoptosis [89, 90], autophagy [91–94], and cortical spreading depression [95, 96]. In the subacute and chronic phases of ischemic stroke, the *neuroregenerative* effects of this noninvasive brain stimulation [14, 23, 62, 97, 98] are more prominent and most likely reflect enhancement of neurogenesis [24, 99], synaptogenesis [100, 101], angiogenesis [17], and neurotransmitter metabolism [102–104]. In many clinical studies, acute and long-term treatment with TES is proved safe and effective in improving functional outcomes [36, 105–107].

2.1.1. Cerebral Molecular Response to TES. The exact molecular mechanism by which TES exhibits beneficial effects in post-stroke patients is still largely unknown (Table 1). Mounting evidence shows that, most likely, TES does not have a singular effect that stimulates recovery but rather influences many processes such as astrocytic calcium and glutamate pathways [108] and reduced the number NMDA receptor 1 (NMDAR1) in the hippocampus [109] resulting in a decrease spontaneously of *peri-infarct depolarization* (PID). The direct consequence of all the molecular effects adds to two main effects. The first is that cathodal tDCS (C-tDCS) decreases the DNA fragmentation and lowers the number of Bax- and caspase-3-positive cells, with a simultaneous increase in Bcl-2 protein expression and Bcl-2/Bax ratio, both reliable markers for the *antiapoptotic pathways* [109]. The second is that C-tDCS lowers the expression of stress proteins and suppresses global protein synthesis, thereby providing neuroprotection [22, 110] by reducing neuronal activity, and thus, it decreases cell metabolism, thereby providing neuroprotection [109] and promoting cell survival after an ischemic lesion. The main molecular pathway involved in in this process is inhibition of caspase-3-dependent apoptosis that seems to be promoted by TES-dependent activation of brain-derived neurotrophic factor (BDNF) and phosphoinositide 3-kinase (PI3K)/Akt/mammalian target of rapamycin (mTOR) pathway [17, 111, 112]. Molecular markers of inflammation, such as hippocampal levels of IL-1b and TNF-a, were found to be decreased, after C-tDCS, in MCAO mice [109]. Likewise, rodents subjected to C-tDCS or A-tDCS had increased levels of superoxide dismutase (SOD) and decreased malondialdehyde (MDA - a membrane lipid peroxidation marker), thus attenuating the *oxidative stress* induced by cerebral ischemia [109].

The consequences of electric stimulation (ES) on the molecular mechanisms also come with functional changes. One of the most interesting observations was the change in membrane polarity induced by direct current stimulation (DCS), which, in turn, modulates Ca^{2+} influx through activation or inhibition of NMDA receptors [102]. This modulation can activate then the enzyme cascades that add or remove glutamatergic AMPA receptors on the postsynaptic membrane, thus strengthening or weakening synaptic connections [113]. The capacity of DCS to influence the strength of neuronal connections has a direct effect on LTP. *In vitro* experiments done on brain slices investigating the connection strength between pyramidal cells of the CA3 hippocampal region and neurons of the CA1 area were able to show that anodal DCS markedly increases LTP, whereas cathodal DCS reduces it. These effects are most likely explained by the increase in Zif268- and C-fos protein-positive cells found in the CA subregions after anodal and cathodal stimulation [114]. Apart from the above-mentioned neuroplastic effects, the GABAergic system seems to play a role in tDCS-induced plasticity. Simultaneous administration of lorazepam (a GABA receptor agonist) to healthy subjects caused a reduction in neuroplastic excitability induced by anodal tDCS in the early phase and an enhancement of it in the late phase [103]. As for synaptic plasticity mediated by BDNF, *in vivo* studies support its enhancement by DCS [115, 116], while an *in vitro* experiment showed the opposite effect [114]. Neuroprotection following ES can be enhanced through the *suppression of autophagy*, another damaging effect excessively triggered by acute and severe cerebral ischemia [117]. The reperfused rat somatosensory cortex that was subjected to ES showed an upregulation of P62 coupled with the suppression of LC32, two apoptotic markers that vary according to the autophagic flux. [111].

At a molecular level, an early A-tDCS application was shown to increase the expression of microtubule-associated protein 2 (MAP-2) and growth-associated protein 43 (GAP-43). This increase directly impacts dendritic plasticity, axonal regrowth, and synaptogenesis both in the ischemic penumbra and in the contralateral cortex with a measurable functional recovery assessed by (improved Barnes maze performance, motor behavioral index scores, and beam balance test) [101]. After global ischemia, A-tDCS increased the expression of postsynaptic density protein 95 and synaptophysin both in the cortex and hippocampus with beneficial effects on recovery assessed by quantitative electroencephalogram, neurological deficit score, and 96 h survival [118].

2.1.2. Cerebral Cellular Response to TES. It is not surprising that all molecular changes following ES will also elicit a cellular response. One of the most important cellular consequences of TES is an increase in *neurogenesis* both in healthy [23] and injured central nervous system [24, 99, 119]. Research data showed that TES (subconvulsive train of 30 mA, 60 pulses/sec, 0.5 ms pulse width, 1 s duration, and in total for 5 s) during the subacute phase of stroke was followed by an increase in the number of $BrdU^+$/tubulin beta III^+ cells in the infarct core. The same stimulation elicited increased subventricular (SVZ) ratio of $BrdU/DCX^+$ cells and an increase in the number of ipsilateral hippocampus neurons positive for doublecortin (DCX) [24] (Figure 1). Other studies showed that MACO rats subjected to C-tDCS (500 μA, 15 minutes, once per day for 5 days in the acute and 5 days in the subacute phase) were able to evoke an increase in the $Nestin^+/Ki67^+$ and $Ng2^+$ cells in the SVZ [99] while A-tDCS increased number of DCX^+ cells in the SVZ, 10 days after stroke [119].

Table 1: Main neuroprotective and neuroregenerative effects of transcranial electric stimulation in experimental research.

Model	Stroke stage	Technique	Types of protocol	Cortical effects	Neurogenesis	Neuroprotection	Neural plasticity	Neuroinflammation	Angiogenesis	Oxidative stress	Neurotransmitter metabolism	BBB permeability	Clinical results	Possible signalling pathway	Data
Healthy animals		C-tDCS or A-tDCS	Continuous administration of C-tDCS or A-tDCS for 15 min at 500 μA using a constant current stimulator to a charge density of 128.571 C/m^2, daily, for 5 consecutive days, followed by a tDCS-free interval of 3 days and another 5 days of electrical stimulation for only half of the animals	Inflammatory modulation through IBA1+ cells, increased ICAM1+ and BrdU+ cells	P	P		P	P				Not analysed	—	Rueger et al., [23]
			1 mA current, for 15 min, the inter-tDCS interval longer than 2 h. At the onset and offset of stimulation, the current was slowly ramped up and ramped down over ~15 s to avoid sudden current change. S-, A-, and C-tDCS were performed in order and repeated for six cycles in each cat	A- and C-tDCS can selectively affect GABAergic and glutamatergic transmissions by reducing GABA and glutamate synthesis			P				P		Reduced glutamate excitotoxicity; A- and C-tDCS can, respectively, enhance and suppress neuronal excitability	Selectively affect GABAergic and glutamatergic transmissions	Zhao et al., [161]
		A-tDCS	3 different doses of weak direct current (0.1, 0.5, and 1 mA) for 20 min (including 30 s ramp up and 30 s ramp down), current density for each dosage being 0.8, 4.0, and 8.0 mA/cm^2	Enhanced BBB dysfunction (transiently); could be used as a convenient, noninvasive, and selective approach for systemic drug delivery to the central nervous system via the BBB								P	BBB permeability modulation	Temporarily disrupting the structural components forming the paracellular pathway of the BBB	Shin DW et al., [114]
MCAO model	Acute/chronic	t-DCS	Subconvulsive train, 30 mA, 60 pulses/sec, 0.5 ms pulse width, 1 s duration and in total for 5 s at 7 and 24 days after stroke	Possibly reduced glutamate excitotoxicity (significantly downregulated genes Gria 3-glutamate receptor) increased the number of BrdU-labeled tubulin beta III cells in the infarct core of ES animals over controls	P	P							Significant beneficial effect on spatial long-term memory, no beneficial effect on complex sensorimotor skills, detrimental effect on the asymmetric sensorimotor deficit	Possibly AKT/mTOR and β-catenin signaling pathways	Balseanu et al., [24], Liu et al., [50]
	Acute		Continuous stimulation for 3 days or 1 week, with	Phosphorylated Akt upregulation of		P		P	P				Ameliorated behavioral impairment; reduced	Stimulation of PI3K/Akt/mTOR pathway	Baba et al., [17]

Table 1: Continued.

Model	Stroke stage	Technique	Types of protocol	Cortical effects	Neurogenesis	Neuroprotection	Neural plasticity	Neuroinflammation	Angiogenesis	Oxidative stress	Neurotransmitter metabolism	BBB permeability	Clinical results	Possible signalling pathway	Data
			square-wave pulses at the duration of 1 ms constant current, with different electric current (0, 100, 200 μA) and frequency (0, 2, 10, 50 Hz). After the 1-week stimulation, the electric stimulation was discontinued	BDNF, GDNF, and VEGF									infarct volumes; increased cerebral blood flow through angiogenesis		
			Electric current of 20 Hz, 2 ms square biphasic pulse, 100 μA for 30 min, starting at 30 min after reperfusion	Inhibits proliferation and activation of microglia and astrocyte upregulation of BDNF		P		P					Attenuated infarction volume and improved functional recovery; neuroprotection	Stimulation of PI3K/Akt/mTOR pathway, autophagy P62-LC3B-related pathway	Wang et al., [166]
		A-tDCS	Early tDCS, 1 day after ischemia for 5 days and late tDCS, 1 week after ischemia for 5 days	Enhanced levels of MAP-2 and GAP-43 for dendritic and axonal regrowth			P						Improved Barnes maze performance; increased motor behavioral index scores and beam balance test	—	Yoon et al., [101]
Asphyxial model of cardiac arrest			1 mA A- tDCS for 0.5 h with a constant direct current generator, repeated for four sessions with a resting interval of 1 h	MAP2, GAP-43, PSD-95, and SYN dramatically higher levels			P						Improves quantitative electroencephalogram; neurological deficit score and 96 h survival	—	Dai C et al., [118]
	Acute +subacute		15 min, once per day, 500 μA administrated for 5 days in the acute and 5 days in the subacute phase, at a corresponding charge density of 128,571 C/m^2 (higher than the one used in clinical trials)	Promoted neural stem cell differentiation to oligodendrocytes and neurons	P		P						Improved locomotor activity and athletic endurance deficits; accelerated recovery of limping gait	Inhibited Notch1 signaling pathway activation (DLL1 and Jagged1 downregulation and NUMB upregulation)	Zhang et al., [99]
MCAO model		C-tDCS	1/2 group-C-tDCS alternating 15 min on and 15 min off starting 45 min after MCAO and lasting 4 h. 1/2 group-same protocol but starting soon after MCAO and lasting 6 h. A constant current intensity of 0.2 mA (current density of 2.86 mA/cm^2)												
	Acute			Reduced oxidative stress		P				P			Decreased number of spreading depolarizations; reduced infarct volume and area	Possibly C-tDCS blocks, the origin and the repeatedly spontaneous cycling of peri-infarction depolarizations	Notturno et al., [22]

Table 1: Continued.

Model	Stroke stage	Technique	Types of protocol	Cortical effects	Neurogenesis	Neuroprotection	Neural plasticity	Neuroinflammation	Angiogenesis	Oxidative stress	Neurotransmitter metabolism	BBB permeability	Clinical results	Possible signalling pathway	Data
			15 min at 500 μA, starting 3 days after ischemia, for 10 days in total (A-tDCS or C-tDCS), with a pause of 2 days in the middle of sessions (5-2-5 days) and a charge density of 128,571 C/m^2	Increased microglia polarization towards an M1 phenotype: iNOS-positive M1-polarized microglia	P		P	P					Accelerated functional recovery; only C-tDCS recruited oligodendrocyte precursors towards the lesion and supported M1-polarization of microglia	—	Braun et al., [113]
			20 min on–20 min off–20 min on of either C-tDCS or A-tDCS, starting after the first 30 min or at 4.5 hours after MCAO	C-tDCS, but not A-tDCS, reduced glutamate excitotoxicity		P		P			P	P	A-tDCS increased BBB permeability, but not C-tDCS; C-tDCS reduced the ischemic volume and brain edema; ameliorated functional deficits	Decrease of cortical glutamate synthesis and downregulation of NR2B NMDAR subunit	Peruzzotti-Jametti et al., [21]
		A-tDCS or/and C-tDCS	30 min daily, A-tDCS and C-tDCS 10 Hz, 0.1 mA, beginning 1 day after stroke for 3, 5, 7, 11, or 14 days	Reduced neuronal membrane permeability and ionic dysregulation			P						Early application of t-DCS from day 7 to day 14 after stroke may result in better motor function improvement than ultraearly intervention (within 3–5 days after stroke); also, it reduced the significantly increased hemichannel pannexin-1 mRNA expression on days 7 and 14	Ischemia may induce opening of the hemichannel pannexin-1 (protein family that forms large-pore nonselective channels in the plasma membrane of cells)	Jiang et al., [100]
4-vessel occlusion model			400 μA constant current applied for 15 min, once, during cerebral ischemia	C-tDCS significantly decreased the levels of IL-1β and TNF-α, MDA, and NOS, while increasing the level of SOD; caused a significant decrease in NMDAR level, Bax and caspase-3 expressions, while increasing the Bcl-2 expression; significantly lower DNA fragmentation and neuronal death			P		P		P	P		Improved learning and memory dysfunctions	Antiapoptotic pathway Bcl-2	Kaviannejad et al., [167]

tDCS: transcranial direct current stimulation; C-tDCS: cathodal transcranial direct current stimulation; A-tDCS: anodal transcranial direct current stimulation; ES: electrical stimulation; mTOR: mammalian target of rapamycin; BDNF: brain-derived neurotrophic factor; GDNF: glial cell line-derived neurotrophic factor; VEGF: vascular endothelial growth factor; PI3K: phosphoinositide 3-kinase; MAP-2: microtubule-associated protein 2; GAP-43: growth-associated protein 43; PSD-95: postsynaptic density protein; SYN: synaptophysin; BBB: blood-brain barrier; DLL1: delta-like 1; MCAO: middle cerebral artery occlusion; iNOS: inducible nitric oxide synthase; NMDAR: N-methyl-D-aspartate receptor; s-tDCS: sham transcranial direct current stimulation; GABA: γ-aminobutyric acid; MDA: malondialdehyde; NOS: nitric oxide synthase; SOD: superoxide dismutase.

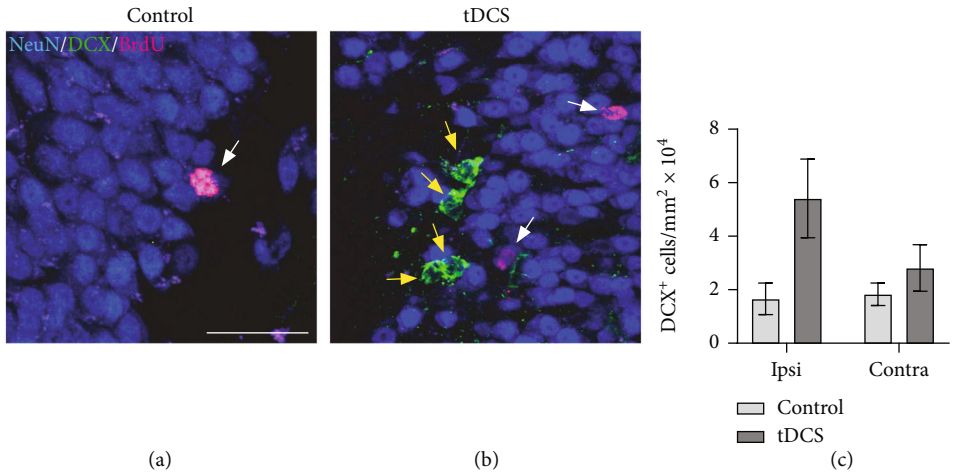

Figure 1: Increase of hippocampus neurogenesis in poststroke mice 14 days after receiving tDCS. (a) Compared to controls, in ES rats, we were able to identify a hippocampal increase in the number of (b) DCX (yellow arrows) and BrdU cells (white arrows). (c) This effect was seen in both the ipsilateral (Ipsi) and contralateral (Contra) hippocampus.

The generation of new brain cells after TES may explain the increase in its structural, functional, and connective reorganization. Increased structural *neuroplasticity* after stroke, evaluated by the density of dendritic spines in the mouse cerebral cortex, was reported after daily sessions of A-tDCS over the ipsilesional motor cortex paired with C-tDCS stimulation of the contralesional motor cortex. Significant improvement in motor function, assessed by beam walking test scores, was observed in the tDCS group compared to the MCAO group [100].

After alteration of inflammatory molecular pathways, MCAO receiving mouse C-tDCS showed reduced levels of macrophage activation markers ($CD68^+$ cells), microglia ($Iba1^+$ cells), lower astrogliosis ($GFAP^+$ cells), less neutrophils (MPO^+), and mononuclear cells ($CD45^+$) in the ischemic penumbra of the cerebral cortex [17, 21, 111]. Interestingly, MCAO mice that received anodal tDCS (A-tDCS) treatment had an increase in $CD45^+$ and MPO^+ cells around the ischemic cortex and in the striatum [21].

An extensive cerebral vasculature is necessary for the support of these neuroprotective and neuroregenerative effects. Thus, TES was shown to enhance *angiogenesis* in animal stroke models through the increased number of laminin-positive vessels in the ischemic penumbra and upregulation of vascular endothelial growth factor (VEGF) [17]. On the other hand, the effects of TES on the postischemic *blood-brain barrier (BBB)* are conflicting. Thus, anodal stimulation amplified the BBB damage with a subsequent increase in edema and ischemic lesion volume probably caused by the accumulation of endogenous IgG in the ipsilateral ischemic hemisphere compared to the contralateral healthy hemisphere and the significant disruption of blood vessel tight junctions [21]. Also, in healthy rat, the brain stimulated with A-tDCS transiently enhanced the permeability of the BBB through activation of nitric oxide synthase, disruption of the endothelial glycocalyx, basement membrane, and the tight junctions, as well as the increase of the gap width between endothelial cells and basement membrane [120]. Some of these effects were also found in an *in vitro* study [121]. However, C-tDCS applied to stroke rat models reduced the ischemic volume, brain edema [21], and nitric oxide synthase level [109]. The integrity of tight junctions after C-tDCS was similar to that of nonstimulated animals, but the IgG leakage was lower compared to both the sham and A-tDCS groups [21].

2.2. Clinical Studies Using TES. Several clinical studies investigated the effects of tDCS on motor recovery in stroke patients (Table 2). In a pilot randomized controlled trial, a current of 1.5 mA or sham current was delivered for 20 minutes hourly over a period of 6 hours and 20 minutes in *hyperacute* middle cerebral artery territory stroke patients receiving reperfusion therapy (intravenous thrombolysis alone or mechanical thrombectomy with or without prior intravenous thrombolysis). Although no major adverse effects (death or neurological deterioration) were reported, the study found no difference between the treated and sham groups. Although the results were not satisfactory, patients receiving reperfusion therapy and ES had smaller infarct volumes. The potential benefits of C-tDCS in patients were also shown for patients with a National Institute of Health Stroke Scale (NIHSS) score of >10 or large vessel occlusion who showed improved functional independence at 3-month poststroke [107]. The lack of a clear benefit in this study was attributed to the fact that on a molecular level, only certain C-tDCS protocols can reduce PID and influence local neuronal networks [107, 122]. On the other hand, C-tDCS exerts its inhibitory effects depending on the organization of cortical neuronal arrangement (i.e., lissencephaly and gyrencephaly) [65]. Building on the partial success of these findings, two clinical trials, TESSERACT and TESSERACT-BA, were approved. The TESSERACT study is testing the use of incremental C-tDCS doses in patients ineligible for reperfusion therapies (URL: https://www.clinicaltrials.gov and unique identifier: NCT03574038) while the TESSERACT-BA study is investigating tDCS in acute stroke patients with substantial salvageable penumbra due to a large vessel occlusion

Table 2: Main clinical outcomes after transcranial electric stimulation.

Model	Stroke stage	Technique	Types of protocol	Reported results	Clinical outcome	Possible signalling pathway	Data
Clinical data	Healthy volunteers	A-tDCS and C-tDCS	Continuous currents for 4 s (excitability shifts during tDCS), 5 (short-lasting excitability shifts), 9 (C-tDCS), or 11 min (A-tDCS), with an intensity of 1.0 mA. A-tDCS was repeated 20 min after the first stimulation	A-tDCS can modulate GABAergic inhibition	Anodal stimulation enhances excitability, cathodal stimulation reduces it enhancement of neurotransmitter metabolism	Might be due to influences of remote cortical or subcortical structures	Nitsche et al., [103]
			A-tDCS 1 mA current, with a ramp up time of 10 s, held at 1 mA for 10 min, and then ramped down over 10 s. For sham stimulation, the current was ramped up over 10 s and then immediately switched off	A-tDCS caused locally reduced GABA, C-tDCS caused reduced glutamatergic neuronal activity with a highly correlated reduction in GABA	A-tDCS - decreased metabolism, C-tDCS - intensive neurotransmitter metabolism	Reduced activity of GAD-67, the rate-limiting enzyme in the major metabolic pathway for GABA synthesis	Stagg et al., [104]
		C-tDCS	A current of 1.5 mA or sham current delivered hourly for 20 min each, over a period of 6 hours and 20 min; C-tDCS started before completion of recanalization procedure in all patients	Reduced infarct volume of stroke patients receiving reperfusion therapy	Better motor improvement and more functional independence at 3 months post stroke; no major adverse effects (death or neurological deterioration); no statistical difference between the treated and sham groups		Pruvost-Robieux et al., [107]
	Acute	C-tDCS, A-tDCS and bilateral tDCS	Each patient received 10 sessions (5 consecutive days for 2 weeks) of real or sham stimulation at 2 mA intensity and current density equivalent to 0.05 A/m^2. For sham stimulation, the current was ramped up over 30 seconds and then turned off	No data	Significant motor recovery sustained at least three months beyond the intervention; decreased risk of falls; only in the bilateral stimulation group was reported an increase in the lower limb's motor skills	No data	Andrade et al., [38]
		C-tDCS vs. A-tDCS	A current of 2 mA for 25 min daily for 6 consecutive days over the motor cortex hand area	A-tDCS over the affected hemisphere may be as effective as C-tDCS on the unaffected hemisphere to enhance recovery after acute ischemic stroke	Clinical improvements not only in the upper limb but also in the lower limb on the affected side		Khedr et al., [106]
	Chronic	A-tDCS	Current (1 mA) remained on for	The effect outlasted the stimulation period	Beneficial influence on skilled motor		Hummel et al., [105]

Table 2: Continued.

Model	Stroke stage	Technique	Types of protocol	Reported results	Clinical outcome	Possible signalling pathway	Data
			20 min in the tDCS session and for up to 30 s in the sham session		functions of the paretic hand in patients suffering from chronic stroke; significant functional improvement of the paretic hand compared with motor therapy alone		
			Applied with the anode positioned over the ipsilesional M1 and the cathode over the contralateral supraorbital region for 20 min (1 mA); sham current applied for only 1 min after which it was slowly tapered down to 0 for the remainder 19 min	Effects maintained 1 and 6 days after the completion of the training	No complications were reported; improved motor performance compared with motor practice or with practice combined with either intervention alone;		Celnik et al., [126]
			30 min of 1.5 mA direct current with the anode placed over the ipsilesional and the cathode over the contralesional motor cortex	Functional reorganization of the ipsilesional motor cortex	No adverse effects were observed; improved motor functions		Lindenberg et al., [36]
		C-tDCS and A-tDCS	Single session of 20 min with 1.5 mA current. The anode was over the M1 contralateral to the paretic limb and the cathode over the M1 contralateral to the nonparetic limb (current density 0.06 mA/cm^2)	Effects maintained for 3 weeks	Improved retention of gains in motor function	Might be modulated through intracortical inhibitory pathways	Goodwill et al., [127]

A-tDCS: anodal transcranial direct current stimulation; C-tDCS: cathodal transcranial direct current stimulation; GABA: γ-aminobutyric acid; GAD-67: glutamate decarboxylase 67; tDCS: transcranial direct current stimulation.

before and after endovascular therapy (URL: https://www.clinicaltrials.gov and unique identifier: NCT04061577). No data had been reported prior to the writing of this review.

2.2.1. TES Influence on the Outcome of Acute and Subacute Stroke. The use of tDCS was not duplicated in other small clinical trials. Bihemispheric tDCS modulation in *acute stroke patients* (48-96 h after stroke) for five continuous days, 40 minutes per day over the primary motor cortex (M1), did not show any clinical benefit beyond the one achieved by the physical therapy alone or through spontaneous recovery [123]. However, some neurophysiological changes were noted (i.e., decrease of the interhemispheric imbalance of excitability and modulation of plasticity), but the lack of clinical improvement was most likely caused by the inappropriate inhibition of the unaffected hemisphere through A-tDCS during the acute stage of stroke [124], as well as the unsuitable tDCS parameters of stimulation [125]. Similarly, A-tDCS applied over the affected motor cortex of acute stroke patients (2 mA for 20 min daily for five consecutive days) showed no significant improvement in NIHSS and Fugl-Meyer scores compared to sham. The lack of efficacy was also attributed to the imbalance of excitability generated through this technique [126].

One targeted study investigated the potential of A-tDCS to improve dysphagia in acute-subacute stroke patients with unilateral ischemic infarction. It is reported that ES sessions (2 mA either twice daily for a total of 20 minutes or

alternating with sham stimulation daily for a total of 20 minutes) performed along with standardized swallowing over five days, starting from day 2 to 6 after stroke onset, did not decrease aspiration risk assessed through Penetration and Aspiration Scale score. Since A-tDCS exerts its effects mainly by modulation of activity in the other intact hemisphere, the limitations, in this case, were most likely due to the extent of damage to the corticobulbar tracts in each case [127].

The use of tDCS on stroke patients during the *subacute period* elicits diverging results. Six consecutive sessions (25 minutes at 2 mA daily) of either C-tDCS over the unaffected hemisphere or A-tDCS over the affected hemisphere administered in early subacute stroke patients seem to have clinical improvements both in the upper and lower limb only after 6 sessions [106]. However, a stimulation of 2 mA using A-tDCS or C-tDCS combined with robot-assisted bilateral arm training applied to subacute stroke patients (3 to 8 weeks from stroke onset) every workday for 6 weeks did not have any additional effect compared to sham [128].

Although some minimal effects were reported, the general consensus seems to be that DCS has a minimal impact on acute and subacute stroke patients. This low efficacy could be explained in several ways. First, a lack of standardization in the way tDCS is applied in stroke patients and the optimal timing of ES. Also, the current characteristics are still unknown. Second, it could be that cellular effects seen in rodent studies have only a limited impact on large lesions or the effect is difficult to quantify in a clinical setting. Whatever the case, the results reported by various clinical studies suggest that some benefits exist and an improvement may be possible.

2.2.2. TES Influence on the Outcome of Chronic Stroke. While the acute and subacute effects of tDCS are still debated, the benefits of tDCS stimulation are far more obvious in *chronic stroke patients*. Several studies showed motor improvement after A-tDCS, especially in association with other recovery strategies. Thus, A-tDCS (1 mA for 20 min on the affected hemisphere) given at 1.9 to 8.9 years after stroke, preceding motor therapy of the upper limb, was able to evoke a significant functional improvement of the paretic hand as measured using the Jebsen–Taylor Hand Function Test compared with motor therapy alone. Furthermore, this effect outlasted the stimulation period [105]. Even patients suffering a stroke up to 7.2 years prior to combined peripheral nerve stimulation of the paretic hand (5 single pulses of 1 ms duration delivered at 10 Hz applied simultaneously over the median and ulnar nerve at the wrist) and A-tDCS applied over the ipsilesional primary motor cortex at an intensity of 1 mA for 20 min showed an improved motor performance, evaluated through the number of correct key presses on a special keyboard containing only 5 keys as compared with motor practice or with practice combined with either intervention alone. This study also reported that the effect outlasted the stimulation and training [129]. Bihemispheric tDCS at 1.5 mA for either 20 min (current density 0.06 mA/cm^2) or 30 min repeated in five sessions done on patients that were subjected to physical/occupational therapy also showed improvements in motor function in chronic stroke patients. The effects were assessed by either Upper Extremity Fugl-Meyer, Wolf Motor Function Test, or Motor Assessment Scale, Tardieu Scale, and grip strength [36, 130].

3. Transcranial Magnetic Stimulation—Short Introduction

Transcranial magnetic stimulation is another noninvasive technique that is able to modulate brain activity already used in different clinical settings. For example, TMS is used as a treatment method for several psychiatric pathologies such as depression [131, 132] or schizophrenia [133]. It is also applied in some neurologic pathologies to improve the outcome of different movement disorders [134, 135], stroke [105], multiple sclerosis [136], Alzheimer's disease [137], and disorders of consciousness [138]. Extensive recent reviews of repetitive TMS on specific poststroke consequences, such as poststroke dementia [139] and poststroke depression [140], have been made, and on the matter, we encourage their reading for further in-depth knowledge.

As is the case with ES, in practice, TMS can also be applied under different protocols. Depending on the applied protocol, TMS can have different effects on brain excitability. Thus, high-frequency repetitive TMS (HF-rTMS) (>1 Hz) [28] and intermittent theta burst stimulation (iTBS) [29] can increase cortical excitability, while TMS protocols using low-frequency repetitive TMS (LF-rTMS) (≤1 Hz) [141] or continuous theta burst stimulation (cTBS) [29] decrease it. One major advantage of using TMS is that its effects last beyond the stimulation period [142]. However, for accurate and meaningful interpretation of TMS results, controls need to be matched at least for age, height, and sex [143].

3.1. Experimental Data Supporting the Use of TMS in Stroke. The molecular and cellular mechanisms through which TMS exerts its effects on stroke are not fully elucidated (Table 3). Although technically TMS is more difficult to use in an experimental setup, especially in rodents that have a small cortical volume, several studies were able to show changes in molecular and cellular responses.

3.1.1. Cerebral Molecular Response to TMS. Extensive molecular research found that cTBS reduces poststroke *neuroinflammation* by lowering the levels of cytokines associated with infiltrating immune cells into the central nervous system (i.e., CNTF, CX3CL1, IFN-r, IL-α, IL-1β, IL-1ra, IL-2, IL-3, IL-6, IL17, and TNFα) or the cytokines related to endothelial inflammation (i.e., CD54, CXCL9, CXCL10, and CCL5) [19, 20]. Adding to this anti-inflammatory effect is the attenuation of *oxidative stress* by reducing the NADPH oxidase activity with subsequent reduction in MDA and 4-hydroxynonenal (another marker of lipid peroxidation) and increasing manganese-superoxide dismutase which clears the free radicals generated by mitochondrial respiration [20, 144, 145].

However, one of the most important molecular effects of TMS is its influence of *neurotransmitter metabolism*. Post TMS, different neurotransmitter levels increase or decrease depending on the investigated region. For example, TBS

Table 3: Main neuroprotective and neuroregenerative effects of transcranial magnetic stimulation.

Model	Stroke stage	Technique	Types of protocol	Results	Neurogenesis	Neuroprotection	Neural plasticity	Neuroinflammation	Angiogenesis	Excitability	Oxidative stress	BBB	Effects	Signalling pathway	Data
Healthy animals		HF-rTMS	Progressive number of trains (15 Hz, 5 s duration, 75 stimuli) separated by 10 s intervals (one treatment was delivered on day 1, up to five on day 5)	Augmented number of thin spines and enhanced dendritic complexity			✓						Did not increase anxiety in mice	Possible BDNF and calcium-dependent signaling pathways	Cambiaghi et al., [25]
Photothrombotic stroke model	Acute	cTBS	rTMS, 1/day, 5 min, days 1-6 after stroke, 3 pulses of 50 Hz, repeated every 200 ms, magnetic field adjusted to 200 gauss	Vascular repair and protection - RECA-1, protein collagen IV with FITC-labelled dextran leakage abated by over 50% in rTMS group rats; upregulation of IGFBP1, TGFβ, VEGF, and PDGFRβ; preserved neuronal morphology and synaptic structure; reduces microgliosis and induces a shift in in microglia phenotype; suppresses proinflammatory cytokine production;		✓	✓	✓	✓		✓	✓	Protected behavioral outcomes; attenuated infarct volume; promoted functional recovery	HIF-1α pathway; antiapoptotic pathways caspase-3 and caspase-9	Zong et al., [19]; Zong et al., [20]
MCAO model		HF-rTMS	Magnetic stimulation for 3 s followed by rest for 50 s and repeated 10 times (300 pulses per day) at a rate of 10 Hz, 3.5 T peak magnetic welds; performed at 24 h, 7 and 14 days after stroke	Increased number of BrdU and NESTIN+ cells; Bcl-2 expression was significantly lower and Bax expression was significantly higher; mRNAs of BDNF and TrkB levels were also significantly higher	✓	✓							Improvement of cognitive impairment	BDNF/TrkB signaling pathway and antiapoptotic pathways Bcl-2 and Bax	Guo et al., [146]
			A 3.5 T peak magnetic weld was applied to conscious rats at day 4 after cerebral ischemia, 10 sessions of stimulation over a 2-week period, seven times of five 1 s strains at a	Greater number of positive Bcl-2 cells and fewer Bax-positive cells in the rTMS group		✓							Beneficial effect on motor function on Barnes maze performance, motor behavioral index scores, and beam balance test	Antiapoptotic pathways Bcl-2 and Bax	Yoon et al., [145]

Table 3: Continued.

Model	Stroke stage	Technique	Types of protocol	Results	Neurogenesis	Neuroprotection	Neural plasticity	Neuroinflammation	Angiogenesis	Excitability	Oxidative stress	BBB	Effects	Signalling pathway	Data
			rate of 10 Hz with a 1 s intertrain interval per day (a total of 3,500 impulses)												
		HF -TMS and iTBS	20 Hz rTMS and iTBS, maximum stimulator output of the magnetic stimulator of 6.0 T, 7 and 14 days	Improvement of functional recovery, reduction of the infarcted area volume, neurogenesis (KI67, DCX, NESTIN)	✓								Elevated protein levels of BDNF and phosphorylated TrkB	BDNF/TrkB signaling pathway	Luo J et al., [148]
		LF-rTMS	2 times a day, 30 pulses each time, with a frequency of 0.5 Hz and magnetic field intensity of 1.33 tesla, when the animals were awake after MCAO, for 1, 7, 14, 21, and 28 days	Higher c-FOS expression, higher BDNF expression in 7, 14, and 21 days after stroke groups			✓						Improved functional outcome	BDNF/TrkB signaling pathway	Zhang et al., [26]
	Acute and chronic	LF-TMS and peripheral nerve stimulation	Paired associative stimulation with a frequency of 0.05 Hz 90 times over 4 weeks (TMS and left tibial nerve stimulation, 1/day); the interpair and interstimulus intervals were 20 seconds and 15 ms, respectively; 7, 14, and 28 days	Higher average BDNF and NMDAR1 expression levels		✓	✓			✓			Learning and memory amelioration, neuroplastic effect	BDNF/TrkB signaling pathway	Hu et al., [149, 150]

MCAO: middle cerebral artery occlusion; HF-rTMS: high-frequency repetitive transcranial magnetic stimulation; rTMS: repetitive transcranial magnetic stimulation; LF-rTMS: low-frequency repetitive transcranial magnetic stimulation; FITC: fluorescein isothiocyanate; IGFBP1: insulin-like growth factor binding protein 1; TGFβ: transforming growth factor β; VEGF: vascular endothelial growth factor; PDGFRβ: platelet-derived grow factor receptor beta; HIF-1α: hypoxia-inducible factor 1α; BDNF: brain-derived neurotrophic factor; TrkB: tropomyosin receptor kinase B; iTBS: intermittent theta burst stimulation; cTBS: continuous theta burst stimulation; NMDAR1: N-methyl-D-aspartate receptor 1.

lowered the level of cerebellar glutamate in the extracellular space of healthy rodents by increasing its uptake from the synaptic cleft and its turnover in neurons. This is done by increasing the number of plasmatic glutamate transporter 1 and by lowering the levels of vesicular glutamate transporter 1 [146]. However, LF-rTMS could not evoke any change in glutamate and glutamine levels in the primary motor cortex but increased GABA levels [147]. Increased extracellular dopamine and glutamate levels in the nucleus accumbens were also found after TMS [148]. Either this heterogeneous response is due to a random way the brain responds to TMS or it can be attributed to the variation in the applied techniques used in animal models. HF-rTMS applied in the subacute phase of stroke in a rat model did not found changes in the expression of NMDA and MAP-2 around the peri-ischemic area, questioning the role of TMS in synaptic plasticity, LTP, and dendritic plasticity in the early phases of stroke. Although no evidence of neuroplasticity was reported, the same groups showed that the animals receiving HF-rTMS had an improvement in functional recovery [149].

The potential of TMS to alter *apoptosis/augmented autophagy* might be of great importance in the clinical practice, as preventing additional cellular death after stroke generates more recovery potential compared to neuronogenesis or anti-inflammatory strategies. In a rat model, HF-rTMS applied during the acute and subacute phase of cerebral ischemia inhibited *apoptosis* by significantly enhancing the expression of Bcl-2 and reducing the expression of Bax compared to controls [149, 150]. The use of c-TBS was reported to have an inhibitory effect on the activation of caspase-3 and caspase-9 [20], while rTMS can increase the ratio of LC3-II/I and decrease p62 through NMDAR–Ca^{2+}–mTOR signaling [151]. Although this TMS effect can be important for poststroke recovery, it is not completely clear if this potentially augmented autophagy of TMS is eliciting a beneficial effect through clearance of the postischemic debris rather than prevention of neuronal death.

Recent reports showed that TMS can influence the integrity of the BBB and promote *angiogenesis*. The observation was done by using rTMS on a rat photothrombotic stroke model. Stimulated animals had less ischemic-induced degeneration and showed an upregulation in important BBB components such as zona occludens-1, claudin-5, occludin, and caveolin-1. In addition, a reduction in the extravasation of IgG into the peri-infarcted area and upregulation of Col IV, an essential element to vascular structure, were also reported [19]. An increase in angiogenesis-related proteins, such as matrix metalloproteinase-9 and VEGF plus the colocalization of vascular endothelial with cellular proliferation markers RECA1/Ki67 and CD31/BrdU, suggests the angiogenic potential of TMS [19].

3.1.2. Cerebral Cellular Response to TMS. After TMS, a plethora of other cellular phenomena has been reported, especially in animal models of stroke. Apart from this molecular effect, cTBS has cellular anti-inflammatory effects as evidenced by decreasing the number of $Iba1^+$ and $GFAP^+$ cells in the peri-infarct region [20]. In the early phase of stroke, both HF-rTMS and iTBS increased the number of Ki67 and DCX/Nestin or $NeuN^+$ cells suggesting that they could promote an increase in the neural stem cells (NSC) followed by a migration to the peri-infarct striatum. Furthermore, by analyzing the SVZ number of $Ki67^+$, an increase was observed after rTMS [152]. IN the subgranular zone, an increase in the ratio BrdU/$Nestin^+$ cells was observed after rTMS in MCAO rats [150]. HF-rTMS applied over the primary motor cortex in healthy mice modulates spinogenesis by increasing the number and complexity of thin spines in apical and basal dendrites [25], showing that it can also have a *neuroplastic effect*.

By combining peripheral nerve stimulation and TMS application, an increase in the expression of MAP-2 and GAP-43 in the ischemic penumbra was reported in the acute phase focal cerebral ischemia and reperfusion, suggesting that TMS is promoting dendritic plasticity and axonal regrowth [153]. The same association was shown to also promote functional neuroplasticity by enhancing LTP at synapses in the CA3 and CA1 regions of the hippocampus through upregulation of mRNA expression of BDNF and NMDAR1, with subsequent amelioration of poststroke impaired learning and memory [154]. If the effects on NMDA-mediated neuroplasticity are paradoxical, neuroplasticity mediated through upregulation of c-Fos and BDNF expressions was supported in a study that applied LF-rTMS in the early phase of stroke in rodents, leading to a neurological function recovery [26]. All this data suggests that the effect of TMS on poststroke recovery might be the overall result of an accumulation of different activity-dependent synaptic plasticity, also known as metaplasticity [155].

3.2. Clinical Studies Using TMS. With the successful use of TMS in other clinical settings [131, 132] and considering the molecular and cellular results from animal models, it did not take long until TMS was tested on stroke patients (Table 4).

3.2.1. TMS Influence on the Outcome of Acute and Subacute Stroke. Compared to DCS, data generated from patients receiving TMS in the *acute period of stroke* was shown to have beneficial effects on *motor function*. One of the first studies used a combination of standard physical rehabilitation strategies (passive limb manipulation from the second day, increasing, by the end of the first week, to more active movements if patients improved function), medical therapies (anticoagulants, antiplatelets, and nootropics), and HF-rTMS (10-second trains of 3 Hz stimulation with 50 seconds between each train for 10 days) over the stroke hemisphere of early postischemic patients. The study reported improvement in clinical scales (Scandinavian Stroke Scale, NIHSS, and Barthel scores) in patients receiving magnetic stimulation [39], suggesting that TMS could impact specific motor impairments. Due to the nature of TMS, specific cortical areas can be targeted, as such, by applying HF-rTMS over the oesophageal cortical area of the affected hemisphere (10 trains of 3 Hz stimulation, 10 min every day for five consecutive days), a clinical improvement of patients suffering

Table 4: Main clinical outcomes after transcranial magnetic stimulation.

Model	Stroke stage	Technique	Types of protocol	Reported results	Clinical outcome	Signalling pathway	Data
Clinical data	Healthy volunteers	LF-rTMS	1 Hz rTMS for 20–22 min at an intensity of 90% RMT (1 Hz rTMS: train of 10 pulses, 1 s wait time between trains, 120 trains, total pulses = 1200; 5 Hz rTMS: train of 25 pulses, 45 s wait time between trains, 24 trains, total pulses = 600); one volunteer additionally received 5 Hz rTMS in a separate session, 3 weeks after the 1 Hz protocol	Modulates neurotransmitter metabolism (increased GABA concentrations)	No significant changes for functional connectivity	No data	Gröhn et al., [143]
		LF-rTMS	20 minutes with 1 Hz rTMS, 5 days per week for a 2-week period	No side effects	Motor improvement and cognitive functions amelioration (unilateral spatial neglect and aphasia)	No data	Zheng et al., [152] Cha and Kim, [42] Weiduschat et al., [154]
			For 20-30 min each time, 1 time/day, and 5 times/week, 4 weeks	Higher SOD levels, lower MDA and ET-1	Improvement in cerebral oxygen metabolism and regulation of brain neurotransmitter	No data	Peng et al., [141]
	Acute and subacute	c-TBS	In every session, 3-pulse bursts at 50 Hz repeated every 200 msec for 40 s were delivered at 80% of the active motor threshold over the left PPC (600 pulses). 15 every day 2 sessions of left PPC cTBS were applied with an interval of 15 minutes. Stimulation lasted for 10 days (5 days per week, Monday to Friday) and was applied daily at the same hour every morning (11 AM) to all patients	Possibly by counteracting the hyperexcitability of left hemisphere parieto-frontal circuits	Recovery from visual spatial neglect	No data	Koch et al., [155]
		HF-rTMS	rTMS (daily at noon) consisted of ten 10-second trains of 3 Hz stimulation with 50 seconds between each train, for 10 days	No side effects	10 consecutive days of rTMS employed as an add-on intervention to normal physical and drug therapies improved immediate clinical outcome in early stroke patients	No data	Khedr et al., [39]
			rTMS applied for 10 min every day for 5 consecutive days, each session consisting of 10 trains of 3 Hz	Increased excitability of the corticobulbar projections from both hemispheres with better	Motor improvement and recovery from dysphagia (maintained for 2 months)	No data	Khedr et al., [40]

Table 4: Continued.

Model	Stroke stage	Technique	Types of protocol	Reported results	Clinical outcome	Signalling pathway	Data
			stimulation for 10 s and then repeated every minute	projection from the stroke hemisphere			
			A daily dose of 1000 pulses of subthreshold 10 Hz rTMS, 10 days	Higher movement accuracy; variable benefits in motor performance	Possible variable functional integrity of the corticospinal tract and different BDNF genotype	No data	Chang et al., [43]; Chang et al., [168]
		iTBS and LF-rTMS	7 days after stroke, for 10 days, iTBS (600 pulses) to the affected hemisphere; 1 Hz stimulation (1200 pulses) of the unaffected motor cortex hand area, also 10 days	No complications; motor improvement by iTBS; spasticity reduction by contralesional 1 Hz stimulation	Enhance motor recovery	No data	Watanabe et al., [41]
		LF-rTMS	1 Hz, 25 minutes, a subthreshold rTMS over the unaffected hemisphere	Increase in the excitability of the affected motor cortex	rTMS improved the motor learning of the affected hand in patients after stroke; enhanced motor skill acquisition and training effect	No data	Takeuchi et al., [44]
	Chronic		Pulses were applied twice daily at 3 Hz for 10 s with a 25-second interval, 20 times per session, alternating between left and right hemispheres (300 pulses for the left hemisphere and 300 pulses for the right hemisphere in one treatment session, 1,200 pulses per day) and were followed by 20 min of intensive swallowing rehabilitation exercise	No deterioration of neurological symptoms or adverse reactions such as convulsions or pneumonia	Improved laryngeal elevation delay time	No data	Momosaki et al., [159]
		HF-rTMS	For the bilateral stimulation group, 500 pulses of 10 Hz rTMS over the ipsilesional and 500 pulses of 10 Hz rTMS over the contralesional motor cortices over the cortical areas that project to the mylohyoid muscles were administered daily, 2 consecutive weeks. For the unilateral stimulation group, 500 pulses of 10 Hz rTMS over the ipsilesional motor cortex over the cortical representation of the mylohyoid muscle and the same amount of	Magnetic stimulation over the cortical areas projecting to the mylohyoid muscles is effective as an additional treatment strategy to traditional dysphagia therapies	Swallowing parameters showed an improvement in the bilateral simulation group	No data	Park et al., [169]

Table 4: Continued.

Model	Stroke stage	Technique	Types of protocol	Reported results	Clinical outcome	Signalling pathway	Data
		LF-rTMS and HF-rTMS	sham rTMS over the contralesional hemisphere were applied 1 Hz rTMS over the unaffected hemisphere, 10 Hz rTMS over the affected hemisphere or bilateral rTMS comprising both the 1 Hz and 10 Hz rTMS	No side effects	An improvement in the motor function of the paretic hand	No data	Takeuchi et al., [156]
		iTBS	Bursts of three pulses at 50 Hz given every 200 milliseconds in two-second trains, repeated every 10 seconds over 200 seconds for a total of 600 pulses	No side effects	Improvements in semantic fluency (language skills), stronger language lateralization to the dominant left hemisphere	No data	Szaflarski et al., [160]

LF-rTMS: low-frequency repetitive transcranial magnetic stimulation; rTMS: repetitive transcranial magnetic stimulation; RMT: resting motor threshold; GABA: γ-aminobutyric acid; PPC: posterior parietal cortex; cTBS: continuous theta burst stimulation; BDNF: brain-derived neurotrophic factor; SOD: superoxide dismutase; MDA: malondialdehyde; ET-1: endothelin-1; iTBS: intermittent theta burst stimulation.

from *poststroke dysphagia* assessed through Dysphagia Outcome and Severity scale was observed. The observed effect was speculated to be a consequence of the increase in corticobulbar projection excitability of both hemispheres [40]. Other LF-rTMS protocols in *subacute stroke patients* also reported encouraging results [156].

With the large motor deficit, capsular stroke patients have generally a poor recovery prognostic [157]. Interesting one of the fists reports that used TMS on capsulat patients utilized two distinct protocols: one using iTBS on the affected side for a total of 600 pulses at an intensity of 80% resting motor threshold (RMT) for 10 days and the other using LF-rTMS on the unaffected hemisphere for a total of 1200 pulses at an intensity of 110% RMT for 10 days. After the two, an enhanced movement and reduced spasticity of the affected limbs compared to the sham group was observed. The study reported improvement in clinical indicators such as Fugl-Meyer Assessment, Stroke Impairment Assessment Set, finger-function test, grip strength, and increase in motor evoked potential amplitude, measured in the first dorsal interosseous on the affected side [41]. However, it should be noted that the results are significant only compared to shams.

The complexity of poststroke disabilities does not restrict to only the motor ones. As such, TMS was used to investigate other nonmotor outcomes. Using a 1 Hz for five minutes with 90% RMT, performed four times, for a total of 1,200 stimulation events, for four weeks, five times each week and 10 minutes each day, LF-rTMS was reported to ameliorate higher-order cerebral functions such as unilateral spatial neglect as assessed by Line Bisection Test and Albert Test [42]. Similarly, 5 days per week for 2 weeks, 20 minutes each day, was shown to improve aphasia (measured by the Aachen Aphasia Test) [158], and even visuospatial neglect (evaluated through Behavioral Inattention Test) was reposted to be impacted by cTBS [159]. Other partial benefits were reported after using different HF-rTMS protocols such as improved the motor function of the affected upper limb, but not the lower one [160].

3.2.2. TMS Influence on the Outcome of Chronic Stroke. While acute and subacute results after TMS are generally encouraging, depending on the type of used protocol, different groups reported diverging recovery outcomes of *chronic stroke patients*. While bilateral TMS using 1 Hz and 50 sec train duration over the unaffected hemisphere, alternating with 10 Hz and 5 sec train duration over the affected hemisphere, with an interval of 5 sec for 20 times and LF-rTMS (1 Hz, 90% RMT, 25 min) applied to these groups of patients was reported to enhance motor skill acquisition in paretic hand movement evaluated through acceleration and pinch force [44, 161], the use of HF-rTMS had less than expected effects when applied to the affected cortex. Further diverging results were reported, with one study (with a protocol of 20 pulses at 10 Hz, 80% RMT, for a total of 160 pulses, in 2 sessions) showing improvements in hand motor performance assessed through movement accuracy and movement time [162], while another (90% RMT, 10 Hz, 1000 stimuli) showed no effect on motor function [161]; however, in this case, there was a lack of a stereotactic system with integrated MRI data or insufficient stimulation power to increase cortical excitability [161].

TMS was also used in an attempt to improve other aspects of poststroke recovery. In chronic poststroke dysphagia, HF-rTMS (10 sessions of rTMS at 3 Hz applied to the pharyngeal motor cortex bilaterally), followed by 20 min of intensive swallowing rehabilitation exercise, improved laryngeal elevation delay time in 4 poststroke patients [163]. The effect was confirmed in a larger study that demonstrated that 500 pulses of 10 Hz rTMS over the

ipsilesional and 500 pulses of 10 Hz rTMS over the contralesional motor administered daily for 2 consecutive weeks over the cortical areas projecting to the mylohyoid muscles are effective as an additional treatment strategy to traditional dysphagia therapies, with improvements in Clinical Dysphagia Scale, Dysphagia Outcome and Severity Scale, Penetration Aspiration Scale, and Videofluoroscopic Dysphagia Scale [164]. iTBS (bursts of three pulses at 50 Hz given every 200 milliseconds in two-second trains, repeated every 10 seconds over 200 seconds for a total of 600 pulses) applied to chronic left middle cerebral artery stroke patients with moderate aphasia (≥12 months prior to study participation) proved to be effective clinically, paraclinically, and subjectively. Thus, after rTMS, patients showed improvements in semantic fluency, being able to generate more appropriate words when prompted with a semantic category. fMRI mapping of post-rTMS showed shifts in activations predominantly of the left hemispheric head regions (fronto-temporo-parietal language networks). Also, patients noted a subjective improvement in the Communicative Activity Log [165].

4. Conclusions

With the increase in the global aged population, an increase in the incidence of stroke is expected. This will become a larger and larger problem as the number of patients increases more compared to the number of healthcare professionals properly trained to deal with such cases. Therefore, other ways to improve patient outcomes are needed. The results of some clinical studies using TMS in acute and subacute stroke patients paired with the ones from DCS applied to chronic patients could be the aid that stroke patients need, to ensure better results of classical medical recovery and, as such, diminish their disability.

Data Availability

Data are available on reasonable request.

Conflicts of Interest

The authors declare that there is no conflict of interest regarding the publication of this paper.

Authors' Contributions

Anca Badoiu, Smaranda Ioana Mitran, and Bogdan Catalin contributed equally to this work.

Acknowledgments

Dr. Raluca Elena Sandu and Dr. Albu Valeria Carmen were supported by grant no. 26/301/4 01.03.2022 "Risk and prognostic factors in ischemic stroke" at the Universitatea de Medicină şi Farmacie din Craiova and E.O. and B.C. by the Romanian National Council for the Financing of Higher Education (grant number CNFIS-FDI-2022-0263)

References

[1] V. L. Feigin, B. A. Stark, C. O. Johnson et al., "Global, regional, and national burden of stroke and its risk factors, 1990-2019: a systematic analysis for the Global Burden of Disease Study 2019," *The Lancet Neurology*, vol. 20, no. 10, pp. 795–820, 2021.

[2] D. Hebert, M. P. Lindsay, A. McIntyre et al., "Canadian stroke best practice recommendations: stroke rehabilitation practice guidelines, update 2015," *International Journal of Stroke*, vol. 11, no. 4, pp. 459–484, 2016.

[3] S. M. A. A. Evers, J. N. Struijs, A. J. H. A. Ament, M. L. L. van Genugten, J. (. H.). C. Jager, and G. A. M. van den Bos, "International comparison of stroke cost studies," *Stroke*, vol. 35, no. 5, pp. 1209–1215, 2004.

[4] A. Patel, V. Berdunov, Z. Quayyum, D. King, M. Knapp, and R. Wittenberg, "Estimated societal costs of stroke in the UK based on a discrete event simulation," *Age and Ageing*, vol. 49, no. 2, pp. 270–276, 2020.

[5] L. Rusu, E. Paun, M. I. Marin et al., "Plantar pressure and contact area measurement of foot abnormalities in stroke rehabilitation," *Brain Sciences*, vol. 11, no. 9, p. 1213, 2021.

[6] R. J. Nudo, G. W. Milliken, W. M. Jenkins, and M. M. Merzenich, "Use-dependent alterations of movement representations in primary motor cortex of adult squirrel monkeys," *The Journal of Neuroscience*, vol. 16, no. 2, pp. 785–807, 1996.

[7] H. Thikey, M. Grealy, F. van Wijck, M. Barber, and P. Rowe, "Augmented visual feedback of movement performance to enhance walking recovery after stroke: study protocol for a pilot randomised controlled trial," *Trials*, vol. 13, no. 1, p. 163, 2012.

[8] M. E. Stoykov and S. Madhavan, "Motor priming in neurorehabilitation," *Journal of Neurologic Physical Therapy*, vol. 39, no. 1, pp. 33–42, 2015.

[9] N. Takeuchi and S. I. Izumi, "Rehabilitation with poststroke motor recovery: a review with a focus on neural plasticity," *Stroke Research and Treatment*, vol. 2013, Article ID 128641, 13 pages, 2013.

[10] E. Burdet, D. W. Franklin, and T. E. Milner, *Human Robotics: Neuromechanics and Motor Control*, MIT Press, 2013.

[11] R. Teasell, N. Foley, K. Salter, S. Bhogal, J. Jutai, and M. Speechley, "Evidence-based review of stroke rehabilitation: executive summary, 12th edition," *Topics in Stroke Rehabilitation*, vol. 16, no. 6, pp. 463–488, 2009.

[12] F. Fregni and A. Pascual-Leone, "Technology Insight: noninvasive brain stimulation in neurology–perspectives on the therapeutic potential of rTMS and tDCS," *Nature Clinical Practice Neurology*, vol. 3, no. 7, pp. 383–393, 2007.

[13] A. B. Caglayan, M. C. Beker, B. Caglayan et al., "Acute and post-acute neuromodulation induces stroke recovery by promoting survival signaling, neurogenesis, and pyramidal tract plasticity," *Frontiers in Cellular Neuroscience*, vol. 13, 2019.

[14] M. A. Nitsche, L. G. Cohen, E. M. Wassermann et al., "Transcranial direct current stimulation: state of the art 2008," *Brain Stimulation*, vol. 1, no. 3, pp. 206–223, 2008.

[15] L. J. Boddington and J. N. J. Reynolds, "Targeting interhemispheric inhibition with neuromodulation to enhance stroke rehabilitation," *Brain Stimulation*, vol. 10, no. 2, pp. 214–222, 2017.

[16] B. Berger, R. Dersch, E. Ruthardt, C. Rasiah, S. Rauer, and O. Stich, "Prevalence of anti-SOX1 reactivity in various

neurological disorders," *Journal of the Neurological Sciences*, vol. 369, pp. 342–346, 2016.

[17] T. Baba, M. Kameda, T. Yasuhara et al., "Electrical stimulation of the cerebral cortex exerts antiapoptotic, angiogenic, and anti-inflammatory effects in ischemic stroke rats through phosphoinositide 3-kinase/Akt signaling pathway," *Stroke*, vol. 40, no. 11, pp. e598–e605, 2009.

[18] M. A. Nitsche and W. Paulus, "Excitability changes induced in the human motor cortex by weak transcranial direct current stimulation," *The Journal of Physiology*, vol. 527, Part 3, pp. 633–639, 2000.

[19] X. Zong, Y. Li, C. Liu et al., "Theta-burst transcranial magnetic stimulation promotes stroke recovery by vascular protection and neovascularization," *Theranostics*, vol. 10, no. 26, pp. 12090–12110, 2020.

[20] X. Zong, Y. Dong, Y. Li et al., "Beneficial effects of theta-burst transcranial magnetic stimulation on stroke injury via improving neuronal microenvironment and mitochondrial integrity," *Translational Stroke Research*, vol. 11, no. 3, pp. 450–467, 2020.

[21] L. Peruzzotti-Jametti, M. Cambiaghi, M. Bacigaluppi et al., "Safety and efficacy of transcranial direct current stimulation in acute experimental ischemic stroke," *Stroke*, vol. 44, no. 11, pp. 3166–3174, 2013.

[22] F. Notturno, M. Pace, F. Zappasodi, E. Cam, C. L. Bassetti, and A. Uncini, "Neuroprotective effect of cathodal transcranial direct current stimulation in a rat stroke model," *Journal of the Neurological Sciences*, vol. 342, no. 1-2, pp. 146–151, 2014.

[23] M. A. Rueger, M. H. Keuters, M. Walberer et al., "Multi-session transcranial direct current stimulation (tDCS) elicits inflammatory and regenerative processes in the rat brain," *PLoS One*, vol. 7, no. 8, article e43776, 2012.

[24] A. T. Balseanu, M. Grigore, L. R. Pinosanu et al., "Electric stimulation of neurogenesis improves behavioral recovery after focal ischemia in aged rats," *Frontiers in Neuroscience*, vol. 14, p. 732, 2020.

[25] M. Cambiaghi, L. Cherchi, L. Masin et al., "High-frequency repetitive transcranial magnetic stimulation enhances layer II/III morphological dendritic plasticity in mouse primary motor cortex," *Behavioural Brain Research*, vol. 410, article 113352, 2021.

[26] X. Zhang, Y. Mei, C. Liu, and S. Yu, "Effect of transcranial magnetic stimulation on the expression of c-Fos and brain-derived neurotrophic factor of the cerebral cortex in rats with cerebral infarct," *Journal of Huazhong University of Science and Technology Medical Sciences*, vol. 27, no. 4, pp. 415–418, 2007.

[27] O. D. Creutzfeldt, G. H. Fromm, and H. Kapp, "Influence of transcortical d-c currents on cortical neuronal activity," *Experimental Neurology*, vol. 5, no. 6, pp. 436–452, 1962.

[28] A. Pascual-Leone, J. Grafman, and M. Hallett, "Modulation of cortical motor output maps during development of implicit and explicit knowledge," *Science*, vol. 263, no. 5151, pp. 1287–1289, 1994.

[29] Y.-Z. Huang, M. J. Edwards, E. Rounis, K. P. Bhatia, and J. C. Rothwell, "Theta burst stimulation of the human motor cortex," *Neuron*, vol. 45, no. 2, pp. 201–206, 2005.

[30] M. Ameli, C. Grefkes, F. Kemper et al., "Differential effects of high-frequency repetitive transcranial magnetic stimulation over ipsilesional primary motor cortex in cortical and subcortical middle cerebral artery stroke," *Annals of Neurology*, vol. 66, no. 3, pp. 298–309, 2009.

[31] S. Wiethoff, M. Hamada, and J. C. Rothwell, "Variability in response to transcranial direct current stimulation of the motor cortex," *Brain Stimulation*, vol. 7, no. 3, pp. 468–475, 2014.

[32] V. López-Alonso, B. Cheeran, D. Río-Rodríguez, and M. Fernández-del-Olmo, "Inter-individual variability in response to non-invasive brain stimulation paradigms," *Brain Stimulation*, vol. 7, no. 3, pp. 372–380, 2014.

[33] J. Veldema and A. Gharabaghi, "Non-invasive brain stimulation for improving gait, balance, and lower limbs motor function in stroke," *Journal of Neuroengineering and Rehabilitation*, vol. 19, no. 1, p. 84, 2022.

[34] Q. Zhao, H. Li, Y. Liu et al., "Non-invasive brain stimulation associated mirror therapy for upper-limb rehabilitation after stroke: systematic review and meta-analysis of randomized clinical trials," *Frontiers in Neurology*, vol. 13, article 918956, 2022.

[35] S. Bornheim, J. L. Croisier, P. Maquet, and J. F. Kaux, "Transcranial direct current stimulation associated with physical-therapy in acute stroke patients - a randomized, triple blind, sham-controlled study," *Brain Stimulation*, vol. 13, no. 2, pp. 329–336, 2020.

[36] R. Lindenberg, V. Renga, L. L. Zhu, D. Nair, and G. Schlaug, "Bihemispheric brain stimulation facilitates motor recovery in chronic stroke patients," *Neurology*, vol. 75, no. 24, pp. 2176–2184, 2010.

[37] X. Bai, Z. Guo, L. He, L. Ren, M. A. McClure, and Q. Mu, "Different therapeutic effects of transcranial direct current stimulation on upper and lower limb recovery of stroke patients with motor dysfunction: a meta-analysis," *Neural Plasticity*, vol. 2019, Article ID 1372138, 13 pages, 2019.

[38] S. M. Andrade, J. J. A. Ferreira, T. S. Rufino et al., "Effects of different montages of transcranial direct current stimulation on the risk of falls and lower limb function after stroke," *Neurological Research*, vol. 39, no. 12, pp. 1037–1043, 2017.

[39] E. M. Khedr, M. A. Ahmed, N. Fathy, and J. C. Rothwell, "Therapeutic trial of repetitive transcranial magnetic stimulation after acute ischemic stroke," *Neurology*, vol. 65, no. 3, pp. 466–468, 2005.

[40] E. M. Khedr, N. Abo-Elfetoh, and J. C. Rothwell, "Treatment of post-stroke dysphagia with repetitive transcranial magnetic stimulation," *Acta Neurologica Scandinavica*, vol. 119, no. 3, pp. 155–161, 2009.

[41] K. Watanabe, Y. Kudo, E. Sugawara et al., "Comparative study of ipsilesional and contralesional repetitive transcranial magnetic stimulations for acute infarction," *Journal of the Neurological Sciences*, vol. 384, pp. 10–14, 2018.

[42] H. G. Cha and M. K. Kim, "Effects of repetitive transcranial magnetic stimulation on arm function and decreasing unilateral spatial neglect in subacute stroke: a randomized controlled trial," *Clinical Rehabilitation*, vol. 30, no. 7, pp. 649–656, 2016.

[43] W. H. Chang, Y. H. Kim, W. K. Yoo et al., "rTMS with motor training modulates cortico-basal ganglia-thalamocortical circuits in stroke patients," *Restorative Neurology and Neuroscience*, vol. 30, no. 3, pp. 179–189, 2012.

[44] N. Takeuchi, T. Tada, M. Toshima, T. Chuma, Y. Matsuo, and K. Ikoma, "Inhibition of the unaffected motor cortex by 1 Hz repetitive transcranical magnetic stimulation enhances

motor performance and training effect of the paretic hand in patients with chronic stroke," *Journal of Rehabilitation Medicine*, vol. 40, no. 4, pp. 298–303, 2008.

[45] P. S. Boggio, S. P. Rigonatti, R. B. Ribeiro et al., "A randomized, double-blind clinical trial on the efficacy of cortical direct current stimulation for the treatment of major depression," *The International Journal of Neuropsychopharmacology*, vol. 11, no. 2, pp. 249–254, 2008.

[46] A. R. Brunoni, R. Ferrucci, M. Bortolomasi et al., "Transcranial direct current stimulation (tDCS) in unipolar vs. bipolar depressive disorder," *Progress in Neuro-Psychopharmacology & Biological Psychiatry*, vol. 35, no. 1, pp. 96–101, 2011.

[47] S. Allida, K. L. Cox, C. F. Hsieh et al., "Pharmacological, psychological, and non-invasive brain stimulation interventions for treating depression after stroke," *Cochrane Database of Systematic Reviews*, vol. 1, article CD003437, no. 1, 2020.

[48] W.-D. Heiss and A. Thiel, "A proposed regional hierarchy in recovery of post-stroke aphasia," *Brain and Language*, vol. 98, no. 1, pp. 118–123, 2006.

[49] M. Balconi, "Dorsolateral prefrontal cortex, working memory and episodic memory processes: insight through transcranial magnetic stimulation techniques," *Neuroscience Bulletin*, vol. 29, no. 3, pp. 381–389, 2013.

[50] Y. Liu, M. Yin, J. Luo et al., "Effects of transcranial magnetic stimulation on the performance of the activities of daily living and attention function after stroke: a randomized controlled trial," *Clinical Rehabilitation*, vol. 34, no. 12, pp. 1465–1473, 2020.

[51] Y. Li, H. Luo, Q. Yu et al., "Cerebral functional manipulation of repetitive transcranial magnetic stimulation in cognitive impairment patients after stroke: an fMRI study," *Frontiers in Neurology*, vol. 11, 2020.

[52] G. Schlaug, V. Renga, and D. Nair, "Transcranial direct current stimulation in stroke recovery," *Archives of Neurology*, vol. 65, no. 12, pp. 1571–1576, 2008.

[53] K. Cuypers, D. J. F. Leenus, B. van Wijmeersch et al., "Anodal tDCS increases corticospinal output and projection strength in multiple sclerosis," *Neuroscience Letters*, vol. 554, pp. 151–155, 2013.

[54] R. Ferrucci, M. Vergari, F. Cogiamanian et al., "Transcranial direct current stimulation (tDCS) for fatigue in multiple sclerosis," *NeuroRehabilitation*, vol. 34, no. 1, pp. 121–127, 2014.

[55] M. A. Nitsche and W. Paulus, "Noninvasive brain stimulation protocols in the treatment of epilepsy: current state and perspectives," *Neurotherapeutics*, vol. 6, no. 2, pp. 244–250, 2009.

[56] R. Ferrucci, F. Mameli, I. Guidi et al., "Transcranial direct current stimulation improves recognition memory in Alzheimer disease," *Neurology*, vol. 71, no. 7, pp. 493–498, 2008.

[57] P. S. Boggio, L. P. Khoury, D. C. Martins, O. E. Martins, E. C. de Macedo, and F. Fregni, "Temporal cortex direct current stimulation enhances performance on a visual recognition memory task in Alzheimer disease," *Journal of Neurology, Neurosurgery, and Psychiatry*, vol. 80, no. 4, pp. 444–447, 2009.

[58] F. Valentino, G. Cosentino, F. Brighina et al., "Transcranial direct current stimulation for treatment of freezing of gait: a cross-over study," *Movement Disorders*, vol. 29, no. 8, pp. 1064–1069, 2014.

[59] D. H. Benninger and M. Hallett, "Non-invasive brain stimulation for Parkinson's disease: current concepts and outlook 2015," *NeuroRehabilitation*, vol. 37, no. 1, pp. 11–24, 2015.

[60] D. P. Purpura and J. G. McMurtry, "Intracellular activities and evoked potential changes during polarization of motor cortex," *Journal of Neurophysiology*, vol. 28, no. 1, pp. 166–185, 1965.

[61] L. J. Bindman, O. C. J. Lippold, and J. W. T. Redfearn, "Long-lasting Changes in the Level of the Electrical Activity of the Cerebral Cortex produced by Polarizing Currents," *Nature*, vol. 196, no. 4854, pp. 584-585, 1962.

[62] L. J. Bindman, O. C. J. Lippold, and J. W. T. Redfearn, "The action of brief polarizing currents on the cerebral cortex of the rat (1) during current flow and (2) in the production of long-lasting after-effects," *The Journal of Physiology*, vol. 172, no. 3, pp. 369–382, 1964.

[63] N. Islam, M. Aftabuddin, A. Moriwaki, Y. Hattori, and Y. Hori, "Increase in the calcium level following anodal polarization in the rat brain," *Brain Research*, vol. 684, no. 2, pp. 206–208, 1995.

[64] B. C. Albensi, D. R. Oliver, J. Toupin, and G. Odero, "Electrical stimulation protocols for hippocampal synaptic plasticity and neuronal hyper-excitability: are they effective or relevant?," *Experimental Neurology*, vol. 204, no. 1, pp. 1–13, 2007.

[65] A. Liu, M. Vöröslakos, G. Kronberg et al., "Immediate neurophysiological effects of transcranial electrical stimulation," *Nature Communications*, vol. 9, no. 1, p. 5092, 2018.

[66] A. Quartarone, F. Morgante, S. Bagnato et al., "Long lasting effects of transcranial direct current stimulation on motor imagery," *Neuroreport*, vol. 15, no. 8, pp. 1287–1291, 2004.

[67] A. Priori, A. Berardelli, S. Rona, N. Accornero, and M. Manfredi, "Polarization of the human motor cortex through the scalp," *Neuroreport*, vol. 9, no. 10, pp. 2257–2260, 1998.

[68] L. Marshall, H. Helgadóttir, M. Mölle, and J. Born, "Boosting slow oscillations during sleep potentiates memory," *Nature*, vol. 444, no. 7119, pp. 610–613, 2006.

[69] A. Antal, K. Boros, C. Poreisz, L. Chaieb, D. Terney, and W. Paulus, "Comparatively weak after-effects of transcranial alternating current stimulation (tACS) on cortical excitability in humans," *Brain Stimulation*, vol. 1, no. 2, pp. 97–105, 2008.

[70] D. Terney, L. Chaieb, V. Moliadze, A. Antal, and W. Paulus, "Increasing human brain excitability by transcranial high-frequency random noise stimulation," *The Journal of Neuroscience*, vol. 28, no. 52, pp. 14147–14155, 2008.

[71] C. J. Stagg, A. Antal, and M. A. Nitsche, "Physiology of transcranial direct current stimulation," *The Journal of ECT*, vol. 34, no. 3, pp. 144–152, 2018.

[72] D. Yang, Y. I. Shin, and K. S. Hong, "Systemic review on transcranial electrical stimulation parameters and EEG/fNIRS features for brain diseases," *Frontiers in Neuroscience*, vol. 15, p. 274, 2021.

[73] H. Mahmoudi, A. B. Haghighi, P. Petramfar, S. Jahanshahi, Z. Salehi, and F. Fregni, "Transcranial direct current stimulation: electrode montage in stroke," *Disability and Rehabilitation*, vol. 33, no. 15–16, pp. 1383–1388, 2011.

[74] S. B. Berger, D. Ballon, M. Graham et al., "Magnetic resonance imaging demonstrates that electric stimulation of cerebellar fastigial nucleus reduces cerebral infarction in rats," *Stroke*, vol. 21, 11 Supplement, pp. III172–III176, 1990.

[75] S. B. Glickstein, E. V. Golanov, and D. J. Reis, "Intrinsic neurons of fastigial nucleus mediate neurogenic neuroprotection

against excitotoxic and ischemic neuronal injury in rat," *The Journal of Neuroscience*, vol. 19, no. 10, pp. 4142–4154, 1999.

[76] S. B. Glickstein, C. P. Ilch, D. J. Reis, and E. V. Golanov, "Stimulation of the subthalamic vasodilator area and fastigial nucleus independently protects the brain against focal ischemia," *Brain Research*, vol. 912, no. 1, pp. 47–59, 2001.

[77] E. Berdichevsky, N. Riveros, S. Sánchez-Armáss, and F. Orrego, "Kainate, N-methylaspartate and other excitatory amino acids increase calcium influx into rat brain cortex cells in vitro," *Neuroscience Letters*, vol. 36, no. 1, pp. 75–80, 1983.

[78] T. M. Bosley, P. L. Woodhams, R. D. Gordon, and R. Balázs, "Effects of anoxia on the stimulated release of amino acid neurotransmitters in the cerebellum in vitro," *Journal of Neurochemistry*, vol. 40, no. 1, pp. 189–201, 1983.

[79] H. Benveniste, J. Drejer, A. Schousboe, and N. H. Diemer, "Elevation of the extracellular concentrations of glutamate and aspartate in rat hippocampus during transient cerebral ischemia monitored by intracerebral microdialysis," *Journal of Neurochemistry*, vol. 43, no. 5, pp. 1369–1374, 1984.

[80] J. Drejer, H. Benveniste, N. H. Diemer, and A. Schousboe, "Cellular origin of ischemia-induced glutamate release from brain tissue in vivo and in vitro," *Journal of Neurochemistry*, vol. 45, no. 1, pp. 145–151, 1985.

[81] M. Schroeter, S. Jander, O. W. Witte, and G. Stoll, "Local immune responses in the rat cerebral cortex after middle cerebral artery occlusion," *Journal of Neuroimmunology*, vol. 55, no. 2, pp. 195–203, 1994.

[82] E. Tarkowski, L. Rosengren, C. Blomstrand et al., "Early intrathecal production of interleukin-6 predicts the size of brain lesion in stroke," *Stroke*, vol. 26, no. 8, pp. 1393–1398, 1995.

[83] C. Iadecola and J. Anrather, "The immunology of stroke: from mechanisms to translation," *Nature Medicine*, vol. 17, no. 7, pp. 796–808, 2011.

[84] O. Peters, T. Back, U. Lindauer et al., "Increased formation of reactive oxygen species after permanent and reversible middle cerebral artery occlusion in the rat," *Journal of Cerebral Blood Flow and Metabolism*, vol. 18, no. 2, pp. 196–205, 1998.

[85] J. P. Bolaños and A. Almeida, "Roles of nitric oxide in brain hypoxia-ischemia," *Biochimica et Biophysica Acta (BBA) - Bioenergetics*, vol. 1411, no. 2–3, pp. 415–436, 1999.

[86] P. H. Chan, "Reactive oxygen radicals in signaling and damage in the ischemic brain," *Journal of Cerebral Blood Flow and Metabolism*, vol. 21, no. 1, pp. 2–14, 2001.

[87] S. J. Bolton, D. C. Anthony, and V. H. Perry, "Loss of the tight junction proteins occludin and zonula occludens-1 from cerebral vascular endothelium during neutrophil-induced blood-brain barrier breakdown *in vivo*," *Neuroscience*, vol. 86, no. 4, pp. 1245–1257, 1998.

[88] S. Fischer, M. Clauss, M. Wiesnet, D. Renz, W. Schaper, and G. F. Karliczek, "Hypoxia induces permeability in brain microvessel endothelial cells via VEGF and NO," *The American Journal of Physiology*, vol. 276, no. 4, pp. C812–C820, 1999.

[89] P. Lipton, "Ischemic cell death in brain neurons," *Physiological Reviews*, vol. 79, no. 4, pp. 1431–1568, 1999.

[90] S. H. Graham and J. Chen, "Programmed cell death in cerebral ischemia," *Journal of Cerebral Blood Flow and Metabolism*, vol. 21, no. 2, pp. 99–109, 2001.

[91] T. Nitatori, N. Sato, S. Waguri et al., "Delayed neuronal death in the CA1 pyramidal cell layer of the gerbil hippocampus following transient ischemia is apoptosis," *The Journal of Neuroscience*, vol. 15, no. 2, pp. 1001–1011, 1995.

[92] N. J. Solenski, C. G. di Pierro, P. A. Trimmer, A.-L. Kwan, G. A. Helm, and G. A. Helms, "Ultrastructural changes of neuronal mitochondria after transient and permanent cerebral ischemia," *Stroke*, vol. 33, no. 3, pp. 816–824, 2002.

[93] C. Liu, Y. Gao, J. Barrett, and B. Hu, "Autophagy and protein aggregation after brain ischemia," *Journal of Neurochemistry*, vol. 115, no. 1, pp. 68–78, 2010.

[94] Y. Mo, Y.-Y. Sun, and K.-Y. Liu, "Autophagy and inflammation in ischemic stroke," *Neural Regeneration Research*, vol. 15, no. 8, pp. 1388–1396, 2020.

[95] R. Gill, P. Andiné, L. Hillered, L. Persson, and H. Hagberg, "The effect of MK-801 on cortical spreading depression in the penumbral zone following focal ischaemia in the rat," *Journal of Cerebral Blood Flow and Metabolism*, vol. 12, no. 3, pp. 371–379, 1992.

[96] A. J. Strong, S. E. Smith, D. J. Whittington et al., "Factors influencing the frequency of fluorescence transients as markers of peri-infarct depolarizations in focal cerebral ischemia," *Stroke*, vol. 31, no. 1, pp. 214–222, 2000.

[97] R. Babona-Pilipos, I. A. Droujinine, M. R. Popovic, and C. M. Morshead, "Adult subependymal neural precursors, but not differentiated cells, undergo rapid cathodal migration in the presence of direct current electric fields," *PLoS One*, vol. 6, no. 8, article e23808, 2011.

[98] J.-F. Feng, J. Liu, X.-Z. Zhang et al., "Guided migration of neural stem cells derived from human embryonic stem cells by an electric field," *Stem Cells*, vol. 30, no. 2, pp. 349–355, 2012.

[99] K. Zhang, L. Guo, J. Zhang et al., "tDCS accelerates the rehabilitation of MCAO-induced motor function deficits via neurogenesis modulated by the Notch1 signaling pathway," *Neurorehabilitation and Neural Repair*, vol. 34, no. 7, pp. 640–651, 2020.

[100] T. Jiang, R. X. Xu, A. W. Zhang et al., "Effects of transcranial direct current stimulation on hemichannel pannexin-1 and neural plasticity in rat model of cerebral infarction," *Neuroscience*, vol. 226, pp. 421–426, 2012.

[101] K. J. Yoon, B.-M. Oh, and D.-Y. Kim, "Functional improvement and neuroplastic effects of anodal transcranial direct current stimulation (tDCS) delivered 1 day vs. 1 week after cerebral ischemia in rats," *Brain Research*, vol. 1452, pp. 61–72, 2012.

[102] M. A. Nitsche, K. Fricke, U. Henschke et al., "Pharmacological modulation of cortical excitability shifts induced by transcranial direct current stimulation in humans," *The Journal of Physiology*, vol. 553, no. 1, pp. 293–301, 2003.

[103] M. A. Nitsche, D. Liebetanz, A. Schlitterlau et al., "GABAergic modulation of DC stimulation-induced motor cortex excitability shifts in humans," *The European Journal of Neuroscience*, vol. 19, no. 10, pp. 2720–2726, 2004.

[104] C. J. Stagg, J. G. Best, M. C. Stephenson et al., "Polarity-sensitive modulation of cortical neurotransmitters by transcranial stimulation," *Journal of Neuroscience*, vol. 29, no. 16, pp. 5202–5206, 2009.

[105] F. Hummel, P. Celnik, P. Giraux et al., "Effects of non-invasive cortical stimulation on skilled motor function in chronic stroke," *Brain*, vol. 128, no. 3, pp. 490–499, 2005.

[106] E. M. Khedr, O. A. Shawky, D. H. El-Hammady et al., "Effect of anodal versus cathodal transcranial direct current

stimulation on stroke rehabilitation: a pilot randomized controlled trial," *Neurorehabilitation and Neural Repair*, vol. 27, no. 7, pp. 592–601, 2013.

[107] E. Pruvost-Robieux, J. Benzakoun, G. Turc et al., "Cathodal transcranial direct current stimulation in acute ischemic stroke: pilot randomized controlled trial," *Stroke*, vol. 52, no. 6, pp. 1951–1960, 2021.

[108] C. Rakers and G. C. Petzold, "Astrocytic calcium release mediates peri-infarct depolarizations in a rodent stroke model," *The Journal of Clinical Investigation*, vol. 127, no. 2, pp. 511–516, 2017.

[109] R. Kaviannejad, S. M. Karimian, E. Riahi, and G. Ashabi, "A single immediate use of the cathodal transcranial direct current stimulation induces neuroprotection of hippocampal region against global cerebral ischemia," *Journal of Stroke and Cerebrovascular Diseases*, vol. 31, no. 3, article 106241, 2022.

[110] T. Back, K. Kohno, and K. A. Hossmann, "Cortical negative DC deflections following middle cerebral artery occlusion and KCl-induced spreading depression: effect on blood flow, tissue oxygenation, and electroencephalogram," *Journal of Cerebral Blood Flow and Metabolism*, vol. 14, no. 1, pp. 12–19, 1994.

[111] L.-C. Wang, W.-Y. Wei, P.-C. Ho, P.-Y. Wu, Y.-P. Chu, and K.-J. Tsai, "Somatosensory cortical electrical stimulation after reperfusion attenuates ischemia/reperfusion injury of rat brain," *Frontiers in Aging Neuroscience*, vol. 13, article 741168, 2021.

[112] G.-B. Liu, Y.-M. Pan, Y.-S. Liu et al., "Ghrelin promotes neural differentiation of adipose tissue-derived mesenchymal stem cell via AKT/mTOR and β-catenin signaling pathways," *The Kaohsiung Journal of Medical Sciences*, vol. 36, no. 6, pp. 405–416, 2020.

[113] M. C. Ashby, S. A. De La Rue, G. S. Ralph, J. Uney, G. L. Collingridge, and J. M. Henley, "Removal of AMPA receptors (AMPARs) from synapses is preceded by transient endocytosis of extrasynaptic AMPARs," *The Journal of Neuroscience*, vol. 24, no. 22, pp. 5172–5176, 2004.

[114] F. Ranieri, M. V. Podda, E. Riccardi et al., "Modulation of LTP at rat hippocampal CA3-CA1 synapses by direct current stimulation," *Journal of Neurophysiology*, vol. 107, no. 7, pp. 1868–1880, 2012.

[115] B. Cheeran, P. Talelli, F. Mori et al., "A common polymorphism in the brain-derived neurotrophic factor gene (BDNF) modulates human cortical plasticity and the response to rTMS," *The Journal of Physiology*, vol. 586, no. 23, pp. 5717–5725, 2008.

[116] B. Fritsch, J. Reis, K. Martinowich et al., "Direct current stimulation promotes BDNF-dependent synaptic plasticity: potential implications for motor learning," *Neuron*, vol. 66, no. 2, pp. 198–204, 2010.

[117] M. Moloudizargari, M. H. Asghari, E. Ghobadi, M. Fallah, S. Rasouli, and M. Abdollahi, "Autophagy, its mechanisms and regulation: implications in neurodegenerative diseases," *Ageing Research Reviews*, vol. 40, pp. 64–74, 2017.

[118] C. Dai, J. Wang, J. Li et al., "Repetitive anodal transcranial direct current stimulation improves neurological recovery by preserving the neuroplasticity in an asphyxial rat model of cardiac arrest," *Brain Stimulation*, vol. 14, no. 2, pp. 407–416, 2021.

[119] R. Braun, R. Klein, H. L. Walter et al., "Transcranial direct current stimulation accelerates recovery of function, induces neurogenesis and recruits oligodendrocyte precursors in a rat model of stroke," *Experimental Neurology*, vol. 279, pp. 127–136, 2016.

[120] D. W. Shin, J. Fan, E. Luu et al., "In vivo modulation of the blood-brain barrier permeability by transcranial direct current stimulation (tDCS)," *Annals of Biomedical Engineering*, vol. 48, no. 4, pp. 1256–1270, 2020.

[121] Y. Xia, Y. Li, W. Khalid, M. Bikson, and B. M. Fu, "Direct current stimulation disrupts endothelial glycocalyx and tight junctions of the blood-brain barrier in vitro," *Frontiers in Cell and Development Biology*, vol. 9, article 731028, 2021.

[122] M. Vöröslakos, Y. Takeuchi, K. Brinyiczki et al., "Direct effects of transcranial electric stimulation on brain circuits in rats and humans," *Nature Communications*, vol. 9, no. 1, p. 483, 2018.

[123] V. Di Lazzaro, M. Dileone, F. Capone et al., "Immediate and late modulation of interhemipheric imbalance with bilateral transcranial direct current stimulation in acute stroke," *Brain Stimulation*, vol. 7, no. 6, pp. 841–848, 2014.

[124] M. Lotze, J. Markert, P. Sauseng, J. Hoppe, C. Plewnia, and C. Gerloff, "The role of multiple contralesional motor areas for complex hand movements after internal capsular lesion," *The Journal of Neuroscience*, vol. 26, no. 22, pp. 6096–6102, 2006.

[125] K. Fricke, A. A. Seeber, N. Thirugnanasambandam, W. Paulus, M. A. Nitsche, and J. C. Rothwell, "Time course of the induction of homeostatic plasticity generated by repeated transcranial direct current stimulation of the human motor cortex," *Journal of Neurophysiology*, vol. 105, no. 3, pp. 1141–1149, 2011.

[126] C. Rossi, F. Sallustio, S. Di Legge, P. Stanzione, and G. Koch, "Transcranial direct current stimulation of the affected hemisphere does not accelerate recovery of acute stroke patients," *European Journal of Neurology*, vol. 20, no. 1, pp. 202–204, 2013.

[127] S. Kumar, S. Marchina, S. Langmore et al., "FEASt: a randomized controlled trial for dysphagia recovery after an acute ischemic stroke," 2022, https://www.researchsquare.com/article/rs-1344219/v1.

[128] S. Hesse, A. Waldner, J. Mehrholz, C. Tomelleri, M. Pohl, and C. Werner, "Combined transcranial direct current stimulation and robot-assisted arm training in subacute stroke patients: an exploratory, randomized multicenter trial," *Neurorehabilitation and Neural Repair*, vol. 25, no. 9, pp. 838–846, 2011.

[129] P. Celnik, N.-J. Paik, Y. Vandermeeren, M. Dimyan, and L. G. Cohen, "Effects of combined peripheral nerve stimulation and brain polarization on performance of a motor sequence task after chronic stroke," *Stroke*, vol. 40, no. 5, pp. 1764–1771, 2009.

[130] A. M. Goodwill, W.-P. Teo, P. Morgan, R. M. Daly, and D. J. Kidgell, "Bihemispheric-tDCS and upper limb rehabilitation improves retention of motor function in chronic stroke: a pilot study," *Frontiers in Human Neuroscience*, vol. 10, p. 258, 2016.

[131] J. I. Kang, H. Lee, K. Jhung et al., "Frontostriatal connectivity changes in major depressive disorder after repetitive transcranial magnetic stimulation: a randomized sham-controlled study," *The Journal of Clinical Psychiatry*, vol. 77, no. 9, pp. e1137–e1143, 2016.

[132] C.-T. Li, J.-C. Hsieh, H.-H. Huang et al., "Cognition-modulated frontal activity in prediction and augmentation of

antidepressant efficacy: a randomized controlled pilot study," *Cerebral Cortex*, vol. 26, no. 1, pp. 202–210, 2016.

[133] L. Bais, A. Vercammen, R. Stewart et al., "Short and long term effects of left and bilateral repetitive transcranial magnetic stimulation in schizophrenia patients with auditory verbal hallucinations: a randomized controlled trial," *PLoS One*, vol. 9, no. 10, article e108828, 2014.

[134] M. S. Kim, W. H. Chang, J. W. Cho et al., "Efficacy of cumulative high-frequency rTMS on freezing of gait in Parkinson's disease," *Restorative Neurology and Neuroscience*, vol. 33, no. 4, pp. 521–530, 2015.

[135] B. W. Badran, C. E. Glusman, C. W. Austelle et al., "A Double-Blind, Sham-Controlled Pilot Trial of Pre-Supplementary Motor Area (Pre-SMA) 1 Hz rTMS to Treat Essential Tremor," *Brain Stimulation*, vol. 9, no. 6, pp. 945–947, 2016.

[136] M. Azin, N. Zangiabadi, F. Iranmanesh, M. R. Baneshi, and S. Banihashem, "Effects of intermittent theta burst stimulation on manual dexterity and motor imagery in patients with multiple sclerosis: a quasi-experimental controlled study," *Iranian Red Crescent Medical Journal*, vol. 18, no. 10, article e27056, 2016.

[137] G. Rutherford, B. Lithgow, and Z. Moussavi, "Short and long-term effects of rTMS treatment on Alzheimer's disease at different stages: a pilot study," *Journal of Experimental Neuroscience*, vol. 9, pp. 43–51, 2015.

[138] X. Xia, Y. Bai, Y. Zhou et al., "Effects of 10 Hz repetitive transcranial magnetic stimulation of the left dorsolateral prefrontal cortex in disorders of consciousness," *Frontiers in Neurology*, vol. 8, p. 182, 2017.

[139] V. Di Lazzaro, R. Bella, A. Benussi et al., "Diagnostic contribution and therapeutic perspectives of transcranial magnetic stimulation in dementia," *Clinical Neurophysiology*, vol. 132, no. 10, pp. 2568–2607, 2021.

[140] M. Cantone, G. Lanza, F. Fisicaro et al., "Evaluation and treatment of vascular cognitive impairment by transcranial magnetic stimulation," *Neural Plasticity*, vol. 2020, Article ID 8820881, 17 pages, 2020.

[141] R. Chen, J. Classen, C. Gerloff et al., "Depression of motor cortex excitability by low-frequency transcranial magnetic stimulation," *Neurology*, vol. 48, no. 5, pp. 1398–1403, 1997.

[142] E. Dayan, N. Censor, E. R. Buch, M. Sandrini, and L. G. Cohen, "Noninvasive brain stimulation: from physiology to network dynamics and back," *Nature Neuroscience*, vol. 16, no. 7, pp. 838–844, 2013.

[143] M. Cantone, G. Lanza, L. Vinciguerra et al., "Age, height, and sex on motor evoked potentials: translational data from a large Italian cohort in a clinical environment," *Frontiers in Human Neuroscience*, vol. 13, p. 185, 2019.

[144] H. J. Bidmon, K. Kato, A. Schleicher, O. W. Witte, and K. Zilles, "Transient increase of manganese-superoxide dismutase in remote brain areas after focal photothrombotic cortical lesion," *Stroke*, vol. 29, no. 1, pp. 203–211, 1998.

[145] Y. Peng, Y. Lin, N.-W. Yu, X.-L. Liao, and L. Shi, "The clinical efficacy and possible mechanism of combination treatment of cerebral ischemic stroke with Ginkgo biloba extract and low-frequency repetitive transcranial magnetic stimulation," *Sichuan Da Xue Xue Bao. Yi Xue Ban = Journal of Sichuan University. Medical Science Edition*, vol. 52, no. 5, pp. 883–889, 2021.

[146] B. Mancic, I. Stevanovic, T. V. Ilic et al., "Transcranial theta-burst stimulation alters GLT-1 and vGluT1 expression in rat cerebellar cortex," *Neurochemistry International*, vol. 100, pp. 120–127, 2016.

[147] H. Gröhn, B. T. Gillick, I. Tkáč et al., "Influence of repetitive transcranial magnetic stimulation on human neurochemistry and functional connectivity: a pilot MRI/MRS study at 7 T," *Frontiers in Neuroscience*, vol. 13, p. 1260, 2019.

[148] A. Zangen and K. Hyodo, "Transcranial magnetic stimulation induces increases in extracellular levels of dopamine and glutamate in the nucleus accumbens," *Neuroreport*, vol. 13, no. 18, pp. 2401–2405, 2002.

[149] K. J. Yoon, Y.-T. Lee, and T. R. Han, "Mechanism of functional recovery after repetitive transcranial magnetic stimulation (rTMS) in the subacute cerebral ischemic rat model: neural plasticity or anti-apoptosis?," *Experimental Brain Research*, vol. 214, no. 4, pp. 549–556, 2011.

[150] F. Guo, J. Lou, X. Han, Y. Deng, and X. Huang, "Repetitive transcranial magnetic stimulation ameliorates cognitive impairment by enhancing neurogenesis and suppressing apoptosis in the hippocampus in rats with ischemic stroke," *Frontiers in Physiology*, vol. 8, p. 559, 2017.

[151] X. Wang, X. Zhou, J. Bao et al., "High-frequency repetitive transcranial magnetic stimulation mediates autophagy flux in human bone mesenchymal stromal cells via NMDA receptor–Ca2+–extracellular signal-regulated kinase–mammalian target of rapamycin signaling," *Frontiers in Neuroscience*, vol. 13, p. 1225, 2019.

[152] J. Luo, H. Zheng, L. Zhang et al., "High-frequency repetitive transcranial magnetic stimulation (rTMS) improves functional recovery by enhancing neurogenesis and activating BDNF/TrkB signaling in ischemic rats," *International Journal of Molecular Sciences*, vol. 18, no. 2, p. 455, 2017.

[153] Y. Hu, X. Zhang, Y. Lu, J. Tian, and T. Guo, "The effects of paired associative stimulation on sensorimotor function and the expression of MAP-2 and GAP-43 after focal cerebral ischemia and reperfasion," *Chinese Journal of Physical Medicine and Rehabilitation*, vol. 12, pp. 733–739, 2018.

[154] Y. Hu, T.-C. Guo, X.-Y. Zhang, J. Tian, and Y.-S. Lu, "Paired associative stimulation improves synaptic plasticity and functional outcomes after cerebral ischemia," *Neural Regeneration Research*, vol. 14, no. 11, pp. 1968–1976, 2019.

[155] M. Cantone, G. Lanza, F. Ranieri, G. M. Opie, and C. Terranova, "Editorial: Non-invasive brain stimulation in the study and modulation of metaplasticity in neurological disorders," *Frontiers in Neurology*, vol. 12, article 721906, 2021.

[156] C. Zheng, W. Liao, and W. Xia, "Effect of combined low-frequency repetitive transcranial magnetic stimulation and virtual reality training on upper limb function in subacute stroke: a double-blind randomized controlled trail," *Journal of Huazhong University of Science and Technology. Medical Sciences*, vol. 35, no. 2, pp. 248–254, 2015.

[157] S. K. Schiemanck, G. Kwakkel, M. W. M. Post, L. J. Kappelle, and A. J. H. Prevo, "Impact of internal capsule lesions on outcome of motor hand function at one year post-stroke," *Journal of Rehabilitation Medicine*, vol. 40, no. 2, pp. 96–101, 2008.

[158] N. Weiduschat, A. Thiel, I. Rubi-Fessen et al., "Effects of repetitive transcranial magnetic stimulation in aphasic stroke," *Stroke*, vol. 42, no. 2, pp. 409–415, 2011.

[159] G. Koch, S. Bonni, V. Giacobbe et al., "Theta-burst stimulation of the left hemisphere accelerates recovery of hemispatial neglect," *Neurology*, vol. 78, no. 1, pp. 24–30, 2012.

[160] W. H. Chang, Y.-H. Kim, O. Y. Bang, S. T. Kim, Y. H. Park, and P. K. W. Lee, "Long-term effects of rTMS on motor recovery in patients after subacute stroke," *Journal of Rehabilitation Medicine*, vol. 42, no. 8, pp. 758–764, 2010.

[161] N. Takeuchi, T. Tada, M. Toshima, Y. Matsuo, and K. Ikoma, "Repetitive transcranial magnetic stimulation over bilateral hemispheres enhances motor function and training effect of paretic hand in patients after stroke," *Journal of Rehabilitation Medicine*, vol. 41, no. 13, pp. 1049–1054, 2009.

[162] Y.-H. Kim, S. H. You, M.-H. Ko et al., "Repetitive transcranial magnetic stimulation–induced corticomotor excitability and associated motor skill acquisition in chronic stroke," *Stroke*, vol. 37, no. 6, pp. 1471–1476, 2006.

[163] R. Momosaki, M. Abo, and W. Kakuda, "Bilateral repetitive transcranial magnetic stimulation combined with intensive swallowing rehabilitation for chronic stroke dysphagia: a case series study," *Case Reports in Neurology*, vol. 6, no. 1, pp. 60–67, 2014.

[164] E. Park, M. S. Kim, W. H. Chang et al., "Effects of Bilateral Repetitive Transcranial Magnetic Stimulation on Post-Stroke Dysphagia," *Brain Stimulation*, vol. 10, no. 1, pp. 75–82, 2017.

[165] J. P. Szaflarski, J. Vannest, S. W. Wu, M. W. DiFrancesco, C. Banks, and D. L. Gilbert, "Excitatory repetitive transcranial magnetic stimulation induces improvements in chronic post-stroke aphasia," *Medical Science Monitor*, vol. 17, no. 3, pp. -CR132–CR139, 2011.

[166] X. Zhao, J. Ding, H. Pan et al., "Anodal and cathodal tDCS modulate neural activity and selectively affect GABA and glutamate syntheses in the visual cortex of cats," *The Journal of Physiology*, vol. 598, no. 17, pp. 3727–3745, 2020.

[167] K. A. Hossmann, "Periinfarct depolarizations," *Cerebrovascular and Brain Metabolism Reviews*, vol. 8, no. 3, pp. 195–208, 1996.

[168] W. H. Chang, K. E. Uhm, Y.-I. Shin, A. Pascual-Leone, and Y.-H. Kim, "Factors influencing the response to high-frequency repetitive transcranial magnetic stimulation in patients with subacute stroke," *Restorative Neurology and Neuroscience*, vol. 34, no. 5, pp. 747–755, 2016.

[169] Y.-F. Hsu, Y.-Z. Huang, Y.-Y. Lin et al., "Intermittent theta burst stimulation over ipsilesional primary motor cortex of subacute ischemic stroke patients: a pilot study," *Brain Stimulation*, vol. 6, no. 2, pp. 166–174, 2013.

Hindawi
Neural Plasticity
Volume 2022, Article ID 2219993, 12 pages
https://doi.org/10.1155/2022/2219993

Research Article

Altered Effective Connectivity of the Primary Motor Cortex in Transient Ischemic Attack

Zeqi Hao,[1,2] **Yulin Song**,[3] **Yuyu Shi**,[1,2] **Hongyu Xi**,[4] **Hongqiang Zhang**,[5] **Mengqi Zhao**,[1,2] **Jiahao Yu**,[1,2] **Lina Huang**,[5] **and Huayun Li**[1,2]

[1]*School of Teacher Education, Zhejiang Normal University, Jinhua, China*
[2]*Key Laboratory of Intelligent Education Technology and Application, Zhejiang Normal University, Jinhua, China*
[3]*Department of Neurology, Anshan Changda Hospital, Anshan, China*
[4]*Faculty of Western Languages, Heilongjiang University, Harbin, China*
[5]*Department of Radiology, Changshu No. 2 People's Hospital, The Affiliated Changshu Hospital of Xuzhou Medical University, Changshu, Jiangsu, China*

Correspondence should be addressed to Lina Huang; 760020220697@xzhmu.edu.cn and Huayun Li; huayun@zjnu.edu.cn

Received 4 August 2022; Revised 2 September 2022; Accepted 19 September 2022; Published 18 November 2022

Academic Editor: Yu Zheng

Objective. This study is aimed at exploring alteration in motor-related effective connectivity in individuals with transient ischemic attack (TIA). *Methods*. A total of 48 individuals with TIA and 41 age-matched and sex-matched healthy controls (HCs) were recruited for this study. The participants were scanned using MRI, and their clinical characteristics were collected. To investigate motor-related effective connectivity differences between individuals with TIA and HCs, the bilateral primary motor cortex (M1) was used as the regions of interest (ROIs) to perform a whole-brain Granger causality analysis (GCA). Furthermore, partial correlation was used to evaluate the relationship between GCA values and the clinical characteristics of individuals with TIA. *Results*. Compared with HCs, individuals with TIA demonstrated alterations in the effective connectivity between M1 and widely distributed brain regions involved in motor, visual, auditory, and sensory integration. In addition, GCA values were significantly correlated with high- and low-density lipoprotein cholesterols in individuals with TIA. *Conclusion*. This study provides important evidence for the alteration of motor-related effective connectivity in TIA, which reflects the abnormal information flow between different brain regions. This could help further elucidate the pathological mechanisms of motor impairment in individuals with TIA and provide a new perspective for future early diagnosis and intervention for TIA.

1. Introduction

Transient ischemic attack (TIA) is defined as a brief episode of neurological dysfunction caused by focal cerebral ischemia that does not result in acute cerebral infarction [1, 2]. Individuals with TIA have been clinically observed to be at high risk of suffering a stroke, and 7.5%–17.4% of individuals with TIA have a stroke within 3 months [3–5]. Nevertheless, timely treatment of individuals with TIA could reduce the risk of stroke by 80% in 3 months [6–8], which has received increasing attention in recent years [9, 10]. To improve the diagnosis and treatment, it is essential to better understand the underlying neural mechanisms of TIA [11–14].

Resting-state functional magnetic resonance imaging (rs-fMRI) is a promising tool for investigating neurophysiological mechanisms [15–17] and has been extensively used to examine alterations in spontaneous neural activity in individuals with TIA [18–21]. In rs-fMRI, functional connectivity (FC) is an extensively adopted method for examining the brain network characteristics of TIA and disturbances in connectivity have been revealed in previous studies of TIA [22–24]. However, FC only reflects the correlation of time series between brain regions and ignores the causal effect of the interactions [25–27]. Previous studies have demonstrated that effective connectivity could reveal the causal effect of the interactions between brain areas [28–30], which

is how damaged brain areas influence other brain areas in a particular direction [31, 32]. Granger causality analysis (GCA) is one of the commonly used effective connectivity methods that can measure causal effects and information flow of fMRI time series, thus reflecting the directionality of interactions between brain regions [33–38]. In contrast to other effective connectivity methods, such as dynamic causal modeling and structural equation modeling, GCA is relatively data driven and does not require a priori anatomical models for data analysis and statistical inference [39, 40]. The method is therefore particularly suitable for exploratory studies on brain interaction in the context of a limited understanding of the pathological mechanisms of TIA, which could provide further evidence of how the disease affects the brains of individuals.

Motor impairment is a typical transient symptom associated with TIA [6, 41, 42], which mainly includes impaired limb dexterity, limb weakness, limb numbness, gait disturbance, and loss of coordination [43–45]. Previous studies have demonstrated that motor impairment is also a key high-risk clinical characteristic of subsequent stroke [46, 47]. TIA patients with motor impairment are twice as likely to have a stroke as those without motor impairment [48]. The primary motor cortex (M1) plays a critical role in the network responsible for voluntary motor functions [49, 50]. The execution of motor commands is accomplished through neuronal signals generated and sent by M1 [51–53] and is closely associated with motor impairment in TIA [54–56]. Therefore, using bilateral M1 as the regions of interest (ROIs) to explore the alteration of motor-related effective connectivity in TIA could advance our understanding of the pathological mechanisms of TIA.

In the current study, we used the GCA with bilateral M1 as ROIs to examine whether individuals with TIA had altered effective connectivity compared to healthy controls (HCs). Subsequently, we investigated the relationship between alterations of effective connectivity and clinical characteristics. According to our hypothesis, there were alterations in effective connectivity in individuals with TIA, which were related to clinical characteristics.

2. Materials and Methods

2.1. Participants. A total of 51 participants with suspected TIA were enrolled at Anshan Changda Hospital between April 2015 and June 2016. Experienced clinical neurologists evaluated all participants for neurological symptoms associated with a possible vascular etiology. Individuals with a current or past history of hemorrhage, leukodystrophy, migraine, epilepsy, or psychiatric or neurological disorders were excluded. In addition, we recruited 41 HCs with no history of psychiatric or neurological disorders via community advertising, matching their age and sex to participants with TIA.

The MRI data of three individuals with TIA were excluded from further analysis because of their poor image quality. Finally, 48 individuals with TIA (25 with nonfirst TIA and 4 with stroke) and 41 HCs were included in this study. Forty of the 48 individuals with TIA had motor impairment; specifically, 31 had impaired limb dexterity, four had limb weakness, and five had limb numbness.

2.2. Physiological and Biochemical Tests. Physiological and biochemical tests were completed for all participants within 24 hours prior to MRI scanning, including systolic blood pressure, diastolic blood pressure, blood sugar level, triglycerides, total cholesterol, high-density lipoprotein cholesterol (HDL-C), and low-density lipoprotein cholesterol (LDL-C). Based on age, blood pressure, clinical characteristics, symptom duration, and history of diabetes for each individual with TIA, we computed the ABCD2 score to assess the risk of subsequent stroke [5].

2.3. Data Acquisition. MRI scans were performed using a GE MR-750 3.0 T scanner (GE Medical Systems Inc., Waukesha, WI, United States). For individuals with TIA, there was a time interval from the latest TIA to the subsequent MRI scan of 6 hours to 16 days. All participants were instructed to relax, stay still, keep their eyes closed but not fall asleep, and not to think systematically during resting-state scanning [15]. Functional MRI scans were acquired using an echo planar imaging sequence with repetition time (TR)/echo time (TE) = 2000 ms/30 ms, flip angle (FA) = 60°, acquisition matrix = 64 × 64, slice thickness = 3.2 mm, gap = 0 mm, and slices = 43. The scanning time for the functional MRI was 8 minutes (240 volumes). The structural MRI data were acquired using a high-resolution anatomic sagittal 3D T1 sequence (voxel size = 1 mm × 1 mm × 1 mm), TR/TE = 8100 ms/3.1 ms, 176 slice acquisition matrix = 256 × 256, slice thickness = 1 mm, and gap = 0 mm. The scanning time for the structural MRI was 5 minutes.

2.4. Data Preprocessing. The Resting-State fMRI Data Analysis Toolkit plus (RESTplus V1.24, http://restfmri.net/forum/restplus) [57] was used in MATLAB 2017b to preprocess rs-fMRI images. For the preprocessing, we removed the first 10 volumes to ensure that the fMRI signal reached a steady state. Then, the rest of the volumes were slice timing corrected to the reference slice to synchronize timing across slices [58] and a six-parameter rigid-body transformation was used for realignment and motion correction [58, 59]. The realigned images were spatially normalized to the standard stereotactic space, as defined by the Montreal Neurological Institute (MNI) using the new segment method. The images were then smoothed using a Gaussian kernel with a full width at a half-maximum of 6 mm, which could improve the signal to noise ratio [12, 18, 60]. To control for motion and physiological nuisance signals, the Friston-24 parameters [61], white matter signals, and cerebrospinal fluid signals were regressed out [62]. Head motion could be further controlled by regressing the Friston-24 parameters, which include six head motion parameters generated by Realign, six head motion parameters at the preceding time point, and their corresponding 12 squared values [63, 64]. Detrending was performed to reduce the undesirable drift caused by the instrument, head motion, and physiological pulse aliasing [65, 66]. Grounded in the previous studies, band-pass filtering was not performed in the current study because of the low model order of GCA [38, 67–69].

2.5. Blind Deconvolution Procedure. Resting-state hemodynamic response function retrieval and deconvolution (RS-HRF, https://www.nitrc.org/projects/rshrf) was used to deconvolve the HRF from rs-fMRI signals, which could reduce the interindividual and interregional HRF variability and further improve the accuracy of effective connectivity estimation [69, 70].

2.6. Granger Causality Analysis. Bivariate voxel-wise GCA with the bilateral M1 as the ROIs was implemented using RESTplus. The ROIs were centered at $x = -12$, $y = -30$, and $z = 54$ and $x = 12$, $y = -30$, and $z = 54$ in the MNI space, with a radius of 6 mm [71]. GCA can estimate the causal effects from ROIs (x) to every other voxel in the whole brain (y) and the causal effects from every other voxel in the whole brain to ROIs [72, 73]. If the prediction of the future values of y can be improved by combining past values of x and y instead of using only past values of y, then x is said to Granger-cause y. Similarly, y is said to Granger-cause x when the future values of x are better predicted by combining the past values of y and x compared to using only the past values of x [36, 38, 74]. We used the signed-path coefficient GCA to reflect the alterations in effective connectivity among brain regions in the current study, and the increased or decreased effectivity activity between two brain regions was indicated by positive or negative GCA coefficients [75, 76]. Finally, the coefficient-based GCA values were converted into normally distributed z scores [76].

2.7. Statistical Analysis. The differences in age and clinical characteristics between individuals with TIA and HCs were analyzed using a two-sample t-test, and the differences in gender were analyzed using a chi-squared test. Statistical Product and Service Solutions (SPSS 20.0) was used in all of the analyses. Statistically significant between-group differences were set at $p < 0.05$.

Two-sample t-tests were conducted to determine the differences in effective connectivity between individuals with TIA and HCs using RESTplus. Subsequently, the Gaussian random field theory was adopted to carry out multiple comparison correction in the statistical analysis results (voxel $p < 0.05$, cluster $p < 0.05$, and two-tailed).

To detect the relationship between alterations of effective connectivity and clinical characteristics in TIA, we conducted partial correlation analysis between GCA values extracted from each region showing group differences and clinical characteristics with age and gender as covariates, including HDL-C, LDL-C, ABCD2 scores, and the time interval from the latest TIA to subsequent MRI scanning. Subsequently, Bonferroni correction was applied to correction for multiple comparison [77–79] and the threshold for statistical significance was set to $p < 0.0125$ (0.05/4).

3. Results

3.1. Demographic and Clinical Characteristics. In the present study, there were no significant differences in age ($p = 0.182$), gender ($p = 0.670$), triglyceride level ($p = 0.213$), and HDL-C level ($p = 0.306$). However, the systolic blood pressure ($p < 0.001$), diastolic blood pressure ($p = 0.007$), blood sugar level ($p = 0.001$), total cholesterol level ($p = 0.045$), and LDL-C level ($p = 0.004$) were significantly higher in the TIA group than in the HC group. The detailed demographic and clinical characteristics of the individuals with TIA and HCs are shown in Table 1.

3.2. GCA Results

3.2.1. GCA Results from the Left M1 to the Whole Brain. The GCA values in individuals with TIA from the left M1 to the right precentral gyrus, bilateral inferior parietal gyrus (IPG), left postcentral gyrus, left superior cerebellum, bilateral middle frontal gyrus (MFG), left superior frontal gyrus (SFG), right angular gyrus (AG), and left inferior cerebellum were higher, but the values in the left fusiform and right insula were lower than those in the HCs (Table 2, Figure 1(a)). Furthermore, brain maps of the alteration of effective connectivity from the left M1 to the whole brain are shown in the Supplementary Materials (Figure S1A).

3.2.2. GCA Results from the Whole Brain to the Left M1. The GCA values in individuals with TIA from the left Rolandic operculum (RO), temporal pole of the right middle temporal gyrus (TP), right inferior cerebellum, left precuneus, orbital part of the right middle frontal gyrus, right supplementary motor area (SMA), right superior occipital gyrus (SOG), and opercular part of the right inferior frontal gyrus to the left M1 were lower than those in the HCs (Table 2, Figure 1(b)). Brain maps of the alteration of effective connectivity from the whole brain to the left M1 are shown in the Supplementary Materials (Figure S1B).

3.2.3. GCA Results from the Right M1 to the Whole Brain. The GCA values in individuals with TIA from the right M1 to the right superior temporal gyrus (STG), right precentral gyrus, right SFG, and opercular part of the right inferior frontal gyrus were higher, but those in the left MFG, left RO, left thalamus, and right lingual gyrus (LG) were lower than those in the HCs (Table 3, Figure 2(a)). Brain maps of the alteration of effective connectivity from the right M1 to the whole brain are shown in Figure S2A of the Supplementary Materials.

3.2.4. GCA Results from the Whole Brain to the Right M1. Compared with the HCs, the GCA values from the right STG and right fusiform to the right M1 were higher in individuals with TIA but those from the left insula, left medial SFG, left middle occipital gyrus (MOG), left IPG, and right calcarine were lower (Table 3, Figure 2(b)). Brain maps of the alteration of effective connectivity from the whole brain to the right M1 are shown in Figure S2B in the Supplementary Materials.

3.3. Partial Correlation between GCA and Clinical Characteristics. Partial correlation analysis (covariates: age and gender) was conducted to investigate the relationship between the alterations of effective connectivity and clinical characteristics. After Bonferroni correction for multiple comparisons, we found that the GCA values from the right SMA to the left M1 were negatively associated with HDL-C

Table 1: Demographic and clinical characteristics for individuals with TIA and HCs.

	TIA group ($n = 48$)	HC group ($n = 41$)	p value
Age (years, mean ± SD)	57.604 ± 9.778	55.024 ± 8.033	0.182[a]
Gender (male/female)	37/11	30/11	0.670[b]
Systolic blood pressure (mmHg, mean ± SD)	145.542 ± 20.753	127.546 ± 19.527	<0.001[a]
Diastolic blood pressure (mmHg, mean ± SD)	86.667 ± 10.383	80.030 ± 10.896	0.007[a]
Blood sugar level (mmol/L, mean ± SD)	6.299 ± 2.113	5.120 ± 0.740	0.001[a]
Total cholesterol (mmol/L, mean ± SD)	5.242 ± 1.135	4.753 ± 1.011	0.045[a]
Triglycerides (mmol/L, mean ± SD)	1.603 ± 0.940	1.917 ± 1.345	0.213[a]
HDL-C (mmol/L, mean ± SD)	1.111 ± 0.238	1.051 ± 0.290	0.306[a]
LDL-C (mmol/L, mean ± SD)	3.314 ± 0.974	2.691 ± 0.904	0.004[a]
Motor impairment, no. (%)	40 (83.3%)	—	—
Time interval (days, mean ± SD)	2.610 ± 2.981	—	—
ABCD2 scores (median)	4 (2–6)	—	—

HDL-C: high-density lipoprotein cholesterol; LDL-C: low-density lipoprotein cholesterol; time interval: time interval from the latest TIA to subsequent MRI scanning. [a]Calculated by two-sample t-test. [b]Calculated by chi-squared t-test; there were 6 missing data of blood sugar level, total cholesterol, triglycerides, HDL-C, and LDL-C and 8 missing data of blood systolic pressure and blood diastolic pressure in the HC group.

Table 2: The differences of GCA with left M1 as ROI between the TIA and HC groups.

	Anatomical label	BA	Number of voxels	Peak MNI coordinates (x, y, z)	t value
$F_{x \longrightarrow y}$	Precentral_R	4	74	57, −12, 45	4.43
	Parietal_Inf_R	40	59	48, −48, 48	4.31
	Postcentral_L	43	47	−57, −9, 30	4.10
	Cerebellum_6_L	18	43	−15, −75, −18	4.07
	Frontal_Mid_L	10	57	−24, 51, 9	4.04
	Frontal_Sup_L	9	45	−9, 54, 33	3.90
	Parietal_Inf_L	7	106	−33, −69, 45	3.83
	Frontal_Mid_R	44	47	39, 21, 36	3.67
	Parietal_Inf_L	40	48	−51, −48, 51	3.44
	Angular_R	39	47	42, −60, 45	3.04
	Cerebellum_8_L	NA	38	−18, −45, −39	2.91
	Fusiform_L	37	42	−21, −42, −18	−3.21
	Insula_R	48	76	33, 21, 12	−3.73
$F_{y \longrightarrow x}$	Rolandic_Oper_L	48	74	−39, −12, 15	−3.58
	Temporal_Pole_Mid_R	20	96	48, 12, −42	−3.59
	Cerebellum_8_R	NA	65	12, −66, −33	−3.62
	Precuneus_L	5	68	−9, −45, 78	−3.82
	Frontal_Mid_Orb_R	11	265	27, 42, −18	−3.83
	Supp_Motor_Area_R	6	138	6, 12, 54	−3.87
	Cerebellum_8_R	NA	74	15, −66, −54	−3.96
	Occipital_Sup_R	19	321	21, −87, 36	−4.10
	Frontal_Inf_Oper_R	48	63	63, 12, 0	−4.29

Precentral_R: right precentral gyrus; Parietal_Inf_R: right inferior parietal gyrus; Postcentral_L: left postcentral gyrus; Cerebellum_6_L: left superior cerebellum; Frontal_Mid_L: left middle frontal gyrus; Frontal_Sup_L: left superior frontal gyrus; Parietal_Inf_L: left inferior parietal gyrus; Frontal_Mid_R: right middle frontal gyrus; Angular_R: right angular gyrus; Cerebellum_8_L: left inferior cerebellum; Fusiform_L: left fusiform; Insula_R: right insula; Rolandic_Oper_L: left Rolandic operculum; Temporal_Pole_Mid_R: temporal pole of the right middle temporal gyrus; Cerebellum_8_R: right inferior cerebellum; Precuneus_L: left precuneus; Frontal_Mid_Orb_R: orbital part of the right middle frontal gyrus; Supp_Motor_Area_R: right supplementary motor area; Occipital_Sup_R: right superior occipital gyrus; Frontal_Inf_Oper_R: opercular part of the right inferior frontal gyrus; BA: Brodmann area; MNI: Montreal Neurological Institute; NA: not available.

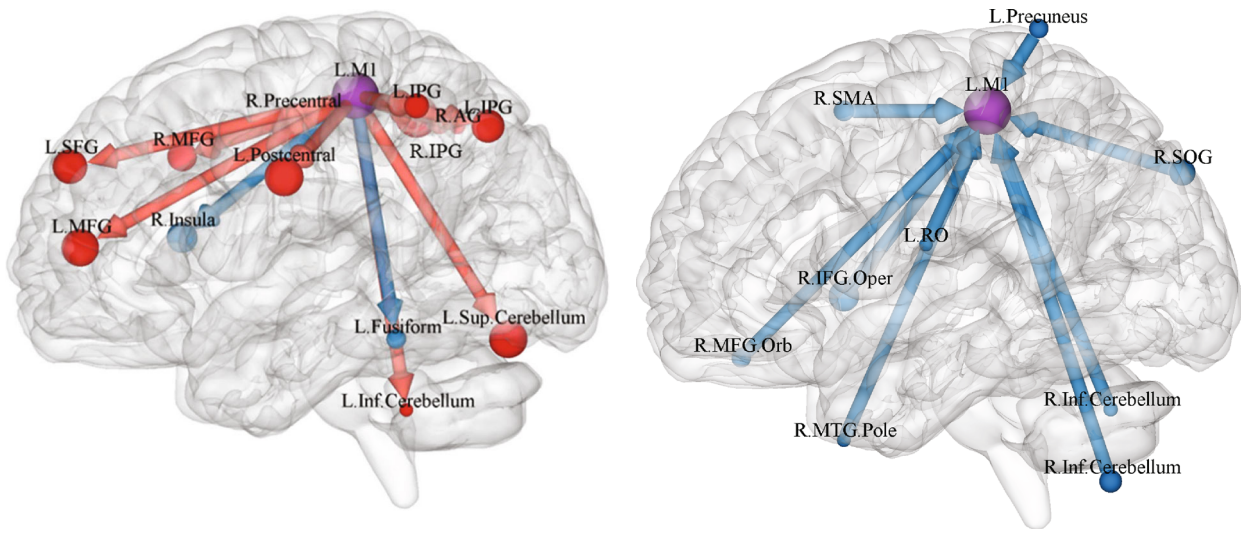

(a) (b)

Figure 1: (a) Between-group differences in effective connectivity from the left M1 to the rest of the brain. (b) Between-group differences in effective connectivity from the rest of the brain to the left M1. The arrow indicated the causal inflow to the left M1 or the causal outflow from the left M1, and the red meant increased and blue meant decreased effective connectivity. L.M1: left primary motor cortex; R. Precentral: right precentral gyrus; R.IPG: right inferior parietal gyrus; L. Postcentral: left postcentral gyrus; L.Sup.Cerebellum: left superior cerebellum; L.MFG: left middle frontal gyrus; L.SFG: left superior frontal gyrus; L.IPG: left inferior parietal gyrus; R.MFG: right middle frontal gyrus; R.AG: right angular gyrus; L.Inf.Cerebellum: left inferior cerebellum; L. Fusiform: left fusiform; R. Insula: right insula; L.RO: left Rolandic operculum; R.MTG.Pole: temporal pole of the right middle temporal gyrus; R.Inf.Cerebellum: right inferior cerebellum; L. Precuneus: left precuneus; R.MFG.Orb: orbital part of the right middle frontal gyrus; R.SMA: right supplementary motor area; R.SOG: right superior occipital gyrus; R.IFG.Oper: opercular part of the right inferior frontal gyrus.

Table 3: The differences of GCA with the right M1 as ROI between the TIA and HC groups.

	Anatomical label	BA	Number of voxels	Peak MNI coordinates (x, y, z)	t value
$F_{x\longrightarrow y}$	Temporal_Sup_R	22	351	60, −51, 18	4.39
	Precentral_R	6	55	48, 0, 45	3.77
	Frontal_Sup_R	9	58	24, 39, 36	3.76
	Frontal_Inf_Oper_R	44	51	39, 18, 33	3.04
	Frontal_Mid_L	46	40	−39, 48, 27	−3.18
	Rolandic_Oper_L	20	86	−30, −18, −3	−3.73
	Thalamus_L	NA	64	−6, −6, 3	−3.85
	Lingual_R	18	55	24, −96, −18	−4.32
$F_{y\longrightarrow x}$	Temporal_Sup_R	21	231	51, −21, −3	4.02
	Fusiform_R	20	76	42, −24, −33	3.88
	Insula_L	48	101	−36, 9, −12	−3.44
	Temporal_Sup_L	42	104	−60, −36, 12	−3.53
	Frontal_Sup_Medial_L	10	389	−3, 63, 3	−4.02
	Occipital_Mid_L	19	389	−48, −81, −6	−4.11
	Parietal_Inf_L	40	463	−36, −48, 51	−4.43
	Calcarine_R	17	411	6, −66, 12	−4.46

Temporal_Sup_R: right superior temporal gyrus; Precentral_R: right precentral gyrus; Frontal_Sup_R: right superior frontal gyrus; Frontal_Inf_Oper_R: opercular part of the right inferior frontal gyrus; Frontal_Mid_L: left middle frontal gyrus; Rolandic_Oper_L: left Rolandic operculum; Thalamus_L: left thalamus; Lingual_R: right lingual gyrus; Fusiform_R: right fusiform; Insula_L: left insula; Temporal_Sup_L: left superior temporal gyrus; Frontal_Sup_Medial_L: left medial superior frontal gyrus; Occipital_Mid_L: left middle occipital gyrus; Parietal_Inf_L: left inferior parietal gyrus; Calcarine_R: right calcarine; BA: Brodmann area; MNI: Montreal Neurological Institute; NA: not available.

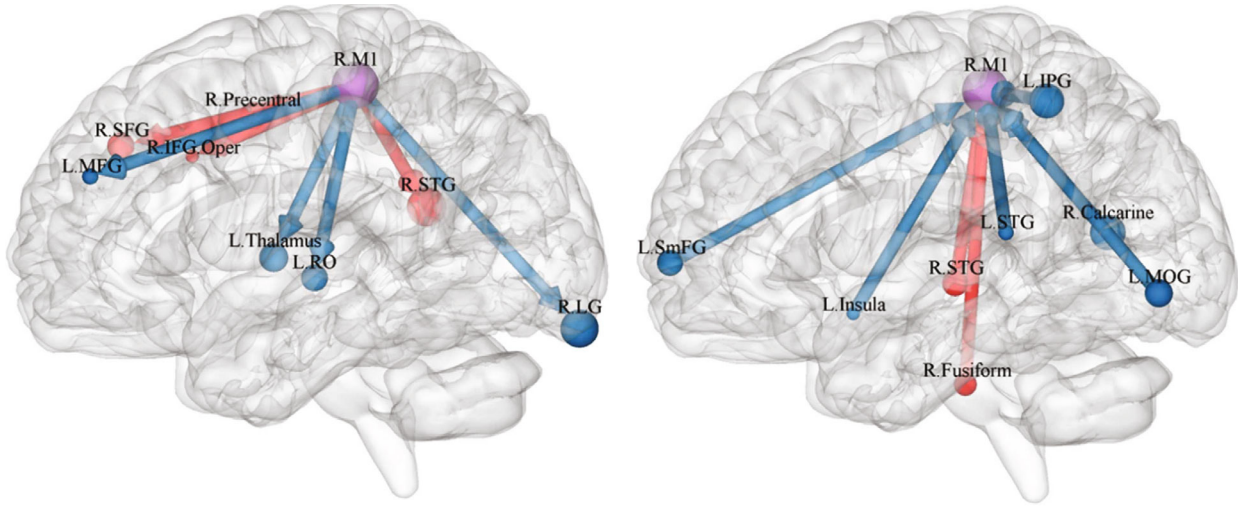

(a) (b)

Figure 2: (a) Between-group differences in effective connectivity from the right M1 to the rest of the brain. (b) Between-group differences in effective connectivity from the rest of the brain to the right M1. The arrow indicated the causal inflow to the right M1 or the causal outflow from the right M1, and the red meant increased and blue meant decreased effective connectivity. R.STG: right superior temporal gyrus; R. Precentral: right precentral gyrus; R.SFG: right superior frontal gyrus; R.IFG.Oper: opercular part of the right inferior frontal gyrus; L.MFG: left middle frontal gyrus; L.RO: left Rolandic operculum; L.Thalamus: left thalamus; R.LG: right lingual gyrus; R. Fusiform: right fusiform; L. Insula: left insula; L.STG: left superior temporal gyrus; L.SmFG: left medial superior frontal gyrus; L.MOG: left middle occipital gyrus; L.IPG: left inferior parietal gyrus; R. Calcarine: right calcarine.

(Figure 3(a)) but the GCA values from the left MOG to the right M1 were positively associated with LDL-C (Figure 3(b)). Specific information is provided in the Supplementary Materials (Tables S1–S4).

4. Discussion

In the present study, we used the GCA with the bilateral M1 as the ROIs to investigate the alteration of motor-related effective connectivity in individuals with TIA. Subsequently, we examined the correlation between altered effective connectivity and the clinical characteristics of individuals with TIA. Our results indicated that individuals with TIA had alterations in effective connectivity between the bilateral M1 and widely distributed brain regions, including motor control brain regions such as the SMA and cerebellum, as well as brain regions indirectly associated with motor function, such as the MOG, STG, and thalamus. These results have an important impact on understanding the pathological mechanisms of TIA from a new perspective and on reducing the risk of subsequent stroke.

The motor network mainly includes areas such as the M1, SMA, and cerebellum [80, 81], and the SMA is crucial for the initiation and control of the motor [82, 83]. Previous studies have demonstrated that stroke patients had decreased FC between the M1 and SMA [84], but it could be restored after treatment with repetitive transcranial magnetic stimulation (rTMS) using M1 as the target of stimulation [85]. Our results found decreased information inflow from the right SMA to the left M1 in TIA, which is consistent with previous studies and provides further directional information. This suggests that the poor motor performance of individuals with TIA may be related to impaired information transmission from the SMA to M1. Furthermore, we also found that decreased information inflow from the SMA to M1 was negatively correlated with HDL-C in individuals with TIA. Previous studies found that increased HDL-C was associated with a decreased risk of ischemic stroke [86, 87], which might suggest that lower effective connectivity from the right SMA to the left M1 is related to a higher risk of subsequent stroke. The cerebellum is involved in motor control as a balance center that coordinates the work of muscles [88–90]. Previous studies have shown that effective connectivity from M1 to the cerebellum was decreased whereas that from the cerebellum to M1 increased in stroke patients [34]. This is inconsistent with our results; we found increased information outflow from the left M1 to the left inferior cerebellum and left superior cerebellum, but the GCA values from the right inferior cerebellum to the left M1 demonstrated the opposite result. This might indicate that the motor impairment caused by TIA recovered and exhibited a bidirectional M1 and cerebellar neural circuit.

The precentral and postcentral gyri are also considered brain regions highly associated with motor function. The postcentral gyrus is one of the core nodes in the primary somatosensory cortex that can receive fiber information from spinal and bulbar motor neurons [91, 92]. The precentral gyrus, as part of the primary motor cortex, is primarily involved in motor execution [93, 94]. The current study showed that effective connectivity from the bilateral M1 to the right precentral gyrus and from the left M1 to the left postcentral gyrus was increased in individuals with TIA. This is consistent with previous FC studies, which found increased FC between the M1 and precentral gyrus in stroke

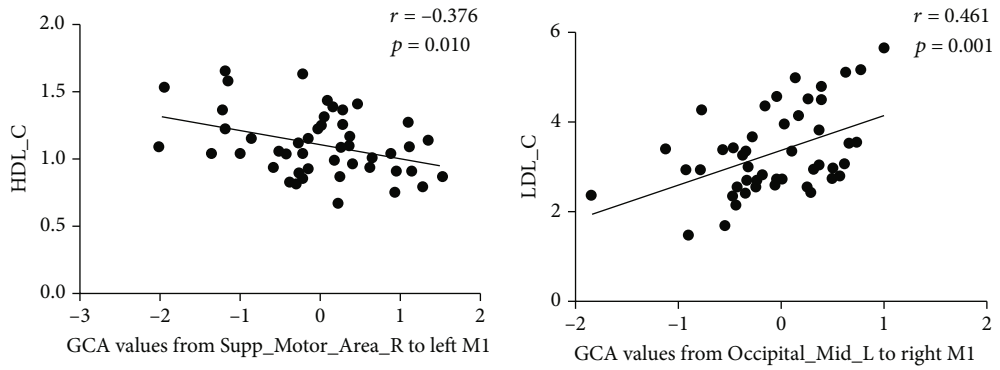

Figure 3: Partial correlation scatterplot between GCA values and the clinical characteristics. (a) Partial correlation scatterplot between GCA values from right SMA to left M1 and HDL-C. (b) Partial correlation scatterplot between GCA values from left MOG to right M1 and LDL-C.

patients and suggested that increased FC might be a compensatory strategy in the early poststroke period and gradually returned to normal levels after treatment [95]. Another study also found that rTMS treatment reduced FC between M1 and the ipsilateral postcentral gyrus [85]. Our results further provide directionality of the interactions between brain regions; that is, the increased FC between M1 and the precentral gyrus and postcentral gyrus might be related to the abnormal excess information transferred from M1 to these brain regions.

Vision and auditory can indirectly affect motor [96–98]. The temporal lobe is primarily responsible for auditory-motor processing skills [99]. Previous studies have demonstrated an increased information inflow from the ipsilateral M1 to the ipsilateral temporal lobe in stroke and have suggested that it might be associated with functional compensation [34]. Our results similarly found increased information outflow from the right M1 to the right STG in individuals with TIA and decreased information inflow from the right TP to the left M1. The increased information transfer between the ipsilateral M1 and temporal lobe may compensate for the information flow between the contralateral M1 and temporal lobe. The occipital lobe, LG, calcarine, fusiform, RO, and precuneus are all involved in the processing of visuospatial information, spatial attention, and vision-motion coordination [100–102]. Previous studies have demonstrated that stroke patients had decreased FC between the M1 and LG, calcarine, MOG, and precuneus [95, 103, 104]. This is consistent with our study, in which we found decreased information inflow from the left precuneus, right occipital lobe, and left RO to the left M1 and increased information inflow from the left occipital lobe and right calcarine to the right M1. This suggests that motor impairment in individuals with TIA might be related to reduced information transfer from these brain regions to the M1. It is noteworthy that the fusiform exhibited information flow in the opposite direction. Specifically, the effective connectivity from the left M1 to the left fusiform decreased but the effective connectivity from the right fusiform to the right M1 increased in the TIA. This suggests a possible functional compensation between the fusiform and M1. Our results also showed that elevated LDL-C was correlated with decreased information transfer from the visuomotor area to the right M1 and elevated LDL-C increased the risk of ischemic stroke [105, 106]. This indicates that impaired effective connectivity between M1 and vision-motion brain regions might not only indirectly affect motor performance in TIA but also increase the subsequent stroke risk in individuals with TIA.

Brain regions including the AG, thalamus, and insula are responsible for the integration of sensory information [85, 107, 108]. Previous studies have shown that the AG can deal with differences between the intended action and the motor result [109]. The thalamus, as a relay station for sensorimotor activity, is associated with motor observation and coordination [110]. We found that information outflow from the right M1 to the left thalamus was reduced in TIA, suggesting that motor impairment in TIA may be related to impaired transmission pathways between the M1 and thalamus. In addition, our study also found increased information outflow from the left M1 to the right AG but decreased information outflow to the right insula. This suggests that although the thalamus, insula, and AG are all associated with sensory integration and neural circuits from M1 to the thalamus and insula are impaired, those from M1 to the AG may be functionally compensated [111].

There are some potential limitations to the present study. First, it was conducted at only one hospital and had a relatively small sample size, which affects the generalizability of our results. In the future, the effective connectivity of TIA should be further explored through large-sample and multisite studies to better reveal the pathological mechanisms of TIA. Second, MRI scans were not conducted in individuals with TIA during the follow-up period, which prevented us from tracking how the motor-related effective connectivity network changed in individuals with TIA. Future longitudinal studies could track the alteration of information transfer between motor-related brain regions in TIA. Finally, the current study found that motor-related effective connectivity was associated with HDL-C and LDL-C levels in individuals with TIA but there was a lack of motor-related clinical data in individuals with TIA.

Future studies should incorporate motor-related clinical measures to further elucidate the clinical significance of altered effective connectivity in TIA.

5. Conclusion

The voxel-wise GCA was used to explore the alteration of the motor-related effective connectivity network in TIA and suggested that the altered information flow between the M1 and right SMA and left MOG might be correlated with the risk of subsequent stroke attack in TIA. This contributes to our comprehension of the underlying pathological mechanism of motor impairment in TIA and suggested that effective connectivity could be beneficial for early screening and urgent intervention for TIA in the future.

Data Availability

All the data supporting the conclusions of this article are available from the authors upon reasonable request.

Ethical Approval

All procedures involving human participants were in accordance with the ethical standards of the institutional and/or national research committee and with the 1964 Helsinki declaration and its later amendments or comparable ethical standards.

Conflicts of Interest

All authors declared no conflicts of interest.

Authors' Contributions

Huayun Li, Lina Huang, and Yulin Song conceived and designed the study; Zeqi Hao and Yuyu Shi analyzed the data and wrote the manuscript; Hongyu Xi, Hongqiang Zhang, Mengqi Zhao, and Jiahao Yu performed the experiments and collected materials. All authors read and approved the final manuscript. Zeqi Hao, Yulin Song, and Yuyu Shi have contributed equally to this work and share the first authorship.

Acknowledgments

We would like to thank all the participants for their participation in this study, and we also thank the Center for Cognition and Brain Disorders, the Affiliated Hospital of Hangzhou Normal University, Hangzhou, China, for the assistance with MRI data acquisition. This study was supported by the Youth Science and Technology Plan of Soochow Science and Technology Bureau and Soochow Health Planning Commission (KJXW2020065) and open research fund of college of teacher education, Zhejiang Normal University (no. jykf20003).

Supplementary Materials

Figure S1: the results of GCA with left M1 as ROI. (A) Between-group differences in effective connectivity from left M1 to the rest of the brain. (B) Between-group differences in effective connectivity from the rest of the brain to left M1. Figure S2: the results of GCA with right M1 as ROI. (A) Between-group differences in effective connectivity from right M1 to the rest of the brain. (B) Between-group differences in effective connectivity from the rest of the brain to right M1. Table S1: the partial correlation between GCA values from left M1 to whole brain and the time interval from the latest TIA to subsequent MRI scanning in individuals with TIA. Table S2: the partial correlation between GCA values from whole brain to left M1 and the time interval from the latest TIA to subsequent MRI scanning in individuals with TIA. Table S3: the partial correlation between GCA values from right M1 to whole brain and the time interval from the latest TIA to subsequent MRI scanning in individuals with TIA. Table S4: the partial correlation between GCA values from whole brain to right M1 and the time interval from the latest TIA to subsequent MRI scanning in individuals with TIA. *(Supplementary Materials)*

References

[1] J. D. Easton, J. L. Saver, G. W. Albers et al., "Definition and evaluation of transient ischemic attack a scientific statement for healthcare professionals from the American Heart Association/American Stroke Association Stroke Council; Council on Cardiovascular Surgery and Anesthesia; Council on Cardiovascular Radiology and Intervention; Council on Cardiovascular Nursing; and the Interdisciplinary Council on Peripheral Vascular Disease The American Academy of Neurology affirms the value of this statement as an educational tool for neurologists," *Stroke*, vol. 40, no. 6, pp. 2276–2293, 2009.

[2] V. Feigin, B. Norrving, C. L. M. Sudlow, and R. L. Sacco, "Updated criteria for population-based stroke and transient ischemic attack incidence studies for the 21st century," *Stroke*, vol. 49, no. 9, pp. 2248–2255, 2018.

[3] V.-A. Lioutas, C. S. Ivan, J. J. Himali et al., "Incidence of transient ischemic attack and association with long-term risk of stroke," *Jama-Journal of the American Medical Association*, vol. 325, no. 4, pp. 373–381, 2021.

[4] A. J. Coull, J. K. Lovett, P. M. Rothwell, and Oxford Vascular Study, "Population based study of early risk of stroke after transient ischaemic attack or minor stroke: implications for public education and organisation of services," *BMJ (Clinical Research Ed.)*, vol. 328, no. 7435, pp. 326–326, 2004.

[5] S. C. Johnston, P. M. Rothwell, M. N. Nguyen-Huynh et al., "Validation and refinement of scores to predict very early stroke risk after transient ischaemic attack," *Lancet*, vol. 369, no. 9558, pp. 283–292, 2007.

[6] P. Amarenco, "Transient ischemic attack," *New England Journal of Medicine*, vol. 383, no. 16, pp. 1596–1598, 2020.

[7] P. C. Lavallee, E. Meseguer, H. Abboud et al., "A transient ischaemic attack clinic with round-the-clock access (SOS-TIA): feasibility and effects," *The Lancet Neurology*, vol. 6, no. 11, pp. 953–960, 2007.

[8] P. M. Rothwell, M. F. Giles, A. Chandratheva et al., "Effect of urgent treatment of transient ischaemic attack and minor stroke on early recurrent stroke (EXPRESS study): a prospective population-based sequential comparison," *Lancet (London, England)*, vol. 370, no. 9596, pp. 1432–1442, 2007.

[9] H.-Q. Gu, X. Yang, C. J. Wang et al., "Clinical characteristics, management, and in-hospital outcomes in patients with stroke or transient ischemic attack in China," *JAMA Network Open*, vol. 4, no. 8, p. e2120745, 2021.

[10] S. Shahjouei, A. Sadighi, D. Chaudhary et al., "A 5-decade analysis of incidence trends of ischemic stroke after transient ischemic attack a systematic review and meta-analysis," *JAMA Neurology*, vol. 78, no. 1, pp. 77–87, 2021.

[11] Y. Lv, W. Wei, X. Han et al., "Multiparametric and multilevel characterization of morphological alterations in patients with transient ischemic attack," *Human Brain Mapping*, vol. 42, no. 7, pp. 2045–2060, 2021.

[12] Y. Lv, W. Wei, Y. Song et al., "Non-invasive evaluation of cerebral perfusion in patients with transient ischemic attack: an fMRI study," *Journal of Neurology*, vol. 266, no. 1, pp. 157–164, 2019.

[13] W. Su, J. Guo, Y. Zhang et al., "A longitudinal functional magnetic resonance imaging study of working memory in patients following a transient ischemic attack: a preliminary study," *Neuroscience Bulletin*, vol. 34, no. 6, pp. 963–971, 2018.

[14] Y. Lv, X. Han, Y. Song et al., "Toward neuroimaging-based network biomarkers for transient ischemic attack," *Human Brain Mapping*, vol. 40, no. 11, pp. 3347–3361, 2019.

[15] B. Biswal, F. Zerrin Yetkin, V. M. Haughton, and J. S. Hyde, "Functional connectivity in the motor cortex of resting human brain using echo- planar mri," *Magnetic Resonance in Medicine*, vol. 34, no. 4, pp. 537–541, 1995.

[16] M. D. Fox and M. E. Raichle, "Spontaneous fluctuations in brain activity observed with functional magnetic resonance imaging," *Nature Reviews. Neuroscience*, vol. 8, no. 9, pp. 700–711, 2007.

[17] S. Ovadia-Caro, D. S. Margulies, and A. Villringer, "The value of resting-state functional magnetic resonance imaging in stroke," *Stroke*, vol. 45, no. 9, pp. 2818–2824, 2014.

[18] Y. Lv, L. Li, Y. Song et al., "The local brain abnormalities in patients with transient ischemic attack: a resting-state fMRI study," *Frontiers in Neuroscience*, vol. 13, p. 24, 2019.

[19] H. Ma, G. Huang, M. Li et al., "The predictive value of dynamic intrinsic local metrics in transient ischemic attack," *Frontiers in Aging Neuroscience*, vol. 13, p. 808094, 2021.

[20] J. Guo, N. Chen, R. Li et al., "Regional homogeneity abnormalities in patients with transient ischaemic attack: a resting-state fMRI study," *Clinical Neurophysiology*, vol. 125, no. 3, pp. 520–525, 2014.

[21] S. Gui, J. Wang, H. Wan, J. Zhang, and C. Yang, "Altered intrinsic brain activities in patients with transient ischemic attack using amplitude of low-frequency fluctuation: a resting-state fMRI study," *International Journal of Clinical and Experimental Medicine*, vol. 11, no. 9, pp. 9559–9565, 2018.

[22] R. Li, S. Wang, L. Zhu et al., "Aberrant functional connectivity of resting state networks in transient ischemic attack," *PLoS One*, vol. 8, no. 8, 2013.

[23] K. Nicolas, P. Goodin, M. M. Visser et al., "Altered functional connectivity and cognition persists 4 years after a transient ischemic attack or minor stroke," *Frontiers in Neurology*, vol. 12, 2021.

[24] W. Zhu, Y. Che, Y. Wang et al., "Study on neuropathological mechanisms of primary monosymptomatic nocturnal enuresis in children using cerebral resting-state functional magnetic resonance imaging," *Scientific Reports*, vol. 9, no. 1, p. 19141, 2019.

[25] M. Allegra, C. Favaretto, N. Metcalf, M. Corbetta, and A. Brovelli, "Stroke-related alterations in inter-areal communication," *Neuroimage-Clinical*, vol. 32, p. 102812, 2021.

[26] Y. Shi, W. Liu, R. Liu et al., "Investigation of the emotional network in depression after stroke: a study of multivariate Granger causality analysis of fMRI data," *Journal of Affective Disorders*, vol. 249, pp. 35–44, 2019.

[27] Z. Zhao, H. Cai, M. Huang et al., "Altered functional connectivity of hippocampal subfields in poststroke dementia," *Journal of Magnetic Resonance Imaging*, vol. 54, no. 4, pp. 1337–1348, 2021.

[28] E. T. Rolls, Y. Zhou, W. Cheng, M. Gilson, G. Deco, and J. Feng, "Effective connectivity in autism," *Autism Research*, vol. 13, no. 1, pp. 32–44, 2020.

[29] M. Wang, N. Zeng, H. Zheng, X. du, M. N. Potenza, and G. H. Dong, "Altered effective connectivity from the pregenual anterior cingulate cortex to the laterobasal amygdala mediates the relationship between internet gaming disorder and loneliness," *Psychological Medicine*, vol. 52, no. 4, pp. 737–746, 2022.

[30] X. Huang, D. Zhang, P. Wang et al., "Altered amygdala effective connectivity in migraine without aura: evidence from resting-state fMRI with Granger causality analysis," *The Journal of Headache and Pain*, vol. 22, no. 1, p. 25, 2021.

[31] K. J. Friston, "Functional and effective connectivity in neuroimaging: a synthesis," *Human Brain Mapping*, vol. 2, no. 1-2, pp. 56–78, 1994.

[32] Z. Li, J. Hu, Z. Wang, R. You, and D. Cao, "Basal ganglia stroke is associated with altered functional connectivity of the left inferior temporal gyrus," *Journal of Neuroimaging*, vol. 32, p. 744, 2022.

[33] F. Liu, C. C. Chen, W. J. Hong et al., "Selectively disrupted sensorimotor circuits in chronic stroke with hand dysfunction," *CNS Neuroscience & Therapeutics*, vol. 28, no. 5, pp. 677–689, 2022.

[34] Z. Zhao, X. Wang, M. Fan et al., "Altered effective connectivity of the primary motor cortex in stroke: a resting-state fMRI study with Granger causality analysis," *PLoS One*, vol. 11, no. 11, p. e0166210, 2016.

[35] R. Goebel, A. Roebroeck, D. S. Kim, and E. Formisano, "Investigating directed cortical interactions in time-resolved fMRI data using vector autoregressive modeling and Granger causality mapping," *Magnetic Resonance Imaging*, vol. 21, no. 10, pp. 1251–1261, 2003.

[36] A. Roebroeck, E. Formisano, and R. Goebel, "Mapping directed influence over the brain using Granger causality and fMRI," *NeuroImage*, vol. 25, no. 1, pp. 230–242, 2005.

[37] L. Wang, J. Cai, M. Zhang et al., "Positive expression of human Cytomegalovirus phosphoprotein 65 in atherosclerosis," *BioMed Research International*, vol. 2016, Article ID 4067685, 7 pages, 2016.

[38] Z. Hao, Y. Shi, L. Huang et al., "The atypical effective connectivity of right temporoparietal junction in autism spectrum disorder: a multi-site study," *Frontiers in Neuroscience*, vol. 16, 2022.

[39] Z. Feng, S. Xu, M. Huang, Y. Shi, B. Xiong, and H. Yang, "Disrupted causal connectivity anchored on the anterior cingulate

cortex in first-episode medication-naive major depressive disorder," *Progress in Neuro-Psychopharmacology & Biological Psychiatry*, vol. 64, pp. 124–130, 2016.

[40] G. B. Chand and M. Dhamala, "Interactions between the anterior cingulate-insula network and the fronto- parietal network during perceptual decision-making," *NeuroImage*, vol. 152, pp. 381–389, 2017.

[41] D. Mozaffarian, E. J. Benjamin, A. S. Go et al., "Heart disease and stroke statistics–2015 update: a report from the American Heart Association," *Circulation*, vol. 131, no. 4, pp. E29–E322, 2015.

[42] L. Simmatis, J. Krett, S. H. Scott, and A. Y. Jin, "Robotic exoskeleton assessment of transient ischemic attack," *PLoS One*, vol. 12, no. 12, p. e0188786, 2017.

[43] C. W. Tsao, A. W. Aday, Z. I. Almarzooq et al., "Heart disease and stroke statistics-2022 update: a report from the American Heart Association," *Circulation*, vol. 145, no. 8, pp. E153–E639, 2022.

[44] J. I. Spark, N. Blest, S. Sandison, P. J. Puckridge, H. A. Saleem, and D. A. Russell, "Stroke and transient ischaemic attack awareness," *Medical Journal of Australia*, vol. 195, no. 1, pp. 16–19, 2011.

[45] E. Low, S. G. Crewther, B. Ong, D. Perre, and T. Wijeratne, "Compromised motor dexterity confounds processing speed task outcomes in stroke patients," *Frontiers in Neurology*, vol. 8, 2017.

[46] N. Lodha, P. Patel, J. Harrell et al., "Motor impairments in transient ischemic attack increase the odds of a positive diffusion-weighted imaging: a meta-analysis," *Restorative Neurology and Neuroscience*, vol. 37, no. 5, pp. 509–521, 2019.

[47] D. J. Gladstone, M. K. Kapral, J. Fang, A. Laupacis, and J. V. Tu, "Management and outcomes of transient ischemic attacks in Ontario," *CMAJ*, vol. 170, no. 7, pp. 1099–1104, 2004.

[48] N. Lodha, J. Harrell, S. Eisenschenk, and E. A. Christou, "Motor impairments in transient ischemic attack increase the odds of a subsequent stroke: a meta-analysis," *Frontiers in Neurology*, vol. 8, 2017.

[49] N. G. Hatsopoulos and A. J. Suminski, "Sensing with the motor cortex," *Neuron*, vol. 72, no. 3, pp. 477–487, 2011.

[50] E. Naito, "Sensing limb movements in the motor cortex: how humans sense limb movement," *The Neuroscientist : A Review Journal Bringing Neurobiology, Neurology and Psychiatry*, vol. 10, no. 1, pp. 73–82, 2004.

[51] S. Bajaj, A. J. Butler, D. Drake, and M. Dhamala, "Functional organization and restoration of the brain motor-execution network after stroke and rehabilitation," *Frontiers in Human Neuroscience*, vol. 9, 2015.

[52] M. M. Morrow and L. E. Miller, "Prediction of muscle activity by populations of sequentially recorded primary motor cortex neurons," *Journal of Neurophysiology*, vol. 89, no. 4, pp. 2279–2288, 2003.

[53] J. A. Gallego, M. G. Perich, R. H. Chowdhury, S. A. Solla, and L. E. Miller, "Long-term stability of cortical population dynamics underlying consistent behavior," *Nature Neuroscience*, vol. 23, no. 2, p. 260, 2020.

[54] K. Figlewski, H. Andersen, T. Stærmose, P. von Weitzel-Mudersbach, J. F. Nielsen, and J. U. Blicher, "Decreased GABA levels in the symptomatic hemisphere in patients with transient ischemic attack," *Heliyon*, vol. 4, no. 9, p. e00790, 2018.

[55] B. A. Radlinska, Y. Blunk, I. R. Leppert, J. Minuk, G. B. Pike, and A. Thiel, "Changes in callosal motor fiber integrity after subcortical stroke of the pyramidal tract," *Journal of Cerebral Blood Flow and Metabolism*, vol. 32, no. 8, pp. 1515–1524, 2012.

[56] A. Nucera, M. R. Azarpazhooh, L. Cardinali et al., "Inhibition of the primary motor cortex and the upgoing thumb sign," *eNeurologicalSci*, vol. 8, pp. 31–33, 2017.

[57] X. Z. Jia, J. Wang, H. Y. Sun et al., "RESTplus: an improved toolkit for resting-state functional magnetic resonance imaging data processing," *Science Bulletin*, vol. 64, no. 14, pp. 953-954, 2019.

[58] Y. Chao-Gan and Z. Yu-Feng, "DPARSF: a MATLAB toolbox for "pipeline" data analysis of resting-state fMRI," *Frontiers in Systems Neuroscience*, vol. 4, p. 13, 2010.

[59] J. D. Power, B. L. Schlaggar, and S. E. Petersen, "Recent progress and outstanding issues in motion correction in resting state fMRI," *NeuroImage*, vol. 105, pp. 536–551, 2015.

[60] K. M. Petersson, T. E. Nichols, J. B. Poline, and A. P. Holmes, "Statistical limitations in functional neuroimaging. II. Signal detection and statistical inference," *Philosophical Transactions of the Royal Society of London. Series B, Biological Sciences*, vol. 354, no. 1387, pp. 1261–1281, 1999.

[61] K. J. Friston, S. Williams, R. Howard, R. S. J. Frackowiak, and R. Turner, "Movement-related effects in fMRI time-series," *Magnetic Resonance in Medicine*, vol. 35, no. 3, pp. 346–355, 1996.

[62] M. D. Fox, A. Z. Snyder, J. L. Vincent, M. Corbetta, D. C. van Essen, and M. E. Raichle, "The human brain is intrinsically organized into dynamic, anticorrelated functional networks," *Proceedings of the National Academy of Sciences of the United States of America*, vol. 102, no. 27, pp. 9673–9678, 2005.

[63] J. E. Chen and G. H. Glover, "Functional magnetic resonance imaging methods," *Neuropsychology Review*, vol. 25, no. 3, pp. 289–313, 2015.

[64] C.-G. Yan, B. Cheung, C. Kelly et al., "A comprehensive assessment of regional variation in the impact of head micromovements on functional connectomics," *NeuroImage*, vol. 76, no. 1, pp. 183–201, 2013.

[65] R. Turner, "Signal sources in bold contrast fMRI," *Advances in Experimental Medicine and Biology*, vol. 413, pp. 19–25, 1997.

[66] M. J. Lowe and D. P. Russell, "Treatment of baseline drifts in fMRI time series analysis," *Journal of Computer Assisted Tomography*, vol. 23, no. 3, pp. 463–473, 1999.

[67] J. P. Hamilton, G. Chen, M. E. Thomason, M. E. Schwartz, and I. H. Gotlib, "Investigating neural primacy in major depressive disorder: multivariate Granger causality analysis of resting-state fMRI time-series data," *Molecular Psychiatry*, vol. 16, no. 7, pp. 763–772, 2011.

[68] W. Liao, J. Ding, D. Marinazzo et al., "Small-world directed networks in the human brain: multivariate Granger causality analysis of resting-state fMRI," *NeuroImage*, vol. 54, no. 4, pp. 2683–2694, 2011.

[69] G. R. Wu, W. Liao, S. Stramaglia, J. R. Ding, H. Chen, and D. Marinazzo, "A blind deconvolution approach to recover effective connectivity brain networks from resting state fMRI data," *Medical Image Analysis*, vol. 17, no. 3, pp. 365–374, 2013.

[70] G. R. Wu, N. Colenbier, S. van den Bossche et al., "rsHRF: a toolbox for resting-state HRF estimation and deconvolution," *NeuroImage*, vol. 244, p. 118591, 2021.

[71] J. Liu, W. Qin, J. Zhang, X. Zhang, and C. Yu, "Enhanced interhemispheric functional connectivity compensates for anatomical connection damages in subcortical stroke," *Stroke*, vol. 46, no. 4, pp. 1045–1051, 2015.

[72] T. Wang, N. Chen, W. Zhan et al., "Altered effective connectivity of posterior thalamus in migraine with cutaneous allodynia: a resting-state fMRI study with granger causality analysis," *Journal of Headache and Pain*, vol. 17, no. 1, p. 17, 2016.

[73] H.-L. Wei, J. Chen, Y. C. Chen et al., "Impaired effective functional connectivity of the sensorimotor network in interictal episodic migraineurs without aura," *Journal of Headache and Pain*, vol. 21, no. 1, p. 111, 2020.

[74] C. W. J. Granger, "Investigating causal relations by econometric models and cross-spectral methods," *Econometrica*, vol. 37, no. 3, pp. 424–438, 1969.

[75] G. Chen, J. P. Hamilton, M. E. Thomason, I. H. Gotlib, Z. S. Saad, and R. W. Cox, "Granger causality via vector autoregression tuned for FMRI data," *Analysis*, vol. 17, p. 1718, 2009.

[76] Z. X. Zang, C. G. Yan, Z. Y. Dong, J. Huang, and Y. F. Zang, "Granger causality analysis implementation on MATLAB: a graphic user interface toolkit for fMRI data processing," *Journal of Neuroscience Methods*, vol. 203, no. 2, pp. 418–426, 2012.

[77] A. C. Nugent, A. Martinez, A. D'Alfonso, C. A. Zarate, and W. H. Theodore, "The relationship between glucose metabolism, resting-state fMRI BOLD signal, and GABAA-binding potential: a preliminary study in healthy subjects and those with temporal lobe epilepsy," *Journal of Cerebral Blood Flow and Metabolism*, vol. 35, no. 4, pp. 583–591, 2015.

[78] J. P. Higgins, J. M. Elliott, and T. B. Parrish, "Brain network disruption in whiplash," *American Journal of Neuroradiology*, vol. 41, no. 6, pp. 994–1000, 2020.

[79] Y. Liu, Y. Chen, X. Liang et al., "Altered resting-state functional connectivity of multiple networks and disrupted correlation with executive function in major depressive disorder," *Frontiers in Neurology*, vol. 11, 2020.

[80] F. A. Middleton and P. L. Strick, "Basal ganglia and cerebellar loops: motor and cognitive circuits," *Brain Research. Brain Research Reviews*, vol. 31, no. 2-3, pp. 236–250, 2000.

[81] Q. Tang, G. Li, T. Liu et al., "Modulation of interhemispheric activation balance in motor-related areas of stroke patients with motor recovery: systematic review and meta-analysis of fMRI studies," *Neuroscience and Biobehavioral Reviews*, vol. 57, pp. 392–400, 2015.

[82] J. G. Nutt, B. R. Bloem, N. Giladi, M. Hallett, F. B. Horak, and A. Nieuwboer, "Freezing of gait: moving forward on a mysterious clinical phenomenon," *Lancet Neurology*, vol. 10, no. 8, pp. 734–744, 2011.

[83] D. Lindenbach and C. Bishop, "Critical involvement of the motor cortex in the pathophysiology and treatment of Parkinson's disease," *Neuroscience and Biobehavioral Reviews*, vol. 37, no. 10, pp. 2737–2750, 2013.

[84] X. Zheng, L. Sun, D. Yin et al., "The plasticity of intrinsic functional connectivity patterns associated with rehabilitation intervention in chronic stroke patients," *Neuroradiology*, vol. 58, no. 4, pp. 417–427, 2016.

[85] J. Li, X. W. Zhang, Z. T. Zuo et al., "Cerebral functional reorganization in ischemic stroke after repetitive transcranial magnetic stimulation: an fMRI study," *CNS Neuroscience & Therapeutics*, vol. 22, no. 12, pp. 952–960, 2016.

[86] P. Amarenco, J. Labreuche, and P.-J. Touboul, "High-density lipoprotein-cholesterol and risk of stroke and carotid atherosclerosis: a systematic review," *Atherosclerosis*, vol. 196, no. 2, pp. 489–496, 2008.

[87] R. Qie, L. Liu, D. Zhang et al., "Dose-response association between high-density lipoprotein cholesterol and stroke: a systematic review and meta-analysis of prospective cohort studies," *Preventing Chronic Disease*, vol. 18, p. E45, 2021.

[88] Z. Xie, F. Cui, Y. Zou, and L. Bai, "Acupuncture enhances effective connectivity between cerebellum and primary sensorimotor cortex in patients with stable recovery stroke," *Evidence-based Complementary and Alternative Medicine*, vol. 2014, Article ID 603909, 9 pages, 2014.

[89] A. J. Bastian, "Moving, sensing and learning with cerebellar damage," *Current Opinion in Neurobiology*, vol. 21, no. 4, pp. 596–601, 2011.

[90] M. L. T. M. Müller, R. L. Albin, V. Kotagal et al., "Thalamic cholinergic innervation and postural sensory integration function in Parkinson's disease," *Brain*, vol. 136, no. 11, pp. 3282–3289, 2013.

[91] X. G. Li, S. L. Florence, and J. H. Kaas, "Areal distributions of cortical neurons projecting to different levels of the caudal brain stem and spinal cord in rats," *Somatosensory & Motor Research*, vol. 7, no. 3, pp. 315–335, 1990.

[92] A. Haseeb, E. Asano, C. Juhász, A. Shah, S. Sood, and H. T. Chugani, "Young patients with focal seizures may have the primary motor area for the hand in the postcentral gyrus," *Epilepsy Research*, vol. 76, no. 2-3, pp. 131–139, 2007.

[93] J. Gao, C. Yang, Q. Li et al., "Hemispheric difference of regional brain function exists in patients with acute stroke in different cerebral hemispheres: a resting-state fMRI study," *Neuroscience*, vol. 13, 2021.

[94] C. A. Sandman, C. Buss, K. Head, and E. P. Davis, "Fetal exposure to maternal depressive symptoms is associated with cortical thickness in late childhood," *Biological Psychiatry*, vol. 77, no. 4, pp. 324–334, 2015.

[95] H. Wang, G. Xu, X. Wang et al., "The reorganization of resting-state brain networks associated with motor imagery training in chronic stroke patients," *IEEE Transactions on Neural Systems and Rehabilitation Engineering*, vol. 27, no. 10, pp. 2237–2245, 2019.

[96] R. Secoli, M. H. Milot, G. Rosati, and D. J. Reinkensmeyer, "Effect of visual distraction and auditory feedback on patient effort during robot-assisted movement training after stroke," *Journal of Neuroengineering and Rehabilitation*, vol. 8, no. 1, p. 21, 2011.

[97] C. C. Berger and H. H. Ehrsson, "Mental imagery induces cross-modal sensory plasticity and changes future auditory perception," *Psychological Science*, vol. 29, no. 6, pp. 926–935, 2018.

[98] J. Reh, G. Schmitz, T. H. Hwang, and A. O. Effenberg, "Loudness affects motion: asymmetric volume of auditory feedback results in asymmetric gait in healthy young adults," *BMC Musculoskeletal Disorders*, vol. 23, no. 1, p. 586, 2022.

[99] C. G. Tsai, L. Y. Fan, S. H. Lee, J. H. Chen, and T. L. Chou, "Specialization of the posterior temporal lobes for audiomotor processing – evidence from a functional magnetic resonance imaging study of skilled drummers," *The European Journal of Neuroscience*, vol. 35, no. 4, pp. 634–643, 2012.

[100] D. S. Margulies, J. L. Vincent, C. Kelly et al., "Precuneus shares intrinsic functional architecture in humans and

monkeys," *Proceedings of the National Academy of Sciences of the United States of America*, vol. 106, no. 47, pp. 20069–20074, 2009.

[101] H. Liu, L. Chen, G. Zhang et al., "Scalp acupuncture enhances the functional connectivity of visual and cognitive-motor function network of patients with acute ischemic stroke," *Evidence-based Complementary and Alternative Medicine*, vol. 2020, Article ID 8836794, 11 pages, 2020.

[102] F. J. A. Deconinck, A. R. P. Smorenburg, A. Benham, A. Ledebt, M. G. Feltham, and G. J. P. Savelsbergh, "Reflections on mirror therapy: a systematic review of the effect of mirror visual feedback on the brain," *Neurorehabilitation and Neural Repair*, vol. 29, no. 4, pp. 349–361, 2015.

[103] J. Li, L. Cheng, S. Chen et al., "Functional connectivity changes in multiple-frequency bands in acute basal ganglia ischemic stroke patients: a machine learning approach," *Neural Plasticity*, vol. 2022, Article ID 1560748, 10 pages, 2022.

[104] J. Chen, D. Sun, Y. Shi et al., "Alterations of static functional connectivity and dynamic functional connectivity in motor execution regions after stroke," *Neuroscience Letters*, vol. 686, pp. 112–121, 2018.

[105] L. Sun, R. Clarke, D. Bennett et al., "Causal associations of blood lipids with risk of ischemic stroke and intracerebral hemorrhage in Chinese adults," *Nature Medicine*, vol. 25, no. 4, p. 569, 2019.

[106] Y. Pan, R. Wangqin, H. Li et al., "LDL-C levels, lipid-lowering treatment and recurrent stroke in minor ischaemic stroke or TIA," *Stroke and Vascular Neurology*, vol. 7, no. 4, pp. 276–284, 2022.

[107] M. L. Seghier, "The angular gyrus: multiple functions and multiple subdivisions," *The Neuroscientist*, vol. 19, no. 1, pp. 43–61, 2013.

[108] C. Farrer, S. H. Frey, J. D. van Horn et al., "The angular gyrus computes action awareness representations," *Cerebral Cortex*, vol. 18, no. 2, pp. 254–261, 2008.

[109] M. Gandolla, L. Niero, F. Molteni, E. Guanziroli, N. S. Ward, and A. Pedrocchi, "Brain plasticity mechanisms underlying motor control reorganization: pilot longitudinal study on post-stroke subjects," *Brain Sciences*, vol. 11, no. 3, p. 329, 2021.

[110] I. C. Brunner, J. S. Skouen, L. Ersland, and R. Grüner, "Plasticity and response to action observation: a longitudinal fMRI study of potential mirror neurons in patients with subacute stroke," *Neurorehabilitation and Neural Repair*, vol. 28, no. 9, pp. 874–884, 2014.

[111] Y. Zhang, H. Liu, L. Wang et al., "Relationship between functional connectivity and motor function assessment in stroke patients with hemiplegia: a resting-state functional MRI study," *Neuroradiology*, vol. 58, no. 5, pp. 503–511, 2016.

Hindawi
Neural Plasticity
Volume 2022, Article ID 1478048, 12 pages
https://doi.org/10.1155/2022/1478048

Research Article

The White Matter Functional Abnormalities in Patients with Transient Ischemic Attack: A Reinforcement Learning Approach

Huibin Ma,[1,2] **Zhou Xie**,[1] **Lina Huang**,[3] **Yanyan Gao**,[4,5] **Linlin Zhan**,[6] **Su Hu**,[4,5] **Jiaxi Zhang**,[4,5] **and Qingguo Ding**[3]

[1]*School of Information and Electronics Technology, Jiamusi University, Jiamusi, China*
[2]*Integrated Medical School, Jiamusi University, Jiamusi, China*
[3]*Department of Radiology, Changshu No.2 People's Hospital, The Affiliated Changshu Hospital of Xuzhou Medical University, Changshu, Jiangsu, China*
[4]*School of Teacher Education, Zhejiang Normal University, Jinhua, China*
[5]*Key Laboratory of Intelligent Education Technology and Application of Zhejiang Province, Zhejiang Normal University, Jinhua, China*
[6]*Faculty of Western Languages, Heilongjiang University, Heilongjiang 150080, China*

Correspondence should be addressed to Jiaxi Zhang; zhangjiaxi@zjnu.edu.cn and Qingguo Ding; lkg980808@zjnu.edu.cn

Received 21 July 2022; Revised 28 August 2022; Accepted 20 September 2022; Published 17 October 2022

Academic Editor: Yu Zheng

Background. Transient ischemic attack (TIA) is a known risk factor for stroke. Abnormal alterations in the low-frequency range of the gray matter (GM) of the brain have been studied in patients with TIA. However, whether there are abnormal neural activities in the low-frequency range of the white matter (WM) in patients with TIA remains unknown. The current study applied two resting-state metrics to explore functional abnormalities in the low-frequency range of WM in patients with TIA. Furthermore, a reinforcement learning method was used to investigate whether altered WM function could be a diagnostic indicator of TIA. *Methods.* We enrolled 48 patients with TIA and 41 age- and sex-matched healthy controls (HCs). Resting-state functional magnetic resonance imaging (rs-fMRI) and clinical/physiological/biochemical data were collected from each participant. We compared the group differences between patients with TIA and HCs in the low-frequency range of WM using two resting-state metrics: amplitude of low-frequency fluctuation (ALFF) and fractional ALFF (fALFF). The altered ALFF and fALFF values were defined as features of the reinforcement learning method involving a *Q*-learning algorithm. *Results.* Compared with HCs, patients with TIA showed decreased ALFF in the right cingulate gyrus/right superior longitudinal fasciculus/left superior corona radiata and decreased fALFF in the right cerebral peduncle/right cingulate gyrus/middle cerebellar peduncle. Based on these two rs-fMRI metrics, an optimal *Q*-learning model was obtained with an accuracy of 82.02%, sensitivity of 85.42%, specificity of 78.05%, precision of 82.00%, and area under the curve (AUC) of 0.87. *Conclusion.* The present study revealed abnormal WM functional alterations in the low-frequency range in patients with TIA. These results support the role of WM functional neural activity as a potential neuromarker in classifying patients with TIA and offer novel insights into the underlying mechanisms in patients with TIA from the perspective of WM function.

1. Introduction

Stroke is one of the leading causes of morbidity, mortality, and loss of function worldwide [1, 2]. The increasing prevalence of stroke places a tremendous economic burden on individuals and society [3]. Transient ischemic attack (TIA), also known as "ministroke," is a serious, reversible, temporary neurological condition caused by focal cerebral nervous system hypoperfusion [4]. It is acknowledged that TIA is a continuum with stoke in the presentation of acute cerebrovascular events [5]. Therefore, precise diagnosis and effective treatment of TIA are paramount to reducing the risk of subsequent stroke

[6–8]. To promote targeted treatment and precise identification of TIA, advanced imaging techniques have been applied to explore the underlying mechanism.

In recent years, resting-state functional magnetic resonance imaging (rs-fMRI) has been considered a promising imaging technique for studying gray matter (GM) alterations based on blood oxygen level-dependent (BOLD) signals [9–13]. However, the signals in white matter (WM) were often neglected as noise, because it was previously thought that WM could not generate BOLD signals due to few postsynaptic potentials [14–17]. Therefore, previous studies of WM in patients with TIA were mainly structural. For instance, structural abnormalities have been found in the superior longitudinal fasciculus in the WM, implying impaired sensorimotor function in patients with TIA [18, 19]. Increasing evidence indicates the existence of functional information in WM that can be reliably detected by BOLD fMRI [20–24], which might open new avenues for studying WM in health and disease. By combining fMRI and dynamic positron emission tomography (PET), BOLD fluctuations in WM have been found to correlate with neural activity through local variations in glucose metabolism, suggesting a possible physiological basis for WM function [25]. Particularly, it has been demonstrated in healthy participants that spontaneous low-frequency BOLD fluctuations in WM can be robustly detected and reflect specific neural activities [26, 27]. During the resting state, Peer et al. [28] applied the Fourier transform of WM functional network signals obtained from healthy participants, and greater neural activity at low frequencies was found to exist in WM networks. A similar feature of neural activity at low-frequency bands in WM has been detected in several neurological or mental diseases, such as schizophrenia [29, 30] and epilepsy [31]. Besides, the WM function estimated by low-frequency BOLD signals can also be modulated by different tasks, suggesting the possibility of estimating the dynamic function of WM fiber bundles using low-frequency BOLD fluctuations [27, 32, 33]. Considered together, these studies provide strong evidence that meaningful signals exist in WM and that low-frequency fluctuations in WM could be effectively detected by BOLD fMRI. Nevertheless, it remains unknown whether there are abnormal functional alterations in low-frequency bands of the WM in patients with TIA. Thus, we expected that unveiling the low-frequency BOLD fluctuation characteristics in the WM of patients with TIA may provide additional information about WM dysfunction in TIA and help better understand the underlying pathological mechanisms of TIA.

Two effective resting-state methods have been raised to characterize the features of low-frequency BOLD fluctuations: amplitude of low-frequency fluctuation (ALFF) and fractional ALFF (fALFF). The ALFF measures the signal intensity in low-frequency oscillations (LFOs) of local spontaneous neural activity of the brain [34] and has been proven to exhibit outstanding test-retest reliability [35]. Previous studies have investigated spontaneous neural activities in the GM and found decreased ALFF in patients with TIA [11, 36], providing evidence of brain dysfunction in TIA. Moreover, based on ALFF, fALFF was raised to characterize the relative contribution of a specific LFO to the whole frequency range, effectively reducing physiological noise and suppressing artifacts in nonspecific brain regions [35, 37]. According to previous studies, the ALFF method has been used to explore WM functional abnormalities in various diseases, such as Parkinson's disease (PD) [38], autism spectrum disorder (ASD) [2], and schizophrenia [39]. Although the fALFF method has not been used in conjunction with the ALFF method to assess the neural activity in the low-frequency range of WM, it is suggested that the combination of these two metrics can help obtain detailed information about brain activity in the low-frequency range than using individual method alone [40–42].

Machine learning algorithms have been widely used for diagnosing neuropsychiatric diseases and are powerful tools for classifying patients and healthy controls (HCs), which show great potential in clinical practice [43–47]. Among the numerous machine learning methods, the reinforcement learning approach is a promising method for addressing the diversity and complexity of the clinical conditions of the disease [48]. Learning through continuous trial-and-error in the interaction between agent and environment, reinforcement learning can adjust its actions according to the environmental feedback signal and arrive at the optimal decision [49–51]. In previous studies, reinforcement learning has been combined with rs-fMRI to recognize patients with early mild cognitive impairment (eMCI) by learning discriminative feature presentations from temporally embedded BOLD signals [52]. Based on probabilistic reinforcement learning tasks, it has been found that patients with treatment-resistant schizophrenia (TRS) and patients with non-treatment-resistant schizophrenia (NTR) can be separated by different neural mechanisms [53]. Additionally, when diagnosing myocarditis, an automatic classification model based on the deep reinforcement learning method can help effectively promote the automatic screening of non-invasive cardiac magnetic resonance (CMR) images [54]. In summary, reinforcement learning can be combined with different methods to distinguish patients from healthy individuals. Hence, we applied the reinforcement learning method to examine whether WM functional abnormalities could effectively differentiate patients with TIA from HCs.

In this study, functional alterations in the WM of patients with TIA were explored using two resting-state metrics (ALFF and fALFF) to determine whether there was WM functional damage in patients with TIA. Furthermore, a reinforcement learning approach was adopted to investigate whether the altered WM function of ALFF and fALFF could serve as effective neuromarkers for identifying patients with TIA.

2. Materials and Methods

2.1. Participants. Data were acquired from 51 patients with suspected TIA in the Department of Neurology at the Anshan Changda Hospital, Liaoning, China. Patients with transient neurological symptoms may have a vascular etiology, according to the assessment of clinical psychiatrists [11, 36]. Blood pressure, clinical features, symptom duration,

and history of diabetes symptoms were assessed for each patient. In addition, ABCD2 scores (a simple score to identify individuals at high early risk of stroke after a TIA) were generated for each patient's risk of secondary stroke [55]. All patients underwent electrocardiography (ECG), carotid duplex ultrasound (CDU), and magnetic resonance imaging (MRI). The information of each patient was recorded as follows: history of TIA and stroke; current smoking and drinking behavior; previous risk factors such as hypertension, diabetes, and coronary artery disease [56]; medications used before MRI scan [57]; in-hospital assessment of arterial stenosis on CDU and magnetic resonance angiography (MR angiography); atrial fibrillation on ECG; brain infarction on diffusion-weighted imaging (DWI) and T2 fluid-attenuated inversion recovery (T2-FLAIR) [58]; and 1-year telephone follow-up for stroke and/or TIA episodes [59]. Participants with migraine, epilepsy, hemorrhage, leukoaraiosis, or psychiatric history were excluded from this study [60].

The 41 HCs matched for age and sex to the TIA group were recruited through an advertising campaign. None of the HCs had a history of physical illnesses, psychiatric disorders, or neurological disorders. This study was approved by the Ethics Committee of the Center for Cognition and Brain Disorders, Hangzhou Normal University. All participants provided written informed consent.

2.2. Physiological and Biochemical Tests. All participants underwent a series of physiological and biochemical tests within 24 h before scanning, which included systolic blood pressure, diastolic blood pressure, blood sugar level, total cholesterol, triglycerides, high-density lipoprotein cholesterol (HDL-C), and low-density lipoprotein cholesterol (LDL-C).

2.3. Data Acquisition. Neuroimaging data were acquired using a GE MR-750 3.0 T scanner (GE Medical Systems, Inc., Waukesha, WI, United States). The parameters for acquiring 3D high resolution T1-weighted anatomical images were as follows: time of repetition (TR) = 8100 ms, time of echo (TE) = 3.1 ms, matrix size = 256 × 256, voxel size = 1 mm × 1 mm × 1 mm, thickness/gap = 1/0 mm, field of view (FOV) = 256 mm^2, and scanning time = 5 min. Gradient echo-planar imaging (EPI) images were captured with TR = 2000 ms, TE = 30 ms, flip angle (FA) = 60°, matrix size = 64 × 64, thickness/gap = 3.2/0 mm, slices = 43, and scanning time = 8 min. During resting-state fMRI scanning, all participants were required to remain still with their eyes closed, remain awake, and not think of anything systematically. All participants reported that they were not asleep during the scanning. The interval between the latest TIA attack time of patients with TIA and the MRI scan time was 6 hours–16 days.

2.4. Data Preprocessing. Preprocessing of rs-fMRI data was performed using SPM12 (http://www.fil.ion.ucl.ac.uk/spm) and RESTplus v1.24 [61] (http://www.restfmri.net/forum/REST) on Matlab 2017b (https://ww2.mathworks.cn/products/matlab.html), which consists of the following steps: (1) removal of the first 10 time points to stabilize magnetization and allow participants to acclimate to the scanning environment, keeping the remaining 230 volumes for further analysis. (2) Slice-time correction to adjust the data scanned simultaneously. (3) Realignment to correct slight head movements during scanning. (4) T1 image segmentation. The T1 images were coregistered with functional images and then segmented into GM, WM, and cerebrospinal fluid (CSF) using the New Segment algorithm [62]. (5) Removal of the linear trend to correct the signal drift. (6) Regression of the noise signals. To avoid eliminating signals of interest, we regressed only head motion (Friston-24 motion parameters [63]) and mean CSF, leaving WM and global signal out [28]. (7) Temporal scrubbing to censor the data at the spike without changing the correlation values by using the motion "spike" as a separate regressor [64, 65]. (8) Spatial smoothing (FWHM = 4 mm) was performed on the WM and GM images separately of each subject, as suggested in previous studies [28, 31]. (9) Normalization to the standard EPI template and resampling to 3 mm^3 voxels using the DARTEL algorithm. (10) Extraction of individual-level WM 4D images. For each participant, we defined each voxel as GM, WM, and CSF based on its maximum probability from the T1 image segmentation results. This resulted in the individual-level WM 4D images. (11) Creation of group-level WM masks based on individual-level WM 4D images for follow-up statistical analysis. Voxels identified as WM in >60% of participants were adopted to create the WM mask [28]. The subcortical regions were then removed from the WM mask based on the Harvard–Oxford Atlas. The WM mask was also coregistered to the functional space and resampled to process the functional image [66]. A flowchart of the study is presented in Figure 1.

2.5. Metric Calculation. Metric calculations were conducted using the RESTplus software [61]. To avoid the mixture of WM and GM signals and reduce the interference of other noises on WM signals as much as possible, all calculations of these metrics were conducted on individual-level WM 4D images (Figure 1).

2.5.1. ALFF Calculation. ALFF was calculated based on a fast Fourier transform (FFT). The time series of each voxel was transformed into the frequency domain, and the power spectrum was obtained. The square root of each power spectrum frequency was then calculated, and the mean square root was obtained for each voxel. Notably, according to Peer et al.'s research, the energy distribution in the frequency domain differs between WM and GM [28]. Additionally, previous studies demonstrated that 0.15 Hz was the highest expected frequency of hemodynamic signals generated by neurons [67, 68]. Therefore, to reduce the contributions of nonneuronal on BOLD fluctuations, the mean square root was calculated in the frequency band of 0.01–0.15 Hz [2, 16, 29, 30, 69]. Finally, the ALFF value for each voxel was divided by the average ALFF value (mALFF). In addition, the results of different frequency bands of 0.01–0.08 Hz [39], 0.01–0.10 Hz [24], and 0.01–0.15 Hz were compared in the case of other parameters that remained constant. The results are provided in detail in Supplementary Materials (Figure S1).

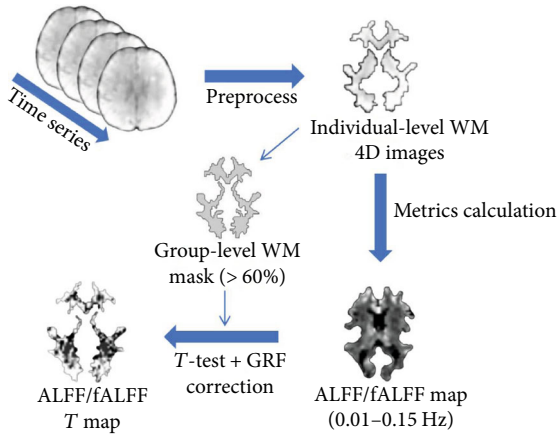

FIGURE 1: Flow chart of preprocessing, metric calculation, and statistical analysis in this study.

2.5.2. fALFF Calculation. As for fALFF, identical to ALFF, 0.01–0.15 Hz was chosen as the frequency band. The ratio of the amplitude in the low-frequency range to the total amplitude in the entire frequency range (0–0.25 Hz) was calculated, representing the relative contribution of the oscillations in the low-frequency range to the signal variation in the entire frequency range. Finally, z-transformation was performed on the ALFF and fALFF maps of each participant. The comparison of different frequency bands is shown in the Supplementary Materials (Figure S2).

2.6. Statistical Analysis. Statistical analysis was performed using the Statistical Package for Social Sciences (SPSS) 26 (IBM Corp., Armonk, N.Y., USA) to examine the differences in demographic and clinical characteristics between patients with TIA and HCs. Age and clinical/physiological/biochemical characteristics were compared between the two groups using Student's t-test, and sex differences were compared using Pearson's chi-squared test. To examine the differences in neural activities in low-frequency bands of WM in patients with TIA and HCs, statistical significance was assessed at voxel-level $P < 0.05$ and cluster-level $P < 0.05$, corrected by Gaussian random fields (GRF) using RESTplus software [61]. In addition, a more rigorous threshold (voxel-level $P < 0.01$, GRF correction) was used to examine the results of the metric calculation and reinforcement learning (see Supplementary Materials Figure S3-S5). Considering the rigor of the statistical analysis, the group-level mask (> 60%) obtained in the preprocessing stage was used for statistical analysis to reduce the interference of non-WM signals. To support the future meta-analysis, we shared the original uncorrected t-maps (http://www.restfmri.net/TIA.tar). Finally, Pearson's correlation analysis was conducted to determine the correlation between resting-state metrics and clinical/physiological/biochemical characteristics. Specifically, the ALFF and fALFF values in WM regions showing group differences between the two groups were extracted and correlated with systolic blood pressure, diastolic blood pressure, blood sugar level, total cholesterol, triglycerides, HDL-C, and LDL-C. Statistical significance was set at $P < 0.05$.

2.7. Feature Extraction and Q-Learning Model Training. To evaluate whether alterations in ALFF and fALFF could serve as potential neuromarkers to distinguish patients with TIA from HCs, we performed a reinforcement learning analysis using the Q-learning algorithm [70, 71]. The steps were as follows: (1) the mean ALFF and fALFF values in WM regions showing significant differences between the two groups were used together to serve as features and were normalized from -1 to 1. According to previous studies on support vector machines (SVM), the combination of features of multiple metrics has a better classification effect than using single metric as the feature [36, 72–74]. (2) The parametric Q-learning method [75] was used to train the approximate Q value function with the linear model and obtain reward feedback by interacting with the environment to find the optimal Q value function and obtain the final classification. In this study, the discount factor γ was 0.9, and the learning rate α was 0.001. Finally, leave-one-out cross-validation (LOOCV) was performed to conduct cross-validation, which could help prevent overfitting [76, 77]. (3) The process described above was applied to each participant to evaluate the overall accuracy of parametric Q-learning. Accuracy, sensitivity, and specificity have been reported to quantify the performance of classification methods. The results of using the ALFF and fALFF features are presented in the Supplementary Materials (Figure S6-S7).

3. Results

3.1. Clinical Data. The final sample size was 89 participants (TIA, $n = 48$; HCs, $n = 41$). Three patients were excluded from further analysis owing to the unsatisfactory quality of multimodal MRI data, including incomplete coverage of the whole brain in the rs-fMRI scan and missing 3D T1 images. Of the 48 patients with TIA, 25 experienced TIA (not a first-time attack), 4 experienced a stroke, and 23 experienced the first episode. Detailed demographic and clinical information of all participants are summarized in Table 1.

As shown in Table 1, the TIA and HC groups were matched for age ($P = 0.182$) and gender ($P = 0.640$). Systolic blood pressure ($P < 0.001$), diastolic blood pressure ($P = 0.007$), blood sugar level ($P = 0.001$), total cholesterol ($P = 0.045$), and LDL-C ($P = 0.004$) were significantly higher in patients with TIA compared to HCs. The median ABCD2 score of patients with TIA was 4.

3.2. Between-Group Differences Results. Brain regions showing differences between groups in the metric analysis were reported based on the ICBM-DTI-81 white-matter label atlas (JHU DTI-based WM atlases, provided by Dr. Susumu Mori, Laboratory of Brain Anatomical MRI, Johns Hopkins University [78, 79]). For the ALFF calculations, patients with TIA showed decreased ALFF in the right cingulate gyrus, right superior longitudinal fasciculus, and left superior corona radiata compared with HCs (Table 2, Figure 2). The right cerebral peduncle, right cingulate gyrus, and middle cerebellar peduncle showed decreased fALFF in patients with TIA (Table 2, Figure 2). Among these brain regions, one cluster with a significant fALFF difference between

Table 1: Demographic and clinical information of all participants.

Variables	TIA ($n = 48$)	HCs ($n = 41$)	P value
Age (year, mean ± SD)	57.60 ± 9.78	55.02 ± 8.03	0.182[t]
Sex (male/female)	37/11	30/11	0.670[χ]
Systolic blood pressure (mmHg, mean ± SD)	145.54 ± 20.75	127.55 ± 19.53[a]	<0.001[t]
Diastolic blood pressure (mmHg, mean ± SD)	86.67 ± 10.38	80.03 ± 10.90[a]	0.007[t]
Blood sugar level (mmol/L, mean ± SD)	6.30 ± 2.11	5.12 ± 0.74[a]	0.001[t]
Total cholesterol (mmol/L, mean ± SD)	5.24 ± 1.14	4.75 ± 1.01[a]	0.045[t]
Triglycerides (mmol/L, mean ± SD)	1.60 ± 0.94	1.92 ± 1.35[a]	0.213[t]
HDL-C (mmol/L, mean ± SD)	1.11 ± 0.24	1.05 ± 0.29[a]	0.306[t]
LDL-C (mmol/L, mean ± SD)	3.31 ± 0.97	2.69 ± 0.90[a]	0.004[t]
ABCD2 scores (median)	4 (2–6)		
Smoking, no. (%)	31 (64.58%)		
Drinking, no. (%)	20 (41.67%)		
Hypertension, no. (%)	22 (45.83%)		
Diabetes, no. (%)	8 (16.67%)		
Coronary artery disease, no. (%)	2 (4.17%)		
Atrial fibrillation, no. (%)	1 (2.08%)		
Medication, no. (%)	—		
Antiplatelets, no. (%)	48 (100%)		
Statins, no. (%)	2 (4.17%)		
DWI hyperintensity, no. (%)	6 (12.50%)		
Vessel stenosis, no. (%)	9 (18.75%)		
TIA/stroke attack in one year follow-up, no. (%)	12 (27.27%)[b]		

Note: [t] The P value was obtained by Student's t-test; [χ] The P value was obtained by two-tailed Pearson chi-square t-test; [a] Data were missing for 6 controls; [b] Four patients dropped out in the one-year follow-up; ABCD2 is a simple score to identify individuals at high early-risk of stroke after a TIA. TIA: transient ischemic attack; HCs: healthy controls; HDL-C: high-density lipoprotein cholesterol; LDL-C: low-density lipoprotein cholesterol.

Table 2: Regions of WM showing abnormal ALFF and fALFF in patients with TIA compared with HCs.

Metrics	Tract (JHU-atlas)	Voxels	MNI coordinates			T value
			x	y	z	
ALFF	Cingulum_R	120	12	0	39	-3.7533
	Superior_longitudinal_fasciculus_R	119	45	-21	30	-4.2423
	Superior_corona_radiata_L	102	-15	-9	45	-3.7579
	Cerebral_peduncle_R	116	12	-24	-15	-3.7614
fALFF	Cingulum_R	109	6	-3	33	-3.9512
	Middle_cerebellar_peduncle	90	-18	-57	-42	-3.8369

Note: The statistical threshold was set at voxel with $P < 0.05$ and cluster with $P < 0.05$ for GRF correction. Cingulum_R: right cingulate gyrus; Superior_longitudinal_fasciculus_R: right superior longitudinal fasciculus; Superior_corona_radiata_L: left superior corona radiate; Cerebral_peduncle_R: right cerebral peduncle; Middle_cerebellar_peduncle: middle cerebellar peduncle; TIA: transient ischemic attack; HCs: healthy controls; MNI: Montreal Neurological Institute; ALFF: amplitude of low-frequency fluctuation; fALFF: fractional ALFF.

patients with TIA and HCs was not reported in Table 2 due to it being off the JHU atlas.

3.3. Correlation Analysis. The ALFF and fALFF values were extracted from WM regions that showed significant differences between patients with TIA and HCs, and correlation analyses between these values and clinical/physiological/biochemical characteristics were conducted. There were no significant differences between the ALFF values in WM regions showing group difference and clinical measurements ($P > 0.05$). There was a significant negative correlation between the fALFF values extracted from the right cerebral peduncle and diastolic blood pressure ($r = -0.316$, $P = 0.029$), and a significant positive correlation between the fALFF values in the right cerebral peduncle and triglycerides ($r = 0.310$, $P = 0.032$). In addition, the fALFF values in the middle cerebellar peduncle showed a significant negative correlation with diastolic blood pressure ($r = -0.320$, $P = 0.027$) and a significant positive correlation with triglycerides ($r = 0.327$, $P = 0.023$).

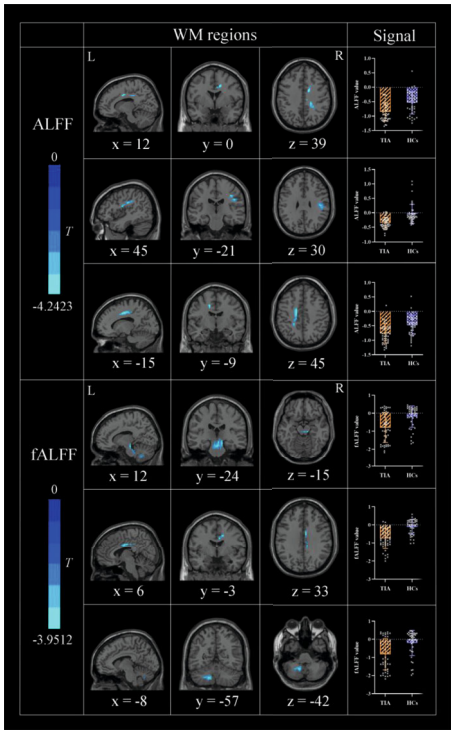

Figure 2: Regions of WM showing group differences in ALFF and fALFF together with signal values extracted from these regions.

3.4. Classification Results. Accuracy, sensitivity, specificity, and precision were calculated to evaluate the classification ability of the parametric *Q*-learning model. The classifier achieved a total accuracy of 82.02%, sensitivity of 85.42%, specificity of 78.05%, precision of 82.00%, and area under the curve (AUC) of 0.87. The receiver operating characteristic (ROC) curve of the classifier is shown in Figure 3.

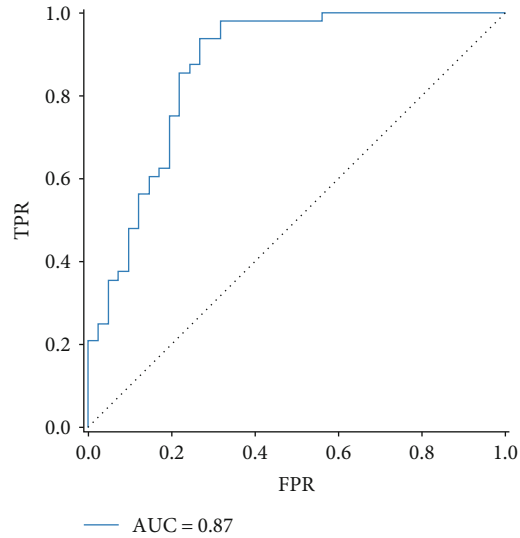

Figure 3: The receiver operating characteristic (ROC) curve of metrics. The image of ROC was displayed using the Matplotlib toolkit in Python. FPR, false positivity rate; TPR, true positivity rate; AUC, area under the ROC curve.

4. Discussion

In this study, two resting-state methods (ALFF and fALFF) were used for the first time to identify abnormalities in the low-frequency range of WM regions in patients with TIA. Moreover, the *Q*-learning algorithm of the reinforcement method was applied to detect neuromarkers that could be used to classify patients with TIA and HCs based on neuroimaging data. Additionally, we explored the relationship between functional abnormalities in WM and the clinical/physiological/biochemical features in patients with TIA. The results showed decreased ALFF in the right cingulate gyrus, right superior longitudinal fasciculus, and left superior corona radiata and decreased fALFF in the right cerebral peduncle, right cingulate gyrus, and middle cerebellar peduncle in patients with TIA. These findings suggest that resting-state metrics can effectively help explore low-frequency BOLD fluctuations in WM in patients with TIA and that these regions of WM showing decreased ALFF and fALFF might indicate that patients with TIA may develop motor and cognitive impairment and emotional problems. Moreover, the *Q*-learning algorithm provided sensitive information for classifying patients with TIA and HCs. These findings may help us gain a deeper understanding of the pathological mechanisms underlying TIA from the perspective of WM dysfunction.

The ALFF is considered a reliable method for detecting the intensity of spontaneous fluctuations and presenting spontaneous brain activity [34]. Recently, ALFF has been demonstrated to effectively reflect functional alterations in WM [32, 38], providing a new perspective for studying WM dysfunction in various diseases. In the present study, we found a decreased ALFF in the right cingulate gyrus, right superior longitudinal fasciculus, and left superior corona radiata in the WM region of patients with TIA. The cingulate gyrus is structurally complex and performs a wide range of functions. Noninvasive imaging has shown that the cingulate gyrus is associated with executive control, emotion, and pain [80]. Damage to the cingulate gyrus may lead to cognitive abnormalities in attention, memory, and emotional processing [81]. Based on prior research and the results of this study, we speculated that patients with TIA may show negative changes in cognitive functions, such as emotion, memory, and executive control. Anatomical studies have shown that the superior longitudinal fasciculus is the biggest associative fiber bundle system in the brain and is connected to the superior frontal gyrus and supplementary motor areas [82]. Patients with TIA are known to exhibit significant cognitive impairment compared with HCs, and the superior longitudinal fasciculus also plays a critical role in a wide range of cognitive functions [19, 83], which might indicate that the onset of TIA may lead to functional impairment in the WM region and affect the patient's cognitive function. The corona radiata consists of numerous tracts involving subcortical motor pathways, which is one of the most prominent motor-related neural fibers [84]. Jiang et al. [85] also found that when an ischemic stroke lesion is located in the corona radiata, it may interfere with the

functional circuitry between the brainstem and frontal cortex, thereby interfering with the patient's emotional expression [86]. We speculated that the decrease in ALFF in the corona radiata may suggest the possibility of developing poststroke depression after a future stroke episode in patients with TIA.

fALFF is calculated as the ratio of the low-frequency range power spectrum to the entire frequency range power spectrum, which is effective in suppressing physiological noise compared to ALFF [35, 87]. To obtain more comprehensive information about low-frequency BOLD fluctuations in WM, we further investigated functional WM abnormalities in patients with TIA using the fALFF method, which is more sensitive to spontaneous neural activity [35]. This study found decreased fALFF in the right cerebral peduncle, right cingulate gyrus, and middle cerebellar peduncle in patients with TIA compared with HCs. Recent diffusion tensor imaging (DTI) studies of cerebral hemorrhage have shown that decreased fractional anisotropy (FA) values in the cerebral peduncle away from the hematoma region indicate neurodegenerative lesions [88, 89]. Koyama et al. [84] also demonstrated that changes in this region are viable predictors of motor outcome. Consistent with the ALFF findings, we also found decreased fALFF in the right cingulate gyrus of patients with TIA, suggesting the possibility of developing cognitive abnormalities in the future. Bilateral middle cerebellar peduncle lesions are commonly associated with cerebrovascular diseases [90]. S.H. Kim and J.S. Kim [91] found unilateral middle cerebellar peduncle lesions in acute stroke patients that manifested clinically as ocular motor abnormalities. Additionally, Zhou et al. [92] found that patients with bilateral middle cerebellar peduncle infarction developed ataxia, characterized by impaired motor coordination. Combined with insights from previous studies, we found that these WM regions with decreased fALFF in patients with TIA were all related to motor function. Hence, we speculated that patients with TIA and decreased fALFF in these WM regions may be at risk of impaired motor coordination and movement disorders (such as local movement disorders) in the future. Our results may shed new light on abnormal changes in these WM regions after the onset of TIA.

In the present study, we noted some variations between the results of the ALFF and fALFF analyses, except for the right cingulate gyrus, which exhibited a decrease in both the ALFF and fALFF. The ALFF reflects the power in the effective frequency range [34], and the fALFF measures the relative spontaneous neural activity in the effective frequency range over the entire frequency range [35]. Owing to the difference in the calculation methods of the two metrics, our results showed slight differences. In addition, the BOLD signal in fMRI reflects the activation of neurons and global physiological fluctuations [93], which may influence the estimation of ALFF. The fALFF is a modified index of ALFF that, relative to the ALFF, can improve the sensitivity and specificity to spontaneous neural activities [87, 94], may provide us with more sensitive information about low-frequency BOLD fluctuations in WM, and validate abnormal functional neural activity in patients with TIA. However, it is noteworthy that the results of ALFF and fALFF analyses both showed decreased low-frequency neural activities in WM of patients with TIA compared with HCs, which may suggest an impaired function in these motor, emotional, and cognitive-related WM regions caused by TIA onset. Combining these two metrics provided us with more comprehensive information on the neural activity in the low-frequency range in WM than using only one method, which also helped examine WM dysfunction in patients with TIA.

Correlation analysis revealed no significant correlations between the ALFF values extracted from WM regions showing group differences and clinical characteristics. In contrast, significant correlations were observed between values in several WM regions showing group differences in fALFF and clinical characteristics. Values in the right cerebral peduncle and middle cerebellar peduncle were negatively correlated with diastolic blood pressure. Demographic information revealed that diastolic blood pressure was significantly higher in patients with TIA than in HCs. According to the World Health Organization Hypertension Guideline, diastolic blood pressure is a risk factor for cardiovascular disease; it is closely associated with mental stress, anxiety, and other emotions [95], which correspond to symptoms presented by some stroke patients since they have developed pathological emotional manifestations such as depression, anxiety disorder, apathy, and psychosis after onset [96, 97]. In this study, we speculated that decreased fALFF values in the right cerebral peduncle and middle cerebellar peduncle may be associated with emotional challenges in patients with TIA. Triglycerides were previously considered a separate risk factor for ischemic stroke in elderly Chinese patients with hypertension [98]. Furthermore, high triglycerides are associated with pathophysiological processes and may contribute to an increased risk of ischemic stroke [99]. Our findings demonstrated that the fALFF values in the right cerebral peduncle and middle cerebellar peduncle of patients with TIA were positively correlated with triglyceride levels. These results imply that the two WM regions may serve as key predictors of ischemic stroke occurrence in the future.

Machine learning has been widely used in neuroscience and for diagnosing neuropsychiatric diseases and has shown good classification performance [100, 101]. More objective diagnostic criteria can be established through machine learning algorithms to help identify neuromarkers for TIA diagnoses. In this study, we combined two indicator features (ALFF and fALFF) and used the *Q*-learning algorithm to distinguish patients with TIA from HCs with an identification accuracy of 82.02% and satisfactory specificity, sensitivity, and precision, which helped establish diagnostic indicators. Therefore, the abnormal ALFF and fALFF values in the WM of the brain could be used as potential imaging biomarkers to differentiate patients with TIA from HCs. Furthermore, *Q*-learning is a promising method for studying these WM functional abnormalities.

5. Limitations

The present study had some limitations that should be interpreted with caution. First, the sample size of this study was

comparatively small, and we would like to validate our results in the future with bigger sample size. Second, fMRI data of patients with TIA were not collected during the follow-up period, to the extent that we have not yet clarified how spontaneous activity in WM changes as TIA progresses. Future studies could be designed longitudinally to test whether current methods can be used to monitor disease progression. Finally, this study lacked information on the emotional condition of patients with TIA, such as depression and anxiety. Considering that our results showed that abnormal WM regions in patients with TIA might also have emotional problems; therefore, future studies can evaluate depression and anxiety in patients using appropriate scales to learn more about the relationship between WM neural activity and scale scores.

6. Conclusion

The present study demonstrated abnormal WM functional alterations in the low-frequency range in patients with TIA. Moreover, WM neural activity in the low-frequency range may serve as a potential neuromarker to differentiate patients with TIA from HCs. These findings provide novel insights into the underlying mechanisms in patients with TIA from the perspective of WM function. Abnormal WM regions may serve as the basis for the clinical diagnosis and prevention of stroke in patients with TIA.

Data Availability

The raw data supporting the conclusions of this study will be made available by the authors, without undue reservation.

Ethical Approval

All procedures involving human participants were in line with the ethical standards of the Institutional and National Research Committee and with the 1964 Helsinki Declaration and its later amendments or comparable ethical standards.

Conflicts of Interest

No conflict of interest is declared by the authors.

Authors' Contributions

Qingguo Ding and Jiaxi Zhang conceived and design the study; Yanyan Gao, Linlin Zhan, and Su Hu performed the experiments and collected materials; Zhou Xie analyzed the data; Huibin Ma, Zhou Xie, and Lina Huang wrote the first manuscript. All authors read and approved the final manuscript. Huibin Ma, Zhou Xie, and Lina Huang contributed equally to this work and share first authorship.

Acknowledgments

We would like to thank all the participants for their participation in this study, and we appreciate the Center for Cognition and Brain Disorders, The Affiliated Hospital of Hangzhou Normal University, Hangzhou, China, for assistance in MRI data acquisition. This study was supported by the Program for Excellent Subject Team of Jiamusi University (JDXKTD_2019008) and the Youth Science and Technology Plan of Soochow Science and Technology Bureau and Soochow Health Planning Commission [KJXW2020065].

Supplementary Materials

Figure S1. Regions of WM showing group differences in ALFF in different frequency bands. Figure S2. Regions of WM showing group differences in fALFF in different frequency bands. Figure S3. Regions of WM showing group differences in ALFF with GRF correction using different thresholds (voxel-level $P < 0.05$ and $P < 0.01$). Figure S4. Regions of WM showing group differences in fALFF with GRF correction using different thresholds (voxel-level $P < 0.05$ and $P < 0.01$). Figure S5. The receiver operating characteristic (ROC) curve of metrics under different thresholds (voxel-level $P < 0.05$ and $P < 0.01$, GRF correction) served as features.[a] By using the mean ALFF and fALFF values in the clusters showing significant differences (voxel-level $P < 0.05$, GRF correction) between the two groups as features, the classifier achieved a total accuracy of 82.02%, sensitivity of 85.42%, specificity of 78.05%, precision of 82.00%, and AUC of 0.87; [b] By using the mean ALFF and fALFF values in the clusters showing significant differences (voxel-level $P < 0.01$, GRF correction) between the two groups as features, the classifier achieved a total accuracy of 80.90%, sensitivity of 77.08%, specificity of 85.37%, precision of 86.05%, and AUC of 0.77. The image of ROC was displayed using the Matplotlib toolkit in Python. FPR, false positivity rate; TPR, true positivity rate; AUC, area under the ROC curve. Figure S6. The receiver operating characteristic (ROC) curve of metrics (ALFF). By using the mean ALFF values in the clusters showing significant differences (voxel-level $P < 0.05$, GRF correction) between the two groups as features, the classifier achieved a total accuracy of 78.65%, sensitivity of 75.00%, specificity of 82.93%, precision of 83.72%, and AUC of 0.77. The image of ROC was displayed using the Matplotlib toolkit in Python. FPR, false positivity rate; TPR, true positivity rate; AUC, area under the ROC curve. Figure S7. The receiver operating characteristic (ROC) curve of metric (fALFF). By using the mean fALFF values in the clusters showing significant differences (voxel-level $P < 0.05$, GRF correction) between the two groups as features, the classifier achieved a total accuracy of 70.79%, sensitivity of 79.17%, specificity of 60.98%, precision of 70.37%, and AUC of 0.75. The image of ROC was displayed using the Matplotlib toolkit in Python. FPR, false positivity rate; TPR, true positivity rate; AUC, area under the ROC curve. *(Supplementary Materials)*

References

[1] E. J. Benjamin, M. J. Blaha, S. E. Chiuve et al., "Heart disease and stroke statistics-2017 update: a report from the American Heart Association," *Circulation*, vol. 135, no. 10, pp. e146–e603, 2017.

[2] H. Chen, J. Long, S. Yang, and B. He, "Atypical functional covariance connectivity between gray and white matter in children with autism spectrum disorder," *Autism Research*, vol. 14, no. 3, pp. 464–472, 2021.

[3] P. A. Heidenreich, N. M. Albert, L. A. Allen et al., "Forecasting the impact of heart failure in the United States: a policy statement from the American Heart Association," *Circulation Heart Failure*, vol. 6, no. 3, pp. 606–619, 2013.

[4] G. W. Albers, L. R. Caplan, J. D. Easton et al., "Transient ischemic attack–proposal for a new definition," *The New England Journal of Medicine*, vol. 347, no. 21, pp. 1713–1716, 2002.

[5] B. Clissold, T. G. Phan, J. Ly, S. Singhal, V. Srikanth, and H. Ma, "Current aspects of TIA management," *Journal of Clinical Neuroscience*, vol. 72, pp. 20–25, 2020.

[6] S. A. Billinger, R. Arena, J. Bernhardt et al., "Physical activity and exercise recommendations for stroke survivors," *Stroke*, vol. 45, no. 8, pp. 2532–2553, 2014.

[7] L. M. de Lau, H. M. den Hertog, E. G. van den Herik, and P. J. Koudstaal, "Predicting and preventing stroke after transient ischemic attack," *Expert Review of Neurotherapeutics*, vol. 9, no. 8, pp. 1159–1170, 2009.

[8] S. Ghozy, S. E. O. Kacimi, M. Elfil et al., "Transient ischemic attacks preceding ischemic stroke and the possible preconditioning of the human brain: a systematic review and meta-analysis," *Frontiers in Neurology*, vol. 12, article 755167, 2021.

[9] J. Li, H. Chen, F. Fan et al., "White-matter functional topology: a neuromarker for classification and prediction in unmedicated depression," *Translational Psychiatry*, vol. 10, no. 1, p. 365, 2020.

[10] B. Biswal, F. Zerrin Yetkin, V. M. Haughton, and J. S. Hyde, "Functional connectivity in the motor cortex of resting human brain using echo- planar mri," *Magnetic Resonance in Medicine*, vol. 34, no. 4, pp. 537–541, 1995.

[11] Y. Lv, L. Li, Y. Song et al., "The local brain abnormalities in patients with transient ischemic attack: a resting-state fMRI study," *Frontiers in Neuroscience*, vol. 13, p. 24, 2019.

[12] M. D. Fox and M. E. Raichle, "Spontaneous fluctuations in brain activity observed with functional magnetic resonance imaging," *Nature Reviews. Neuroscience*, vol. 8, no. 9, pp. 700–711, 2007.

[13] H. J. Park and K. Friston, "Structural and functional brain networks: from connections to cognition," *Science*, vol. 342, no. 6158, p. 1238411, 2013.

[14] J. Li, G. R. Wu, B. Li et al., "Transcriptomic and macroscopic architectures of intersubject functional variability in human brain white-matter," *Communications Biology*, vol. 4, no. 1, p. 1417, 2021.

[15] N. K. Logothetis, J. Pauls, M. Augath, T. Trinath, and A. Oeltermann, "Neurophysiological investigation of the basis of the fMRI signal," *Nature*, vol. 412, no. 6843, pp. 150–157, 2001.

[16] P. Wang, C. Meng, R. Yuan et al., "the organization of the human corpus callosum estimated by intrinsic functional connectivity with white-matter functional networks," *Cerebral Cortex*, vol. 30, no. 5, pp. 3313–3324, 2020.

[17] P. Wang, Z. Wang, J. Wang et al., "Altered homotopic functional connectivity within white matter in the early stages of Alzheimer's disease," *Frontiers in Neuroscience*, vol. 15, article 697493, 2021.

[18] J. K. Ferris, J. D. Edwards, J. A. Ma, and L. A. Boyd, "Changes to white matter microstructure in transient ischemic attack: a longitudinal diffusion tensor imaging study," *Human Brain Mapping*, vol. 38, no. 11, pp. 5795–5803, 2017.

[19] F. Vergani, P. Ghimire, D. Rajashekhar, F. Dell'acqua, and J. P. Lavrador, "Superior longitudinal fasciculus (SLF) I and II: an anatomical and functional review," *Journal of Neurosurgical Sciences*, vol. 65, no. 6, pp. 560–565, 2021.

[20] M. Fabri, G. Polonara, G. Mascioli, U. Salvolini, and T. Manzoni, "Topographical organization of human corpus callosum: an fMRI mapping study," *Brain Research*, vol. 1370, pp. 99–111, 2011.

[21] M. Fabri and G. Polonara, "Functional topography of human corpus callosum: an FMRI mapping study," *Neural Plasticity*, vol. 2013, Article ID 251308, 15 pages, 2013.

[22] J. R. Gawryluk, E. L. Mazerolle, K. D. Brewer, S. D. Beyea, and R. C. N. D'Arcy, "Investigation of fMRI activation in the internal capsule," *BMC Neuroscience*, vol. 12, no. 1, p. 56, 2011.

[23] J. R. Gawryluk, E. L. Mazerolle, and R. C. D'Arcy, "Does functional MRI detect activation in white matter? A review of emerging evidence, issues, and future directions," *Frontiers in Neuroscience*, vol. 8, p. 239, 2014.

[24] J. Li, B. B. Biswal, Y. Meng et al., "A neuromarker of individual general fluid intelligence from the white-matter functional connectome," *Translational Psychiatry*, vol. 10, no. 1, p. 147, 2020.

[25] B. Guo, F. Zhou, M. Li, J. C. Gore, and Z. Ding, "Correlated functional connectivity and glucose metabolism in brain white matter revealed by simultaneous MRI/positron emission tomography," *Magnetic Resonance in Medicine*, vol. 87, no. 3, pp. 1507–1514, 2022.

[26] Z. Ding, A. T. Newton, R. Xu, A. W. Anderson, V. L. Morgan, and J. C. Gore, "Spatio-temporal correlation tensors reveal functional structure in human brain," *PLoS One*, vol. 8, no. 12, article e82107, 2013.

[27] Z. Ding, Y. Huang, S. K. Bailey et al., "Detection of synchronous brain activity in white matter tracts at rest and under functional loading," *Proceedings of the National Academy of Sciences of the United States of America*, vol. 115, no. 3, pp. 595–600, 2018.

[28] M. Peer, M. Nitzan, A. S. Bick, N. Levin, and S. Arzy, "Evidence for functional networks within the human brain's white matter," *The Journal of Neuroscience*, vol. 37, no. 27, pp. 6394–6407, 2017.

[29] Y. Jiang, C. Luo, X. Li et al., "White-matter functional networks changes in patients with schizophrenia," *NeuroImage*, vol. 190, pp. 172–181, 2019.

[30] Y. S. Fan, Z. Li, X. Duan et al., "Impaired interactions among white-matter functional networks in antipsychotic- naive first-episode schizophrenia," *Human Brain Mapping*, vol. 41, no. 1, pp. 230–240, 2020.

[31] Y. Jiang, L. Song, X. Li et al., "Dysfunctional white-matter networks in medicated and unmedicated benign epilepsy with centrotemporal spikes," *Human Brain Mapping*, vol. 40, no. 10, pp. 3113–3124, 2019.

[32] G. J. Ji, W. Liao, F. F. Chen, L. Zhang, and K. Wang, "Low-frequency blood oxygen level-dependent fluctuations in the brain white matter: more than just noise," *Science Bulletin*, vol. 62, no. 9, pp. 656-657, 2017.

[33] X. Wu, Z. Yang, S. K. Bailey et al., "Functional connectivity and activity of white matter in somatosensory pathways

under tactile stimulations," *NeuroImage*, vol. 152, pp. 371–380, 2017.

[34] Z. Yu-Feng, H. Yong, Z. Chao-Zhe et al., "Altered baseline brain activity in children with ADHD revealed by resting-state functional MRI," *Brain and Development*, vol. 29, no. 2, pp. 83–91, 2007.

[35] Q. H. Zou, C. Z. Zhu, Y. Yang et al., "An improved approach to detection of amplitude of low-frequency fluctuation (ALFF) for resting-state fMRI: fractional ALFF," *Journal of Neuroscience Methods*, vol. 172, no. 1, pp. 137–141, 2008.

[36] H. Ma, G. Huang, M. Li et al., "The predictive value of dynamic intrinsic local metrics in transient ischemic attack," *Frontiers in Aging Neuroscience*, vol. 13, article 808094, 2021.

[37] J. Bai, H. Wen, J. Tai et al., "Altered spontaneous brain activity related to neurologic and sleep dysfunction in children with obstructive sleep apnea syndrome," *Frontiers in Neuroscience*, vol. 15, article 595412, 2021.

[38] G. J. Ji, C. Ren, Y. Li et al., "Regional and network properties of white matter function in Parkinson's disease," *Human Brain Mapping*, vol. 40, no. 4, pp. 1253–1263, 2019.

[39] C. Yang, W. Zhang, L. Yao et al., "Functional alterations of white matter in chronic never-treated and treated schizophrenia patients," *Journal of Magnetic Resonance Imaging*, vol. 52, no. 3, pp. 752–763, 2020.

[40] W. Cao, X. Sun, D. Dong, S. Yao, and B. Huang, "Sex differences in spontaneous brain activity in adolescents with conduct disorder," *Frontiers in Psychology*, vol. 9, p. 1598, 2018.

[41] X. He, J. Hong, Q. Wang et al., "Altered spontaneous brain activity patterns and functional connectivity in adults with intermittent exotropia: a resting-state fMRI study," *Frontiers in Neuroscience*, vol. 15, article 746882, 2021.

[42] L. Yang, Y. Yan, Y. Wang et al., "Gradual disturbances of the amplitude of low-frequency fluctuations (ALFF) and fractional ALFF in Alzheimer spectrum," *Frontiers in Neuroscience*, vol. 12, p. 975, 2018.

[43] Q. D. Buchlak, N. Esmaili, J. C. Leveque, C. Bennett, F. Farrokhi, and M. Piccardi, "Machine learning applications to neuroimaging for glioma detection and classification: an artificial intelligence augmented systematic review," *Journal of Clinical Neuroscience*, vol. 89, pp. 177–198, 2021.

[44] J. Cui, J. Yang, K. Zhang et al., "Machine learning-based model for predicting incidence and severity of acute ischemic stroke in anterior circulation large vessel occlusion," *Frontiers in Neurology*, vol. 12, article 749599, 2021.

[45] K. H. Madsen, L. G. Krohne, X. L. Cai, Y. Wang, and R. C. K. Chan, "Perspectives on machine learning for classification of Schizotypy using fMRI data," *Schizophrenia Bulletin*, vol. 44, suppl_2, pp. S480–s490, 2018.

[46] K. S. Na and Y. K. Kim, "The application of a machine learning-based brain magnetic resonance imaging approach in major depression," *Advances in Experimental Medicine and Biology*, vol. 1305, pp. 57–69, 2021.

[47] F. Pereira, T. Mitchell, and M. Botvinick, "Machine learning classifiers and fMRI: a tutorial overview," *NeuroImage*, vol. 45, no. 1, pp. S199–S209, 2009.

[48] V. Ardulov, V. R. Martinez, K. Somandepalli et al., "Robust diagnostic classification via Q-learning," *Scientific Reports*, vol. 11, no. 1, p. 11730, 2021.

[49] S. Ohnishi, E. Uchibe, Y. Yamaguchi, K. Nakanishi, Y. Yasui, and S. Ishii, "Constrained deep Q-learning gradually approaching ordinary Q-learning," *Frontiers in Neurorobotics*, vol. 13, p. 103, 2019.

[50] G. Viejo, M. Khamassi, A. Brovelli, and B. Girard, "Modeling choice and reaction time during arbitrary visuomotor learning through the coordination of adaptive working memory and reinforcement learning," *Frontiers in Behavioral Neuroscience*, vol. 9, p. 225, 2015.

[51] W. Xue, Z. Feng, C. Xu, Z. Meng, and C. Zhang, "Adaptive object tracking via multi-angle analysis collaboration," *Sensors (Basel)*, vol. 18, no. 11, p. 3606, 2018.

[52] J. Lee, W. Ko, E. Kang, H. I. Suk, and Alzheimer's Disease Neuroimaging Initiative, "A unified framework for personalized regions selection and functional relation modeling for early MCI identification," *NeuroImage*, vol. 236, p. 118048, 2021.

[53] L. D. Vanes, E. Mouchlianitis, T. Collier, B. B. Averbeck, and S. S. Shergill, "Differential neural reward mechanisms in treatment-responsive and treatment-resistant schizophrenia," *Psychological Medicine*, vol. 48, pp. 1–10, 2018.

[54] S. V. Moravvej, R. Alizadehsani, S. Khanam et al., "RLMD-PA: a reinforcement learning-based myocarditis diagnosis combined with a population-based algorithm for pretraining weights," *Contrast Media & Molecular Imaging*, vol. 2022, article 8733632, 15 pages, 2022.

[55] S. C. Johnston, P. M. Rothwell, M. N. Nguyen-Huynh et al., "Validation and refinement of scores to predict very early stroke risk after transient ischaemic attack," *The Lancet*, vol. 369, no. 9558, pp. 283–292, 2007.

[56] B. I. Ön, X. Vidal, U. Berger et al., "Antidepressant use and stroke or mortality risk in the elderly," *European Journal of Neurology*, vol. 29, no. 2, pp. 469–477, 2022.

[57] G. M. Turner, C. McMullan, L. Atkins, R. Foy, J. Mant, and M. Calvert, "TIA and minor stroke: a qualitative study of long-term impact and experiences of follow-up care," *BMC Family Practice*, vol. 20, no. 1, p. 176, 2019.

[58] S. B. Coutts, "Diagnosis and management of transient ischemic attack," *Continuum (Minneap Minn)*, vol. 23, pp. 82–92, 2017.

[59] P. M. Rothwell and C. P. Warlow, "Timing of TIAs preceding stroke: time window for prevention is very short," *Neurology*, vol. 64, no. 5, pp. 817–820, 2005.

[60] R. J. Adams, G. Albers, M. J. Alberts et al., "Update to the AHA/ASA recommendations for the prevention of stroke in patients with stroke and transient ischemic attack," *Stroke*, vol. 39, no. 5, pp. 1647–1652, 2008.

[61] X. Z. Jia, J. Wang, H. Y. Sun et al., "RESTplus: An Improved Toolkit for Resting-State Functional Magnetic Resonance Imaging Data Processing," *Science Bulletin*, vol. 64, pp. 953-954, 2019.

[62] J. Ashburner, "A fast diffeomorphic image registration algorithm," *NeuroImage*, vol. 38, no. 1, pp. 95–113, 2007.

[63] K. J. Friston, S. Williams, R. Howard, R. S. J. Frackowiak, and R. Turner, "Movement-related effects in fMRI time-series," *Magnetic Resonance in Medicine*, vol. 35, no. 3, pp. 346–355, 1996.

[64] J. D. Power, K. A. Barnes, A. Z. Snyder, B. L. Schlaggar, and S. E. Petersen, "Spurious but systematic correlations in functional connectivity MRI networks arise from subject motion," *NeuroImage*, vol. 59, no. 3, pp. 2142–2154, 2012.

[65] T. D. Satterthwaite, M. A. Elliott, R. T. Gerraty et al., "An improved framework for confound regression and filtering

for control of motion artifact in the preprocessing of resting-state functional connectivity data," *NeuroImage*, vol. 64, pp. 240–256, 2013.

[66] R. S. Desikan, F. Ségonne, B. Fischl et al., "An automated labeling system for subdividing the human cerebral cortex on MRI scans into gyral based regions of interest," *NeuroImage*, vol. 31, no. 3, pp. 968–980, 2006.

[67] O. Josephs and R. N. Henson, "Event-related functional magnetic resonance imaging: modelling, inference and optimization," *Philosophical Transactions of the Royal Society of London. Series B, Biological Sciences*, vol. 354, no. 1387, pp. 1215–1228, 1999.

[68] T. Tong, Y. Zhenwei, and F. Xiaoyuan, "Transient ischemic attack and stroke can be differentiated by analyzing the diffusion tensor imaging," *Korean Journal of Radiology*, vol. 12, no. 3, pp. 280–288, 2011.

[69] X. Bu, K. Liang, Q. Lin et al., "Exploring white matter functional networks in children with attention-deficit/hyperactivity disorder," *Brain Communications*, vol. 2, no. 2, article fcaa113, 2020.

[70] R. S. Sutton and A. G. Barto, *Introduction to reinforcement learning*, MIT press, 1998.

[71] C. Watkins, J. Christopher, and P. J. M. L. Dayan, "Q-learning," *Machine Learning*, vol. 8, no. 3, pp. 279–292, 1992.

[72] Y. Tang, L. Meng, C. M. Wan et al., "Identifying the presence of Parkinson's disease using low-frequency fluctuations in BOLD signals," *Neuroscience Letters*, vol. 645, pp. 1–6, 2017.

[73] Q. Chen, Y. Bi, X. Zhao et al., "Regional amplitude abnormities in the major depressive disorder: a resting- state fMRI study and support vector machine analysis," *Journal of Affective Disorders*, vol. 308, pp. 1–9, 2022.

[74] M. Yuan, C. Qiu, Y. Meng et al., "Pre-treatment resting-state functional MR imaging predicts the long-term clinical outcome after short-term paroxtine treatment in post-traumatic stress disorder," *Frontiers in Psychiatry*, vol. 9, p. 532, 2018.

[75] L. F. Yang and M. Wang, "Sample-optimal parametric q-learning using linearly additive features," *International Conference on Machine Learning*, vol. 97, pp. 6995–7004, 2019.

[76] R. B. Rao and G. Fung, "On the dangers of cross-validation. An experimental evaluation," in *Proceedings of the SIAM International Conference on Data Mining, SDM*, Atlanta, Georgia, USA, 2008.

[77] Z. Wang, J. Yang, H. Wu, J. Zhu, and M. Sawan, "Power efficient refined seizure prediction algorithm based on an enhanced benchmarking," *Scientific Reports*, vol. 11, no. 1, p. 23498, 2021.

[78] K. Hua, J. Zhang, S. Wakana et al., "Tract probability maps in stereotaxic spaces: analyses of white matter anatomy and tract-specific quantification," *NeuroImage*, vol. 39, no. 1, pp. 336–347, 2008.

[79] S. Wakana, A. Caprihan, M. M. Panzenboeck et al., "Reproducibility of quantitative tractography methods applied to cerebral white matter," *NeuroImage*, vol. 36, no. 3, pp. 630–644, 2007.

[80] E. J. Bubb, C. Metzler-Baddeley, and J. P. Aggleton, "The cingulum bundle: anatomy, function, and dysfunction," *Neuroscience and Biobehavioral Reviews*, vol. 92, pp. 104–127, 2018.

[81] B. A. Vogt and S. Laureys, "Posterior cingulate, precuneal and retrosplenial cortices: cytology and components of the neural network correlates of consciousness," *Progress in Brain Research*, vol. 150, pp. 205–217, 2005.

[82] F. Janelle, C. Iorio-Morin, S. D'amour, and D. Fortin, "Superior longitudinal fasciculus: a review of the anatomical descriptions with functional correlates," *Frontiers in Neurology*, vol. 13, article 794618, 2022.

[83] V. Guyomard, A. K. Metcalf, M. F. Naguib, R. A. Fulcher, J. F. Potter, and P. K. Myint, "Transient ischaemic attack, vascular risk factors and cognitive impairment: a case-controlled study," *Age and Ageing*, vol. 40, no. 5, pp. 641–644, 2011.

[84] T. Koyama, M. Tsuji, H. Nishimura, H. Miyake, T. Ohmura, and K. Domen, "Diffusion tensor imaging for intracerebral hemorrhage outcome prediction: comparison using data from the corona radiata/internal capsule and the cerebral peduncle," *Journal of Stroke and Cerebrovascular Diseases*, vol. 22, no. 1, pp. 72–79, 2013.

[85] C. Jiang, L. Yi, S. Cai, and L. Zhang, "Ischemic stroke in pontine and corona radiata: location specific impairment of neural network investigated with resting state fMRI," *Frontiers in Neurology*, vol. 10, p. 575, 2019.

[86] Y. Shi, Y. Zeng, L. Wu et al., "A study of the brain functional network of post-stroke depression in three different lesion locations," *Scientific Reports*, vol. 7, no. 1, p. 14795, 2017.

[87] X. N. Zuo, A. di Martino, C. Kelly et al., "The oscillating brain: complex and reliable," *NeuroImage*, vol. 49, no. 2, pp. 1432–1445, 2010.

[88] T. Koyama, M. Tsuji, H. Miyake, T. Ohmura, and K. Domen, "Motor outcome for patients with acute intracerebral hemorrhage predicted using diffusion tensor imaging: an application of ordinal logistic modeling," *Journal of Stroke and Cerebrovascular Diseases*, vol. 21, no. 8, pp. 704–711, 2012.

[89] H. Yoshioka, T. Horikoshi, S. Aoki et al., "Diffusion tensor tractography predicts motor functional outcome in patients with spontaneous intracerebral hemorrhage," *Neurosurgery*, vol. 62, no. 1, pp. 97–103, 2008, discussion 103.

[90] J. Jiang, J. Wang, M. Lin, X. Wang, J. Zhao, and X. Shang, "Bilateral middle cerebellar peduncle lesions: neuroimaging features and differential diagnoses," *Brain and Behavior: A Cognitive Neuroscience Perspective*, vol. 10, no. 10, article e01778, 2020.

[91] S. H. Kim and J. S. Kim, "Eye movement abnormalities in middle cerebellar peduncle strokes," *Acta Neurologica Belgica*, vol. 119, no. 1, pp. 37–45, 2019.

[92] C. Zhou, H. Fan, H. Chen et al., "Evaluation of clinical features and stroke etiology in patients with bilateral middle cerebellar peduncle infarction," *European Neurology*, vol. 83, no. 3, pp. 271–278, 2020.

[93] J. Y. Li, X. L. Suo, N. N. Li et al., "Altered spontaneous brain activity in essential tremor with and without resting tremor: a resting-state fMRI study," *Magnetic Resonance Materials in Physics, Biology and Medicine*, vol. 34, no. 2, pp. 201–212, 2021.

[94] C. Kong, D. Xu, Y. Wang et al., "Amplitude of low-frequency fluctuations in multiple-frequency bands in patients with intracranial tuberculosis: a prospective cross-sectional study," *Quantitative Imaging in Medicine and Surgery*, vol. 12, no. 8, pp. 4120–4134, 2022.

[95] A. Al-Makki, D. DiPette, P. K. Whelton et al., "Hypertension pharmacological treatment in adults: a World Health Organization guideline executive summary," *Hypertension*, vol. 79, no. 1, pp. 293–301, 2022.

[96] D. Mozaffarian, E. J. Benjamin, A. S. Go et al., "Heart disease and stroke statistics–2015 update: a report from the American Heart Association," *Circulation*, vol. 131, no. 4, pp. e29–322, 2015.

[97] R. G. Robinson and R. E. Jorge, "Post-stroke depression: a review," *The American Journal of Psychiatry*, vol. 173, no. 3, pp. 221–231, 2016.

[98] Y. Q. Huang, J. Y. Huang, L. Liu et al., "Relationship between triglyceride levels and ischaemic stroke in elderly hypertensive patients," *Postgraduate Medical Journal*, vol. 96, no. 1133, pp. 128–133, 2020.

[99] N. Antonios, D. J. Angiolillo, and S. Silliman, "Hypertriglyceridemia and ischemic stroke," *European Neurology*, vol. 60, no. 6, pp. 269–278, 2008.

[100] C. P. Santana, E. A. de Carvalho, I. D. Rodrigues, G. S. Bastos, A. D. de Souza, and L. L. de Brito, "Rs-fMRI and machine learning for ASD diagnosis: a systematic review and meta-analysis," *Scientific Reports*, vol. 12, no. 1, p. 6030, 2022.

[101] M. S. Sirsat, E. Fermé, and J. Câmara, "Machine learning for brain stroke: a review," *Journal of Stroke and Cerebrovascular Diseases*, vol. 29, no. 10, article 105162, 2020.